# ANALYTICAL MODELING OF FIBER REINFORCED COMPOSITE DEEP BEAMS

A THESIS SUBMITTED TO
THE GRADUATE SCHOOL OF NATURAL AND APPLIED SCIENCES
OF
MIDDLE EAST TECHNICAL UNIVERSITY

BY
EREN YAĞMUR

IN PARTIAL FULFILLMENT OF THE REQUIREMENTS
FOR
THE DEGREE OF DOCTOR OF PHILOSOPHY
IN
CIVIL ENGINEERING

OCTOBER 2018

Approval of the Thesis:

**ANALYTICAL MODELING OF FIBER REINFORCED COMPOSITE DEEP BEAMS**

submitted by **EREN YAĞMUR** in partial fulfilment of the requirements for the degree of **Doctor of Philosophy in Civil Engineering Department, Middle East Technical University** by,

Prof. Dr. Halil KALIPÇILAR ________________
Dean, Graduate School of **Natural and Applied Sciences**

Prof. Dr. İsmail Özgür YAMAN ________________
Head of Department, **Civil Engineering**

Assoc. Prof. Dr. Burcu BURAK BAKIR ________________
Supervisor, **Civil Engineering Department, METU**

**Examining Committee Members:**

Prof. Dr. Erdem CANBAY ________________
Civil Engineering Department, METU

Assoc. Prof. Dr. Burcu BURAK BAKIR ________________
Civil Engineering Department, METU

Prof. Dr. Özgür ANIL ________________
Civil Engineering Department, Gazi University

Assoc. Prof. Dr. Eray BARAN ________________
Civil Engineering Department, METU

Asst. Prof. Dr. Halit Cenan MERTOL ________________
Civil Engineering Department, Atılım University

**Date:** 24.10.2018

**I hereby declare that all information in this document has been obtained and presented in accordance with academic rules and ethical conduct. I also declare that, as required by these rules and conduct, I have fully cited and referenced all material and results that are not original to this work.**

Name, Last Name: Eren YAĞMUR

Signature:

**ABSTRACT**

**ANALYTICAL MODELING OF FIBER REINFORCED COMPOSITE DEEP BEAMS**



YAĞMUR, Eren
Ph.D., Department of Civil Engineering
Supervisor: Assoc. Prof. Dr. Burcu Burak Bakır



October 2018, 203 pages



Discrete fibers are often used as reinforcement to increase the tensile and shear strengths of concrete. For many years, the behavior of fiber reinforced composite members has been investigated both experimentally and analytically. The influence of fibers on the behavior of shear critical members is quite significant, therefore, it is inevitable to develop a method, which estimates the shear strength of fiber reinforced composite deep beams realistically. This is why one of the main objectives of this study is to propose a shear strength equation and a method to obtain the flexural strength of deep beams and coupling beams with different types and amounts of fibers and reinforcement detailing under varying loading conditions. The predicted shear strengths and strengths computed from equations recommended by other researchers are then compared with the experimental results that are tabulated in a database constructed for this analytical study. Another main purpose of this study is to recommend a model that can be utilized in the nonlinear analysis of coupling beams. When the analytical results obtained from the proposed method are compared with the experimental results, it is observed that the behavior is predicted with adequate accuracy, even for coupled wall systems.

**Keywords :** Shear strength, fiber reinforced composites (FRC), high performance fiber reinforced composites (HPFRC), deep beams, coupling beams, nonlinear behavior.

# ÖZ

## LİFLİ BETON İLE ÜRETİLMİŞ DERİN KİRİŞLERİN ANALİTİK MODELLENMESİ



YAĞMUR, Eren
Doktora, İnşaat Mühendisliği Bölümü
Tez Danışmanı: Doç. Dr. Burcu Burak Bakır



Ekim 2018, 203 sayfa



Lifler, betonun çekme ve kesme dayanımlarını artırmak amacı ile sıklıkla kullanılan takviyelerdir. Uzun yıllar boyunca, lif takviyeli kompozit elemanların davranışı hem deneysel hem de analitik olarak farklı araştırmacılar tarafından irdelenmiştir. Liflerin, kesmede kritik olan elemanların davranışına etkisi son derece belirgindir, bundan dolayı lif takviyeli kompozit derin kirişlerin kesme mukavemetini gerçekçi bir şekilde tahmin eden bir yöntemin geliştirilmesi kaçınılmazdır. Bu nedenle, bu çalışmanın temel amaçlarından biri farklı miktar ve çeşitlilikte liflere ve donatı detaylarına sahip olan derin ve bağ kirişlerin farklı yüklemeler altındaki kesme dayanımlarının gerçekçi tahmini için bir bağıntı önermek ve bu kirişlerin eğilme dayanımlarını elde etmek için bir yöntem geliştirmektir. Bu doğrultuda, malzeme ve deney elemanlarının özellikleri ile deney sonuçlarını içeren bir veritabanı oluşturulmuş ve geliştirilen yöntem kullanılarak elde edilen kesme dayanımı ile diğer araştırmacılar tarafından önerilen denklemlerden elde edilen kesme dayanımları veritabanında toplanan deneysel sonuçlarla karşılaştırılmıştır. Bu çalışmanın diğer bir amacı, bağ kirişlerin doğrusal olmayan analizinde kullanılabilecek bir model önermektir. Önerilen model kullanılarak yapılan doğrusal olmayan analizlerin sonuçları deney sonuçları ile karşılaştırıldığında, davranışın gerçekçi bir şekilde tahmin edilebildiği görülmektedir.

**Anahtar Kelimeler :** Kesme dayanımı, lifli beton, derin kirişler, bağ kirişler, doğrusal olmayan davranış.

*To my parents*

## ACKNOWLEDGEMENTS

Firstly, I would like to express my sincere gratitude to my supervisor Assoc. Prof. Dr. Burcu Burak Bakır for her guidance, advice, criticism, encouragements and insight throughout the research.

Besides my advisor, I would like to thank the rest of my thesis committee: Prof. Dr. Erdem Canbay, and Prof. Dr. Özgür Anıl, for their insightful comments and encouragement.

I am thankful to Prof. Dr. Yalın Arıcı, Prof. Dr. Özgür Kurç, and Prof. Dr. Kağan Tuncay for not hesitating to answer my questions. I am grateful to Dr. Engin Karaesmen, and Dr. Erhan Karaesmen for their support and motivation.

I thank my friends and collegues; Başak Varlı Bingöl, Yavuz Semerdöken, Dr. Vesile Hatun Akansel, and Umut Varlı for their friendship and the times we spent together.

My special thanks goes to Başak Varlı Bingöl, Yavuz Semerdöken, and Ayhan Öner Yücel for their friendship and support.

Last but not the least, I would like to thank to my family for providing me with unfailing support and continuous encouragement throughtout my life. This accomplishment would not have been possible without you.

I would like to thank for the financial support, provided to my study by "2211-A" program of Turkish Scientific and Technical Research Council (TÜBİTAK).

# TABLE OF CONTENTS

## LIST OF TABLES

### TABLES

# LIST OF FIGURES

## FIGURES

# CHAPTER 1

# INTRODUCTION

## 1.1. Problem Statement and Objectives

Under seismic loading, reinforced concrete beams have flexural or shear failure based on material or cross sectional properties of the members. Flexural failure is the preferred mode of failure to provide adequate ductility and energy dissipation capacity required under earthquake loading. In a reinforced concrete beam, when principle tensile stresses exceed the tensile strength of concrete in the shear span (Khuntia and Stojadinovic, 2001), a diagonal crack is formed and a sudden and brittle shear failure is observed. In order to avoid this type of brittle failure, randomly distributed short fibers are added to the concrete mix, which increase the tensile and shear strength and provide load transfer in between crack surfaces.

Numerous experimental and analytical research studies have been conducted to determine the effect of different parameters on the seismic behavior of fiber reinforced composite (FRC) and high performance fiber reinforced composite (HPFRC) beams. The main difference of FRC and HPFRC beams is the tensile behavior after the formation of the first crack.

Many researchers estimated the shear strength of fiber reinforced composite (FRC) beams without transverse reinforcement. However, the results of various experimental studies indicated that the use of fibers improves the shear capacity of members even for members that already have transverse reinforcement (Kwak et al., 2002; Cucchiara et al., 2004; Ding et al., 2011). For this reason, a database which includes deep beams, FRC and HPFRC coupling beams is constructed. In the light of these experimental studies, the key parameters that influence the strength and behavior of shear critical beams are selected and a method is developed to compute the shear and flexural strengths of the beams. In order to verify the accuracy of the predicted shear and flexural strengths, the analytical results are compared with the experimental ones and the information gathered from this comparison is presented. Moreover, nonlinear models are developed to determine the behavior of FRC and HPFRC coupling beams. The results of the nonlinear analysis are also compared with the experimental results obtained from the coupling beam specimens and recommendations are made to further improve the accuracy of the proposed method. Two large scale four-story coupled-wall specimens are analyzed by using the proposed model as well, in order to examine the efficiency of this model in predicting the overall system response.

## 1.2. Organization of the Thesis

In Chapter 2, mechanical properties of fiber reinforced composites (FRC), parameters that influence the behavior of FRC members, the difference between FRC and high performance fiber reinforced composites (HPFRC), and the failure mechanisms for reinforced concrete and FRC members are discussed. The existing shear and flexural strength prediction methods for FRC members are also presented in this chapter. The construction of a detailed database of experimental results to be utilized in the development of an analytical model to predict the behavior of fiber reinforced composite beams is discussed in Chapter 3 and the resulting database is presented. Chapter 4 gives detailed information on the proposed shear and flexural strengths and the comparison of the predicted values with existing equations. The development of a nonlinear model for fiber reinforced composite coupling beams and the comparison of analytical results with the experimental ones are presented in Chapter 5. The thesis is finalized with Chapter 6, in which a general summary, conclusions drawn from the results of the analytical study and recommendations for future research are provided.

# CHAPTER 2

# LITERATURE REVIEW

Fiber reinforced composites (FRC) contain short discrete fibers that are uniformly distributed and randomly oriented. The properties of fiber-reinforced composites vary based on fiber characteristics such as geometry, distribution, orientation, and volume fraction. The addition of fibers to the mix especially influences the behavior of shear critical members such as deep beams, since this increases both the tensile and shear strengths of the composite. The experimental and analytical investigations on the behavior of FRC deep beams along with the material properties are discussed in this chapter.

## 2.1. Mechanical Properties of FRC

Fiber reinforced composite (FRC) is a material composed of cement, water, and randomly distributed short fibers. When aggregates are added to the mix, the term fiber reinforced concrete can be used. Fibers are small discrete reinforcing materials that have various shapes and sizes, which are produced from various materials like steel, plastic, glass, carbon and natural materials such as sisal, bamboo and jute (ACI Committee 440, 1997). The first known example of the use of fibers as reinforcement is the use of horsehair and straw to strengthen bricks. The type, properties and the amount of fibers used in the mixture significantly affect the mechanical properties of concrete. Prior experimental research illustrated that the use of fibers improves flexural, compressive and tensile strength, ductility, energy dissipation capacity, impact resistance and toughness of concrete (Kurtz and Balaguru, 2000; Luo et al., 2000; Puertas et al., 2003).

### 2.1.1. Definition of FRC and HPFRC

Based on the tensile behavior, fiber reinforced composites can be classified into two groups as fiber reinforced composites (FRC) and high performance fiber reinforced composites (HPFRC) (Shah et al.,1999). The main difference between the two is the behavior of the members after the formation of the first crack. Members made up of FRC have strain-softening response and the ones built with HPFRC have strain-hardening response (Fig. 2.1) (Naaman and Reinhardt, 2006). Strain-hardening response is preferred in seismic design, since this will provide multiple cracking with significant increase in both ductility and energy dissipation capacity of the structural member.

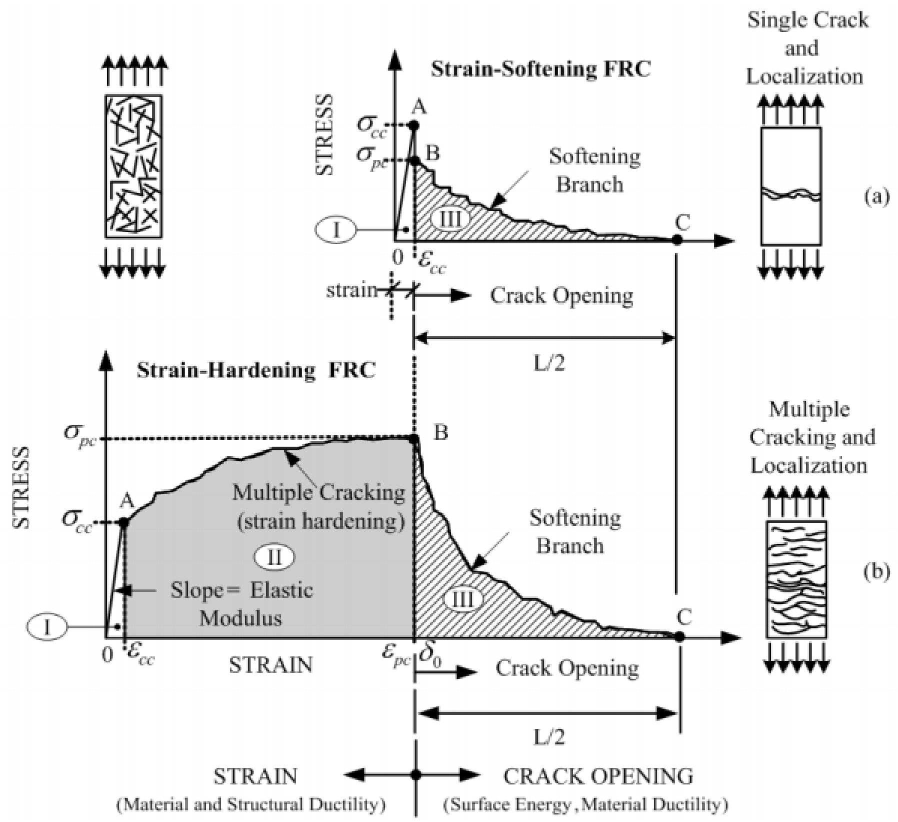


*Figure 2.1.* Tensile stress-strain relationship for FRC and HPFRC members (Naaman and Reinhardt, 1996).

#### 2.1.1.1. Cracking Tensile Strength and Post-Cracking Tensile Strength

FRC members exhibit strain-softening response in which the maximum post-cracking strength ($\sigma_{pc}$) is smaller than the tensile strength of the composite at first cracking ($\sigma_{cc}$). However, for HPFRC members, the strength continues to increase after reaching $\sigma_{cc}$ and multiple cracking can be observed up to the post-cracking strength, which is always higher than the cracking strength (Naaman, 2007).

Many analytical studies have been conducted to determine the cracking and post-cracking strengths of composites and formulations have been derived since the early seventies (Naaman, 1972; Naaman, 1974; Naaman, 1987; Naaman and Reinhardt, 1995).

Naaman and Reinhardt (1996) proposed the following equations to calculate the cracking and post-cracking tensile strengths:

$$\sigma_{cc} = \sigma_{mu}\left(1 - V_f\right) + \frac{\alpha_1\,\alpha_2\,\tau\,V_f\,L}{d}\,(MPa) \qquad (2-1)$$

where, $\sigma_{mu}$ :tensile strength of the matrix,

$V_f$ : volume fraction of fibers,

$\alpha_1$ : coefficient representing the fraction of bond mobilized at first matrix cracking,

$\alpha_2$ : efficiency factor of fiber orientation in the uncracked state of the composite,

$\tau$ : average bond strength at the fiber matrix interface,

$L$ : fiber length,

$d$ : fiber diameter,

$L/d$ : fiber aspect ratio.

$$\sigma_{pc} = \lambda_{pc}\, V_f (L/d)\, \tau \qquad (MPa) \tag{2-2}$$

where, $\lambda_{pc} = \lambda_1\, \lambda_2\, \lambda_3$ $(2-3)$

$$\lambda_2 = 4\, \alpha_2\, \lambda_4\, \lambda_5 \tag{2-4}$$

$\lambda_1$ : expected pull-out length ratio,

$\lambda_2$ : efficiency factor of fiber orientation in the cracked state of the composite,

$\lambda_3$ : group reduction factor depending on the number of fibers in the unit area,

$\lambda_4$ : reduction factor to consider the pulley effect,

$\lambda_5$ : reduction in pull-out response, when fiber orientation angle is greater than $60^0$.

The composite can be classified as high performance fiber reinforced composite, which has a ductile strain hardening behavior, if the post-cracking strength is more than the cracking strength.

#### 2.1.1.2. Critical Fiber Volume Fraction

The required volumetric ratio of the fibers required to ensure that the post-cracking strength is higher than the cracking strength is referred to as the critical fiber volume fraction, $(V_f)_{cri}$ (Fig. 2.2). If the composite has more than the critical volume fraction of fibers, strain hardening response with multiple cracking will be observed (Naaman and Reinhardt, 1995). Naaman and Reinhardt (1995) recommended Eqn. (2.5) to obtain critical value of the volume fraction of reinforcement. It can be concluded from this equation that if the fiber aspect ratio, $L/d$, or the ratio of average bond strength at the fiber matrix interface to cracking strength of the matrix, $\tau/\sigma_{mu}$, increases, the critical volume fraction decreases. This will result in obtaining higher performance from the composite with lower amount of fibers.

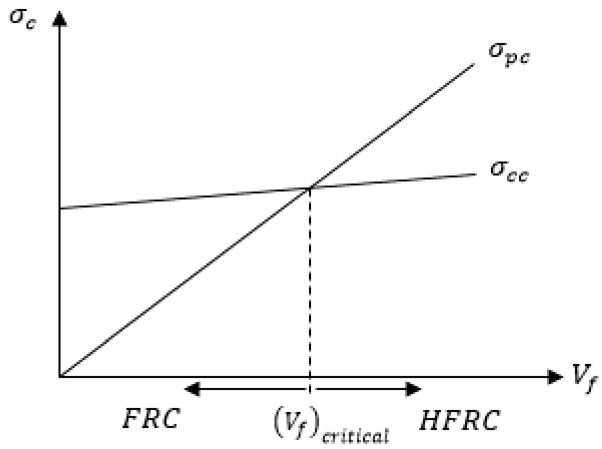


*Figure 2.2*. Critical fiber volume fraction (Hull and Clyne, 1996)

$$V_f \geq \left(V_f\right)_{cri} = \frac{1}{1+\frac{\tau}{\sigma_{mu}d}\frac{L}{(\lambda_1\,\lambda_2\,\lambda_3-\alpha_1\,\alpha_2)}} \qquad (2-5)$$

where, $V_f$ : volume fraction of fibers,

$\left(V_f\right)_{cri}$ : critical volume fraction of fibers,

$\tau$ : average bond strength at the fiber matrix interface,

$\sigma_{mu}$ : tensile strength of the matrix,

$L/d$ : fiber aspect ratio,

$\lambda_1$ : expected pull-out length ratio,

$\lambda_2$ : efficiency factor of fiber orientation in the cracked state of the composite,

$\lambda_3$ : group reduction factor depending on the number of fibers in the unit area,

$\alpha_1$ : coefficient representing the fraction of bond mobilized at first matrix cracking,

$\alpha_2$ : efficiency factor of fiber orientation in the uncracked state of the composite.

## 2.2. Main Parameters Affecting the Shear Capacity of FRC Beams

Numerous experimental studies were conducted to investigate the factors that affect the shear capacity of FRC beams. Based on the results of these experimental studies, the key factors that are explained in detail below, can be listed as: fiber pull-out stress, concrete compressive strength, beam reinforcement ratio, cross-sectional dimensions and length of the beam and shear span-to-depth ratio.

### 2.2.1. Fiber Pull-Out Strength

Pull-out test is used to identify the characteristic bond stress of the fiber matrix interface (Guerrero, 1999). The bond between fibers and the matrix significantly influences the tensile, shear and bending capacities of fiber reinforced composites. A theoretical model was developed by Wang et al. (1987) to calculate the cracking stress based on the load applied to synthetic FRC. At the same year, Shah and Jenq (1987) studied the bond properties by conducting an investigation on pullout test results and Gopalaratnam and Cheng (1987) formulated the pull-out problem in one dimension by assuming that the fiber and matrix both behave elastically. Then, Naaman et al. (1989) examined the pull-out stress considering bond shear stress versus slip relationship. The pull-out strength of fiber reinforced composites is influenced mainly by fiber type and shape, fiber aspect ratio ($l_f/d_f$), fiber-matrix interface bond stress($\tau$), and volumetric ratio of fibers ($V_f$).

Bond strength, $\tau$, is the most difficult parameter to determine and usually assumed to be constant. However, it directly influences the cracking and post-cracking strengths, toughness, ductility and energy absorption capacity of the composite (Naaman, 2003); therefore, choosing an appropriate value for the bond strength is crucial in defining the cracking and post-cracking behavior.

$l_f/d_f$ ratio is another important parameter to be considered in obtaining the composite strength. Naaman et al. (1989) stated that when all other properties kept the same, higher cracking strength is obtained with lower fiber aspect ratio, since shorter fibers exhibit more homogeneous bond shear stress distributions at the fiber-matrix interface. The force transmission between the fiber and the matrix is a result of the shear stress at the interface between the fiber and the surrounding matrix (Naaman et al., 1991). Moreover, the selected $l_f/d_f$ ratio affects workability and placement of composites (ACI 544.3R, 1997).

$V_f$ is one of the most effective parameters in determining the shear strength of FRC members. Majdzadeh et al. (2006) recommended 1% volumetric ratio of fiber reinforcement as the optimum value and stated that no improvement was observed in the behavior, if more than this percentage of fibers were used. In addition, Dinh et al. (2010) stated that up to 0.75% volume fraction, fibers were effective in increasing the shear strength, whereas when this ratio was more than 1%, the contribution of fibers had not further improved the capacity.

### 2.2.2. Concrete Compressive Strength

The effect of concrete compressive strength on the shear resistance has been studied by many researchers for beams with and without transverse reinforcement. First known studies on the failure mechanism of reinforced concrete beams without transverse reinforcement were conducted by Ritter (1899). Then, Moody et al. (1954) tested 42 simply supported reinforced concrete beams and determined that longitudinal reinforcement ratio, concrete compressive strength, and shear span-to-depth ratio influenced the shear strength of simply supported beams.

Mansur et al. (1986) stated that the shear capacity of FRC members depend on compressive strength of the matrix as much as the fiber properties. Moreover, Imam et al. (1994) observed that as the compressive strength of steel fiber reinforced composites (SFRCs) increased, the load carrying capacity and ultimate shear strength of the members also improved.

### 2.2.3. Transverse and Longitudinal Reinforcement Ratios

The amount of transverse reinforcement in a member could change the failure mode from brittle shear failure to more ductile flexural failure, while increasing the ultimate shear strength. When shear forces are applied to a beam, inclined shear cracks are formed and splitting cracks may be observed along the longitudinal reinforcement. However, to increase the shear capacity and modify the mode of failure, extensive transverse reinforcement may be required, which will result in problems with reinforcement congestion. Therefore, to relax the reinforcement detailing of stirrups, randomly distributed discrete fibers have been used as transverse reinforcement in fiber reinforced composites.

Batson et al. (1972) investigated the effect of different types of steel fibers with varying volumetric ratios and observed that the required shear capacity could be obtained with the use of fibers. Moreover, Swamy and Bahia (1985) observed that fibers behaved just like stirrups due to dowel action and controlled the crack formation. Greenough and Nehdi (2008) claimed that the minimum shear reinforcement ratio required by ACI 318-05 can be provided by using steel fibers. Similar findings were also observed by Dinh et al. (2010), which was accepted by the ACI Committee 318 in 2008. Kwak et al. (2002), Cuchiara et al. (2004), and Ding et al. (2011) believed that instead of using just fibers as transverse reinforcement, the use of transverse reinforcement with steel fibers was more effective in improving the shear capacity of members.

Longitudinal reinforcement ratio has also an important factor effect on the shear behavior of FRC beams. Crack width and length depend on the amount of longitudinal reinforcement. Swamy and Bahia (1985) stated that tension reinforcement ratios up to 1.95% increased the shear strength of FRC beams, and after that limit, its contribution diminished.

### 2.2.4. Shear Span-to-Depth Ratio

It is a well known fact that shear span-to-depth ratio, $a/d$, affects the behavior and strength of reinforced concrete beams. Shear span can be defined as the maximum moment divided by the maximum shear $(M/V)$. Shear span-to-depth ratio affects the crack inclination and mode of failure. Based on ACI 318-14 code provisions, beams with a shear span-to-depth ratio less than 2 should be considered as deep beams, for which the shear failure is more critical. However, beams could be classified into four categories based on the shear span-to-depth ratio as: very short, short, slender and very slender beams, which will have different failure modes (Fig. 2.3).

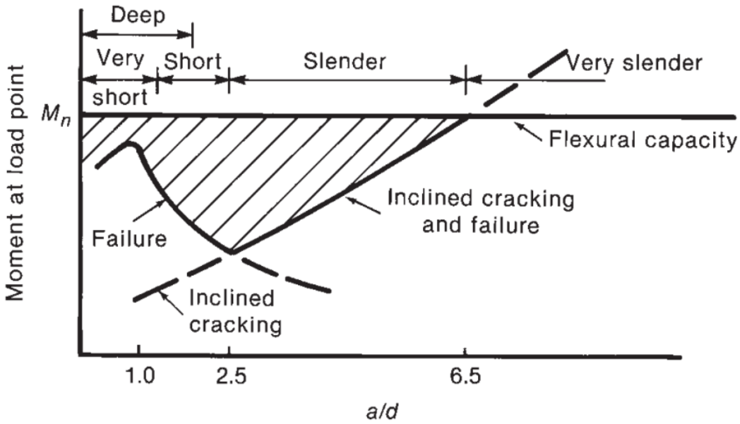


*Figure 2.3.* Moment capacity based on $a/d$ ratio (Wight and MacGregor, 2016)

## 2.3. Deep Beams

Reinforced concrete deep beams are commonly used in a wide range of different structures, from tall buildings to offshore structures (Sanad and Saka, 2001). In order for a beam to be classified as a deep beam, the American Concrete Institute Building Code Requirements for Structural Concrete and Commentary (ACI-318, 2014) requires that:

$$l_n \leq 4h \quad or \quad \frac{a}{h} \leq 2 \qquad (2-6)$$

where, $l_n$ : clear span length of member,

$h$ : overall member depth,

$a/h$ : shear span-to-overall depth ratio.

One of the most common shear failure types is the diagonal tension failure, because plain concrete is weak under tension. The tensile strength of concrete is almost only 10% of its compressive strength. Therefore, to increase the shear strength and reduce the brittleness of deep beams, it is necessary to increase the longitudinal and transverse reinforcement ratios or use fiber reinforced composites. Due to the reinforcement congestion in these beams, the use of randomly distributed discrete short fibers gets more widespread with time.

Narayanan and Darwish (1989) tested 12 steel fiber reinforced composite (SFRC) deep beams with varying fiber volumetric ratios, shear span-to-depth ratios, and concrete compressive strengths and observed that the shear strength was improved by the addition of fibers. Mansur et al. (1991) and Li et al. (1992) stated that including discrete fibers in the matrix significantly improved the shear strength and deformation capacity of deep beams. Champione (2012) compared the behavior of reinforced concrete and hooked-end steel fiber reinforced composite beams and confirmed that using SFRC increased the shear strength and ductility.

### 2.3.1. Coupling Beams

Window and door openings divide the reinforced concrete walls into two or more segments connected by deep and short beams, which are called coupling beams. The strength, stiffness, and energy dissipation capacity of coupling beams have crucial influence on the behavior of coupled walls under seismic loading. During an earthquake, the primary function of the coupling beam is to enable the load transfer between two shear wall segments. The deformed shape of a coupled wall system subjected to earthquake loading is given in Fig. 2.4. Prior studies have shown that well-designed coupling beams develop plastic hinges over the height of the building which results in high energy dissipation capacity (Shui et al., 1981; Aristizabal and Ochoa, 1982).

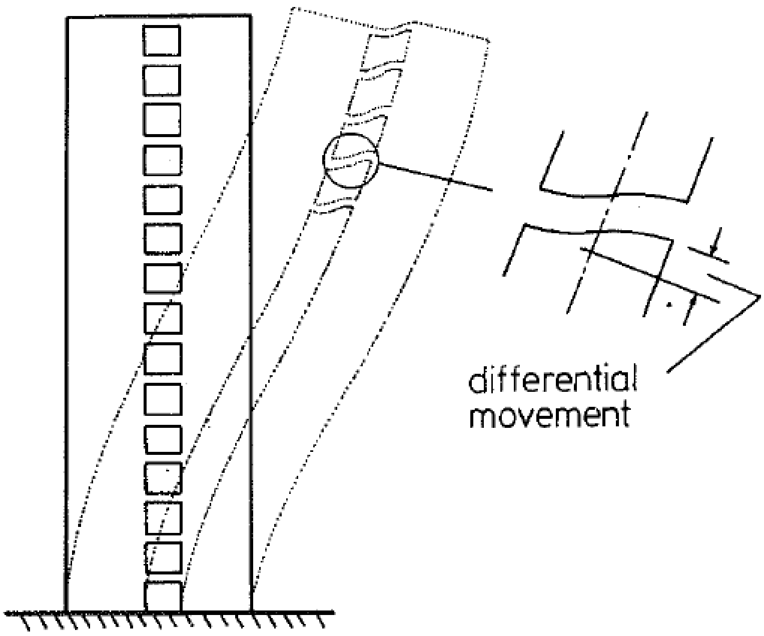


*Figure 2.4.* Differential movement of coupling beam (Subedi, 1991)

Experimental studies of Paulay (1971) showed that conventionally reinforced coupling beams behaved deficiently under large load reversals. Paulay and Biney (1974) then recommended the use of diagonally reinforced coupling beams. Currently, ACI 318-14also requires diagonal reinforcement detailing for coupling beams, which delays failure due to diagonal tension failure (Fig. 2.5). Barney et al. (1978), Tassios et al. (1996), Galano and Vignoli (2000) also investigated the effect of diagonal reinforcement on the shear capacity and observed that this type of detailing improves ductility, stiffness retention and energy dissipation capacities of coupling beams.

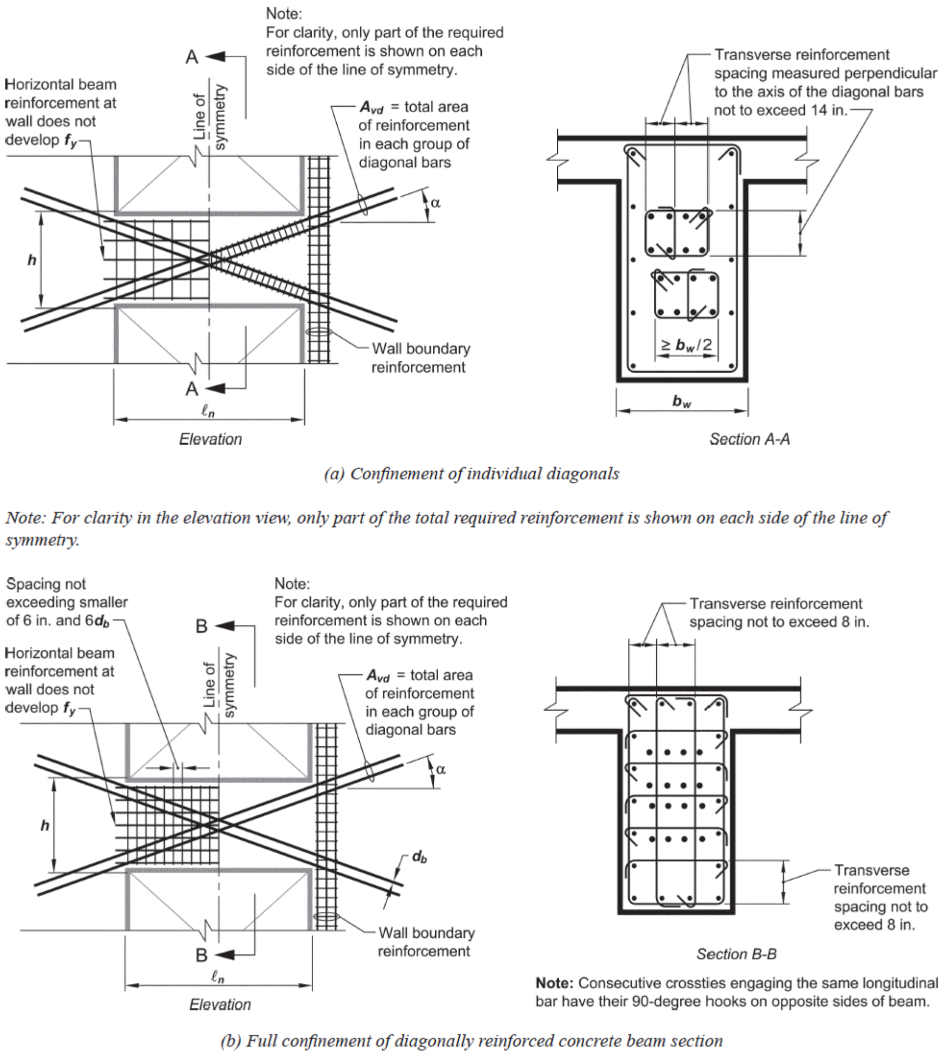


*Figure 2.5.* Reinforcement detailing of diagonally reinforced coupling beams (ACI 318-14)

However, construction of coupling beams becomes quite demanding with the use of this complex reinforcement detailing. Recent experimental research proved that the use of fiber reinforced composites also improved the shear strength, ductility, stiffness retention and energy dissipation capacities of coupling beams, while relaxing the detailing requirements (Canbolat et al., 2005; Lequesne, 2011; Setkit, 2012; Parra-Montesinos et al., 2017).

### 2.4. Shear Failure Mechanisms

First, the behavior of plain concrete beams will be discussed in this section, which will be helpful in understanding the different possible shear failure modes. Although the shear strength of a concrete beam is relatively high, its tensile strength is very low. Moreover, commonly the beams will not only be under pure shear but also flexural loads.

For the simply supported prismatic plain concrete beam presented in Fig. 2.6 under concentrated load, an equilibrium equation can be written that shows the relationship between the moment and shear in the shear span of the beam:

$$M = V\,x\,,\ x \leq a \qquad (2-7)$$

where, $V$ : applied shear,

$x$ : distance of any selected section between the support and the point of application of the concentrated load from the support,

$a$ : shear span.

From the beam theory, flexural and shear stresses can be calculated by using the following equations:

$$f(x) = \sigma(x) = \frac{M\,y}{I} \qquad (2-8)$$

where, $f(x)\ or\ \sigma(x)$ : flexural stress at any point on the section located at a distance y away from the neutral axis,

$y$ : distance from the neutral axis,

$I$ : moment of inertia of the section about the neutral axis.

$$\tau = \frac{V\,Q}{I\,b} \qquad (2-9)$$

where, τ : shear stress at any point on the section located at a distance y away from the neutral axis,

$Q$ : first moment of area about the neutral axis of the section at a distance located $y$ away from the neutral axis,

$b$ : beam width,

$I$ : moment of inertia.

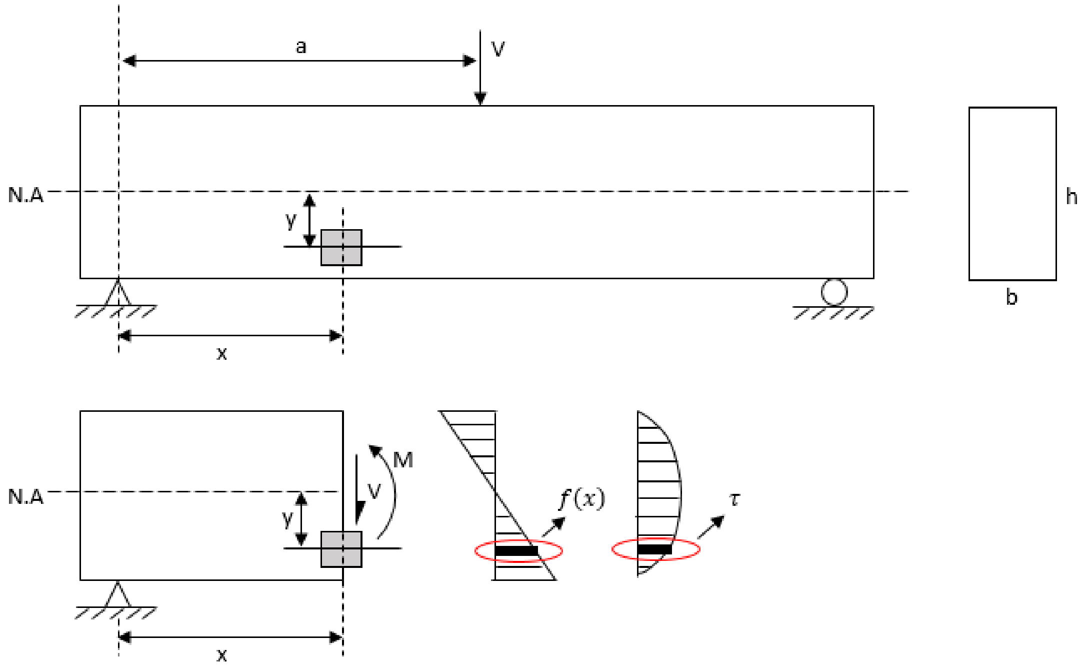


*Figure 2.6.* Shear and flexural stresses for plain concrete beam subjected to a concentrated load.

Longitudinal reinforcement in the beam (Fig. 2.6) transfers the shear stresses in the cracking zone by the dowel action and controls the crack propagation. The typical cracking pattern for a simply supported beam is shown in Fig. 2.7. First, vertical cracks due to flexural stresses start to form at the bottom of the member, where the flexural stresses are higher. Secondly, diagonal tension cracks start to appear near the support due to combined shear and flexure. Then, the cracks get wider and shear failure is observed. After the formation of the shear crack, longitudinal reinforcement carries the shear force together with concrete under compression at any section. The contribution of the longitudinal reinforcement is called the dowel action.

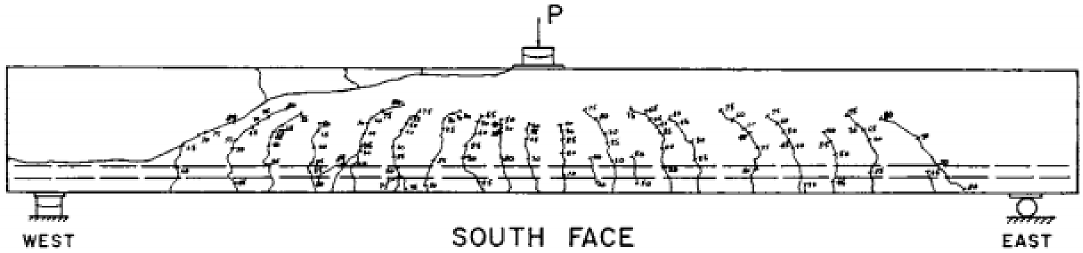


*Figure 2.7.* Typical crack pattern for a simply-supported reinforced concrete beam (Bresler and Scordelis, 1963)

The behavior of a beam under shear loading is mainly related to the shear span-to-depth ratio $(a/d)$, where $a$ is the shear span, and $d$ is the effective depth of the beam. This ratio is a dimensionless quantity and is important in determining the failure mode and shear strength of reinforced concrete beams. Deep beams have low $a/d$ ratios, which make them shear critical. Researchers set different limitations for the $a/d$ ratios to differentiate deep and slender beams, but, mostly this limit is accepted to be 2 or 2.5.

Beams can be classified into four categories: very short, short, slender, and very slender beams (Fig. 2.3). Very short beams, with $a/d$ ratios between 0 and 1, develop inclined cracks between the applied load and the support. The most common mode of failure in such a beam is an anchorage failure at the ends of the tension tie. Short beams with $a/d$ ratios ranging from1 to 2.5 develop inclined cracks and, after a redistribution of internal forces, are able to carry additional load, in part by arch action. The final failure of such beams is caused by a bond failure, a splitting failure, or a dowel failure along the tension reinforcement, or by crushing of the compression zone. The latter is referred to as the shear compression failure. Because the inclined crack generally extends higher into the beam than does a flexural crack, failure occurs at a moment lower than the flexural capacity. In slender beams, those having $a/d$ ratios from 2.5 to 6.5, the inclined cracks disrupt equilibrium to such an extent that the beam fails under diagonal tension failure and with the formation of an inclined crack. For very slender beams, with $a/d$ ratios greater than 6.5, the mode of failure changes from shear to flexural.

The shear strength of a beam with no transverse reinforcement is lower than its flexural strength due to formation of the principal tensile crack. Since concrete is a brittle material, cracking occurs even at small strain levels and the use of transverse reinforcement cannot prevent crack formation. The purpose of placing stirrups is to transfer tensile stresses between concrete surfaces throughout the diagonal crack and control the crack width.

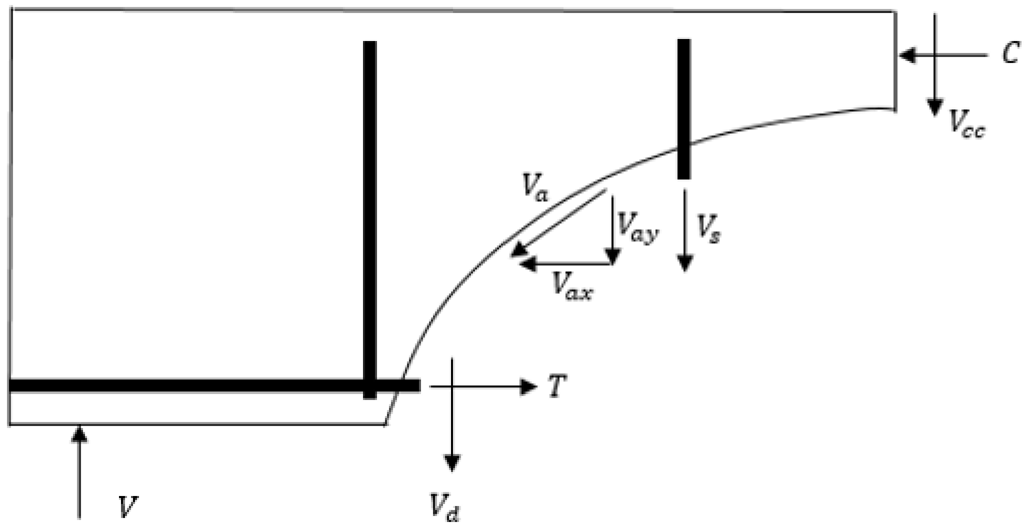


*Figure 2.8.* Shear resisting forces in a beam with transverse reinforcement

In a cracked beam, shear force is resisted by $V_{cc}$ , $V_{ay}$ , $V_s$, and $V_d$ as presented in Fig. 2.8. $V_{cc}$ is the shear carried by concrete under compression, $V_{ay}$ is the vertical component of the aggregate interlock, $V_s$ is the shear force resisted by transverse reinforcement, and $V_d$ is the shear force carried by the longitudinal reinforcement due to dowel action. Therefore, the total shear strength turns out to be:

$$V = V_{cc} + V_{ay} + V_d + V_s \qquad (2-10)$$

In design, $V_{cc}$ , $V_{ay}$ , and $V_d$ are lumped together as $V_c$ and considered to be the shear carried by concrete. Thus, the nominal shear strength, $V_n$ , can be considered as:

$$V_n = V_c + V_s \qquad (2-11)$$

In this equation, $V_c$ is computed for only the section which is under compression. If discrete fibers are placed in the concrete mixture, they will not only act as shear reinforcement, but also transfer the tensile stresses within the cracked region. The contribution of the cracked region and the increase in the tensile strength and strain capacity of reinforced concrete due to the addition of fibers will significantly increase the shear strength of the member. Since the distributed fibers minimize the crack width and delay the shear failure, new cracks are formed, which leads to multiple cracking and higher energy dissipation capacity.

### 2.5. Shear Strength of FRC Beams

Numerous analytical equations were proposed to predict the shear strength of fiber reinforced composite deep beams, which were based on the test results obtained from simply supported deep beams.

Sharma (1986) recommended an empirical equation to compute the nominal shear strength of deep and slender FRC beams obtained by examining the experimental results of 41 previously tested beams and got reasonable results. The formula is composed of two parts, fiber and transverse reinforcement contribution:

$$V_{nf} = V_{cf} + V_s \qquad (2-12)$$

where, $V_{nf}$ : nominal shear strength of the FRC beam,

$V_{cf}$ : shear strength of fibrous concrete,

$V_s$ : shear strength provided by the web reinforcement.

In Eqn. (2.12), the shear strength provided by the web reinforcement is computed following the requirements of ACI-318-83 (1983) as follows:

$$V_s = \frac{A_v f_y d}{s} \qquad (2-13)$$

where, $A_v$ : cross sectional area of the transverse reinforcement,

$f_y$ : yield strength of transverse reinforcement,

$d$ : effective depth,

$s$ : stirrup spacing.

The contribution of the fibrous concrete to the shear strength is given as:

$$V_{cf} = k\, f_t'(d/a)^{0.25} \qquad (2-14)$$

where, $d/a$ : effective depth-to-shear span ratio,

$f_t'$ : tensile strength of concrete obtained from results of indirect tension tests on 150x300 mm. cylinders,

$k$ : constant taken equal to 2/3.

Mansur et al. (1986) predicted the ultimate strength of fibrous normal weight reinforced concrete beams without stirrups by considering equilibrium of forces in Fig. 2.9. The total shear force represented by $V$ was then obtained as:

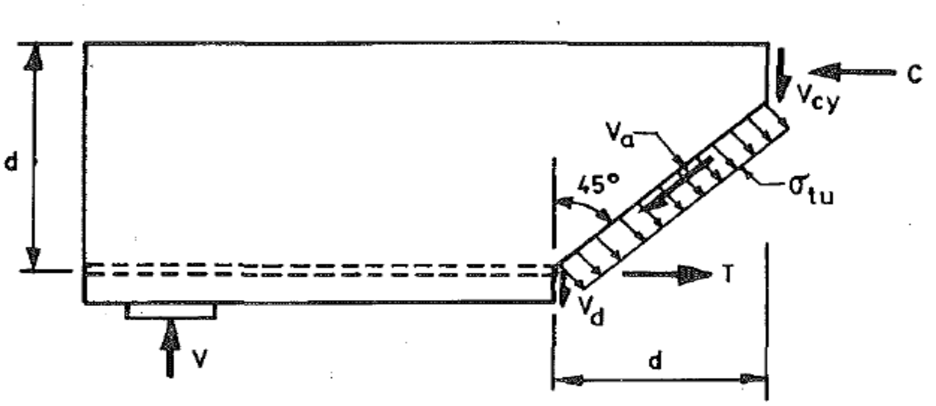


*Figure 2.9.* Forces through a diagonal crack of a FRC beam without transverse reinforcement (Mansur et al., 1986)

$$V_u = V_{cy} + V_{ay} + V_d + \sigma_{tu}\, b\, d \tag{2-15}$$

where, $V_{cy}$ : contribution of the concrete in the compression zone,

$V_{ay}$ : aggregate interlock action in the $y$ direction,

$V_d$ : dowel action of longitudinal bars,

$\sigma_{tu}$ : residual strength of fibrous concrete in tension,

$b$ : beam width,

$d$ : effective beam depth.

In this equation, it is hard to estimate the first three components ($V_{cy}$, $V_{ay}$, $V_d$) separately. Therefore, they are lumped and referred to as the cracking shear strength, $V_{cr}$.

$$V_u = V_{cr} + \sigma_{tu}\, b\, d \tag{2-16}$$

The following formula proposed for $V_{cr}$ by American Concrete Institute Committee, The Shear Strength of Reinforced Concrete Members (ACI-ASCE 426, 1973) was used as the cracking strength:

$$V_{cr} = \left(0.16\sqrt{f_c'} + 17.2\,\rho\,\frac{d}{a}\right) b\, d \tag{2-17}$$

The residual strength of FRC under tension was considered to be:

$$\sigma_{tu} = 0.41\left(\tau \ V_f \frac{L}{d}\right) \qquad (2-18)$$

The final proposed ultimate shear strength equation which is applicable to both fiber reinforced composite and reinforced concrete beams without any transverse reinforcement becomes:

$$v_u = \left(0.16\sqrt{f_c'} + 17.2\,\rho\,\frac{d}{a}\right) + 0.41\left(\tau\, V_f\,\frac{L}{d}\right) \qquad (2-19)$$

where, $V_{cr}$ : cracking shear strength,

$f_c'$ : concrete compressive strength,

$\rho$ : longitudinal reinforcement ratio,

$a/d$ : shear span-to-depth ratio,

$\tau$ : ultimate bond stress between fiber and matrix,

$V_f$ : fiber volume fraction,

$L/d$ : fiber aspect ratio.

$b$ : beam width,

$d$ : effective depth.

Narayanan and Darwish (1987) proposed two separate shear strength formulae for deep ($a/d \leq 2.8$) and slender beams ($a/d > 2.8$). The parameters used in these equations are fiber volume fraction ($V_f$) and fiber aspect ratio ($L/d$), concrete compressive strength ($f_{cuf}$), longitudinal reinforcement ratio ($\rho$), and shear span-to-depth ratio ($a/d$).

$$v_u = e\left[A' f_{ct} + B'\,\rho\,\frac{d}{a}\right] + v_b \qquad (2-20)$$

where, $e$ : nondimensional arch action factor and is given by:

$$e = \begin{cases} 1.0 \; for \;\; a/d > 2.8 \\ 2.8 \;\; d/a \;\; for \;\; a/d \leq 2.8 \end{cases}$$

$A'$ and $B'$: constants determined by the regression analysis of 91 tests as:

$A'$= 0.24 and $B'$= 80 MPa .

$v_b$ : fiber pull-out stress, $v_b = 0.41 \frac{L}{d} \rho \tau$ , where the bond stress, $\tau$ is considered to be 4.15 MPa.

$f_{ct}$ : strength related to cube compressive strength, $f_{cuf}$ as:

$$f_{ct} = \frac{f_{cuf}}{20 - \sqrt{V_f \frac{L}{d} \beta}} + 0.7 + \sqrt{V_f \; \frac{L}{d} \; \beta} (MPa) \qquad (2-21)$$

$\beta$ : bond factor adopted from Narayanan et al (1984) and taken as 0.5 for round, 0.75 for crimped, and 1.0 for indented fibers.

Zsutty (1968) proposed an equation to predict the shear strength of reinforced concrete beams with no transverse reinforcement:

$$v_u = 60 \left( f_c' \; \rho \frac{d}{a} \right)^{\frac{1}{3}} \quad for \quad a/d \; \geq 2.5 \qquad (2-22)$$

$$v_u = 150 (f_c' \; \rho)^{1/3} \left( \frac{d}{a} \right)^{4/3} \quad for \quad a/d < 2.5 \qquad (2-23)$$

where, $v_u$ : ultimate shear strength,

$f_c'$ : concrete compressive strength,

$\rho$ : longitudinal reinforcement ratio,

$a/d$ : shear span-to-depth ratio.

Ashour et al. (1992) modified Zsutty's equation (1968) for predicting the shear strength of reinforced concrete, to fiber reinforced composites by utilizing the fiber factor, F. In this study the specimens were divided into two groups as slender ($a/d \geq$

2.5) and deep ($a/d < 2.5$) beams, considering a different limit of shear span-to-depth ratio. The proposed ultimate shear strength equations are given below:

For slender beams:

$$v_u = \left(2.11\sqrt[3]{f_c'} + 7\,F\right)\left(\rho\,\frac{d}{a}\right)^{0.333}\,(MPa) \qquad (2-24)$$

For deep beams:

$$v_u = \left(2.11\sqrt[3]{f_c'} + 7\,F\right)\left(\rho\,\frac{d}{a}\right)^{0.333}\frac{2.5}{a/d} + v_b\left(2.5 - \frac{a}{d}\right)(MPa) \qquad (2-25)$$

where, $F = \left(\frac{L_f}{D_f}\right) V_f\,d_f$ (2 − 26)

$L_f$ : fiber length,

$D_f$ : fiber diameter,

$V_f$ : fiber volume fraction,

$d_f$ : factor that accounts for varying bond characteristics of fibers taken equal to 0.5 for round fibers, 0.75 for crimped fibers, and 1.0 for indented fibers.

$v_b$ : fiber pull-out stress, $v_b = 0.41\tau F$ (2 − 27)

$\tau$ : ultimate bond stress between fiber and matrix and taken as 4.15 MPa.

Li et al. (1992) tested 252 mortar and 60 reinforced concrete beams that have steel, acrylic, aramid and high-strength polyethylene fibers with various reinforcement detailing and shear span-to-depth ratios. The equations of Zsutty (1968) for plain concrete members are also modified in this study for slender ($a/d \geq 2.5$) and deep ($a/d < 2.5$) beams as:

For slender beams:

$$v_u = \alpha + \beta \left[ \left(f_f f_t\right)^{3/4} \left(\rho \frac{d}{a}\right)^{1/3} (d)^{-1/3} \right] \qquad (2-28)$$

For deep beams:

$$v_u = 9.16 \left[ \left(f_f\right)^{2/3} (\rho)^{1/3} \left(\frac{d}{a}\right) \right] \qquad (2-29)$$

where, $\alpha = 0.53$ for mortar and $\alpha = 1.25$ for reinforced concrete beams,

$\beta = 5.47$ for mortar and $\beta = 4.68$ for reinforced concrete beams,

$f_f$ : flexural strength of the composite,

$f_t$ : splitting strength of the mortar or concrete,

$\rho$ : longitudinal reinforcement ratio,

$d$ : effective depth,

$a$ : shear span length.

Khuntia et al. (1999) also predicted the ultimate shear strength of FRC beams without any transverse reinforcement as:

$$v_u = (0.167\, \alpha + 0.25\, F)\sqrt{f_c'}(MPa) \qquad (2-30)$$

where, $\alpha$ : arch action factor, $\alpha = \begin{cases} 1, \text{when } a/d \geq 2.5 \\ 2.5\ d/a \leq 3, \text{when } a/d < 2.5 \end{cases}$,

$F$ : fiber factor taken as $F = V_f\ (L/d)$.

Kwak et al. (2002) also proposed a shear prediction equation in the form of the recommendation by Zsutty (1967):

$$v_u = 3.7\, e\, \left(f_{spcf}\right)^{2/3} \left(\rho\, \frac{d}{a}\right)^{1/3} + 0.8\, v_b \qquad (2-31)$$

where, $v_b$ : fiber pull-out strength given in Eqn. (2-27),

$$f_{spcf} = \frac{f_{cuf}}{20-\sqrt{F}} + 0.7 + \sqrt{F}(MPa) \qquad (2-32)$$

where, $f_{spcf}$ : split-cylinder strength of fiber reinforced composite,

$f_{cuf}$ : cube compressive strength of concrete,

$F$ : fiber factor computed by Eqn. (2-26),

$$e = \begin{cases} 1.0 \text{ for } a/d > 3.4 \\ 3.4\, d/a \text{ for } a/d < 3.4 \end{cases}.$$

Shahnevaz and Alam (2014) also developed two separate equations for deep $(a/d \leq 2.8)$ and slender beams $(a/d > 2.8)$ given below by performing parametric analysis on 358 prior test results. Key parameters of these equations are shear span-to-depth ratio $(a/d)$, concrete compressive strength $(f_c')$, longitudinal reinforcement ratio $(\rho)$, fiber volumetric ratio $\left(V_f\right)$ and aspect ratio $\left(l_f/d_f\right)$ of fibers.

For slender beams:

$$\begin{aligned} V_u = {} & 0.205 + 0.072(f_c')^{0.85} + 12.52\rho^{0.084} - 23.61(a/d)^{0.068} + 13.5V_f^{0.071} \\ & +456.7\left(l_f/d_f\right)^{-1.61} - 0.0002\left[(a/d)V_f\right]^{3.91} - 27.69\left[(a/d)\left(l_f/d_f\right)\right]^{-0.84} \\ & +1181\left[\left(l_f/d_f\right)V_f\right]^{-2.69} - 21.89\left[(a/d)V_f\left(l_f/d_f\right)\right]^{-0.9} \end{aligned} \qquad (2-33)$$

For deep beams:

$$V_u = 0.2 + 0.034f_c' + 19\rho^{0.087} - 5.8(a/d)^{0.5} + 3.4V_f^{0.4} + 800\left(l_f/d_f\right)^{-1.6}$$
$$-12\left[(a/d)V_f\right]^{0.05} - 197\left[(a/d)\left(l_f/d_f\right)\right]^{-1.4} + 105\left[\left(l_f/d_f\right)V_f\right]^{-2.12} \quad (2-34)$$

### 2.5.2. Shear Strength of FRC Coupling Beams

The shear strength prediction equation by Canbolat (2004) takes into account the properties of fiber reinforced composite, diagonal and transverse reinforcement detailing, respectively:

$$V = \left(\sigma_{pc}\ b_w\ h\right) + \left(2\ A_{vd}\ f_{yd}\ sin\alpha\right) + \left(\frac{A_w\ f_{yw}\ d}{s}\right) \quad (2-35)$$

where, $\sigma_{pc}$ : post-cracking tensile strength of FRC,

$2\ A_{vd}$ : total area of diagonal reinforcement,

$f_{yd}$: tensile yield strength of diagonal reinforcing bar,

$\alpha$ : angle of inclination of diagonal reinforcement with relative to the beam longitudinal axis.

Lequesne (2011) developed an equation for the shear strength of coupling beams, which has the same considered parameters as in Canbolat's equation (2004):

$$V = \left(0.4\sqrt{f_c'}\ b_w\ d\right) + \left(2\ A_{vd} f_{yd}\ sin\alpha\right) + \left(\frac{A_w\ f_{yw}\ d}{s}\right) \quad (2-36)$$

## 2.6. Flexural Strength of FRC Beams

Obtaining an accurate flexural strength for FRC beams is as important as the prediction of shear strength in order to assess the failure mode of the member. A more ductile, flexural failure can be achieved even for short span FRC beams with increasing fiber reinforcement ratios. To perform sectional analysis of single reinforced steel fiber reinforced composite (SFRC) beams, Hanegar and Doherty (1976) recommended using the stress and strain distribution given in Fig. 2.10. As it can be observed from this figure, uniform stress distribution was considered in the tension zone and the contribution of fibers was added to the flexural capacity of the section while computing the ultimate moment capacity.

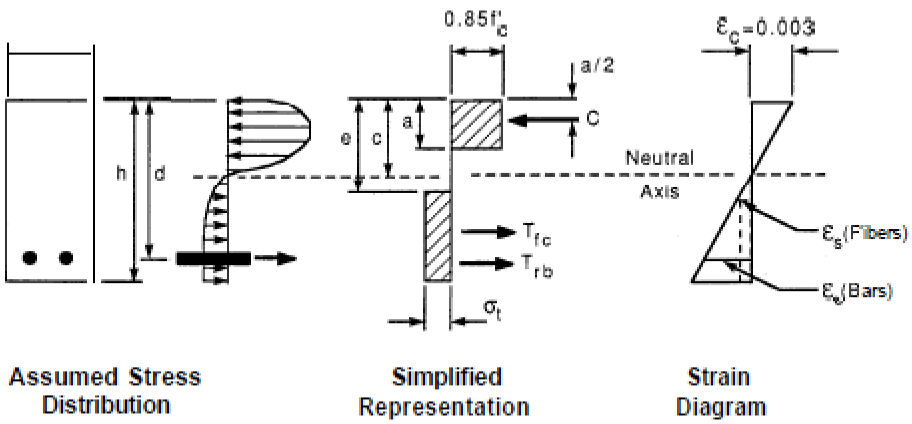


*Figure 2.10.* Stress and Strain Distributions for Single Reinforced SFRC Beams (Hanegar and Doherty, 1976)

The nominal moment capacity was then defined as:

$$M_n = A_s f_y \left(d - \frac{a}{2}\right) + \sigma_t\, b\, (h - e)\left(\frac{h}{2} + \frac{e}{2} - \frac{a}{2}\right) \qquad (2-37)$$

$$e = [\varepsilon_f + 0.003]\frac{c}{0.003} \qquad (2-38)$$

$$\sigma_t = 0.772\, \frac{l}{d_f} \rho_f\, F_{be} \qquad (2-39)$$

where, $\rho_f$ : volumetric ratio fibers,

$F_{be}$ : bond efficiency which varies from 1.0 to 1.2 depending on fiber characteristics,

$c$ : neutral axis depth,

$\varepsilon_s$ : tensile strain for steel bars $\varepsilon_s = f_y/E_s$,

$\varepsilon_f$ : tensile strain for fibers $\varepsilon_f = \sigma_f/E_s$,

$\sigma_t$ : tensile strength of FRC,

$T_{fc}$ : tensile force carried by the composite = $\sigma_t \, b \, (h - e)$,

$T_{rb}$ : tensile force carried by reinforcing bars = $A_s \, f_y$.

Imam et al. (1995) predicted the ultimate moment of steel fiber high-strength concrete beams without any transverse reinforcement as:

$$M_u = 0.6 \, b \, d^2 \, \psi \, \sqrt[3]{\omega} \left[ {f_c}'^{(0.44)} \left(\frac{a}{d}\right) + 275 \sqrt{\frac{\omega}{(a/d)^3}} \right] \qquad (2-40)$$

where, $\psi$ : size effect factor defined as $\psi = \left[1 + \sqrt{(5.08/d_a)}\right] / \sqrt{1 + d/(25 \, d_a)}$,

$d_a$ : maximum aggregate size,

$\omega$ : reinforcement factor,$\omega = \rho \, (1 + 4 \, F)$,

$\rho$ : longitudinal reinforcement ratio,

$F$ : fiber factor, $F = (L_f/D_f) \, V_f d_f$,

$d_f$ : efficiency factor, $d_f = \begin{cases} 1.0 \text{ for hooked fibers} \\ 0.9 \text{ for deformed fibers} \end{cases}$.

Casanova and Rossi (1997) defined the ultimate bending moment resistance of a section under a given axial load based on the ultimate limit crack opening considering stress-strain relationship given in Fig. 2.11.

$$M_u = \frac{1}{w_u - w_i} \int_{w_i}^{w_u} M(w) \, dw \qquad (2-41)$$

where, $M_u$ : ultimate bending moment resistance,

$w$ : crack width,

$w_i$ : initial crack width,

$w_u$ : ultimate crack width.

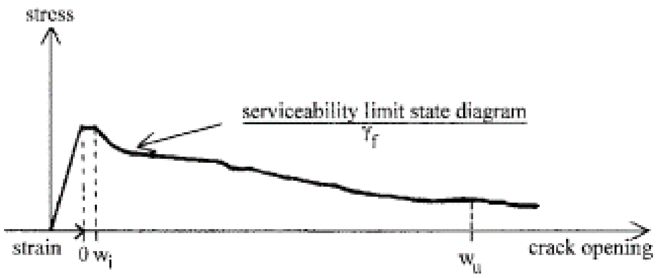


*Figure 2.11.* Characteristic stress-strain relationship (Casanova and Rossi, 1997)

Dinh et al. (2011) developed a model to predict the shear strength of steel FRC beams without transverse reinforcement:

$$V_n = V_{cc} + V_{FRC} \tag{2 – 42}$$

where, $V_{cc}$ : shear carried by concrete in the compression zone,

$$V_{cc} = 0.11\, f'_c\, \beta_1\, c\, b \tag{2 – 43}$$

$\beta_1 = 0.85$ for $f'_c \leq 27.6\ MPa$ and $\beta_1 = 0.65$ for $f'_c \geq 55.1\ MPa$.

Linear interpolation was used for values in between these two.

$b$ : beam width.

$c$ : neutral axis depth, $c = \dfrac{A_s\, f_y}{k_1\, k_3\, f'_c\, b}$ (2 – 44)

$A_s$ : area of tension reinforcement,

$f_y$ : yield strength of the tension reinforcement.

$k_1 k_3 = 0.85\, \beta_1$ (2 – 45)

$V_{FRC}$ : vertical component of the diagonal tension resistance provided by fibers,

$$V_{FRC} = (\sigma_t)_{avg}\, b\, (d - c)\, cotan(45) \qquad (2-46)$$

$(\sigma_t)_{avg}$ : average tensile stress, $(\sigma_t)_{avg} = \frac{2\, M}{(h-c)\, b\, h}$ $\quad (2-47)$

$M$ : moment at the cracked section,

$h$ : beam depth.

In this equation, the failure criterion proposed by Bresler and Pister (1958) (Fig. 2.12) was used to obtain $V_{cc}$.

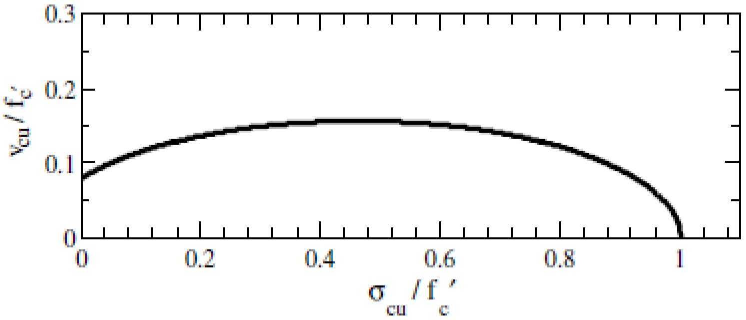


*Figure 2.12.* Bresler and Pister's failure criterion for concrete subjected to combined compression and shear stresses.

$$\frac{v_{cu}}{f'_c} = 0.1\, \left[0.62 + 7.86\left(\frac{\sigma_{cu}}{f'_c}\right) - 8.46\left(\frac{\sigma_{cu}}{f'_c}\right)^2\right]^{1/2} \qquad (2-48)$$

where, $v_{cu}$ : acting shear stress at failure,

$\sigma_{cu}$ : normal compressive stress at failure,

$f'_c$ : concrete compressive stress.

# CHAPTER 3

# DATABASE CONSTRUCTION

The seismic behavior of fiber reinforced composite (FRC) shear critical beams is affected by many different parameters related to structural and material properties. Therefore, accurately predicting the shear and flexural capacities and the mode of failure for such beams and coming up with design recommendations is a challenge. The construction of a detailed database of experimental results constitutes an essential step towards the development of an analytical model to predict the behavior of fiber reinforced composite beams under earthquake loading. A large variety of shear critical beam subassemblies having different geometric, material and loading characteristics are presented in the database, however, certain limitations are taken into consideration, in order not to lose the accuracy and applicability of the analytical model. In this chapter, a database of experimental studies for shear critical beams referred to as deep beams, for the subassemblies that were tested as simply supported members under concentrated point loading, and coupling beams that were built in between two reinforced concrete walls and tested with more realistic boundary conditions, was presented. The compiled database includes test results of 387 deep beams and 59 coupling beams obtained from 51 different prior experimental studies. In this chapter, selection criteria of the experiments are discussed and the resulting database including properties of the specimens and the experimental results is presented.

## 3.1. Selection Criteria and Properties of Specimens

Experimental studies on the behavior of fiber reinforced concrete deep and coupling beams are investigated and included in the database. Tests on continuous beams are not included, because there is insufficient data in the literature to verify if the developed model accurately predicts their behavior. Although all the beams investigated in this analytical study are shear critical deep beams, they are grouped into two based on the boundary conditions of the test setup and the loading schemes. The term deep beams is used while referring to the simply supported beams tested under monotonic loading. The term coupling beams is used to represent the subassemblies, which have two reinforced concrete wall segments on either side of the beam that were tested under cyclic loading. Moreover, the experimental studies on precast high-performance fiber reinforced concrete coupling beams are included in this investigation.

In the database, the shear span-to-depth and length-to-depth ratios of the beams are first tabulated. Then the geometrical properties of the beams, reinforcement ratios and the material properties are presented in the table. As for the geometric features; width, depth, and effective depth of members, longitudinal and transverse reinforcement detailing are considered. Furthermore, when the diagonal reinforcement and/or dowel bars were used, these details are also included in the database. The compressive strength of the composition the test date, the reinforcement yield strength, fiber types, volumetric ratios and aspect ratios are gathered as the material properties for all selected specimens.

The standard cylinder concrete compressive strength is considered in this database. Therefore, if the cube compressive strength was provided in the literature, it was multiplied by 0.8 to convert the value to the cylinder compressive strength.

If circular fibers were used in the specimens, the fiber diameter can be obtained directly. However, if the fiber has any other cross-sectional shape than a circle, the equivalent diameter should be used. For this purpose, a parameter defined as the fiber intrinsic efficiency ratio (FIER) proposed by Naaman (1998) is utilized:

$$FIER = \left(\frac{lateral\ surface\ area\ of\ the\ fiber}{fiber\ cross\ sectional\ area}\right) = \left(\frac{\psi\ l_f}{A}\right) \qquad (3-1)$$

where, $A$ : cross sectional area of the fiber,

$\psi$ : perimeter of the fiber cross section,

$l_f$ : fiber length. The embedded length of the fiber can be considered here or simply as the unit length can be taken when fibers are compared to one another.

The area, perimeter, equivalent diameter and FIER computations for fibers with common cross-sections are presented in Fig. 3.1.

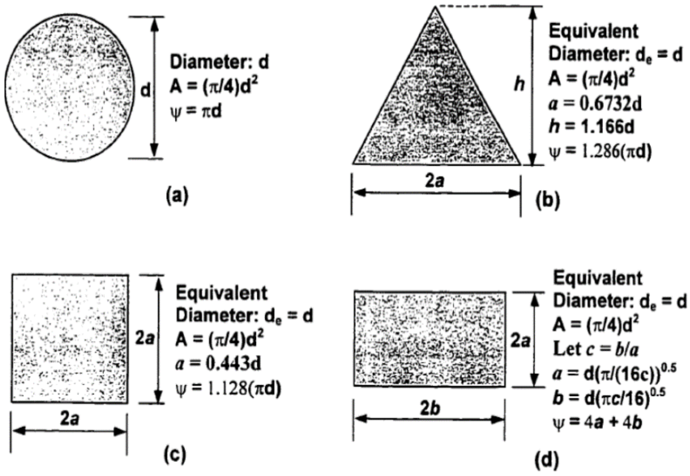


*Figure 3.1.* Equivalent cross-sections: a) circular, b) triangular, c) square, d) rectangular

Tensile reinforcement ratio ($\rho$) is computed as the area of reinforcing bars located in the tension zone divided by the effective concrete area, taken as beam width times the effective depth. A similar computation is performed to obtain the compression reinforcement ratio ($\rho'$) for the bars located in the compression zone.

Fiber types that were used in the tests included in the database are hooked-end, crimped, straight and torex steel fibers, polyvinyl alcohol (PVA) fibers, and polyethylene (PE) fibers (Fig. 3.2).

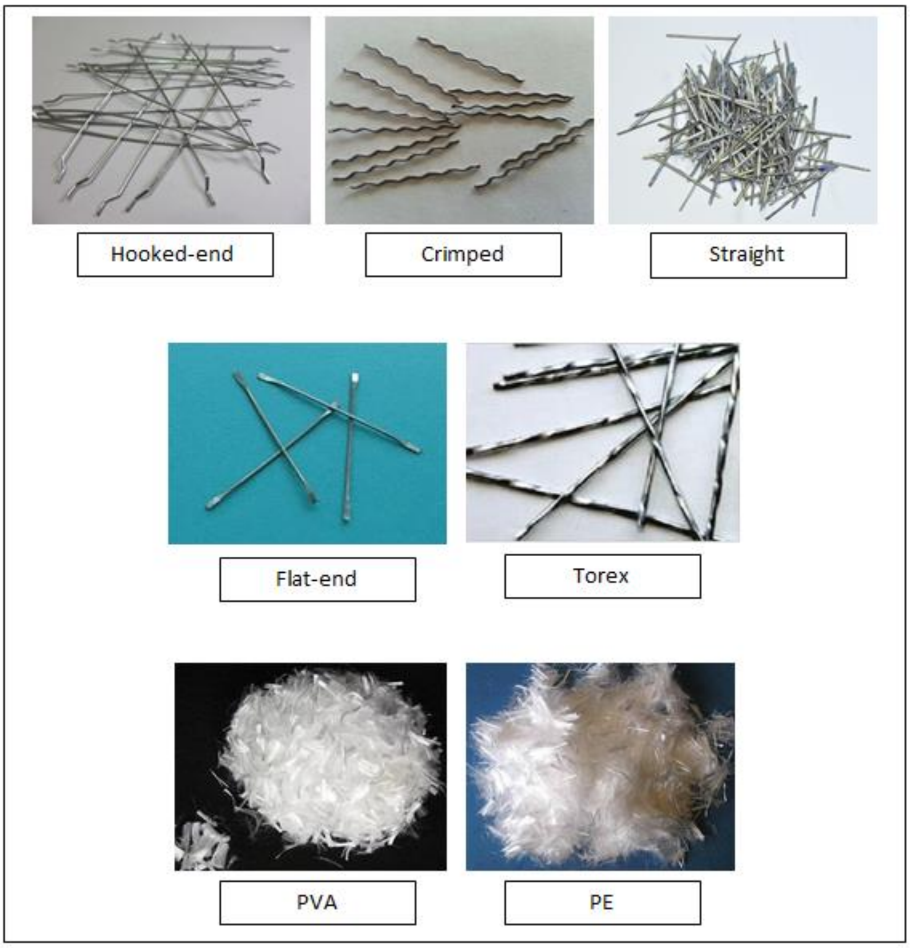


*Figure 3.2.* Fiber types included in the database

### 3.1.1. Selected Experiments

The database is basically divided into two main groups as deep and coupling beams based on support conditions and applied loads. The term deep beam is used, when the shear critical beams are loaded from the top monotonically with concentrated loads within twice the member depth from the support and simply supported at the bottom so that compression struts develop between the point loads and supports (Seo et al., 2004). On the other hand, the term coupling beam is used when the tested shear critical beam has two reinforced concrete wall segments on each end, which is a more realistic representation of the boundary conditions. During an earthquake, coupling beams enable the shear transfer between reinforced concrete walls, therefore, the strength, stiffness, and energy dissipation capacity of coupling beams have significant influence on the behavior of coupled wall systems. The fiber reinforced composite (FRC) properties are also taken into account while constructing the database.

Based on the tensile behavior, fiber reinforced composites can be classified into two groups as fiber reinforced composites (FRC) and high performance fiber reinforced composites (HPFRC) (Shah et al.,1999). The main difference between the two is the behavior of the members after the formation of the first crack. Members made up of FRC have strain-softening response and the ones built with HPFRC have strain-hardening response (Naaman and Reinhardt, 2006). Strain-hardening response is preferred in seismic design, since this will provide multiple cracking with significant increase in both ductility and energy dissipation capacity of the structural member. FRC members exhibit strain-softening response in which the maximum post cracking strength ($\sigma_{pc}$) is smaller than the tensile strength of the composite at first cracking ($\sigma_{cc}$). However, for HPFRC members, the strength continues to increase after reaching $\sigma_{cc}$ and multiple cracking can be observed up to the post-cracking strength, which is always higher than the cracking strength (Naaman, 2007).

#### 3.1.1.1. Deep Beams

In this analytical study, all members selected for the deep beam database are steel fiber reinforced composite (SFRC) beams. The database is divided into two parts based on the shear span-to-depth ratio ($a/d$). ASCE-ACI Committee 445 (1998) classifies beams into deep beams (when $a/d < 1.0$), short beams (when $1.0 < a/d < 2.5$), and ordinary shallow beams (when $a/d > 2.5$). The first part of the database with low shear span-to-depth ratios ($a/d \leq 2.5$) contains 125 test results on SFRC beams, while the second part with higher shear span-to-depth ratios ($a/d > 2.5$) has 262 data points. The parameters considered in the database include shear span-to-effective depth ratio ($a/d$), clear length-to-effective depth ratio ($l_n/d$), beam depth ($h$), effective beam depth ($d$), beam width ($b_w$), concrete compressive strength ($f'_c$), tension reinforcement ratio ($\rho$), yield strength of tension reinforcement ($f_y$), compression reinforcement ratio ($\rho'$), yield strength of compression reinforcement (${f'}_y$), transverse reinforcement ratio ($\rho_t$), yield strength of transverse reinforcement ($f_{yt}$), fiber type, aspect ratio of fibers ($l_f\ /d_f$), and fiber volumetric ratio ($V_f$). The range of all considered parameters are displayed for the specimens with and without transverse reinforcement in Table 3.1 and Table 3.2, respectively. The database includes both normal and high-strength composites. Although all the collected data for the deep beam specimens are for SFRC beams, several steel fiber types were used in the experiments such as hooked, crimped, straight, and flat-end steel fibers.

Table 3.1. *Parameters considered in the database for deep beams with transverse reinforcement*

| | Deep Beams ($a/d \leq 2.5$) | Deep Beams ($a/d > 2.5$) |
|---|---|---|
| Parameter | Range | Range |
| $a\ /\ d$ | 12 - 2.5 | 2.6 - 6.5 |
| $l_n\ /\ d$ | 4.3 - 14.4 | 8 - 14.4 |
| $h\ (mm)$ | 152.4 - 390 | 100 - 300 |
| $d\ (mm)$ | 127 - 340 | 85 - 262.5 |
| $b_w\ (mm)$ | 101.6 - 150 | 100 - 200 |
| $f_c'\ (MPa)$ | 39.8 - 62.3 | 24 - 56.24 |
| $V_f$ (%) | 0.5 - 2 | 0.22 - 2 |
| $l_f/d_f$ | 46.18 - 101.6 | 33.42 - 127.7 |
| $\rho$ (%) | 1.32 - 3.08 | 0.19 - 4.01 |
| $f_y(MPa)$ | 280 - 610 | 276 - 617 |
| $\rho'$(%) | 1.1 - 2.68 | 0.85 - 3.36 |
| $f_y'(MPa)$ | 278 - 661 | 276 - 565 |
| $\rho_t$ (%) | 0.18 - 3.04 | 0.13 - 3.04 |
| $f_{yt}(MPa)$ | 280 - 661 | 276 - 617 |
| $N^s$ | 18 | 99 |

$N^s$ = *Number of data points.*

Table 3.2. *Parameters considered in the database for deep beams without transverse reinforcement*

| | Deep Beams ($a/d \leq 2.5$) | Deep Beams ($a/d > 2.5$) |
|---|---|---|
| Parameter | Range | Range |
| $a\ /\ d$ | 0.8 - 2.5 | 2.75 - 6 |
| $l_n\ /\ d$ | 1.37 - 10.8 | 5.53 - 14.33 |
| $h\ (mm)$ | 127 - 375 | 100 - 1000 |
| $d\ (mm)$ | 102 - 340 | 85 - 923 |
| $b_w\ (mm)$ | 63.5 - 200 | 63.5 - 310 |
| $f_c'\ (MPa)$ | 22.7 -110 | 19.6 - 111.5 |
| $V_f$ (%) | 0.25 - 2 | 0.25 - 2 |
| $l_f/d_f$ | 28.5 - 100 | 28.5 - 100 |
| $\rho$ (%) | 0.37 - 4.58 | 0.37 - 4.58 |
| $f_y(MPa)$ | 343 - 610 | 350 - 610 |
| $\rho'$ (%) | 0.32 - 3.94 | 0.32 - 3.94 |
| $f'_y(MPa)$ | 0 - 417 | 0 - 590 |
| $N^s$ | 107 | 163 |

*$N^s$ = Number of data points.*

### 3.1.1.2 Coupling Beams

The database for coupling beams is divided into four parts based on the tensile behavior of the composites as FRC and HPFRC and whether the specimens had transverse reinforcement or not. The first set contained 29 test results on FRC coupling beams with transverse reinforcement and 8 test results on FRC coupling beams without transverse reinforcement. The second set contained 20 test results on HPFRC coupling beams with transverse reinforcement and 2 test results on HPFRC coupling beams without transverse reinforcement. The variables used in the experimental investigations include shear span-to-effective depth ratio ($a/d$), clear length-to-effective depth ratio ($l_n/d$), beam depth ($h$), effective depth ($d$), beam width ($b_w$), concrete compressive strength ($f'_c$), tension reinforcement ratio ($\rho$), yield strength of tension reinforcement ($f_y$), compression reinforcement ratio ($\rho'$), yield strength of compression reinforcement ($f'_y$), transverse reinforcement ratio ($\rho_t$), yield strength of transverse reinforcement ($f_{yt}$), diagonal reinforcement ratio ($\rho_d$), yield strength of diagonal reinforcement ($f_{yd}$), fiber type, aspect ratio of fibers ($l_f\ /d_f$), and fiber volumetric ratio ($V_f$). The range of all variables are displayed for beams with transverse reinforcement in Table 3.3 and without transverse reinforcement in Table

3.4. Several fiber types were used in the experiments such as hooked-end and torex steel fibers, polyvinyl alcohol (PVA) and polyethylene (PE) fibers.

Table 3.3. *Parameters considered in the database for coupling beams with transverse reinforcement*

| | FRC Coupling Beams | HPFRC Coupling Beams |
|---|---|---|
| Parameter | Range | Range |
| $l_n$ / $d$ | 1.1 - 3.9 | 1.1 - 4.2 |
| $h$ $(mm)$ | 300 - 457.2 | 300 - 609.6 |
| $d$ $(mm)$ | 260 - 412.7 | 250 - 571.5 |
| $b_w$ $(mm)$ | 100 - 152.4 | 150 -250 |
| $f_c'$ $(MPa)$ | 31.4 - 80.7 | 34 - 68.2 |
| $V_f$ (%) | 0.5 - 2.5 | 0.7 - 2 |
| $l_f/d_f$ | 42 - 79 | 78.9 - 342.1 |
| $\rho$ (%) | 1.1 - 5.9 | 0.4 - 5.7 |
| $f_y(MPa)$ | 363.4 - 600 | 421 - 545 |
| $\rho'$ (%) | 0.9 - 5.3 | 0.4 -4.7 |
| $f'_y(MPa)$ | 363.4 - 600 | 421 - 545 |
| $\rho_t$ (%) | 5.5 - 1.2 | 0.2 - 1.8 |
| $f_{yt}(MPa)$ | 295.6 - 510 | 291 - 586 |
| $\rho_d$ (%) | - | 0 - 4.4 |
| $f_{yd}(MPa)$ | - | 0 - 572 |
| $N^s$ | 29 | 20 |

$N^s$ = *Number of data points.*

Table 3.4. *Parameters considered in the database for coupling beams without transverse reinforcement*

| | FRC Coupling Beams | HPFRC Coupling Beams |
|---|---|---|
| Parameter | Range | Range |
| $l_n$ / $d$ | 2.68 - 2.68 | 2.15 - 4.05 |
| $h$ $(mm)$ | 610 - 610 | 300 - 525 |
| $d$ $(mm)$ | 559.5 - 559.5 | 259.5 - 488.5 |
| $b_w$ $(mm)$ | 150 - 150 | 250 - 250 |
| $f_c'$ $(MPa)$ | 40.8 - 56.5 | 41 - 41 |
| $V_f$ (%) | 0.4 - 1.5 | 2 - 2 |
| $l_f/d_f$ | 60 - 100 | 307.7 - 307.7 |
| $\rho$ (%) | 2.2 - 2.2 | - |
| $f_y(MPa)$ | 570 - 570 | - |
| $\rho'$ (%) | 2.1 - 2.1 | - |
| $f'_y(MPa)$ | 570 - 570 | - |
| $\rho_d$ (%) | - | 4.5 - 4.5 |
| $f_{yd}(MPa)$ | - | 438 - 442 |
| $N^s$ | 8 | 2 |

$N^s$ = *Number of data points.*

## 3.2. Resulting Database

The resulting database consists of 8 groups: $a/d \leq 2.5$ deep beams with transverse reinforcement, $a/d \leq 2.5$ deep beams without transverse reinforcement, $a/d > 2.5$ deep beams with transverse reinforcement, $a/d > 2.5$ deep beams without transverse reinforcement, FRC coupling beams with transverse reinforcement, FRC coupling beams without transverse reinforcement, HPFRC coupling beams with transverse reinforcement, and HPFRC coupling beams without transverse reinforcement, which are presented in Tables 3.5 - 3.12. The fiber types used in the experiments are abbreviated in these tables as:

H: hooked-end steel fibers

S: straight steel fibers

C: crimped steel fibers

F: flat-end steel fibers

T: torex steel fibers

PVA: polyvinyl alcohol fibers

PE: polyethylene fibers

Table 3.5. *Deep Beams ( $a/d \leq 2.5$ ) with transverse reinforcement*

| $Researcher$ | $Specimen$ | $a/d$ | $l_n/d$ | $b_w$ $(mm)$ | $h$ $(mm)$ | $d$ $(mm)$ | $\rho$ (%) | $\rho'$ (%) | $\rho_t$ (%) | $f_c'$ $(MPa)$ | $Fiber$ Type | $V_f$ (%) | $l_f/d_f$ |
|---|---|---|---|---|---|---|---|---|---|---|---|---|---|
| Cuchiara et al. (2004) | B11 | 2.0 | 10.5 | 150.0 | 250.0 | 219.0 | 1.9 | 1.7 | 0.2 | 40.9 | H | 1.0 | 60.0 |
| | B21 | 2.0 | 10.5 | 150.0 | 250.0 | 219.0 | 1.9 | 1.7 | 0.2 | 43.2 | H | 2.0 | 60.0 |
| | B12 | 2.0 | 10.5 | 150.0 | 250.0 | 219.0 | 1.9 | 1.7 | 0.6 | 40.9 | H | 1.0 | 60.0 |
| Cho and Kim (2003) | F60-0.5-13S | 1.4 | 4.3 | 120.0 | 200.0 | 167.5 | 2.1 | 1.8 | 0.5 | 57.8 | H | 0.5 | 60.0 |
| | F60-1.0-13S | 1.4 | 4.3 | 120.0 | 200.0 | 167.5 | 2.1 | 1.8 | 0.5 | 61.5 | H | 1.0 | 60.0 |
| | F60-1.5-13S | 1.4 | 4.3 | 120.0 | 200.0 | 167.5 | 1.3 | 1.1 | 0.5 | 60.6 | H | 1.5 | 60.0 |
| | F60-2.0-13S | 1.4 | 4.3 | 120.0 | 200.0 | 167.5 | 1.3 | 1.1 | 0.5 | 62.3 | H | 2.0 | 60.0 |
| Batson et al. (1972) | K1 | 2.2 | 14.4 | 101.6 | 152.4 | 127.0 | 3.1 | 2.6 | 3.0 | 39.8 | S | 1.8 | 101.6 |
| | K2 | 2.4 | 14.4 | 101.6 | 152.4 | 127.0 | 3.1 | 2.6 | 3.0 | 39.8 | S | 1.8 | 101.6 |
| | U2 | 2.2 | 14.4 | 101.6 | 152.4 | 127.0 | 3.1 | 2.6 | 3.0 | 39.8 | C | 1.8 | 46.2 |
| | V1 | 1.8 | 14.4 | 101.6 | 152.4 | 127.0 | 3.1 | 2.6 | 3.0 | 39.8 | C | 1.8 | 46.2 |
| | V2 | 1.8 | 14.4 | 101.6 | 152.4 | 127.0 | 3.1 | 2.6 | 3.0 | 39.8 | C | 1.8 | 46.2 |
| | V3 | 2.0 | 14.4 | 101.6 | 152.4 | 127.0 | 3.1 | 2.6 | 3.0 | 39.8 | C | 1.8 | 46.2 |
| | W1 | 1.2 | 14.4 | 101.6 | 152.4 | 127.0 | 3.1 | 2.6 | 3.0 | 39.8 | C | 1.8 | 46.2 |
| | W2 | 1.2 | 14.4 | 101.6 | 152.4 | 127.0 | 3.1 | 2.6 | 3.0 | 39.8 | C | 1.8 | 46.2 |
| | W3 | 1.4 | 14.4 | 101.6 | 152.4 | 127.0 | 3.1 | 2.6 | 3.0 | 39.8 | C | 1.8 | 46.2 |
| Araújo et al. (2014) | V-1-0.21 | 2.5 | 6.5 | 150.0 | 390.0 | 340.0 | 3.1 | 2.7 | 0.2 | 52.9 | H | 1.0 | 65.0 |
| | V-2-0.21 | 2.5 | 6.5 | 150.0 | 390.0 | 340.0 | 3.1 | 2.7 | 0.2 | 57.9 | H | 2.0 | 65.0 |

Table 3.6. *Deep Beams ( $a/d \leq 2.5$ ) without transverse reinforcement*

| $Researcher$ | $Specimen$ | $a/d$ | $l_n/d$ | $b_w$ $(mm)$ | $h$ $(mm)$ | $d$ $(mm)$ | $\rho$ (%) | $\rho'$ (%) | $f_c'$ $(MPa)$ | $Fiber$ Type | $V_f$ (%) | $l_f/d_f$ |
|---|---|---|---|---|---|---|---|---|---|---|---|---|
| Mansur et al. (1986) | B1 | 2.0 | 10.2 | 150.0 | 225.0 | 197.0 | 1.4 | 1.2 | 29.1 | H | 0.5 | 60.0 |
| | C1 | 2.0 | 10.2 | 150.0 | 225.0 | 197.0 | 1.4 | 1.2 | 29.9 | H | 0.8 | 60.0 |
| | D1 | 2.0 | 10.2 | 150.0 | 225.0 | 197.0 | 1.4 | 1.2 | 30.0 | H | 1.0 | 60.0 |
| Lim et al. (1987) | 2/1,0/1,5 | 1.5 | 7.2 | 152.0 | 254.0 | 221.0 | 1.2 | 1.0 | 34.0 | H | 1.0 | 60.0 |
| | 2/1,0/2,5 | 2.5 | 9.5 | 152.0 | 254.0 | 221.0 | 1.2 | 1.0 | 34.0 | H | 1.0 | 60.0 |
| | 2/0.5/1.5 | 1.5 | 7.2 | 152.0 | 254.0 | 221.0 | 1.2 | 1.0 | 34.0 | H | 0.5 | 60.0 |
| | 2/0,5/2,5 | 2.5 | 9.5 | 152.0 | 254.0 | 221.0 | 1.2 | 1.0 | 34.0 | H | 0.5 | 60.0 |
| | 4/1/1.5 | 1.5 | 7.2 | 152.0 | 254.0 | 221.0 | 2.4 | 2.1 | 34.0 | H | 1.0 | 60.0 |
| | 4/1,0/2,5 | 2.5 | 9.5 | 152.0 | 254.0 | 221.0 | 2.4 | 2.1 | 34.0 | H | 1.0 | 60.0 |
| | 4/0.5/1.5 | 1.5 | 7.2 | 152.0 | 254.0 | 221.0 | 2.4 | 2.1 | 34.0 | H | 0.5 | 60.0 |
| | 4/0,5/2,5 | 2.5 | 9.5 | 152.0 | 254.0 | 221.0 | 2.4 | 2.1 | 34.0 | H | 0.5 | 60.0 |
| Cuchiara et al. (2004) | B10 | 2.0 | 10.5 | 150.0 | 240.0 | 219.0 | 1.9 | 1.7 | 40.9 | H | 1.0 | 60.0 |
| | B20 | 2.0 | 10.5 | 150.0 | 240.0 | 219.0 | 1.9 | 1.7 | 43.2 | H | 2.0 | 60.0 |
| Şen (2005) | BEAM-03 | 2.0 | 9.3 | 125.0 | 250.0 | 215.0 | 1.5 | 1.3 | 60.2 | H | 0.5 | 65.0 |
| | BEAM-05 | 2.0 | 9.3 | 125.0 | 250.0 | 215.0 | 1.5 | 1.3 | 61.7 | H | 0.8 | 65.0 |
| | BEAM-07 | 2.0 | 9.3 | 125.0 | 250.0 | 215.0 | 1.5 | 1.3 | 60.9 | H | 0.5 | 80.0 |
| | BEAM-09 | 2.0 | 9.3 | 125.0 | 250.0 | 215.0 | 1.5 | 1.3 | 63.6 | H | 0.8 | 80.0 |
| Kwak et al. (2002) | FHB2-2 | 2.0 | 5.9 | 125.0 | 250.0 | 212.0 | 1.5 | 1.3 | 63.8 | H | 0.5 | 62.5 |
| | FHB3-2 | 2.0 | 5.9 | 125.0 | 250.0 | 212.0 | 1.5 | 1.3 | 68.6 | H | 0.8 | 62.5 |
| | FNB2-2 | 2.0 | 5.9 | 125.0 | 250.0 | 212.0 | 1.5 | 1.3 | 30.8 | H | 0.5 | 62.5 |
| Rosenbusch and Teutsch (2003) | 2.2/2 | 1.5 | 8.8 | 200.0 | 300.0 | 260.0 | 1.8 | 1.6 | 41.2 | H | 0.3 | 65.0 |
| | 2.2/3 | 1.5 | 8.8 | 200.0 | 300.0 | 260.0 | 1.8 | 1.6 | 40.3 | H | 0.8 | 65.0 |
| | 2.3/2 | 2.5 | 8.8 | 200.0 | 300.0 | 260.0 | 1.2 | 1.0 | 40.0 | H | 0.3 | 65.0 |
| | 2.3/3 | 2.5 | 8.8 | 200.0 | 300.0 | 260.0 | 1.2 | 1.0 | 38.7 | H | 0.8 | 65.0 |
| | 2.4/2 | 2.5 | 8.8 | 200.0 | 300.0 | 260.0 | 1.8 | 1.6 | 40.0 | H | 0.3 | 65.0 |
| | 2.4/3 | 2.5 | 8.8 | 200.0 | 300.0 | 260.0 | 1.8 | 1.6 | 38.7 | H | 0.8 | 65.0 |

Table 3.6. *Deep Beams ( $a/d \leq 2.5$ ) without transverse reinforcement (continued)*

| *Researcher* | *Specimen* | $a/d$ | $l_n/d$ | $b_w$ $(mm)$ | $h$ $(mm)$ | $d$ $(mm)$ | $\rho$ (%) | $\rho'$ (%) | $f_c'$ $(MPa)$ | *Fiber* Type | $V_f$ (%) | $l_f/d_f$ |
|---|---|---|---|---|---|---|---|---|---|---|---|---|
| Dupont and Vandewalle (2003) | 14 | 1.5 | 8.8 | 200.0 | 300.0 | 260.0 | 1.8 | 1.6 | 40.7 | H | 0.3 | 65.0 |
| | 15 | 1.5 | 8.8 | 200.0 | 300.0 | 260.0 | 1.8 | 1.6 | 42.4 | H | 0.8 | 65.0 |
| | 17 | 2.5 | 8.8 | 200.0 | 300.0 | 262.0 | 1.2 | 1.0 | 39.1 | H | 0.3 | 65.0 |
| | 18 | 2.5 | 8.8 | 200.0 | 300.0 | 262.0 | 1.2 | 1.0 | 38.6 | H | 0.8 | 65.0 |
| | 20 | 2.5 | 8.8 | 200.0 | 300.0 | 260.0 | 1.8 | 1.6 | 39.1 | H | 0.3 | 65.0 |
| | 21 | 2.5 | 8.8 | 200.0 | 300.0 | 260.0 | 1.8 | 1.6 | 38.6 | H | 0.8 | 65.0 |
| | 26 | 2.5 | 8.8 | 200.0 | 300.0 | 262.0 | 1.2 | 1.0 | 26.5 | H | 0.3 | 45.0 |
| | 27 | 2.5 | 8.8 | 200.0 | 300.0 | 262.0 | 1.2 | 1.0 | 27.2 | H | 0.8 | 45.0 |
| | 29 | 2.5 | 8.8 | 200.0 | 300.0 | 260.0 | 1.8 | 1.6 | 26.5 | H | 0.3 | 45.0 |
| | 30 | 2.5 | 8.8 | 200.0 | 300.0 | 260.0 | 1.8 | 1.6 | 27.2 | H | 0.8 | 45.0 |
| | 31 | 2.5 | 8.8 | 200.0 | 300.0 | 262.0 | 1.2 | 1.0 | 47.4 | H | 0.5 | 65.0 |
| | 32 | 2.5 | 8.8 | 200.0 | 300.0 | 260.0 | 1.8 | 1.6 | 46.8 | H | 0.5 | 65.0 |
| | 33 | 2.5 | 8.8 | 200.0 | 300.0 | 262.0 | 1.2 | 1.0 | 45.3 | H | 0.5 | 80.0 |
| | 34 | 2.5 | 8.8 | 200.0 | 300.0 | 262.0 | 1.2 | 1.0 | 50.0 | H | 0.8 | 80.0 |
| | 41 | 2.5 | 10.7 | 200.0 | 350.0 | 305.0 | 1.0 | 0.9 | 34.4 | H | 0.6 | 80.0 |
| | 42 | 2.5 | 10.7 | 200.0 | 350.0 | 305.0 | 1.0 | 0.9 | 30.1 | H | 0.9 | 80.0 |
| | 43 | 2.5 | 10.7 | 200.0 | 350.0 | 305.0 | 1.0 | 0.9 | 30.2 | H | 0.4 | 80.0 |
| Imam et al. (1994) | B15 | 1.8 | 10.8 | 200.0 | 350.0 | 300.0 | 1.9 | 1.6 | 108.5 | H | 0.8 | 75.0 |
| | B5 | 2.5 | 10.8 | 200.0 | 350.0 | 300.0 | 1.9 | 1.6 | 110.0 | H | 0.8 | 75.0 |
| | B16 | 1.8 | 10.8 | 200.0 | 350.0 | 300.0 | 3.1 | 2.6 | 109.5 | H | 0.8 | 75.0 |
| | B6 | 2.5 | 10.8 | 200.0 | 350.0 | 300.0 | 3.1 | 2.6 | 110.0 | H | 0.8 | 75.0 |
| Tan et al. (1993) | 2 | 2.0 | 5.0 | 140.0 | 375.0 | 340.0 | 1.7 | 1.5 | 35.0 | H | 0.5 | 60.0 |
| | 3 | 2.0 | 5.0 | 140.0 | 375.0 | 340.0 | 1.7 | 1.5 | 33.0 | H | 0.8 | 60.0 |
| | 4 | 2.0 | 5.0 | 140.0 | 375.0 | 340.0 | 1.7 | 1.5 | 36.0 | H | 1.0 | 60.0 |
| | 5 | 2.5 | 5.0 | 140.0 | 375.0 | 340.0 | 1.7 | 1.5 | 36.0 | H | 1.0 | 60.0 |
| | 6 | 1.5 | 5.0 | 140.0 | 375.0 | 340.0 | 1.7 | 1.5 | 36.0 | H | 1.0 | 60.0 |

Table 3.6. *Deep Beams ( $a/d \leq 2.5$ ) without transverse reinforcement (continued)*

| $Researcher$ | $Specimen$ | $a/d$ | $l_n/d$ | $b_w$ $(mm)$ | $h$ $(mm)$ | $d$ $(mm)$ | $\rho$ (%) | $\rho'$ (%) | $f_c'$ $(MPa)$ | $Fiber$ Type | $V_f$ (%) | $l_f/d_f$ |
|---|---|---|---|---|---|---|---|---|---|---|---|---|
| Ashour et al. (1992) | B-2-l.O-L | 2.0 | 6.3 | 125.0 | 250.0 | 215.0 | 0.4 | 0.3 | 92.0 | H | 1.0 | 75.0 |
| | B-1-0.5-A | 1.0 | 4.3 | 125.0 | 250.0 | 215.0 | 2.8 | 2.4 | 99.0 | H | 0.5 | 75.0 |
| | B-2-0.5-A | 2.0 | 6.3 | 125.0 | 250.0 | 215.0 | 2.8 | 2.4 | 99.1 | H | 0.5 | 75.0 |
| | B-1-l.O-A | 1.0 | 4.3 | 125.0 | 250.0 | 215.0 | 2.8 | 2.4 | 95.3 | H | 1.0 | 75.0 |
| | B-2-l.O-A | 2.0 | 6.3 | 125.0 | 250.0 | 215.0 | 2.8 | 2.4 | 95.3 | H | 1.0 | 75.0 |
| | B-1-1.5-A | 1.0 | 4.3 | 125.0 | 250.0 | 215.0 | 2.8 | 2.4 | 96.4 | H | 1.5 | 75.0 |
| | B-2-1.5-A | 2.0 | 6.3 | 125.0 | 250.0 | 215.0 | 2.8 | 2.4 | 96.6 | H | 1.5 | 75.0 |
| | B-2-l.O-M | 2.0 | 6.3 | 125.0 | 250.0 | 215.0 | 4.6 | 3.9 | 94.5 | H | 1.0 | 75.0 |
| Cho and Kim (2003) | F30-0.5-13 | 1.4 | 4.3 | 120.0 | 200.0 | 167.5 | 1.3 | 1.1 | 25.7 | H | 0.5 | 60.0 |
| | F30-1.0-13 | 1.4 | 4.3 | 120.0 | 200.0 | 167.5 | 1.3 | 1.1 | 25.3 | H | 1.0 | 60.0 |
| | F30-1.5-13 | 1.4 | 4.3 | 120.0 | 200.0 | 167.5 | 1.3 | 1.1 | 23.9 | H | 1.5 | 60.0 |
| | F30-2.0-13 | 1.4 | 4.3 | 120.0 | 200.0 | 167.5 | 1.3 | 1.1 | 28.8 | H | 2.0 | 60.0 |
| | F60-0.5-13 | 1.4 | 4.3 | 120.0 | 200.0 | 167.5 | 2.1 | 1.8 | 57.8 | H | 0.5 | 60.0 |
| | F60-1.0-13 | 1.4 | 4.3 | 120.0 | 200.0 | 167.5 | 2.1 | 1.8 | 61.5 | H | 1.0 | 60.0 |
| | F60-1.5-13 | 1.4 | 4.3 | 120.0 | 200.0 | 167.5 | 1.3 | 1.1 | 60.6 | H | 1.5 | 60.0 |
| | F60-2.0-13 | 1.4 | 4.3 | 120.0 | 200.0 | 167.5 | 1.3 | 1.1 | 62.3 | H | 2.0 | 60.0 |
| | F70-0.5-19 | 1.4 | 4.3 | 120.0 | 200.0 | 167.5 | 2.8 | 2.4 | 70.5 | H | 0.5 | 60.0 |
| | F70-1.0-19 | 1.4 | 4.3 | 120.0 | 200.0 | 167.5 | 2.8 | 2.4 | 67.3 | H | 1.0 | 60.0 |
| | F70-1.5-19 | 1.4 | 4.3 | 120.0 | 200.0 | 167.5 | 2.8 | 2.4 | 67.3 | H | 1.5 | 60.0 |
| | F70-2.0-19 | 1.4 | 4.3 | 120.0 | 200.0 | 167.5 | 2.8 | 2.4 | 69.6 | H | 2.0 | 60.0 |
| | F80-0.5-16 | 1.4 | 4.3 | 120.0 | 200.0 | 167.5 | 2.0 | 1.7 | 82.4 | H | 0.5 | 60.0 |
| | F80-1.0-16 | 1.4 | 4.3 | 120.0 | 200.0 | 167.5 | 2.0 | 1.7 | 81.1 | H | 1.0 | 60.0 |
| | F80-1.5-16 | 1.4 | 4.3 | 120.0 | 200.0 | 167.5 | 2.0 | 1.7 | 83.0 | H | 1.5 | 60.0 |
| | F80-2.0-16 | 1.4 | 4.3 | 120.0 | 200.0 | 167.5 | 2.0 | 1.7 | 82.2 | H | 2.0 | 60.0 |
| | F80-0.5-19 | 1.4 | 4.3 | 120.0 | 200.0 | 167.5 | 2.8 | 2.4 | 86.1 | H | 0.5 | 60.0 |
| | F80-1.0-19 | 1.4 | 4.3 | 120.0 | 200.0 | 167.5 | 2.8 | 2.4 | 89.4 | H | 1.0 | 60.0 |
| | F80-1.5-19 | 1.4 | 4.3 | 120.0 | 200.0 | 167.5 | 2.8 | 2.4 | 82.7 | H | 1.5 | 60.0 |
| | F80-2.0-19 | 1.4 | 4.3 | 120.0 | 200.0 | 167.5 | 2.8 | 2.4 | 89.9 | H | 2.0 | 60.0 |

Table 3.6. *Deep Beams ( $a/d \leq 2.5$ ) without transverse reinforcement (continued)*

| $Researcher$ | $Specimen$ | $a/d$ | $l_n/d$ | $b_w$ $(mm)$ | $h$ $(mm)$ | $d$ $(mm)$ | $\rho$ (%) | $\rho'$ (%) | $f_c'$ $(MPa)$ | $Fiber$ Type | $V_f$ (%) | $l_f/d_f$ |
|---|---|---|---|---|---|---|---|---|---|---|---|---|
| Li et al. (1992) | M11 | 63.5 | 127.0 | 102.0 | 2.4 | 1.9 | 54.1 | 63.5 | 127.0 | C | 1.0 | 57.0 |
| | M12 | 63.5 | 127.0 | 102.0 | 2.4 | 1.9 | 54.1 | 63.5 | 127.0 | C | 1.0 | 57.0 |
| | M13 | 63.5 | 127.0 | 102.0 | 2.4 | 1.9 | 54.1 | 63.5 | 127.0 | C | 1.0 | 57.0 |
| | M14 | 63.5 | 127.0 | 102.0 | 2.4 | 1.9 | 54.1 | 63.5 | 127.0 | C | 1.0 | 57.0 |
| | M15 | 63.5 | 127.0 | 102.0 | 2.4 | 1.9 | 62.6 | 63.5 | 127.0 | C | 1.0 | 28.5 |
| | M16 | 63.5 | 127.0 | 102.0 | 2.4 | 1.9 | 62.6 | 63.5 | 127.0 | C | 1.0 | 28.5 |
| | C4 | 63.5 | 127.0 | 102.0 | 1.2 | 1.0 | 22.7 | 63.5 | 127.0 | H | 1.0 | 60.0 |
| Khaloo and Kim (1997) | LC-0.5-16 | 125.0 | 220.0 | 190.0 | 1.3 | 1.1 | 33.5 | 125.0 | 220.0 | H | 0.5 | 29.0 |
| | LC-1.0-16 | 125.0 | 220.0 | 190.0 | 1.3 | 1.1 | 30.9 | 125.0 | 220.0 | H | 0.5 | 58.0 |
| | LC-1.5-16 | 125.0 | 220.0 | 190.0 | 1.3 | 1.1 | 29.8 | 125.0 | 220.0 | H | 1.0 | 29.0 |
| | LC-0.5-32 | 125.0 | 220.0 | 190.0 | 1.3 | 1.1 | 35.5 | 125.0 | 220.0 | H | 1.0 | 58.0 |
| | LC-1.0-32 | 125.0 | 220.0 | 190.0 | 1.3 | 1.1 | 32.8 | 125.0 | 220.0 | H | 1.5 | 29.0 |
| | LC-1.5-32 | 125.0 | 220.0 | 190.0 | 1.3 | 1.1 | 29.0 | 125.0 | 220.0 | H | 1.5 | 58.0 |
| | NC-0.5-16 | 125.0 | 220.0 | 190.0 | 1.3 | 1.1 | 45.3 | 125.0 | 220.0 | H | 0.5 | 29.0 |
| | NC-1.0-16 | 125.0 | 220.0 | 190.0 | 1.3 | 1.1 | 45.3 | 125.0 | 220.0 | H | 0.5 | 58.0 |
| | NC-1.5-16 | 125.0 | 220.0 | 190.0 | 1.3 | 1.1 | 48.7 | 125.0 | 220.0 | H | 1.0 | 29.0 |
| | NC-0.5-32 | 125.0 | 220.0 | 190.0 | 1.3 | 1.1 | 45.2 | 125.0 | 220.0 | H | 1.0 | 58.0 |
| | NC-1.0-32 | 125.0 | 220.0 | 190.0 | 1.3 | 1.1 | 47.8 | 125.0 | 220.0 | H | 1.5 | 29.0 |
| | NC-1.5-32 | 125.0 | 220.0 | 190.0 | 1.3 | 1.1 | 41.5 | 125.0 | 220.0 | H | 1.5 | 58.0 |
| | MC-0.5-16 | 125.0 | 220.0 | 190.0 | 2.0 | 1.7 | 56.4 | 125.0 | 220.0 | H | 0.5 | 29.0 |
| | MC-1.0-16 | 125.0 | 220.0 | 190.0 | 2.0 | 1.7 | 59.5 | 125.0 | 220.0 | H | 0.5 | 58.0 |
| | MC-1.5-16 | 125.0 | 220.0 | 190.0 | 1.3 | 1.1 | 55.6 | 125.0 | 220.0 | H | 1.0 | 29.0 |
| | MC-0.5-32 | 125.0 | 220.0 | 190.0 | 1.3 | 1.1 | 56.4 | 125.0 | 220.0 | H | 1.0 | 58.0 |
| | MC-1.0-32 | 125.0 | 220.0 | 190.0 | 1.3 | 1.1 | 58.3 | 125.0 | 220.0 | H | 1.5 | 29.0 |
| | MC-1.5-32 | 125.0 | 220.0 | 190.0 | 1.3 | 1.1 | 55.1 | 125.0 | 220.0 | H | 1.5 | 58.0 |
| Shin et al. (1994) | 1 | 100.0 | 200.0 | 175.0 | 3.6 | 3.1 | 80.0 | 100.0 | 200.0 | S | 0.5 | 100.0 |
| | 2 | 100.0 | 200.0 | 175.0 | 3.6 | 3.1 | 80.0 | 100.0 | 200.0 | S | 1.0 | 100.0 |

Table 3.7. *Deep Beams ( $a/d$ > 2.5 ) with transverse reinforcement*

| *Researcher* | *Specimen* | $a/d$ | $l_n/d$ | $b_w$ $(mm)$ | $h$ $(mm)$ | $d$ $(mm)$ | $\rho$ (%) | $\rho'$ (%) | $\rho_t$ (%) | $f_c'$ $(MPa)$ | *Fiber* Type | $V_f$ (%) | $l_f/d_f$ |
|---|---|---|---|---|---|---|---|---|---|---|---|---|---|
| Swamy and Bahia (1985) | B52 | 4.5 | 9.0 | 175.0 | 250.0 | 210.0 | 4.0 | 3.4 | 0.2 | 35.5 | C | 0.4 | 100.0 |
| | B53 | 4.5 | 9.0 | 175.0 | 250.0 | 210.0 | 4.0 | 3.4 | 0.2 | 37.4 | C | 0.8 | 100.0 |
| | B54 | 4.5 | 9.0 | 175.0 | 250.0 | 210.0 | 4.0 | 3.4 | 0.2 | 39.8 | C | 1.2 | 100.0 |
| | B55 | 4.5 | 9.0 | 175.0 | 250.0 | 210.0 | 3.1 | 2.6 | 0.2 | 38.2 | C | 0.8 | 100.0 |
| | B56 | 4.5 | 9.0 | 175.0 | 250.0 | 210.0 | 2.0 | 1.6 | 0.2 | 41.8 | C | 0.8 | 100.0 |
| | B63R | 4.5 | 9.0 | 175.0 | 250.0 | 210.0 | 2.0 | 1.6 | 0.2 | 35.1 | C | 0.8 | 100.0 |
| Batson et al. (1972) | A1 | 4.8 | 14.4 | 101.6 | 152.4 | 127.0 | 3.1 | 2.6 | 3.0 | 33.2 | S | 0.2 | 101.6 |
| | A2 | 4.8 | 14.4 | 101.6 | 152.4 | 127.0 | 3.1 | 2.6 | 3.0 | 33.2 | S | 0.2 | 101.6 |
| | A3 | 4.8 | 14.4 | 101.6 | 152.4 | 127.0 | 3.1 | 2.6 | 3.0 | 33.2 | S | 0.2 | 101.6 |
| | B1 | 4.4 | 14.4 | 101.6 | 152.4 | 127.0 | 3.1 | 2.6 | 3.0 | 33.2 | S | 0.2 | 101.6 |
| | B2 | 4.4 | 14.4 | 101.6 | 152.4 | 127.0 | 3.1 | 2.6 | 3.0 | 33.2 | S | 0.2 | 101.6 |
| | B3 | 4.4 | 14.4 | 101.6 | 152.4 | 127.0 | 3.1 | 2.6 | 3.0 | 33.2 | S | 0.2 | 101.6 |
| | C1 | 4.2 | 14.4 | 101.6 | 152.4 | 127.0 | 3.1 | 2.6 | 3.0 | 33.2 | S | 0.2 | 101.6 |
| | C2 | 4.2 | 14.4 | 101.6 | 152.4 | 127.0 | 3.1 | 2.6 | 3.0 | 33.2 | S | 0.2 | 101.6 |
| | C3 | 4.2 | 14.4 | 101.6 | 152.4 | 127.0 | 3.1 | 2.6 | 3.0 | 33.2 | S | 0.2 | 101.6 |
| | D1 | 4.3 | 14.4 | 101.6 | 152.4 | 127.0 | 3.1 | 2.6 | 3.0 | 33.2 | S | 0.2 | 101.6 |
| | D2 | 4.3 | 14.4 | 101.6 | 152.4 | 127.0 | 3.1 | 2.6 | 3.0 | 33.2 | S | 0.2 | 101.6 |
| | D3 | 4.3 | 14.4 | 101.6 | 152.4 | 127.0 | 3.1 | 2.6 | 3.0 | 33.2 | S | 0.2 | 101.6 |
| | E1 | 4.2 | 14.4 | 101.6 | 152.4 | 127.0 | 3.1 | 2.6 | 3.0 | 40.2 | S | 0.4 | 101.6 |
| | E2 | 4.2 | 14.4 | 101.6 | 152.4 | 127.0 | 3.1 | 2.6 | 3.0 | 40.2 | S | 0.4 | 101.6 |
| | E3 | 4.2 | 14.4 | 101.6 | 152.4 | 127.0 | 3.1 | 2.6 | 3.0 | 40.2 | S | 0.4 | 101.6 |
| | F1 | 4.0 | 14.4 | 101.6 | 152.4 | 127.0 | 3.1 | 2.6 | 3.0 | 40.2 | S | 0.4 | 101.6 |
| | F2 | 4.0 | 14.4 | 101.6 | 152.4 | 127.0 | 3.1 | 2.6 | 3.0 | 40.2 | S | 0.4 | 101.6 |
| | F3 | 4.0 | 14.4 | 101.6 | 152.4 | 127.0 | 3.1 | 2.6 | 3.0 | 40.2 | S | 0.4 | 101.6 |
| | G1 | 4.4 | 14.4 | 101.6 | 152.4 | 127.0 | 3.1 | 2.6 | 3.0 | 33.2 | S | 0.2 | 101.6 |
| | G2 | 4.4 | 14.4 | 101.6 | 152.4 | 127.0 | 3.1 | 2.6 | 3.0 | 33.2 | S | 0.2 | 101.6 |
| | G3 | 4.4 | 14.4 | 101.6 | 152.4 | 127.0 | 3.1 | 2.6 | 3.0 | 33.2 | S | 0.2 | 101.6 |

Table 3.7. *Deep Beams ( $a/d$ > 2.5 ) with transverse reinforcement (continued)*

| *Researcher* | *Specimen* | $a/d$ | $l_n/d$ | $b_w$ $(mm)$ | $h$ $(mm)$ | $d$ $(mm)$ | $\rho$ (%) | $\rho'$ (%) | $\rho_t$ (%) | $f_c'$ $(MPa)$ | *Fiber* Type | $V_f$ (%) | $l_f/d_f$ |
|---|---|---|---|---|---|---|---|---|---|---|---|---|---|
| Batson et al. (1972) | H1 | 3.8 | 14.4 | 101.6 | 152.4 | 127.0 | 3.1 | 2.6 | 3.0 | 39.8 | S | 0.9 | 101.6 |
| | H2 | 3.8 | 14.4 | 101.6 | 152.4 | 127.0 | 3.1 | 2.6 | 3.0 | 39.8 | S | 0.9 | 101.6 |
| | H3 | 3.8 | 14.4 | 101.6 | 152.4 | 127.0 | 3.1 | 2.6 | 3.0 | 39.8 | S | 0.9 | 101.6 |
| | I1 | 3.6 | 14.4 | 101.6 | 152.4 | 127.0 | 3.1 | 2.6 | 3.0 | 39.8 | S | 0.9 | 101.6 |
| | I2 | 3.6 | 14.4 | 101.6 | 152.4 | 127.0 | 3.1 | 2.6 | 3.0 | 39.8 | S | 0.9 | 101.6 |
| | I3 | 3.6 | 14.4 | 101.6 | 152.4 | 127.0 | 3.1 | 2.6 | 3.0 | 39.8 | S | 0.9 | 101.6 |
| | J1 | 2.8 | 14.4 | 101.6 | 152.4 | 127.0 | 3.1 | 2.6 | 3.0 | 39.8 | S | 1.8 | 101.6 |
| | J2 | 2.8 | 14.4 | 101.6 | 152.4 | 127.0 | 3.1 | 2.6 | 3.0 | 39.8 | S | 1.8 | 101.6 |
| | J3 | 2.8 | 14.4 | 101.6 | 152.4 | 127.0 | 3.1 | 2.6 | 3.0 | 39.8 | S | 1.8 | 101.6 |
| | K3 | 2.6 | 14.4 | 101.6 | 152.4 | 127.0 | 3.1 | 2.6 | 3.0 | 39.8 | S | 1.8 | 101.6 |
| | U1 | 4.0 | 14.4 | 101.6 | 152.4 | 127.0 | 3.1 | 2.6 | 3.0 | 33.2 | C | 0.2 | 101.6 |
| | U3 | 4.0 | 14.4 | 101.6 | 152.4 | 127.0 | 3.1 | 2.6 | 3.0 | 33.2 | C | 0.2 | 101.6 |
| | L1 | 4.0 | 14.4 | 101.6 | 152.4 | 127.0 | 3.1 | 2.6 | 3.0 | 33.2 | S | 0.2 | 101.6 |
| | L2 | 4.6 | 14.4 | 101.6 | 152.4 | 127.0 | 3.1 | 2.6 | 3.0 | 33.2 | S | 0.2 | 46.2 |
| | L3 | 4.4 | 14.4 | 101.6 | 152.4 | 127.0 | 3.1 | 2.6 | 3.0 | 33.2 | S | 0.2 | 46.2 |
| | M1 | 4.4 | 14.4 | 101.6 | 152.4 | 127.0 | 3.1 | 2.6 | 3.0 | 33.2 | C | 0.2 | 46.2 |
| | M2 | 5.0 | 14.4 | 101.6 | 152.4 | 127.0 | 3.1 | 2.6 | 3.0 | 33.2 | C | 0.2 | 46.2 |
| | M3 | 4.8 | 14.4 | 101.6 | 152.4 | 127.0 | 3.1 | 2.6 | 3.0 | 33.2 | C | 0.2 | 46.2 |
| | N1 | 5.0 | 14.4 | 101.6 | 152.4 | 127.0 | 3.1 | 2.6 | 3.0 | 33.2 | C | 0.2 | 46.2 |
| | N2 | 4.0 | 14.4 | 101.6 | 152.4 | 127.0 | 3.1 | 2.6 | 3.0 | 40.2 | C | 0.4 | 46.2 |
| | N3 | 4.4 | 14.4 | 101.6 | 152.4 | 127.0 | 3.1 | 2.6 | 3.0 | 40.2 | C | 0.4 | 46.2 |
| | O1 | 4.8 | 14.4 | 101.6 | 152.4 | 127.0 | 3.1 | 2.6 | 3.0 | 40.2 | C | 0.4 | 46.2 |
| | O2 | 4.2 | 14.4 | 101.6 | 152.4 | 127.0 | 3.1 | 2.6 | 3.0 | 40.2 | C | 0.4 | 46.2 |
| | O3 | 4.2 | 14.4 | 101.6 | 152.4 | 127.0 | 3.1 | 2.6 | 3.0 | 40.2 | C | 0.4 | 46.2 |
| | P1 | 4.2 | 14.4 | 101.6 | 152.4 | 127.0 | 3.1 | 2.6 | 3.0 | 40.2 | C | 0.4 | 46.2 |
| | P2 | 3.8 | 14.4 | 101.6 | 152.4 | 127.0 | 3.1 | 2.6 | 3.0 | 39.8 | C | 0.4 | 46.2 |
| | P3 | 3.8 | 14.4 | 101.6 | 152.4 | 127.0 | 3.1 | 2.6 | 3.0 | 39.8 | C | 0.4 | 46.2 |

Table 3.7. *Deep Beams ( $a/d$ > 2.5 ) with transverse reinforcement (continued)*

| *Researcher* | *Specimen* | $a/d$ | $l_n/d$ | $b_w$ $(mm)$ | $h$ $(mm)$ | $d$ $(mm)$ | $\rho$ (%) | $\rho'$ (%) | $\rho_t$ (%) | $f'_c$ $(MPa)$ | *Fiber* Type | $V_f$ (%) | $l_f/d_f$ |
|---|---|---|---|---|---|---|---|---|---|---|---|---|---|
| Batson et al. (1972) | Q1 | 4.4 | 14.4 | 101.6 | 152.4 | 127.0 | 3.1 | 2.6 | 3.0 | 40.2 | C | 0.4 | 46.2 |
| | Q2 | 4.4 | 14.4 | 101.6 | 152.4 | 127.0 | 3.1 | 2.6 | 3.0 | 40.2 | C | 0.4 | 46.2 |
| | Q3 | 4.4 | 14.4 | 101.6 | 152.4 | 127.0 | 3.1 | 2.6 | 3.0 | 40.2 | C | 0.4 | 46.2 |
| | R1 | 3.2 | 14.4 | 101.6 | 152.4 | 127.0 | 3.1 | 2.6 | 3.0 | 39.7 | C | 0.9 | 46.2 |
| | R2 | 3.4 | 14.4 | 101.6 | 152.4 | 127.0 | 3.1 | 2.6 | 3.0 | 39.7 | C | 0.9 | 46.2 |
| | R3 | 3.6 | 14.4 | 101.6 | 152.4 | 127.0 | 3.1 | 2.6 | 3.0 | 39.7 | C | 0.9 | 46.2 |
| | S1 | 3.4 | 14.4 | 101.6 | 152.4 | 127.0 | 3.1 | 2.6 | 3.0 | 39.7 | C | 0.9 | 46.2 |
| | S2 | 3.4 | 14.4 | 101.6 | 152.4 | 127.0 | 3.1 | 2.6 | 3.0 | 39.7 | C | 0.9 | 46.2 |
| | S3 | 3.4 | 14.4 | 101.6 | 152.4 | 127.0 | 3.1 | 2.6 | 3.0 | 39.7 | C | 0.9 | 46.2 |
| | T1 | 3.6 | 14.4 | 101.6 | 152.4 | 127.0 | 3.1 | 2.6 | 3.0 | 39.7 | C | 0.9 | 46.2 |
| | T2 | 3.6 | 14.4 | 101.6 | 152.4 | 127.0 | 3.1 | 2.6 | 3.0 | 39.7 | C | 0.9 | 46.2 |
| | T3 | 3.6 | 14.4 | 101.6 | 152.4 | 127.0 | 3.1 | 2.6 | 3.0 | 39.7 | C | 0.9 | 46.2 |
| | X1 | 4.8 | 14.4 | 101.6 | 152.4 | 127.0 | 3.1 | 2.6 | 3.0 | 33.2 | C | 0.2 | 46.2 |
| | X2 | 4.8 | 14.4 | 101.6 | 152.4 | 127.0 | 3.1 | 2.6 | 3.0 | 33.2 | C | 0.2 | 46.2 |
| | X3 | 4.8 | 14.4 | 101.6 | 152.4 | 127.0 | 3.1 | 2.6 | 3.0 | 33.2 | C | 0.2 | 46.2 |
| EI-Niema (1991) | 2,00 | 3.9 | 10.3 | 100.0 | 200.0 | 175.0 | 2.3 | 2.0 | 0.5 | 26.0 | C | 0.4 | 127.7 |
| | 3,00 | 3.9 | 10.3 | 100.0 | 200.0 | 175.0 | 2.3 | 2.0 | 0.5 | 28.5 | C | 0.7 | 127.7 |
| | 4,00 | 3.9 | 10.3 | 100.0 | 200.0 | 175.0 | 2.3 | 2.0 | 0.5 | 30.0 | C | 1.0 | 127.7 |
| | 5,00 | 3.9 | 10.3 | 100.0 | 200.0 | 175.0 | 2.3 | 2.0 | 0.5 | 25.0 | C | 0.4 | 95.8 |
| | 6,00 | 3.9 | 10.3 | 100.0 | 200.0 | 175.0 | 2.3 | 2.0 | 0.5 | 25.0 | C | 0.7 | 95.8 |
| | 7,00 | 3.9 | 10.3 | 100.0 | 200.0 | 175.0 | 2.3 | 2.0 | 0.5 | 25.0 | C | 1.0 | 95.8 |
| | 8,00 | 3.9 | 10.3 | 100.0 | 200.0 | 175.0 | 2.3 | 2.0 | 0.5 | 24.0 | C | 0.4 | 63.8 |
| | 9,00 | 3.9 | 10.3 | 100.0 | 200.0 | 175.0 | 2.3 | 2.0 | 0.5 | 25.0 | C | 0.7 | 63.8 |
| | 10,00 | 3.9 | 10.3 | 100.0 | 200.0 | 175.0 | 2.3 | 2.0 | 0.5 | 25.0 | C | 1.0 | 63.8 |
| Swamy and Alta'an(1981) | DR11 | 6.5 | 12.9 | 130.0 | 203.2 | 174.2 | 1.0 | 0.9 | 0.3 | 31.6 | C | 0.5 | 100.0 |
| | DR12 | 6.5 | 12.9 | 130.0 | 203.2 | 174.2 | 1.0 | 0.9 | 0.3 | 32.0 | C | 1.0 | 100.0 |
| | DR21 | 6.5 | 12.9 | 130.0 | 203.2 | 174.2 | 1.8 | 1.5 | 0.3 | 29.8 | C | 0.5 | 100.0 |

Table 3.7. *Deep Beams ( $a/d$ > 2.5 ) with transverse reinforcement (continued)*

| $Researcher$ | $Specimen$ | $a/d$ | $l_n/d$ | $b_w$ $(mm)$ | $h$ $(mm)$ | $d$ $(mm)$ | $\rho$ (%) | $\rho'$ (%) | $\rho_t$ (%) | $f_c'$ $(MPa)$ | $Fiber$ Type | $V_f$ (%) | $l_f/d_f$ |
|---|---|---|---|---|---|---|---|---|---|---|---|---|---|
| Swamy and Alta'an(1981) | DR22 | 6.5 | 12.9 | 130.0 | 203.2 | 174.2 | 1.0 | 0.9 | 0.3 | 31.2 | C | 0.5 | 100.0 |
| | DR31 | 6.5 | 12.9 | 130.0 | 203.2 | 174.2 | 1.0 | 0.9 | 0.3 | 32.7 | C | 1.0 | 100.0 |
| | DR32 | 3.8 | 10.6 | 100.0 | 100.0 | 85.0 | 1.7 | 1.4 | 0.2 | 54.8 | C | 1.0 | 33.4 |
| Furlan and Hanai (1997) | P3A | 3.8 | 10.6 | 100.0 | 100.0 | 85.0 | 1.7 | 1.4 | 0.2 | 50.0 | C | 2.0 | 33.4 |
| | P4A | 3.8 | 10.6 | 100.0 | 100.0 | 85.0 | 1.7 | 1.4 | 0.2 | 49.3 | C | 1.0 | 50.1 |
| | P5A | 3.8 | 10.6 | 100.0 | 100.0 | 85.0 | 1.7 | 1.4 | 0.2 | 53.7 | C | 2.0 | 50.1 |
| | P6A | 3.8 | 10.6 | 100.0 | 100.0 | 85.0 | 1.7 | 1.4 | 0.2 | 53.5 | C | 0.5 | 50.1 |
| | P7A | 2.8 | 10.5 | 150.0 | 250.0 | 219.0 | 1.9 | 1.7 | 0.2 | 40.9 | C | 1.0 | 60.0 |
| Cuchiara et al. (2004) | A11 | 2.8 | 10.5 | 150.0 | 250.0 | 219.0 | 1.9 | 1.7 | 0.2 | 43.2 | H | 2.0 | 60.0 |
| | A21 | 2.8 | 10.5 | 150.0 | 250.0 | 219.0 | 1.9 | 1.7 | 0.6 | 40.9 | H | 1.0 | 60.0 |
| | A12 | 3.0 | 8.0 | 200.0 | 300.0 | 262.5 | 2.8 | 2.5 | 0.1 | 52.1 | H | 0.3 | 65.0 |
| Ding et al. (2011) | SFSCCB25-250 | 3.0 | 8.0 | 200.0 | 300.0 | 262.5 | 2.8 | 2.5 | 0.1 | 56.2 | H | 0.5 | 65.0 |
| | SFSCCB50-250 | 3.0 | 8.0 | 200.0 | 300.0 | 262.5 | 2.8 | 2.5 | 0.2 | 52.1 | H | 0.3 | 65.0 |
| | SFSCCB25-150 | 3.0 | 8.0 | 200.0 | 300.0 | 262.5 | 2.8 | 2.5 | 0.2 | 56.2 | H | 0.5 | 65.0 |
| | SFSCCB50-150 | 2.7 | 8.7 | 100.0 | 180.0 | 150.0 | 2.7 | 2.2 | 0.3 | 38.7 | H | 1.0 | 60.0 |
| Lim and Oh (1999) | S0.50V1 | 2.7 | 8.7 | 100.0 | 180.0 | 150.0 | 2.7 | 2.2 | 0.4 | 38.7 | S | 1.0 | 60.0 |
| | S0.75V1 | 2.7 | 8.7 | 100.0 | 180.0 | 150.0 | 2.7 | 2.2 | 0.4 | 42.4 | S | 2.0 | 60.0 |
| | S0.50V2 | 6.5 | 12.9 | 130.0 | 203.2 | 174.2 | 1.0 | 0.9 | 0.3 | 31.2 | S | 0.5 | 100.0 |

Table 3.8. *Deep Beams ( $a/d$ > 2.5 ) without transverse reinforcement*

| $Researcher$ | $Specimen$ | $a/d$ | $l_n/d$ | $b_w$ $(mm)$ | $h$ $(mm)$ | $d$ $(mm)$ | $\rho$ (%) | $\rho'$ (%) | $f_c'$ $(MPa)$ | $Fiber$ Type | $V_f$ (%) | $l_f/d_f$ |
|---|---|---|---|---|---|---|---|---|---|---|---|---|
| Dinh et al. (2010) | B18-1a | 3.4 | 8.2 | 152.0 | 455.0 | 381.0 | 2.0 | 1.6 | 44.8 | H | 0.8 | 55.0 |
| | B18-1b | 3.4 | 8.2 | 152.0 | 455.0 | 381.0 | 2.0 | 1.6 | 44.8 | H | 0.8 | 55.0 |
| | B18-2a | 3.5 | 5.9 | 152.0 | 455.0 | 381.0 | 2.0 | 1.6 | 38.1 | H | 1.0 | 55.0 |
| | B18-2b | 3.5 | 5.9 | 152.0 | 455.0 | 381.0 | 2.0 | 1.6 | 38.1 | H | 1.0 | 55.0 |
| | B18-2c | 3.5 | 5.9 | 152.0 | 455.0 | 381.0 | 2.6 | 2.2 | 38.1 | H | 1.0 | 55.0 |
| | B18-2d | 3.5 | 5.9 | 152.0 | 455.0 | 381.0 | 2.6 | 2.2 | 38.1 | H | 1.0 | 55.0 |
| | B18-3a | 3.4 | 8.2 | 152.0 | 455.0 | 381.0 | 2.6 | 2.2 | 31.0 | H | 1.5 | 55.0 |
| | B18-3b | 3.4 | 8.2 | 152.0 | 455.0 | 381.0 | 2.6 | 2.2 | 31.0 | H | 1.5 | 55.0 |
| | B18-3c | 3.4 | 8.2 | 152.0 | 455.0 | 381.0 | 2.6 | 2.2 | 44.9 | H | 1.5 | 55.0 |
| | B18-3d | 3.4 | 8.2 | 152.0 | 455.0 | 381.0 | 2.6 | 2.2 | 44.9 | H | 1.5 | 55.0 |
| | B18-5a | 3.4 | 8.2 | 152.0 | 455.0 | 381.0 | 2.6 | 2.2 | 49.2 | H | 1.0 | 80.0 |
| | B18-5b | 3.4 | 8.2 | 152.0 | 455.0 | 381.0 | 2.6 | 2.2 | 49.2 | H | 1.0 | 80.0 |
| | B18-7a | 3.4 | 8.2 | 152.0 | 455.0 | 381.0 | 2.0 | 1.6 | 43.3 | H | 0.8 | 80.0 |
| | B18-7b | 3.4 | 8.2 | 152.0 | 455.0 | 381.0 | 2.0 | 1.6 | 43.3 | H | 0.8 | 80.0 |
| | B27-1a | 3.4 | 5.8 | 203.0 | 685.0 | 610.0 | 2.0 | 1.8 | 50.8 | H | 0.8 | 55.0 |
| | B27-1b | 3.4 | 5.8 | 203.0 | 685.0 | 610.0 | 2.0 | 1.8 | 50.8 | H | 0.8 | 55.0 |
| | B27-2a | 3.4 | 5.8 | 203.0 | 685.0 | 610.0 | 2.0 | 1.8 | 28.7 | H | 0.8 | 80.0 |
| | B27-2b | 3.4 | 5.8 | 203.0 | 685.0 | 610.0 | 2.0 | 1.8 | 28.7 | H | 0.8 | 80.0 |
| | B27-3a | 3.5 | 5.8 | 203.0 | 685.0 | 610.0 | 1.5 | 1.4 | 42.3 | H | 0.8 | 55.0 |
| | B27-3b | 3.5 | 5.8 | 203.0 | 685.0 | 610.0 | 1.5 | 1.4 | 42.3 | H | 0.8 | 55.0 |
| | B27-4a | 3.5 | 5.8 | 203.0 | 685.0 | 610.0 | 1.5 | 1.4 | 29.6 | H | 0.8 | 80.0 |
| | B27-4b | 3.5 | 5.8 | 203.0 | 685.0 | 610.0 | 1.5 | 1.4 | 29.6 | H | 0.8 | 80.0 |
| | B27-5 | 3.5 | 5.8 | 203.0 | 685.0 | 610.0 | 2.0 | 1.8 | 44.2 | H | 1.5 | 55.0 |
| | B27-6 | 3.5 | 5.8 | 203.0 | 685.0 | 610.0 | 2.0 | 1.8 | 42.8 | H | 1.5 | 80.0 |
| Lim et al. (1987) | 2/1,0/3,5 | 3.5 | 9.5 | 152.0 | 254.0 | 221.0 | 1.2 | 1.0 | 34.0 | H | 1.0 | 60.0 |
| | 2/0,5/3,5 | 3.5 | 9.5 | 152.0 | 254.0 | 221.0 | 1.2 | 1.0 | 34.0 | H | 0.5 | 60.0 |
| | 4/1,0/3,5 | 3.5 | 9.5 | 152.0 | 254.0 | 221.0 | 2.4 | 2.1 | 34.0 | H | 1.0 | 60.0 |

Table 3.8. *Deep Beams ( $a/d$ > 2.5 ) without transverse reinforcement (continued)*

| $Researcher$ | $Specimen$ | $a/d$ | $l_n/d$ | $b_w$ $(mm)$ | $h$ $(mm)$ | $d$ $(mm)$ | $\rho$ (%) | $\rho'$ (%) | $f_c'$ $(MPa)$ | $Fiber$ Type | $V_f$ (%) | $l_f/d_f$ |
|---|---|---|---|---|---|---|---|---|---|---|---|---|
| Lim et al. (1987) | 4/0,5/3,5 | 254.0 | 221.0 | 2.4 | 2.1 | 34.0 | 254.0 | 221.0 | 2.4 | H | 0.5 | 60.0 |
| Cuchiara et al. (2004) | A10 | 240.0 | 219.0 | 1.9 | 1.7 | 40.9 | 240.0 | 219.0 | 1.9 | H | 1.0 | 60.0 |
| | A20 | 240.0 | 219.0 | 1.9 | 1.7 | 43.2 | 240.0 | 219.0 | 1.9 | H | 2.0 | 60.0 |
| Cohen (2012) | M15-0.5% | 250.0 | 212.5 | 1.3 | 1.1 | 59.4 | 250.0 | 212.5 | 1.3 | H | 0.5 | 55.0 |
| | M15-1.0% | 250.0 | 212.5 | 1.3 | 1.1 | 51.5 | 250.0 | 212.5 | 1.3 | H | 1.0 | 55.0 |
| | M15-1.5% | 250.0 | 212.5 | 1.3 | 1.1 | 55.8 | 250.0 | 212.5 | 1.3 | H | 1.5 | 55.0 |
| | M15-0.5%H | 250.0 | 212.5 | 1.3 | 1.1 | 49.6 | 250.0 | 212.5 | 1.3 | H | 0.5 | 80.0 |
| | M15-0.75%H | 250.0 | 212.5 | 1.3 | 1.1 | 45.9 | 250.0 | 212.5 | 1.3 | H | 0.8 | 80.0 |
| | M20-0.75% | 250.0 | 210.0 | 2.4 | 2.0 | 44.7 | 250.0 | 210.0 | 2.4 | H | 0.8 | 55.0 |
| | M20-1.0% | 250.0 | 210.0 | 2.4 | 2.0 | 45.0 | 250.0 | 210.0 | 2.4 | H | 1.0 | 55.0 |
| | M20-1.0%A | 250.0 | 210.0 | 2.4 | 2.0 | 54.5 | 250.0 | 210.0 | 2.4 | H | 1.0 | 55.0 |
| | M20-1.5%A | 250.0 | 210.0 | 2.4 | 2.0 | 52.6 | 250.0 | 210.0 | 2.4 | H | 1.5 | 55.0 |
| | M20-1.0%B | 250.0 | 210.0 | 2.4 | 2.0 | 50.5 | 250.0 | 210.0 | 2.4 | H | 1.0 | 55.0 |
| | M20-1.5%B | 250.0 | 210.0 | 2.4 | 2.0 | 51.5 | 250.0 | 210.0 | 2.4 | H | 1.5 | 55.0 |
| Şen (2005) | BEAM-04 | 250.0 | 215.0 | 1.5 | 1.3 | 60.2 | 250.0 | 215.0 | 1.5 | H | 0.5 | 65.0 |
| | BEAM-06 | 250.0 | 215.0 | 1.5 | 1.3 | 61.7 | 250.0 | 215.0 | 1.5 | H | 0.8 | 65.0 |
| | BEAM-08 | 250.0 | 215.0 | 1.5 | 1.3 | 60.9 | 250.0 | 215.0 | 1.5 | H | 0.5 | 80.0 |
| | BEAM-10 | 250.0 | 215.0 | 1.5 | 1.3 | 63.6 | 250.0 | 215.0 | 1.5 | H | 0.8 | 80.0 |
| Kwak et al. (2002) | FHB2-3 | 250.0 | 212.0 | 1.5 | 1.3 | 63.8 | 250.0 | 212.0 | 1.5 | H | 0.5 | 62.5 |
| | FHB3-3 | 250.0 | 212.0 | 1.5 | 1.3 | 68.6 | 250.0 | 212.0 | 1.5 | H | 0.8 | 62.5 |
| | FNB2-3 | 250.0 | 212.0 | 1.5 | 1.3 | 30.8 | 250.0 | 212.0 | 1.5 | H | 0.5 | 62.5 |
| | FHB2-4 | 250.0 | 212.0 | 1.5 | 1.3 | 63.8 | 250.0 | 212.0 | 1.5 | H | 0.5 | 62.5 |
| | FHB3-4 | 250.0 | 212.0 | 1.5 | 1.3 | 68.6 | 250.0 | 212.0 | 1.5 | H | 0.8 | 62.5 |
| | FNB2-4 | 250.0 | 212.0 | 1.5 | 1.3 | 30.8 | 250.0 | 212.0 | 1.5 | H | 0.5 | 62.5 |

Table 3.8. *Deep Beams ( $a/d$ > 2.5 ) without transverse reinforcement (continued)*

| *Researcher* | *Specimen* | $a/d$ | $l_n/d$ | $b_w$ $(mm)$ | $h$ $(mm)$ | $d$ $(mm)$ | $\rho$ (%) | $\rho'$ (%) | $f_c'$ $(MPa)$ | *Fiber* Type | $V_f$ (%) | $l_f/d_f$ |
|---|---|---|---|---|---|---|---|---|---|---|---|---|
| Rosenbusch and Teutsch (2003) | 1.2/2 | 300.0 | 260.0 | 3.6 | 3.1 | 46.9 | 300.0 | 260.0 | 3.6 | H | 0.3 | 65.0 |
| | 1.2/3 | 300.0 | 260.0 | 3.6 | 3.1 | 43.7 | 300.0 | 260.0 | 3.6 | H | 0.5 | 65.0 |
| | 1.2/4 | 300.0 | 260.0 | 3.6 | 3.1 | 48.3 | 300.0 | 260.0 | 3.6 | H | 0.8 | 65.0 |
| | 2.6/2 | 300.0 | 260.0 | 1.8 | 1.6 | 41.2 | 300.0 | 260.0 | 1.8 | H | 0.3 | 65.0 |
| | 2.6/3 | 300.0 | 260.0 | 1.8 | 1.6 | 40.3 | 300.0 | 260.0 | 1.8 | H | 0.8 | 65.0 |
| | 3.1/1 | 300.0 | 260.0 | 2.8 | 2.5 | 37.7 | 300.0 | 260.0 | 2.8 | H | 0.5 | 65.0 |
| | 3.1/1 F2 | 300.0 | 260.0 | 2.8 | 2.5 | 38.8 | 300.0 | 260.0 | 2.8 | H | 0.5 | 65.0 |
| Dupont and Vandewalle (2003) | 2 | 300.0 | 260.0 | 3.6 | 3.1 | 46.4 | 300.0 | 260.0 | 3.6 | H | 0.3 | 65.0 |
| | 3 | 300.0 | 260.0 | 3.6 | 3.1 | 43.2 | 300.0 | 260.0 | 3.6 | H | 0.5 | 65.0 |
| | 4 | 300.0 | 260.0 | 3.6 | 3.1 | 47.6 | 300.0 | 260.0 | 3.6 | H | 0.8 | 65.0 |
| | 23 | 300.0 | 260.0 | 1.8 | 1.6 | 40.7 | 300.0 | 260.0 | 1.8 | H | 0.3 | 65.0 |
| | 24 | 300.0 | 260.0 | 1.8 | 1.6 | 42.4 | 300.0 | 260.0 | 1.8 | H | 0.8 | 65.0 |
| Imam et al. (1994) | B4 | 350.0 | 300.0 | 1.9 | 1.6 | 109.0 | 350.0 | 300.0 | 1.9 | H | 0.8 | 75.0 |
| | B11 | 350.0 | 300.0 | 1.9 | 1.6 | 110.5 | 350.0 | 300.0 | 1.9 | H | 0.8 | 75.0 |
| | B7 | 350.0 | 300.0 | 3.1 | 2.6 | 111.5 | 350.0 | 300.0 | 3.1 | H | 0.8 | 75.0 |
| | B12 | 350.0 | 300.0 | 3.1 | 2.6 | 110.8 | 350.0 | 300.0 | 3.1 | H | 0.8 | 75.0 |
| Aoude et al. (2012) | A0.5 | 250.0 | 202.0 | 1.2 | 0.9 | 21.3 | 250.0 | 202.0 | 1.2 | H | 0.5 | 55.0 |
| | A1 | 250.0 | 202.0 | 1.2 | 0.9 | 19.6 | 250.0 | 202.0 | 1.2 | H | 1.0 | 55.0 |
| | B0.5 | 500.0 | 437.0 | 1.5 | 1.3 | 21.3 | 500.0 | 437.0 | 1.5 | H | 0.5 | 55.0 |
| | B1 | 500.0 | 437.0 | 1.5 | 1.3 | 19.6 | 500.0 | 437.0 | 1.5 | H | 1.0 | 55.0 |
| Ashour et al. (1992) | B-4-1 .0-L | 250.0 | 215.0 | 0.4 | 0.3 | 92.6 | 250.0 | 215.0 | 0.4 | H | 1.0 | 75.0 |
| | B-6-l.O-L | 250.0 | 215.0 | 0.4 | 0.3 | 93.7 | 250.0 | 215.0 | 0.4 | H | 1.0 | 75.0 |
| | B-4-0.5-A | 250.0 | 215.0 | 2.8 | 2.4 | 95.1 | 250.0 | 215.0 | 2.8 | H | 0.5 | 75.0 |
| | B-6-0.5-A | 250.0 | 215.0 | 2.8 | 2.4 | 95.8 | 250.0 | 215.0 | 2.8 | H | 0.5 | 75.0 |
| | B-4-l.O-A | 250.0 | 215.0 | 2.8 | 2.4 | 97.5 | 250.0 | 215.0 | 2.8 | H | 1.0 | 75.0 |
| | B-6-l.O-A | 250.0 | 215.0 | 2.8 | 2.4 | 100.5 | 250.0 | 215.0 | 2.8 | H | 1.0 | 75.0 |
| | B-4-1.5-A | 250.0 | 215.0 | 2.8 | 2.4 | 97.1 | 250.0 | 215.0 | 2.8 | H | 1.5 | 75.0 |

Table 3.8. *Deep Beams ( $a/d$ > 2.5 ) without transverse reinforcement (continued)*

| $Researcher$ | $Specimen$ | $a/d$ | $l_n/d$ | $b_w$ $(mm)$ | $h$ $(mm)$ | $d$ $(mm)$ | $\rho$ (%) | $\rho'$ (%) | $f_c'$ $(MPa)$ | $Fiber$ Type | $V_f$ (%) | $l_f/d_f$ |
|---|---|---|---|---|---|---|---|---|---|---|---|---|
| Ashour et al. (1992) | B-6-1.5-A | 6.0 | 14.3 | 125.0 | 250.0 | 215.0 | 2.8 | 2.4 | 101.3 | H | 1.5 | 75.0 |
| | B-4-l.O-M | 4.0 | 10.3 | 125.0 | 250.0 | 215.0 | 4.6 | 3.9 | 93.8 | H | 1.0 | 75.0 |
| | B-6-l.O-M | 6.0 | 14.3 | 125.0 | 250.0 | 215.0 | 4.6 | 3.9 | 95.0 | H | 1.0 | 75.0 |
| Ding et al. (2012) | SF20-0 | 4.0 | 9.3 | 100.0 | 150.0 | 122.0 | 3.3 | 2.7 | 36.0 | H | 0.3 | 80.0 |
| | SF40-0 | 4.0 | 9.3 | 100.0 | 150.0 | 122.0 | 3.3 | 2.7 | 32.5 | H | 0.5 | 80.0 |
| | SF60-0 | 4.0 | 9.3 | 100.0 | 150.0 | 122.0 | 3.3 | 2.7 | 41.2 | H | 0.8 | 80.0 |
| Furlan and Hanai (1997) | P3B | 3.8 | 10.6 | 100.0 | 100.0 | 85.0 | 1.7 | 1.4 | 54.8 | C | 1.0 | 33.0 |
| | P4B | 3.8 | 10.6 | 100.0 | 100.0 | 85.0 | 1.7 | 1.4 | 50.0 | C | 2.0 | 33.0 |
| | P5B | 3.8 | 10.6 | 100.0 | 100.0 | 85.0 | 1.7 | 1.4 | 49.3 | C | 1.0 | 50.0 |
| | P6B | 3.8 | 10.6 | 100.0 | 100.0 | 85.0 | 1.7 | 1.4 | 53.7 | C | 2.0 | 50.0 |
| | P7B | 3.8 | 10.6 | 100.0 | 100.0 | 85.0 | 1.7 | 1.4 | 53.5 | C | 0.5 | 50.0 |
| Shin et al. (1994) | 3 | 3.0 | 6.0 | 100.0 | 200.0 | 175.0 | 3.6 | 3.1 | 80.0 | S | 0.5 | 100.0 |
| | 4 | 3.0 | 6.0 | 100.0 | 200.0 | 175.0 | 3.6 | 3.1 | 80.0 | S | 1.0 | 100.0 |
| | 5 | 4.5 | 9.0 | 100.0 | 200.0 | 175.0 | 3.6 | 3.1 | 80.0 | S | 0.5 | 100.0 |
| | 6 | 4.5 | 9.0 | 100.0 | 200.0 | 175.0 | 3.6 | 3.1 | 80.0 | S | 1.0 | 100.0 |
| Mansur et al. (1986) | B2 | 2.8 | 10.2 | 150.0 | 225.0 | 197.0 | 1.4 | 1.2 | 29.1 | H | 0.5 | 60.0 |
| | B3 | 3.6 | 10.2 | 150.0 | 225.0 | 197.0 | 1.4 | 1.2 | 29.1 | H | 0.5 | 60.0 |
| | B4 | 4.4 | 10.2 | 150.0 | 225.0 | 197.0 | 1.4 | 1.2 | 29.1 | H | 0.5 | 60.0 |
| | C2 | 2.8 | 10.2 | 150.0 | 225.0 | 197.0 | 1.4 | 1.2 | 29.9 | H | 0.8 | 60.0 |
| | C3 | 3.6 | 10.2 | 150.0 | 225.0 | 197.0 | 1.4 | 1.2 | 29.9 | H | 0.8 | 60.0 |
| | C4 | 4.4 | 10.2 | 150.0 | 225.0 | 197.0 | 1.4 | 1.2 | 29.9 | H | 0.8 | 60.0 |
| | C5 | 2.8 | 12.5 | 150.0 | 225.0 | 200.0 | 0.8 | 0.7 | 29.9 | H | 0.8 | 60.0 |
| | C6 | 2.8 | 10.2 | 150.0 | 225.0 | 197.0 | 2.0 | 1.8 | 29.9 | H | 0.8 | 60.0 |
| | D2 | 2.8 | 10.2 | 150.0 | 225.0 | 197.0 | 1.4 | 1.2 | 30.0 | H | 1.0 | 60.0 |
| | D3 | 3.6 | 10.2 | 150.0 | 225.0 | 197.0 | 1.4 | 1.2 | 30.0 | H | 1.0 | 60.0 |
| | D4 | 4.4 | 10.2 | 150.0 | 225.0 | 197.0 | 1.4 | 1.2 | 30.0 | H | 1.0 | 60.0 |
| | E1 | 2.8 | 12.5 | 150.0 | 225.0 | 200.0 | 0.8 | 0.7 | 20.6 | H | 0.8 | 60.0 |

Table 3.8. *Deep Beams ( $a/d$ > 2.5 ) without transverse reinforcement (continued)*

| $Researcher$ | $Specimen$ | $a/d$ | $l_n/d$ | $b_w$ $(mm)$ | $h$ $(mm)$ | $d$ $(mm)$ | $\rho$ (%) | $\rho'$ (%) | $f_c'$ $(MPa)$ | $Fiber$ Type | $V_f$ (%) | $l_f/d_f$ |
|---|---|---|---|---|---|---|---|---|---|---|---|---|
| Mansur et al. (1986) | E2 | 2.8 | 10.2 | 150.0 | 225.0 | 197.0 | 1.4 | 1.2 | 20.6 | H | 0.8 | 60.0 |
| | E3 | 2.8 | 10.2 | 150.0 | 225.0 | 197.0 | 2.0 | 1.8 | 20.6 | H | 0.8 | 60.0 |
| | F1 | 2.8 | 12.5 | 150.0 | 225.0 | 200.0 | 0.8 | 0.7 | 33.4 | H | 0.8 | 60.0 |
| | F2 | 2.8 | 10.2 | 150.0 | 225.0 | 197.0 | 1.4 | 1.2 | 33.4 | H | 0.8 | 60.0 |
| | F3 | 2.8 | 10.2 | 150.0 | 225.0 | 197.0 | 2.0 | 1.8 | 33.4 | H | 0.8 | 60.0 |
| Shoaib et al. (2014) | N31 | 3.0 | 6.0 | 310.0 | 308.0 | 258.0 | 2.5 | 2.1 | 23.0 | H | 1.0 | 55.0 |
| | N32 | 3.0 | 6.0 | 310.0 | 308.0 | 240.0 | 4.0 | 3.1 | 41.0 | H | 1.0 | 55.0 |
| | H31 | 3.0 | 6.0 | 310.0 | 308.0 | 258.0 | 2.5 | 2.1 | 41.0 | H | 1.0 | 55.0 |
| | H32 | 3.0 | 6.0 | 310.0 | 308.0 | 240.0 | 4.0 | 3.1 | 80.0 | H | 1.0 | 55.0 |
| | N61 | 3.0 | 6.0 | 300.0 | 600.0 | 531.0 | 1.8 | 1.6 | 23.0 | H | 1.0 | 55.0 |
| | N62 | 3.0 | 6.0 | 300.0 | 600.0 | 523.0 | 2.5 | 2.2 | 23.0 | H | 1.0 | 55.0 |
| | E2 | 3.0 | 6.0 | 300.0 | 600.0 | 531.0 | 1.8 | 1.6 | 41.0 | H | 1.0 | 55.0 |
| | E3 | 3.0 | 6.0 | 300.0 | 600.0 | 523.0 | 2.5 | 2.2 | 41.0 | H | 1.0 | 55.0 |
| | F1 | 3.0 | 6.0 | 300.0 | 1000.0 | 923.0 | 1.4 | 1.3 | 41.0 | H | 1.0 | 55.0 |
| | F2 | 3.0 | 6.0 | 300.0 | 1000.0 | 920.0 | 2.0 | 1.9 | 41.0 | H | 1.0 | 55.0 |
| | F3 | 3.0 | 6.0 | 300.0 | 1000.0 | 923.0 | 1.4 | 1.3 | 80.0 | H | 1.0 | 55.0 |
| | N31 | 3.0 | 6.0 | 300.0 | 1000.0 | 920.0 | 2.0 | 1.9 | 80.0 | H | 1.0 | 55.0 |
| Noghabai (2000) | 3typeB | 2.8 | 5.5 | 200.0 | 300.0 | 235.0 | 4.3 | 3.4 | 91.4 | H | 1.0 | 50.0 |
| | 5 type A | 3.3 | 6.7 | 200.0 | 250.0 | 180.0 | 4.5 | 3.2 | 80.5 | H | 0.5 | 86.0 |
| | 6 type A | 3.3 | 6.7 | 200.0 | 250.0 | 180.0 | 4.5 | 3.2 | 80.5 | H | 0.8 | 86.0 |
| | 7 type C | 2.9 | 7.3 | 200.0 | 500.0 | 410.0 | 2.0 | 1.6 | 69.3 | H | 0.5 | 86.0 |
| | 8 type C | 2.9 | 7.3 | 200.0 | 500.0 | 410.0 | 3.1 | 2.5 | 69.3 | H | 0.5 | 86.0 |
| | 9 type C | 2.9 | 7.3 | 200.0 | 500.0 | 410.0 | 3.1 | 2.5 | 60.2 | H | 0.8 | 86.0 |
| | 10 type C | 2.9 | 7.3 | 200.0 | 500.0 | 410.0 | 3.1 | 2.5 | 75.7 | H | 0.8 | 86.0 |
| | 4 type D | 3.0 | 8.8 | 300.0 | 700.0 | 570.0 | 2.9 | 2.3 | 60.2 | H | 0.8 | 86.0 |
| Majdzadeh et al. (2006) | B12 | 3.0 | 6.7 | 150.0 | 150.0 | 120.0 | 2.6 | 2.1 | 45.5 | H | 0.5 | 80.0 |
| | B13 | 3.0 | 6.7 | 150.0 | 150.0 | 120.0 | 2.6 | 2.1 | 44.6 | H | 1.0 | 80.0 |

Table 3.8. *Deep Beams ( $a/d$ > 2.5 ) without transverse reinforcement (continued)*

| $Researcher$ | $Specimen$ | $a/d$ | $l_n/d$ | $b_w$ $(mm)$ | $h$ $(mm)$ | $d$ $(mm)$ | $\rho$ (%) | $\rho'$ (%) | $f_c'$ $(MPa)$ | $Fiber$ Type | $V_f$ (%) | $l_f/d_f$ |
|---|---|---|---|---|---|---|---|---|---|---|---|---|
| Majdzadeh et al. (2006) | B14 | 150.0 | 150.0 | 120.0 | 2.6 | 2.1 | 40.9 | 150.0 | 150.0 | H | 1.5 | 80.0 |
| Ding et al. (2011) | SFSCCB25-∞ | 200.0 | 300.0 | 262.5 | 2.8 | 2.5 | 52.1 | 200.0 | 300.0 | H | 0.3 | 65.0 |
| | SFSCCB50-∞ | 200.0 | 300.0 | 262.5 | 2.8 | 2.5 | 56.2 | 200.0 | 300.0 | H | 0.6 | 65.0 |
| Li et al. (1992) | M1 | 63.5 | 127.0 | 102.0 | 2.4 | 1.9 | 53.0 | 63.5 | 127.0 | C | 1.0 | 28.5 |
| | M2 | 127.0 | 228.0 | 204.0 | 2.2 | 2.0 | 53.0 | 127.0 | 228.0 | C | 1.0 | 28.5 |
| | M3 | 63.5 | 127.0 | 102.0 | 2.4 | 1.9 | 50.2 | 63.5 | 127.0 | C | 2.0 | 28.5 |
| | M4 | 127.0 | 228.0 | 204.0 | 2.2 | 2.0 | 50.2 | 127.0 | 228.0 | C | 2.0 | 28.5 |
| | M5 | 63.5 | 127.0 | 102.0 | 2.4 | 1.9 | 62.6 | 63.5 | 127.0 | C | 1.0 | 28.5 |
| | M6 | 127.0 | 228.0 | 204.0 | 2.2 | 2.0 | 62.6 | 127.0 | 228.0 | C | 1.0 | 28.5 |
| | M7 | 63.5 | 127.0 | 102.0 | 2.4 | 1.9 | 57.0 | 63.5 | 127.0 | C | 2.0 | 28.5 |
| | M8 | 63.5 | 127.0 | 102.0 | 2.4 | 1.9 | 62.6 | 63.5 | 127.0 | C | 1.0 | 57.0 |
| | M9 | 127.0 | 228.0 | 204.0 | 2.2 | 2.0 | 62.6 | 127.0 | 228.0 | C | 1.0 | 57.0 |
| | M10 | 127.0 | 228.0 | 204.0 | 2.2 | 2.0 | 57.0 | 127.0 | 228.0 | C | 2.0 | 57.0 |
| | M17 | 63.5 | 127.0 | 102.0 | 2.4 | 1.9 | 62.6 | 63.5 | 127.0 | C | 1.0 | 28.5 |
| | M18 | 63.5 | 127.0 | 102.0 | 1.2 | 1.0 | 62.6 | 63.5 | 127.0 | C | 1.0 | 28.5 |
| | M19 | 63.5 | 127.0 | 102.0 | 3.6 | 2.9 | 62.6 | 63.5 | 127.0 | C | 1.0 | 28.5 |
| | M20 | 63.5 | 127.0 | 102.0 | 3.6 | 2.9 | 54.1 | 63.5 | 127.0 | C | 1.0 | 57.0 |
| | C1 | 127.0 | 228.0 | 204.0 | 2.2 | 2.0 | 22.7 | 127.0 | 228.0 | H | 1.0 | 60.0 |
| | C2 | 63.5 | 127.0 | 102.0 | 2.4 | 1.9 | 22.7 | 63.5 | 127.0 | H | 1.0 | 60.0 |
| | C3 | 63.5 | 127.0 | 102.0 | 1.2 | 1.0 | 22.7 | 63.5 | 127.0 | H | 1.0 | 60.0 |
| | C5 | 127.0 | 228.0 | 204.0 | 2.2 | 2.0 | 26.0 | 127.0 | 228.0 | H | 1.0 | 100.0 |
| | C6 | 63.5 | 127.0 | 102.0 | 2.4 | 1.9 | 26.0 | 63.5 | 127.0 | H | 1.0 | 100.0 |

Table 3.8. *Deep Beams ( $a/d$ > 2.5 ) without transverse reinforcement (continued)*

| $Researcher$ | $Specimen$ | $a/d$ | $l_n/d$ | $b_w$ $(mm)$ | $h$ $(mm)$ | $d$ $(mm)$ | $\rho$ (%) | $\rho'$ (%) | $f_c'$ $(MPa)$ | $Fiber$ Type | $V_f$ (%) | $l_f/d_f$ |
|---|---|---|---|---|---|---|---|---|---|---|---|---|
| Greenough and Nehdi (2008) | S-HE-50-0.5 | 200.0 | 300.0 | 265.0 | 1.8 | 1.6 | 47.9 | 200.0 | 300.0 | H | 0.5 | 50.0 |
| | S-HE-50-0.75 | 200.0 | 300.0 | 265.0 | 1.8 | 1.6 | 38.0 | 200.0 | 300.0 | H | 0.8 | 50.0 |
| | S-HE-50-1.0 | 200.0 | 300.0 | 265.0 | 1.8 | 1.6 | 42.2 | 200.0 | 300.0 | H | 1.0 | 50.0 |
| | S-FE-50-0.5 | 200.0 | 300.0 | 265.0 | 1.8 | 1.6 | 45.4 | 200.0 | 300.0 | F | 0.5 | 50.0 |
| | S-FE-50-0.75 | 200.0 | 300.0 | 265.0 | 1.8 | 1.6 | 44.4 | 200.0 | 300.0 | F | 0.8 | 50.0 |
| | S-FE-50-1.0 | 200.0 | 300.0 | 265.0 | 1.8 | 1.6 | 40.3 | 200.0 | 300.0 | F | 1.0 | 50.0 |
| | S-FE-30-0.5 | 200.0 | 300.0 | 265.0 | 1.8 | 1.6 | 53.7 | 200.0 | 300.0 | F | 0.5 | 43.0 |
| | S-FE-30-0.75 | 200.0 | 300.0 | 265.0 | 1.8 | 1.6 | 46.0 | 200.0 | 300.0 | F | 0.8 | 43.0 |
| | S-FE-30-1.0 | 200.0 | 300.0 | 265.0 | 1.8 | 1.6 | 42.2 | 200.0 | 300.0 | F | 1.0 | 43.0 |

Table 3.9. *FRC Coupling Beams with transverse reinforcement*

| $Researcher$ | $Specimen$ | $l_n/d$ | $b_w$ $(mm)$ | $h$ $(mm)$ | $d$ $(mm)$ | $\rho$ (%) | $\rho'$ (%) | $\rho_t$ (%) | $f_c'$ $(MPa)$ | $Fiber$ Type | $V_f$ (%) | $l_f/d_f$ |
|---|---|---|---|---|---|---|---|---|---|---|---|---|
| Cai et al. (2016) | CCB3-30-2-1F-S | 2.2 | 150.0 | 400.0 | 359.0 | 6.0 | 5.4 | 0.6 | 40.5 | S | 1.0 | 42.0 |
| | CCB3-40-2-1F-S | 2.2 | 150.0 | 400.0 | 359.0 | 6.0 | 5.4 | 0.6 | 43.1 | S | 1.0 | 42.0 |
| | CCB3-50-2-1F-S | 2.2 | 150.0 | 400.0 | 359.0 | 6.0 | 5.4 | 0.6 | 52.9 | S | 1.0 | 42.0 |
| | CCB3-60-2-1F-S | 2.2 | 150.0 | 400.0 | 359.0 | 6.0 | 5.4 | 0.6 | 66.7 | S | 1.0 | 42.0 |
| | CCB3-70-2-1F-S | 2.2 | 150.0 | 400.0 | 359.0 | 6.0 | 5.4 | 0.6 | 70.1 | S | 1.0 | 42.0 |
| | CCB3-80-2-1F-S | 2.2 | 150.0 | 400.0 | 359.0 | 6.0 | 5.4 | 0.6 | 80.7 | S | 1.0 | 42.0 |
| | CCB3-40-1-1F-S | 1.1 | 150.0 | 400.0 | 359.0 | 6.0 | 5.4 | 0.6 | 43.1 | S | 1.0 | 42.0 |
| | CCB3-40-1.5-1F-S | 1.7 | 150.0 | 400.0 | 359.0 | 6.0 | 5.4 | 0.6 | 43.1 | S | 1.0 | 42.0 |
| | CCB3-40-2.5-1F-F/S | 2.8 | 150.0 | 400.0 | 359.0 | 6.0 | 5.4 | 0.6 | 43.1 | S | 1.0 | 42.0 |
| | CCB3-40-3.0-1F-F/S | 3.3 | 150.0 | 400.0 | 359.0 | 6.0 | 5.4 | 0.6 | 43.1 | S | 1.0 | 42.0 |
| | CCB3-40-3.5-1F-F | 3.9 | 150.0 | 400.0 | 359.0 | 6.0 | 5.4 | 0.6 | 43.1 | S | 1.0 | 42.0 |
| | CCB3-50-2-0.5F-S | 2.2 | 150.0 | 400.0 | 359.0 | 6.0 | 5.4 | 0.6 | 54.5 | S | 0.5 | 42.0 |
| | CCB3-55-2-1F-S | 2.2 | 150.0 | 400.0 | 359.0 | 6.0 | 5.4 | 0.6 | 54.8 | S | 1.0 | 42.0 |
| | CCB3-50-2-1.5F-S | 2.2 | 150.0 | 400.0 | 359.0 | 6.0 | 5.4 | 0.6 | 55.9 | S | 1.5 | 42.0 |
| | CCB3-50-2-2F-S | 2.2 | 150.0 | 400.0 | 359.0 | 6.0 | 5.4 | 0.6 | 55.3 | S | 2.0 | 42.0 |
| | CCB3-50-2.5F-F/S | 2.2 | 150.0 | 400.0 | 359.0 | 6.0 | 5.4 | 0.6 | 54.1 | S | 2.5 | 42.0 |
| Baczkowski (2007) | C-10/M | 1.1 | 100.0 | 400.0 | 360.0 | 1.7 | 1.6 | 0.6 | 33.7 | H | 1.0 | 47.6 |
| | C-15/M | 1.7 | 100.0 | 400.0 | 360.0 | 1.7 | 1.6 | 0.6 | 32.8 | H | 1.0 | 47.6 |
| | C-15/S | 1.7 | 100.0 | 400.0 | 360.0 | 1.7 | 1.6 | 1.1 | 31.9 | H | 1.0 | 47.6 |
| | C-20/M | 2.2 | 100.0 | 400.0 | 360.0 | 1.7 | 1.6 | 0.6 | 32.2 | H | 1.0 | 47.6 |
| | C-30/M | 3.1 | 100.0 | 300.0 | 260.0 | 2.4 | 2.1 | 0.6 | 31.4 | H | 1.0 | 47.6 |
| Pérez-Irizarry and Parra-Montesinos (2016) | CB1 | 3.4 | 152.4 | 457.2 | 412.8 | 3.0 | 2.7 | 1.0 | 53.7 | H | 1.3 | 64.0 |
| | CB2 | 3.4 | 152.4 | 457.2 | 412.8 | 2.1 | 1.9 | 1.0 | 59.9 | H | 1.3 | 64.0 |
| | CB3 | 3.4 | 152.4 | 457.2 | 412.8 | 2.1 | 1.9 | 1.0 | 58.5 | H | 1.3 | 55.0 |
| | CB4 | 3.4 | 152.4 | 457.2 | 412.8 | 1.8 | 1.7 | 1.0 | 63.3 | H | 1.0 | 55.0 |
| | CB5 | 3.4 | 152.4 | 457.2 | 412.8 | 1.8 | 1.7 | 1.0 | 67.5 | H | 1.0 | 79.0 |
| | CB6 | 2.4 | 152.4 | 457.2 | 393.7 | 1.1 | 1.0 | 1.2 | 57.4 | H | 1.5 | 64.0 |
| | CB7 | 2.4 | 152.4 | 457.2 | 393.7 | 1.1 | 1.0 | 1.2 | 70.4 | H | 1.5 | 79.0 |
| | CB8 | 2.4 | 152.4 | 457.2 | 393.7 | 1.1 | 1.0 | 1.2 | 58.7 | H | 1.5 | 79.0 |

Table 3.10. *FRC Coupling Beams without transverse reinforcement*

| $Researcher$ | $Specimen$ | $l_n/d$ | $b_w$ $(mm)$ | $h$ $(mm)$ | $d$ $(mm)$ | $\rho$ (%) | $\rho'$ (%) | $f_c'$ $(MPa)$ | $Fiber$ Type | $V_f$ (%) | $l_f/d_f$ |
|---|---|---|---|---|---|---|---|---|---|---|---|
| Adebar et al. (1997) | FC2 | 2.7 | 150.0 | 610.0 | 559.5 | 2.2 | 2.1 | 54.1 | H | 0.8 | 60.0 |
| | FC3 | 2.7 | 150.0 | 610.0 | 559.5 | 2.2 | 2.1 | 49.9 | H | 1.5 | 60.0 |
| | FC5 | 2.7 | 150.0 | 610.0 | 559.5 | 2.2 | 2.1 | 54.1 | H | 0.8 | 60.0 |
| | FC6 | 2.7 | 150.0 | 610.0 | 559.5 | 2.2 | 2.1 | 49.9 | H | 1.5 | 60.0 |
| | FC8 | 2.7 | 150.0 | 610.0 | 559.5 | 2.2 | 2.1 | 54.8 | H | 0.4 | 60.0 |
| | FC9 | 2.7 | 150.0 | 610.0 | 559.5 | 2.2 | 2.1 | 56.5 | H | 0.6 | 60.0 |
| | FC10 | 2.7 | 150.0 | 610.0 | 559.5 | 2.2 | 2.1 | 46.9 | H | 0.4 | 100.0 |
| | FC11 | 2.7 | 150.0 | 610.0 | 559.5 | 2.2 | 2.1 | 40.8 | H | 0.6 | 100.0 |

Table 3.11. *HPFRC Coupling Beams with transverse reinforcement*

| *Researcher* | *Specimen* | $l_n/d$ | $b_w$ $(mm)$ | $h$ $(mm)$ | $d$ $(mm)$ | $\rho$ (%) | $\rho'$ (%) | $\rho_t$ (%) | $\rho_d$ (%) | $f_c'$ $(MPa)$ | *Fiber* Type | $V_f$ (%) | $l_f/d_f$ |
|---|---|---|---|---|---|---|---|---|---|---|---|---|---|
| Shin et al. (2014) | 1CF2Y | 4.2 | 250.0 | 300.0 | 250.0 | 3.2 | 2.7 | 1.4 | 0.0 | 49.2 | PVA | 2.0 | 307.7 |
| | 1DF2Y | 4.2 | 250.0 | 300.0 | 250.0 | 1.1 | 0.9 | 0.9 | 1.5 | 49.2 | PVA | 2.0 | 307.7 |
| Yun et al. (2008) | CB2 | 1.1 | 200.0 | 600.0 | 570.0 | 0.5 | 0.4 | 0.2 | 2.0 | 57.0 | PE+T | 0.75+0.75 | 342.1+100 |
| | CB3 | 1.1 | 200.0 | 600.0 | 570.0 | 0.5 | 0.4 | 0.2 | 0.0 | 57.0 | PE+T | 0.75+0.75 | 342.1+100 |
| Setkit (2012) | CB-1 | 2.9 | 152.4 | 609.6 | 571.5 | 1.8 | 1.7 | 0.5 | 3.7 | 49.6 | H | 1.5 | 80.0 |
| | CB-2 | 2.9 | 152.4 | 609.6 | 571.5 | 1.1 | 1.0 | 0.6 | 3.7 | 59.0 | H | 1.5 | 80.0 |
| | CB-3 | 3.6 | 152.4 | 508.0 | 469.9 | 1.5 | 1.4 | 0.6 | 3.1 | 61.0 | H | 1.5 | 80.0 |
| | CB-5 | 3.6 | 152.4 | 508.0 | 469.9 | 3.0 | 2.8 | 1.1 | 0.0 | 68.0 | H | 1.5 | 80.0 |
| | CB-6 | 2.9 | 152.4 | 609.6 | 571.5 | 2.3 | 2.1 | 1.1 | 0.0 | 67.6 | H | 1.5 | 80.0 |
| Canbolat (2004) | Specimen 2 | 1.1 | 150.0 | 600.0 | 570.0 | 0.8 | 0.8 | 0.3 | 0.0 | 57.0 | PE | 2.0 | 342.1 |
| | Specimen 3 | 1.1 | 150.0 | 600.0 | 570.0 | 0.6 | 0.6 | 0.3 | 3.7 | 57.0 | PE | 2.0 | 342.1 |
| | Specimen 4 | 1.1 | 150.0 | 600.0 | 565.0 | 0.6 | 0.6 | 0.5 | 1.5 | 63.4 | T | 1.5 | 100.0 |
| Lequesne (2011) | CB-1 | 1.8 | 150.0 | 600.0 | 570.0 | 1.6 | 1.5 | 0.6 | 2.9 | 45.0 | H | 1.5 | 78.9 |
| | CB-2 | 1.8 | 150.0 | 600.0 | 570.0 | 1.4 | 1.3 | 0.6 | 2.9 | 52.0 | H | 1.5 | 78.9 |
| | CB-3 | 1.8 | 150.0 | 600.0 | 570.0 | 1.4 | 1.3 | 0.5 | 2.9 | 34.0 | H | 1.5 | 78.9 |
| C18 Han et al. (2015) | FC-05-2,0 | 2.1 | 250.0 | 525.0 | 495.0 | 0.9 | 0.9 | 0.6 | 4.5 | 41.0 | PVA | 2.0 | 307.7 |
| | FC-0,5-3,5 | 3.9 | 250.0 | 300.0 | 270.0 | 0.9 | 0.8 | 0.6 | 4.6 | 41.0 | PVA | 2.0 | 307.7 |
| Parra-Montesinos et al. (2017) | 1 | 2.4 | 150.0 | 475.0 | 437.5 | 2.5 | 2.3 | 1.8 | 0.0 | 63.0 | H | 1.5 | 78.9 |
| | 2 | 2.9 | 150.0 | 600.0 | 562.5 | 2.3 | 2.2 | 1.2 | 0.0 | 68.3 | H | 1.5 | 78.9 |
| | 3 | 3.6 | 150.0 | 500.0 | 462.5 | 3.1 | 2.9 | 1.2 | 0.0 | 68.3 | H | 1.5 | 78.9 |

Table 3.12. *HPFRC Coupling Beams without transverse reinforcement*

| $Researcher$ | $Specimen$ | $l_n/d$ | $b_w$ $(mm)$ | $h$ $(mm)$ | $d$ $(mm)$ | $\rho_d$ (%) | $f_c'$ $(MPa)$ | $Fiber$ Type | $V_f$ (%) | $l_f/d_f$ |
|---|---|---|---|---|---|---|---|---|---|---|
| Kwon et al. (2013) | FC-0.0 | 2.2 | 250.0 | 525.0 | 488.5 | 4.5 | 41.0 | PVA | 2.0 | 307.7 |
| Han et al. (2015) | FC-0-3.5 | 4.1 | 250.0 | 300.0 | 259.5 | 4.6 | 41.0 | PVA | 2.0 | 307.7 |

# CHAPTER 4

# ANALYTICAL MODELING

One of the main purposes of this analytical study is to obtain the load carrying capacity of shear critical deep beams. Generally, the failure mode of a deep beam is shear failure, however, depending on the reinforcement detailing, cross sectional properties and length of the beam, flexural failure may also be observed. Therefore, it is important to accurately predict not only the shear strength but also the flexural strength of a beam so that the failure mode and the load carrying capacity of the member can be determined properly. For this purpose, a shear strength formulation and a methodology to obtain the flexural strength are proposed in this chapter. The two capacities are then compared to obtain the mode of failure. Resulting member capacities and comparison with experimental results are also presented for the beams that are considered in the database provided in Chapter 3.

## 4.1. Flexural Strength of FRC and HPFRC Beams

In structural members, internal flexural and shear forces occur as a result of external loading. Members with shear span-to-depth ratios ($a/d$) less than 2.5 (ASCE-ACI Committee 445, 1998) are considered to be deep members, where Bernoulli's hypothesis of plane sections remain plane after bending does not hold true. However, for more slender beams for which the $a/d$ ratio is more than 2.5, Bernoulli's equations are applicable and used to obtain their flexural capacities. The shear capacity corresponding to the deep beam flexural failure ($V$) is computed as $M/a$, where $M$ is the beam flexural capacity and $a$ is the shear span of the member. For the coupling beams considered in the database, the shear strength corresponding to flexural failure is computed as $V = M/(l_n/2)$, where M is the internal moment and $l_n$ is the clear length of the member measured from face-to-face of supports. Bernoulli's hypothesis states that the strain distribution over the depth of the member is linear. The section reaches ultimate moment capacity, when the outermost concrete fiber under compression reaches its maximum strain capacity, generally after the tension reinforcement yields. Hence, the strain capacity of concrete under compression should be determined first. The maximum compressive strain value for reinforced concrete is accepted as 0.003 in the American Concrete Institute Building Code Requirements for Structural Concrete and Commentary to have a conservative design as shown in Fig. 4.1.

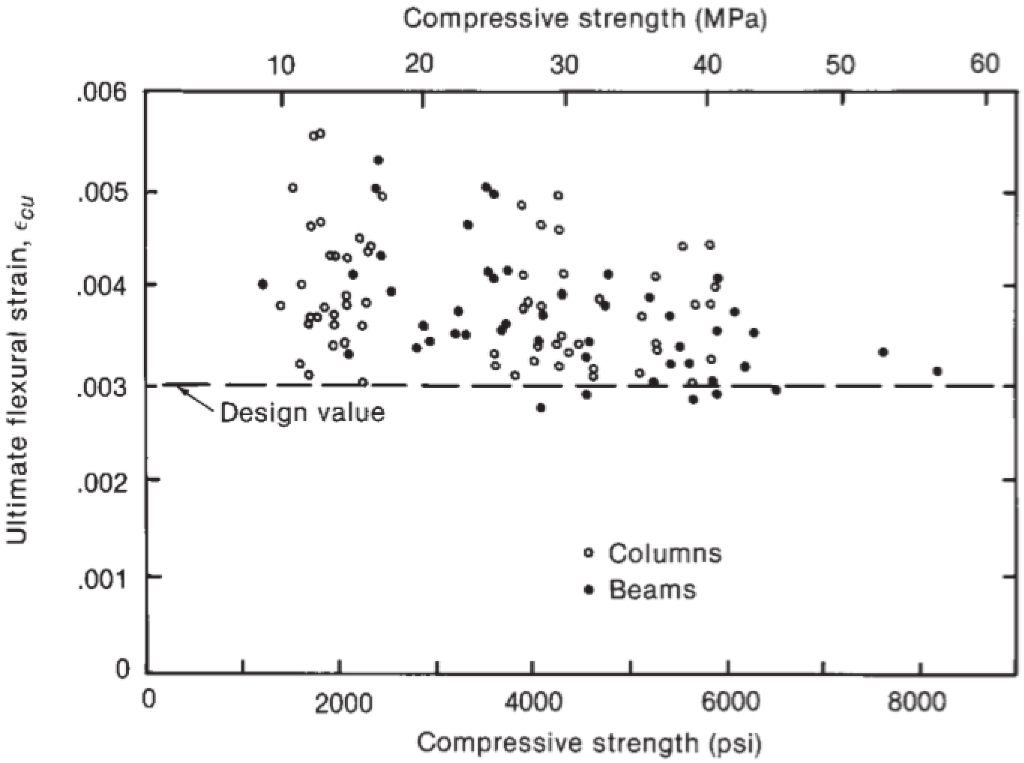


*Figure 4.1.* Concrete compressive strain limit for reinforced concrete members (Mattock et al., 1961)

Moreover, Guide to Design with Fiber Reinforced Concrete (ACI 544.4R-18, 2018) recommends 0.003 as the maximum compressive strain for fiber reinforced composite to be conservative, as well. In this analytical study, 0.003 is selected as the limiting compressive strain for both fiber reinforced composite and high performance fiber reinforced composite beams. In the tests selected for the database, the maximum moment is observed at the midspan of the member for deep beam specimens and at the beam ends for coupling beam subassemblies. The diagonal and dowel bars placed in the coupling beams are taken into account in flexural capacity computations. The increase in the flexural capacity due to strain-hardening of the reinforcement is not accounted for to be conservative. Rectangular concrete stress block, first proposed by Whitney (1937), is utilized in the compression zone. The equivalent rectangular stress distribution does not represent the actual stress distribution in the compression zone at nominal strength, but provides essentially the same nominal combined flexural and axial compressive strengths (Mattock et al. 1961).The depth of the equivalent compressive block is considered to be $a = \beta_1\ c$ , where, $c$ is the neutral axis depth and the factor $\beta_1$ is computed from Table 4.1.

Table 4.1. $\beta_1$ *Values*

| $f'_c$ **(MPa)** | $\boldsymbol{\beta_1}$ |
|---|---|
| $17.12 \leq f'_c \leq 27.6$ | 0.85 |
| $27.6 < f'_c < 55.2$ | $0.85 - \frac{0.05(f'_c - 27.6)}{6.9}$ |
| $f'_c \geq 55.2$ | 0.65 |

For reinforced concrete sections, the tensile strength of concrete is neglected in flexural capacity computations. However, fibers transfer tensile stresses across the cracked surfaces. Therefore, the post cracking tensile strength of fiber reinforced composites is taken into account with a constant distribution throughout the tension zone. The resulting stress distribution and equivalent forces are given in Fig. 4.2. In this figure, $C$ is the concrete compression force, $T_f$ is the tensileforce resisted by fibers and $T_s$ is the force carried by the reinforcement. The formulation of compressive force, $C$, and the total tensile force, $T$, are given below:

$$C = 0.85 f_c{}' b_w a \qquad (4-1)$$

$$T = A_s f_y + \sigma_{pc} b_w (h - c) \qquad (4-2)$$

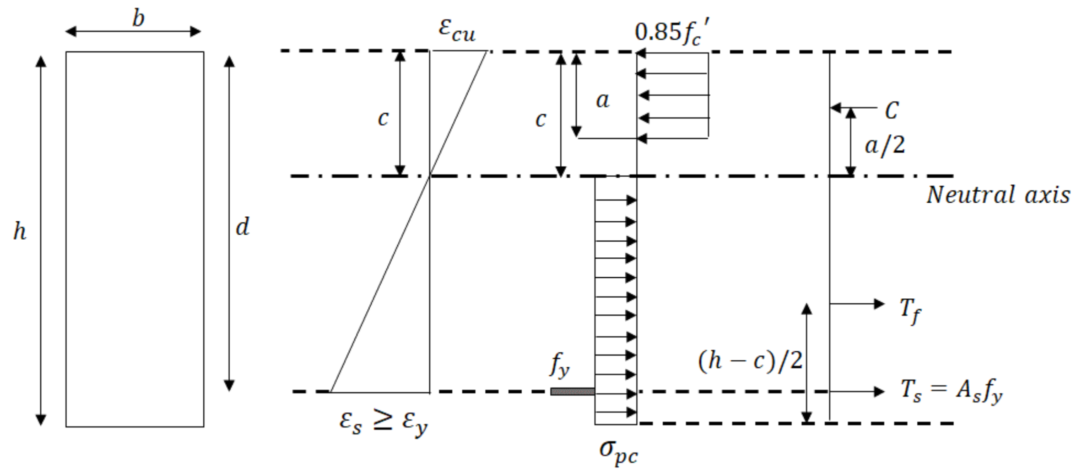


*Figure 4.2.* Considered stress distribution and equivalent forces for rectangular single reinforced section

### 4.1.1. Tensile Strength of Fiber Reinforced Composites

Based on the tensile behavior, composites can be classified into two groups as fiber reinforced composites (FRC) and high performance fiber reinforced composites (HPFRC) (Shah et al., 1999). The main difference between the two is the behavior of the members after the formation of the first crack. FRC members exhibit strain-softening response in which the maximum post-cracking strength ($\sigma_{pc}$) is smaller than the tensile strength of the composite at first cracking ($\sigma_{cc}$). However, for HPFRC members, the strength continues to increase after reaching $\sigma_{cc}$ and multiple cracking can be observed up to the post-cracking strength, which is always higher than the cracking strength (Naaman, 2007). The post-cracking tensile strength,$\sigma_{pc}$, significantly influences the structural performance of FRC beams (Choi et al, 2007).

Many analytical studies have been conducted to determine the cracking and post-cracking strengths of composites and formulations have been derived since the early seventies (Naaman, 1972; Naaman, 1974; Naaman, 1987; Naaman and Reinhardt, 1996). Naaman and Reinhardt (1996) proposed the following equation to calculate the post-cracking tensile strength:

$$\sigma_{pc} = \lambda_{pc} V_f \left(l_f/d_f\right)\tau \qquad (4-3)$$

where, $\lambda_{pc} = \lambda_1 \lambda_2 \lambda_3$ $(4-4)$

$V_f$ : fiber volume fraction,

$l_f/d_f$ : fiber aspect ratio,

$\lambda_1$ : expected pull-out length ratio,

$\lambda_2 = 4\alpha_2\lambda_4\lambda_5$ : orientation efficiency factor for cracked state,

$\lambda_3$ : group reduction factor depending on the number of fibers in the unit area,

$\alpha_2$ : efficiency factor of fiber orientation in the uncracked state of the composite,

$\lambda_4$ : Pulley Effect,

$\lambda_5$ : General reduction in pull-out response when fiber orientation angle is oriented at greater than $60^0$,

$\tau$ : average interfacial bond stress.

Table 4.2 presents widely accepted values for $\lambda_1$, $\lambda_2, \lambda_3$, $\alpha_2$ factors and the modulus of elasticity, $E$, for the fiber types that are included in the database.

Table 4. 2. *Fiber Properties*

| **Fiber Type** | $\boldsymbol{\alpha_2}$ | $\boldsymbol{\lambda_1}$ | $\boldsymbol{\lambda_2}$ | $\boldsymbol{\lambda_3}$ | **Modulus of Elasticity (GPa)** |
|---|---|---|---|---|---|
| Steel | 0.5 | 0.25 | 1.2 | 1 | 200 |
| PVA | 0.5 | 0.25 | 0.7 | 1 | 25 |
| PE | 0.5 | 0.25 | 0.5 | 1 | 117 |

#### 4.1.1.1. Bond Strength

The behavior of fiber reinforced composites depends also on the interfacial bond characteristics between the fiber and the matrix. After cracking, if the bond between the fiber and the matrix is well established, fibers prevent the extension of micro cracks and initiate the formation of new cracks. However, as the cracks get wider, the fibers pull-out or fracture. Long fibers are more effective for large crack widths than short ones due to their higher adherence. The bond strength is linearly proportional with the fiber length, while it is inversely proportional with the fiber diameter.

The difficulty in mixing a large volume of discontinuous fibers may result in some air voids in the composites, which could lead to erroneous evaluation of the fiber bond strength (Guerrero 1999).

The tensile strength of the matrix also has an effect on crack formation. The lower the cracking strength of the matrix, the faster the crack gets wider and this will reduce the stress transfer surface between the fiber and the matrix. Therefore, the cracking tensile strength of the matrix can be considered to be the splitting tensile strength. There is a range of bond strength values for different fiber types proposed by various researchers based on the average results of single fiber pull-out tests (Fig. 4.3), some of which are tabulated in Table 4.3. However, considering a constant bond strength value based on only the fiber type is a huge simplification. Bond strength depends not only on the fiber type but also matrix and fiber properties such as length and diameter of the fiber as discussed before. Taking these into account, a simple formulation is proposed to compute the interfacial bond strength based on the tensile strength of the matrix and key fiber properties, which significantly affect the member behavior (Eqn. 4-5). In this equation, the widely accepted formula to compute the average splitting tensile strength of normal weight concrete (Hasson, 1961 and Ivey et al., 1967) given in Eqn. 4-6 is used to obtain the cracking tensile strength of the matrix. The range of the calculated interfacial bond strengths for the subassemblies in the database by using Eqn. 4-5 is tabulated in Table 4.4.

$$\tau = \left(l_f/d_f\right)^{V_f}\sigma_{mu} \quad (MPa) \qquad (4-5)$$

where, $l_f/d_f$ : fiber aspect ratio,

$V_f$ : fiber volume fraction,

$\sigma_{mu}$ : average splitting tensile strength of normal weight concrete.

$$\sigma_{mu} = \begin{cases} 6.7\sqrt{f_c{}'}(psi) \\ 0.556\sqrt{f_c{}'}(MPa) \end{cases} \qquad (4-6)$$

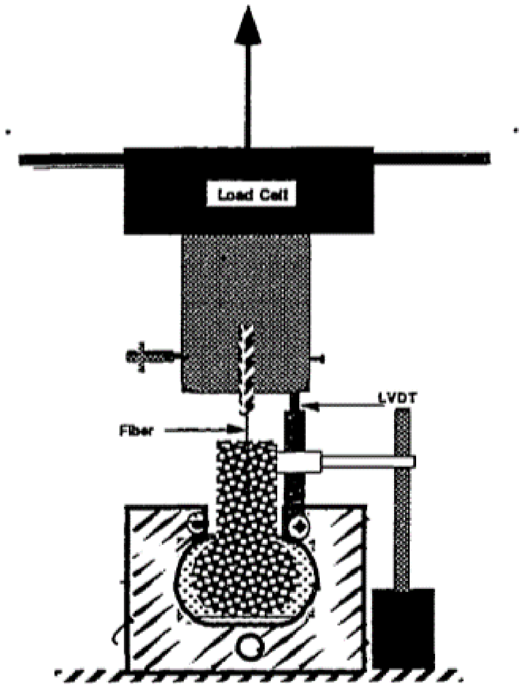


*Figure 4.3.* Single fiber pull-out test setup (Guerrero, 1999)

Table 4.3. *Bond Strength Values Proposed in Prior Studies*

| Fiber Type | Range of Proposed Bond Strengths (MPa) |
|---|---|
| Hooked-end | 4.5 (Parra-Montesinos, 2000) - 19.2 (Li et al., 1992) |
| Crimped | 4.1 (Batson et al., 1972) - 30.4 (Li et al., 1992) |
| Straight | 9.4 (Lim and Oh, 1999) - 60.6 (Cai et al., 2016) |
| Flat-end | 45.3 - 130.5 (Greenough and Nehdi, 2008) |
| Torex | 6.15 - 23.0 (Sujivorakol, 2003) |
| PVA | 2.3 (Han et al., 2015) - 4.0 (Kwon et al., 2013) |
| PE | 3.62 (Canbolat, 2004) - 11.0 (Yun et al., 2008) |

Table 4.4. *Bond Strength Values Proposed in Current Study*

| Fiber Type | Range of Proposed Bond Strengths (MPa) (Obtained from Eqn. 4-5) |
|---|---|
| Hooked-end | 3.65 - 4.91 |
| Crimped | 2.77 - 4.55 |
| Straight | 3.68 - 5.18 |
| Flat-end | 3.67 - 4.15 |
| Torex | 4.35 - 4.75 |
| PVA | 3.99 - 4.38 |
| PE | 4.39 - 4.72 |

## 4.2. Shear Strength of FRC and HPFRC Beams

When a shear crack is formed in a beam, the shear resisting forces can be referred to as $V_{cc}, V_{ay}, V_s$, $V_{dowel}$ and $V_d$ as shown in Fig. 4.4. In this figure, $V_{cc}$ is the shear carried by concrete under compression, $V_{ay}$ is the vertical component of aggregate interlock, $V_s$ is the shear force resisted by vertical reinforcement, $V_{dowel}$ is the shear force carried by the longitudinal reinforcement due to dowel action, and $V_d$ is the vertical component of the shear carried by diagonal reinforcement.

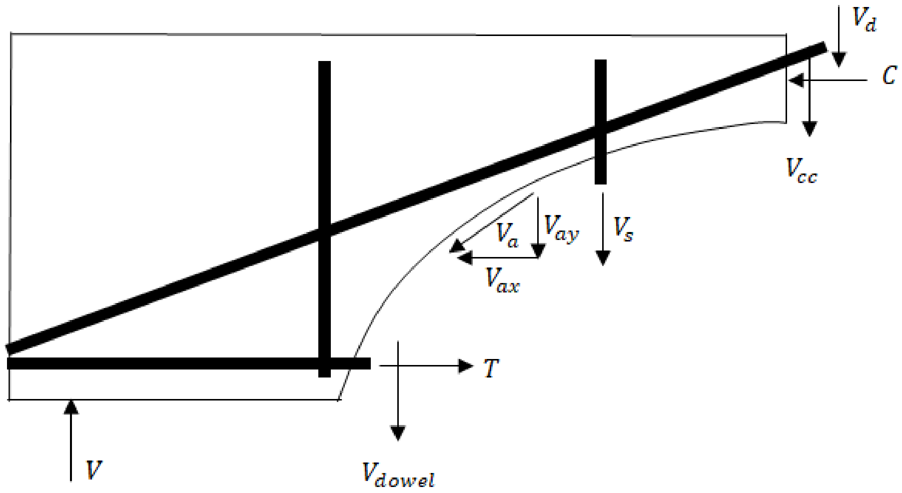


*Figure 4.4.* Shear resisting forces in a beam after the formation of a shear crack

$$V = V_{cc} + V_{ay} + V_{dowel} + V_s + V_d \qquad (4-7)$$

In design, $V_{cc}, V_{ay}$, and $V_{dowel}$ are lumped together as the shear carried by concrete, $V_c$. Thus, the nominal shear strength, $V_n$, can be defined as:

$$V_n = V_c + V_s + V_d \qquad (4-8)$$

where, $V_c = 0.17\sqrt{f_c{}'} b_w\, d$ $\qquad (4-9)$

$$V_s = \frac{A_t f_t d}{s} \qquad (4-10)$$

$$V_d = 2\, A_{vd}\, f_{yd}\, sin\alpha \qquad (4-11)$$

Then, the equation becomes,

$$V_n = \left(0.17\,\sqrt{f_c{}'}\; b_w\; d + \frac{A_t\, f_t\, d}{s} + 2\, A_{vd}\, f_{yd}\, sin\alpha\right) \qquad (4-12)$$

where, $f_c'$ : concrete compressive strength,

$b_w$ : section width,

$d$ : effective depth,

$A_t$ : cross sectional area of the transverse reinforcement,

$f_t$ : yield strength of the transverse reinforcement,

$s$ : transverse reinforcement spacing,

$2\ A_{vd}$ : total area of diagonal reinforcement in coupling beam,

$f_{yd}$ : yield strength of the diagonal reinforcement.

$\alpha$ : angle of inclination of the diagonal reinforcement with respect to the beam longitudinal axis.

Prior research studies have shown that decreasing the shear span-to-depth ratio leads to an increase in shear resistance because of the anchoring action in between loading points and supports (Shahnewaz and Alam, 2014). Moreover, Ashour et al. (1992) stated that the failure mode depended on the shear span-to-depth ratio; when this ratio was higher than 2.5, flexural failure was expected, whereas a lower shear span-to-depth ratio commonly resulted in shear failure.

### 4.2.1. Proposed Shear Strength Prediction Equation

Based on the constructed database of 446 shear critical deep beams, a shear strength prediction equation is proposed that can be used for both FRC and HPFRC beams with or without transverse and diagonal reinforcement. The key parameter of this equation is selected to be the effective depth to clear span length ratio, $d/l_n$, since the shear span depends on the loading conditions. The proposed equation is based on Eqn. 4-12, however the contribution of concrete, transverse and diagonal reinforcement to shear are modified to take into account the contribution of fibers.

$$V = X_1\left(0.5\sqrt{f_c'}\ b_w d + X_2 \frac{A_t f_t d}{s} + 0.8\ (2\ A_{vd}\ f_{yd}\ sin\alpha)\right) \qquad (4-13)$$

where,

$$X_1 = \begin{cases} 1.4\,(d/l_n)^{0.4} & \text{if } (d/l_n) > 1/3 \\ 1.4\,(0.65) & \text{if } (d/l_n) \le 1/3 \end{cases} \tag{4-14}$$

$$X_2 = \begin{cases} 0.5 & \text{if } \rho_t \ge 0.005 \\ 1.0 & \text{if } \rho_t < 0.005 \end{cases} \tag{4-15}$$

where, $f_c'$ : concrete compressive strength,

$b_w$ : section width,

$d$ : effective depth,

$l_n$ : clear length,

$A_t$ : cross sectional area of the transverse reinforcement,

$f_t$ : yield strength of the transverse reinforcement,

$s$ : transverse reinforcement spacing,

$2\,A_{vd}$ : total area of diagonal reinforcement in the cross-section,

$f_{yd}$ : yield strength of the diagonal reinforcement,

$\alpha$ : angle of inclination of the diagonal reinforcement with respect to the beam longitudinal axis.

#### 4.2.1.1. Concrete Contribution

Normally, the tensile strength of concrete increases with increasing compressive strength, however, the ratio of the tensile to compressive strength decreases. The tensile strength of concrete is generally considered as proportional to the square root of its compressive strength. The distribution of $\sqrt{f_c'}$ vs experimental shear strength for the subassemblies included in the database is given in Fig. 4.5.

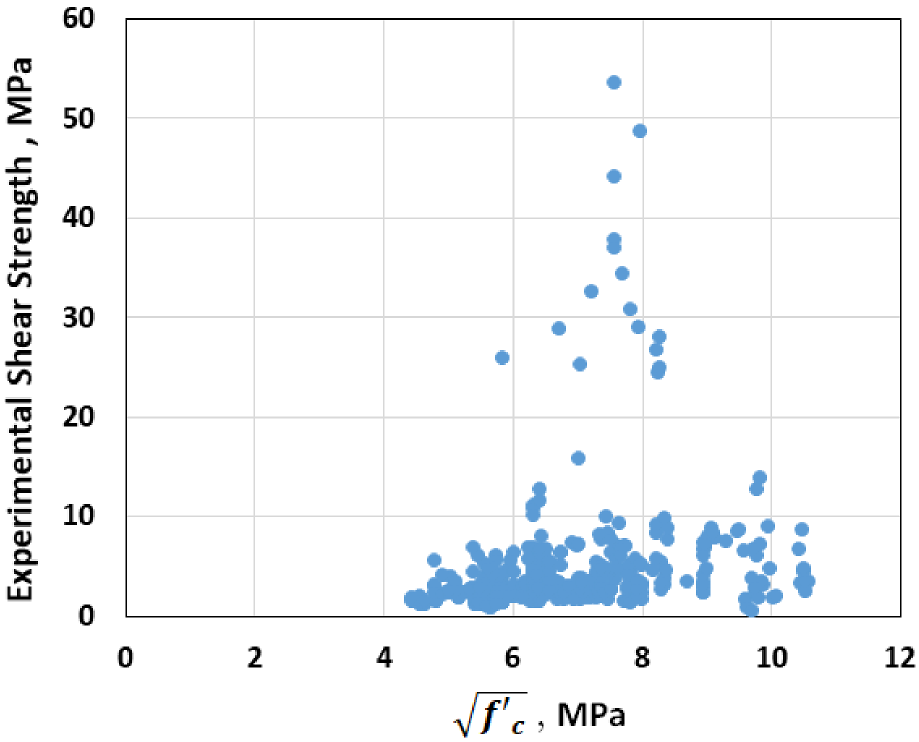


*Figure 4.5*. Influence of $\sqrt{f_c'}$ on shear strength of FRC beams

The shear capacity of reinforced concrete members without transverse reinforcement is given as Eqn. 4-16 (ACI 318-14).

$$V_c = 0.17\sqrt{f_c'}\, b_w d \qquad (N) \qquad (4-16)$$

This formula provides reasonable accuracy for reinforced concrete members however, for FRC and HPFRC beams due to the stress transfer across inclined cracks, a higher contribution of the composite to shear carrying capacity is considered in the proposed equation.

#### 4.2.1.2. Contribution of the Transverse Reinforcement

Transverse reinforcement increases the shear strength of a member and with proper detailing a more ductile mode of failure, namely flexural failure, will be observed in the members with transverse reinforcement. Before the formation of the inclined cracks, the strain value on the legs of a stirrup is equal to the strain value of concrete and the stresses on the transverse reinforcement are very low. When the crack widths increase, the stress on stirrup legs will also increase and they will eventually yield. After yielding of the stirrups, crack widths increase rapidly. Fiber reinforced composite deep beams have multiple cracking before failure with a much higher number of cracks when compared to reinforced concrete beams (Fig. 4.6). Since the crack widths are narrower, the strains on the legs of the stirrups are reduced when fibers are added to the composite; furthermore, fibers also withstand the widening of the diagonal cracks (Ding et al. 2011). Therefore, in the proposed equation, the contribution of the transverse reinforcement to shear carrying capacity is reduced, when the shear reinforcement ratio, $\rho_t$, computed as $A_t/(b_w\, s)$, is higher than 0.5%. The influence of the transverse reinforcement ratio on the shear strength is presented in Fig. 4.7.

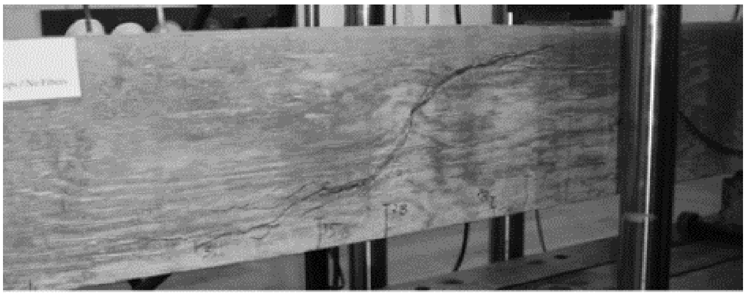

a) Reinforced concrete beam

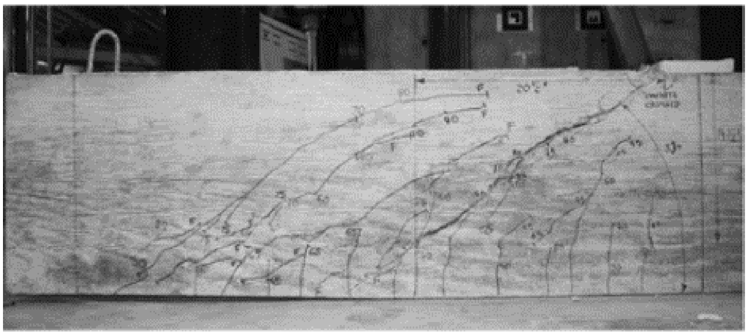

b) FRC beam

*Figure 4.6.* Cracking pattern for RC and FRC beams (Dinh et al. 2010)

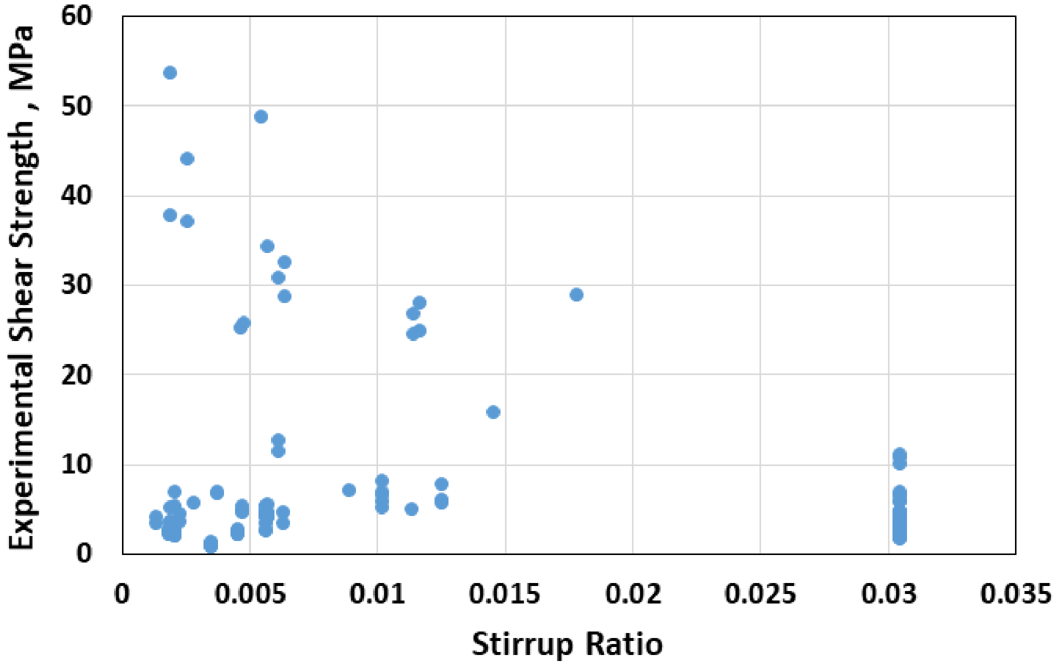


*Figure 4.7.* Influence of the stirrup ratio on shear strength of FRC beams

#### 4.2.1.3. Contribution of the Diagonal Reinforcement

The vertical component of the force on the diagonal reinforcement contributes to the shear capacity. The stress on the diagonal reinforcement depends on the crack width, as in the case for the transverse reinforcement. Therefore, the contribution of the diagonal reinforcement is also reduced with a constant factor of 0.8 in the proposed equation.

### 4.2.4. Effect of Shear Span-to-Depth Ratio

In prior research studies, the shear span-to-depth ratio is considered to be one of the most important parameters that affects the shear strength of members. The failure mode also depends on the shear span-to-depth ratio ($a/d$). When this ratio is higher than 2.5, flexural failure is expected and when it is lower, shear becomes more dominant. Ashour et al. (1992) mentioned that the shear capacity was much higher for smaller $a/d$ ratios. In the proposed procedure the flexural and shear capacities of the beams are compared for beams that have $a/d$ ratios more than 2.5 to determine the failure mode and accurately predict the shear strength. For beams with $a/d$ ratios less than 2.5, the strain distribution due to flexural loading does not remain linear because of the increased shear strains. Therefore, only the proposed shear capacity equation is used to determine the capacity of beams that have $a/d$ ratios less than 2.5. The effect of shear span-to-effective depth ratio ($a/d$) on the shear strength for fiber reinforced composite shear critical beams is shown in Fig. 4.8.

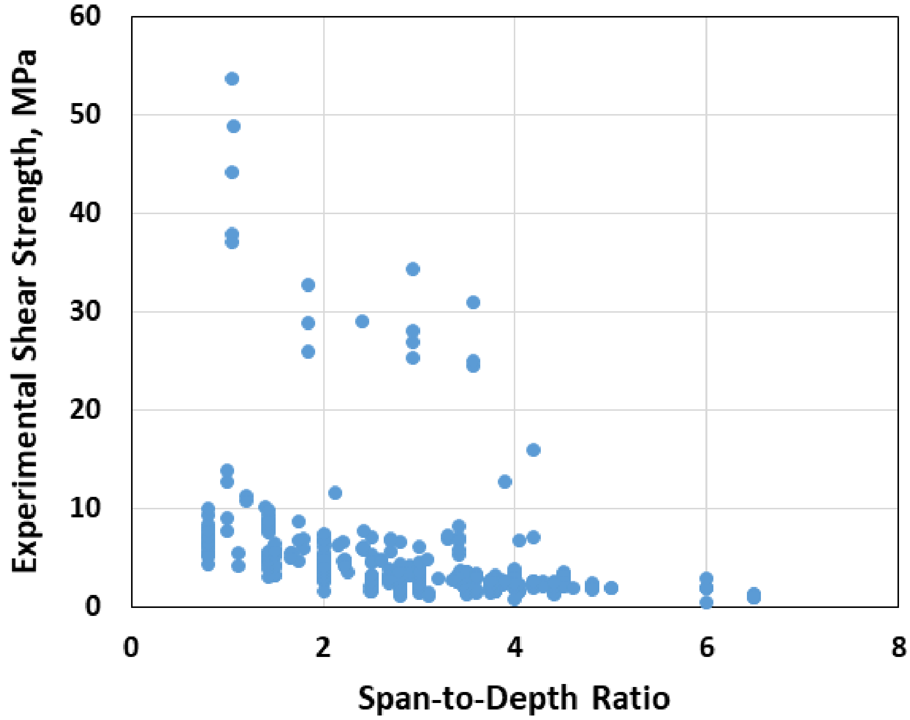


*Figure 4.8.* Influence of the shear span-to-depth ratio on shear strength of FRC beams

The shear span depends on the clear length of the member and the loading conditions. In this study, it is observed that the shear strength is more prone to variation of $d/l_n$ ratio especially for the coupling beams, as in the case of reinforced concrete walls (ACI 318-14). Therefore, $d/l_n$ ratio is considered in the proposed equation. Another advantage of using this ratio is the fact that it remains constant for all loading conditions, which will make it more suitable to be used in design recommendations.

### 4.3. Comparison of Existing Prediction Equations with the Proposed One

Numerous equations were proposed by different researchers to predict the ultimate shear strength of fiber reinforced composite beams. Most of these equations only consider shear failure, without taking into account the flexural capacity. Moreover, most of them are only applicable to steel fiber reinforced composites, while other fiber types were not considered. These formulations are presented in this section and the predictions from these equations, as well as the proposed equation are compared with the experimental results.

Statistical parameters are used in the comparison such as the ratio of predicted shear strength to experimental shear strength, mean, standard deviation and average absolute error calculated by the equations given below. All the shear prediction equations given in Table 4.5 are discussed in detail in Chapter 2.

$$Mean = \overline{V_{pre}} = \frac{\sum_1^n V_{pre}}{n} \qquad (4-17)$$

$$Standard\ Deviation = \sqrt{\frac{\sum_1^n (V_{pre} - \overline{V_{pre}})^2}{n-1}} \qquad (4-18)$$

$$Average\ Absolute\ Error\ (\%) = \frac{1}{n}\left(\frac{V_{exp} - V_{pre}}{V_{exp}}\right)100 \qquad (4-19)$$

where, $n$ : number of specimens in each group,

$V_{exp}$ : experimental shear strength (MPa),

$V_{pre}$ : predicted shear strength (MPa) obtained by using the proposed equations.

Table 4.5. *Shear Strength Prediction Equations*

| Equation Number | Reference | Shear Strength Formulation |
|---|---|---|
| (1) | ACI 318-14 (2014) | $V_n = 0.75\ (0.83\sqrt{f_c{}'}b_w d)$ for deep beams |
| | | $V_n = 2\ A_{vd}\, f_y\ sin\alpha \le 0.83\ \sqrt{f_c{}'}b_w\ d$ for coupling beams |
| (2) | Sharma (1986) | $V = \frac{A_v\ f_y\ d}{s} + (k\ f_t' \left(\frac{d}{a}\right)^{0.25}\ b_w\ d)$ |
| (3) | Mansur et al. (1986) | $V = \left[\left(0.16\sqrt{f_c'} + 17.2\ \rho\ \frac{d}{a}\right) + 0.41\left(\tau\ V_f\ \frac{L}{d}\right)\right] b_w\ d$ |
| (4) | Narayanan and Darwish (1987) | $V = \left(2.8\ \frac{d}{a}\left[0.24\ f_{ct} + 80\ \rho\ \frac{d}{a}\right] + v_b\right) b_w\ d\quad for\ \frac{a}{d} \le 2.8$ |
| | | $V = \left(\left[0.24\ f_{ct} + 80\ \rho\ \frac{d}{a}\right] + v_b\right) b_w\ d\quad for\ \frac{a}{d} > 2.8$ |
| (5) | Ashour et al. (1992) | $V = \left[\left(2.11\sqrt[3]{f_c'} + 7\ F\right)\left(\rho\frac{d}{a}\right)^{0.333}\frac{2.5}{a/d} + v_b\left(2.5 - \frac{a}{d}\right)\right] b_w\ d\ for\ \frac{a}{d} < 2.5$ |
| | | $V = \left(2.11\sqrt[3]{f_c'} + 7\ F\right)\left(\rho\ \frac{d}{a}\right)^{0.333} b_w\ d\quad for\ \frac{a}{d} > 2.5$ |
| (6) | Khuntia et al. (1999) | $V = \left(0.167 \times 2.5\frac{d}{a} + 0.25\ F\right)\sqrt{f_c'}b_w\ d\quad for\ \frac{a}{d} < 2.5$ |
| | | $V = (0.167 + 0.25\ F)\sqrt{f_c'}\ b_w\ d\quad for\ \frac{a}{d} \ge 2.5$ |
| (7) | Kwak et al. (2002) | $V = \left[3.7\left(3.5\frac{d}{a} \le 3\right)\left(f_{spcf}\right)^{2/3}\left(\rho\ \frac{d}{a}\right)^{1/3} + 0.8\ v_b\right] b_w\ d\ \ for\ \frac{a}{d} < 3.5$ |
| | | $V = \left[3.7\left(f_{spcf}\right)^{2/3}\left(\rho\ \frac{d}{a}\right)^{1/3} + 0.8\ v_b\right] b_w\ d\quad for\ \frac{a}{d} > 3.5$ |
| (8) | Canbolat(2004) | $V = (\sigma_{pc} b_w\ h) + (2\ A_{vd} f_{yd}\ sin\alpha) + \left(\frac{A_w f_{yw}\ d}{s}\right)$ |
| (9) | Lequesne(2011) | $V = \left(0.4\sqrt{f_c'}\ \ b_w\ d\right) + (2\ A_{vd} f_{yd}\ sin\alpha) + \left(\frac{A_w\ f_{yw}\ d}{s}\right)$ |
| (10) | Cai et al. (2016) | $V = \left(0.29\sqrt{f_{cfrc}}\ 0.8\ b_w\ d\right) + \left(\frac{A_w\ f_{yw} 0.8\ d}{s}\right) + (0.055 + 1.7\rho_f) f_{cfrc}\ b_w\ d$ |
| (11) | Dinh et al. (2011) | $V = 0.13\ A_s f_y + (\sigma_t)_{ave}\ b\ (d - c)\ cotan(45)$ for $\frac{a}{d} > 2.5$ |
| (12) | Shear Strength Equation for the Proposed Method | $V = X_1\left(0.5\sqrt{f_c{}'}b_w\ d + X_2\frac{A_t f_{yt} d}{s} + 0.8\ \left(2\ A_{vd} f_{yd}\ sin\alpha\right)\right)$ <br> $X_1 = \begin{cases} 1.4\left({}^{d}/{}_{l_n}\right)^{0.4} & \text{if } \left({}^{d}/{}_{l_n}\right) > 1/3 \\ 1.4\ (0.65) & \text{if } \left({}^{d}/{}_{l_n}\right) \le 1/3 \end{cases}$ <br> $X_2 = \begin{cases} 0.5 & \text{if } \rho_t \ge 0.005 \\ 1.0 & \text{if } \rho_t < 0.005 \end{cases}$ |

Considering the limitations of the prediction equations, the shear capacities of all specimens belonging to each different group of the database are compared with the experimental values. The following tables include all applicable equations for different groups of specimens and their comparisons with experimental shear strengths for the proposed method and the methods recommended by ACI 318-14 (2014), Sharma (1986), Mansur et al. (1986), Narayanan and Darwish (1987), Ashour et al. (1992), Khuntia et al. (1999), Kwak et al. (2002), Canbolat et al. (2005), Lequesne (2011), Cai et al. (2016), Dinh et al. (2011). Only the proposed method and the method recommended by Dinh et. al. (2011) considered flexural failure as well as shear failure, therefore, in addition to the values obtained from the shear prediction equations, the shear capacities corresponding to the flexural failure are also computed for members with $a/d$ ratios more than 2.5 for these two methods. Although ACI 318-14 (2014) equations are valid for reinforced concrete members, they are included in these tables, since the values obtained from these equations could be considered as a lower bound for the shear strength.

### 4.3.1. Comparison of Shear Prediction Equations for Deep Beams ($a/d \leq 2.5$) with Transverse Reinforcement

From Fig. 4.9 (1), it can be observed that the shear formulation of ACI 318-14 (2014) is conservative in shear strength estimation. The shear strength values obtained from Eqn. (2) by Sharma (1986) overpredict the experimental shear strength for nearly half of the specimens. Moreover, the mean (1.35), standard deviation (0.35) and AAE (44.25%) are higher than these values for the other predictions. The comparison of the proposed method is given in Fig. 4.9 (12). For the majority of the members, the experimental results are underestimated, which makes the equation conservative for design purposes (Table 4.6). Furthermore, mean (0.73), standard deviation (0.12), and AAE (27.54%) of the proposed equation are lower than those of the other models. Standard deviation is a significant parameter that indicates the scatter of the data. Therefore, it can be concluded that when compared with the other prediction equations, the proposed method enhances the accuracy of the predicted shear strength.

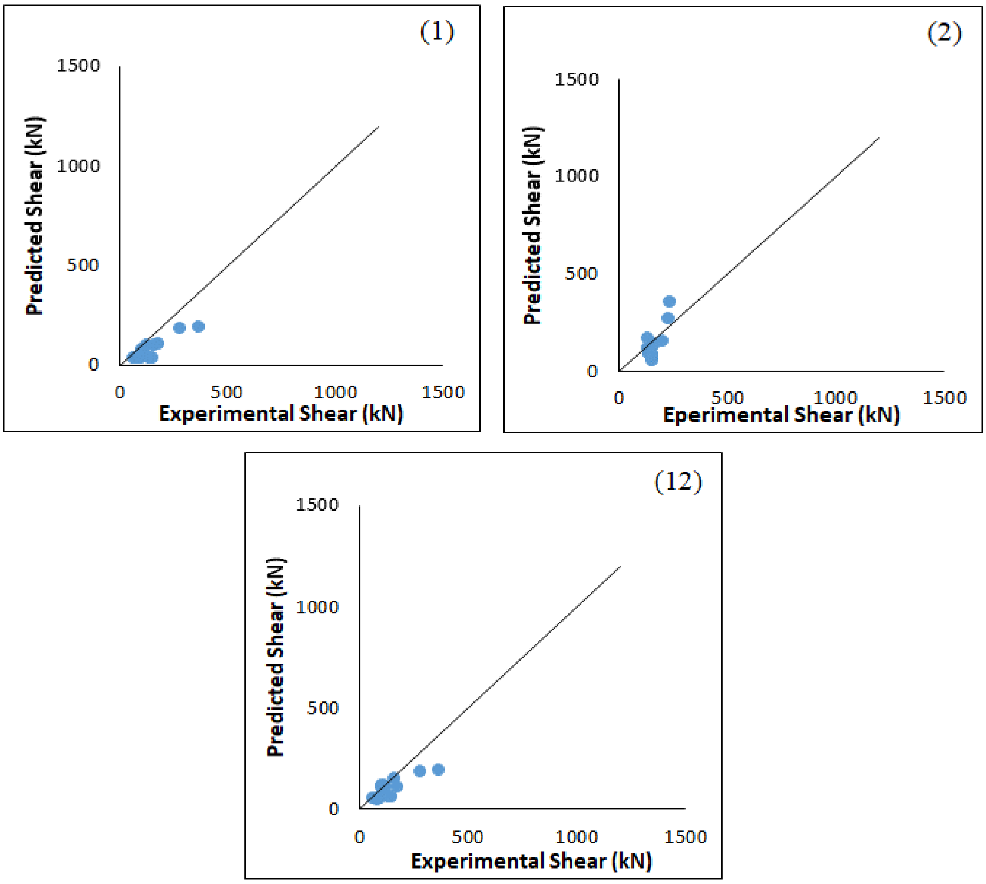


*Figure 4.9.* Shear strength predictions for Deep Beams ($a/d \leq 2.5$) with transverse reinforcement: (1) ACI 318-14 (2014); (2) Sharma (1986); (12) Proposed method

Table 4. 6. *Statistical Parameters for Deep Beams ($a/d \leq 2.5$) with transverse reinforcement*

| Equation Number | Shear Equation | Mean | Range | Standard Deviation | Avg. Absolute Error (%) |
|---|---|---|---|---|---|
| (1) | ACI 318-14 (2014) | 0.73 | 0.35 -1.08 | 0.22 | 28.31 |
| (2) | Sharma (1986) | 1.35 | 0.65 - 2.39 | 0.35 | 44.25 |
| (12) | Proposed Method | 0.73 | 0.56 - 1.03 | 0.12 | 27.54 |

Table 4.7. *Comparison of Predicted versus Experimental Strengths for Deep Beams ( $a/d \leq 2.5$ ) with transverse reinforcement*

| $Researcher$ | $Specimen$ | $a/d$ | $l_n/d$ | $\rho_t$ (%) | $Fiber$ Type | $V_f$ (%) | $l_f/d_f$ | $V_{exp}$ $(MPa)$ | $V_{pre}/V_{exp}$ | | |
|---|---|---|---|---|---|---|---|---|---|---|---|
| | | | | | | | | | (1) | (2) | (12) |
| Cuchiara et al. (2004) | B11 | 2.0 | 10.5 | 0.2 | H | 1.0 | 60.0 | 121.0 | 0.86 | 1.03 | 1.03 |
| | B21 | 2.0 | 10.5 | 0.2 | H | 2.0 | 60.0 | 173.0 | 0.62 | 0.74 | 0.73 |
| | B12 | 2.0 | 10.5 | 0.6 | H | 1.0 | 60.0 | 156.6 | 0.67 | 1.27 | 0.92 |
| Choand Kim (2003) | F60-0.5-13S | 1.4 | 4.3 | 0.5 | H | 0.5 | 60.0 | 97.3 | 0.78 | 1.36 | 0.78 |
| | F60-1.0-13S | 1.4 | 4.3 | 0.5 | H | 1.0 | 60.0 | 97.3 | 0.81 | 1.39 | 0.82 |
| | F60-1.5-13S | 1.4 | 4.3 | 0.5 | H | 1.5 | 60.0 | 96.2 | 0.81 | 1.40 | 0.84 |
| | F60-2.0-13S | 1.4 | 4.3 | 0.5 | H | 2.0 | 60.0 | 109.0 | 0.72 | 1.24 | 0.77 |
| Batson et al. (1972) | K1 | 2.2 | 14.4 | 3.0 | S | 1.8 | 101.6 | 84.9 | 0.48 | 1.71 | 0.58 |
| | K2 | 2.4 | 14.4 | 3.0 | S | 1.8 | 101.6 | 76.3 | 0.53 | 1.89 | 0.59 |
| | U2 | 2.2 | 14.4 | 3.0 | C | 1.8 | 46.2 | 60.8 | 0.67 | 2.39 | 0.77 |
| | V1 | 1.8 | 14.4 | 3.0 | C | 1.8 | 46.2 | 90.2 | 0.45 | 1.63 | 0.64 |
| | V2 | 1.8 | 14.4 | 3.0 | C | 1.8 | 46.2 | 76.9 | 0.53 | 1.91 | 0.74 |
| | V3 | 2.0 | 14.4 | 3.0 | C | 1.8 | 46.2 | 86.2 | 0.47 | 1.69 | 0.60 |
| | W1 | 1.2 | 14.4 | 3.0 | C | 1.8 | 46.2 | 145.0 | 0.28 | 1.04 | 0.59 |
| | W2 | 1.2 | 14.4 | 3.0 | C | 1.8 | 46.2 | 139.3 | 0.29 | 1.08 | 0.62 |
| | W3 | 1.4 | 14.4 | 3.0 | C | 1.8 | 46.2 | 131.8 | 0.31 | 1.13 | 0.56 |
| Araújo et al. (2014) | V-1-0.21 | 2.5 | 6.5 | 0.2 | H | 1.0 | 65.0 | 275.5 | 0.67 | 0.82 | 0.84 |
| | V-2-0.21 | 2.5 | 6.5 | 0.2 | H | 2.0 | 65.0 | 360.0 | 0.54 | 0.65 | 0.67 |

### 4.3.2. Comparison of Shear Prediction Equations for Deep Beams ($a/d \leq 2.5$) without Transverse Reinforcement

In Fig. 4.10, (3) and (6), the shear strength formulations of Mansur et al. (1986) and Khuntia et al. (1999) are shown, respectively. From Table 4.8, it can be observed that the mean values of these equations are very low. Underestimation is more conservative; however the majority of these results are below half of the actual experimental shear strengths. Moreover, AAE values are 52.47% and 57.63%, respectively, which correspond to the two highest errors in Table 4.8. Eqn. (1) has the highest mean and overestimates the shear strength for most of the subassemblies. The mean values of Eqns. (2), (7), and (12) are similar. However, the standard deviation (0.21) and AAE (26.31%) for Eqn. (7) by Kwak et al. (2002) are the lowest and this prediction gives the most uniform distribution within these three equations. The mean of Eqns. (4), and (5), are 0.92, 0.94; standard deviations are 0.33, 0.32; and AAE values are 28.38, 27.67, respectively. Standard deviations are very close to one another, however, these two equations have the most uncorservative results. It should be remembered that some of these equations are not applicable to all the specimens considered in the database, therefore, only the equations applicable for these types of specimens are used in the comparisons.

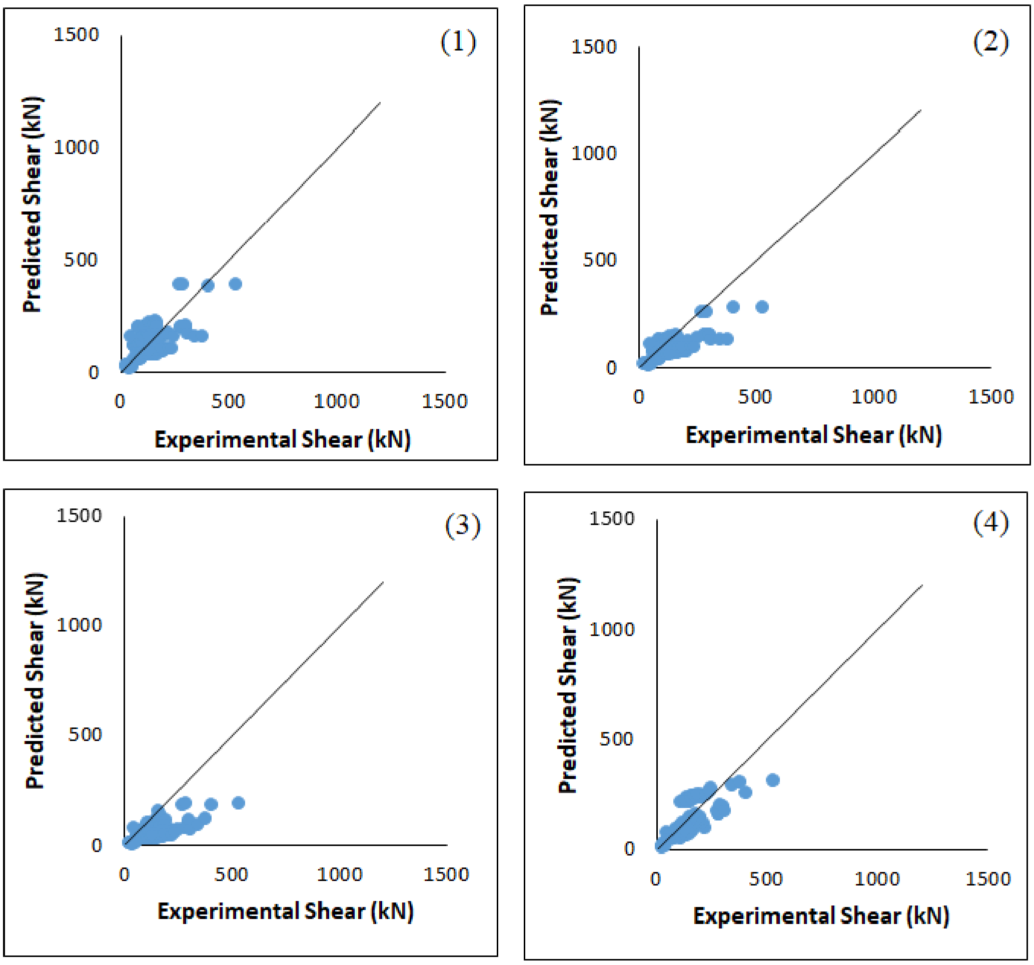


*Figure 4.10.* Shear strength predictions for Deep Beams ($a/d \leq 2.5$) without transverse reinforcement: (1) ACI 318-14 (2014); (2) Sharma (1986); (3) Mansur et al. (1986); (4) Narayanan and Darwish (1987)

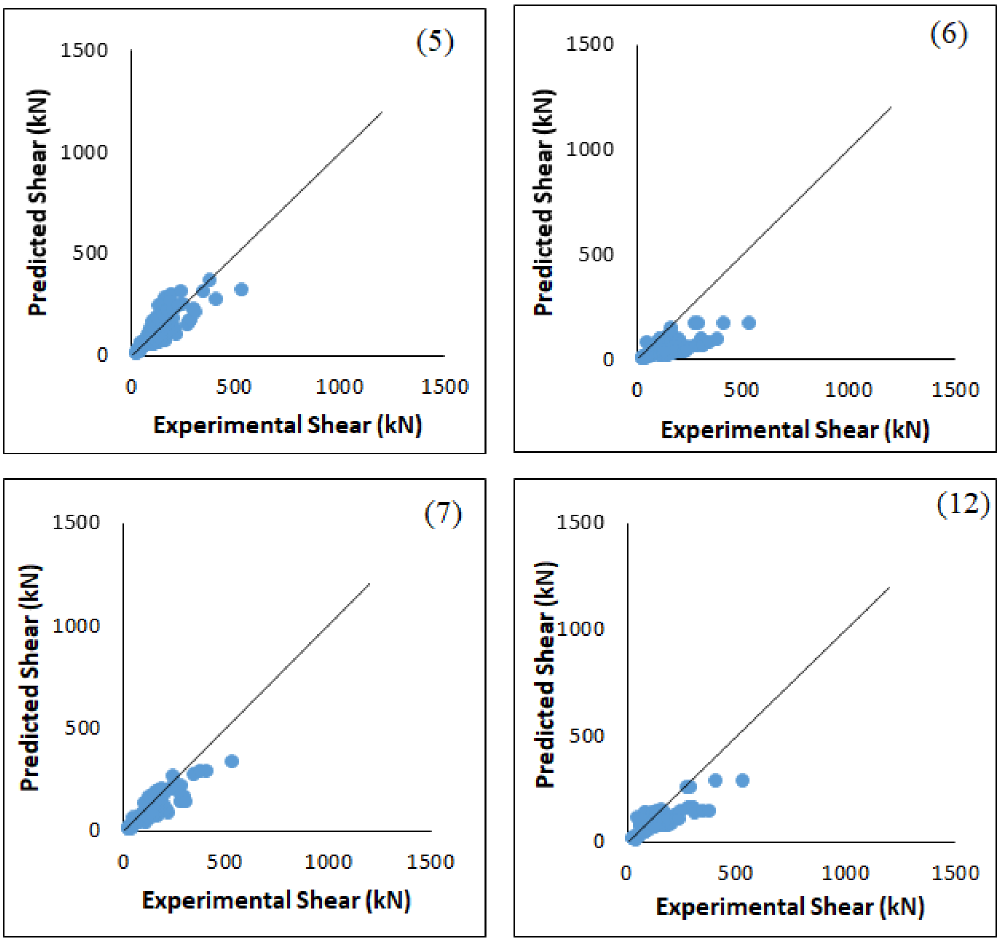


*Figure 4.10.* Shear strength predictions for Deep Beams ($a/d \leq 2.5$) without transverse reinforcement (continued):

(5) Ashour et al. (1992); (6) Khuntia et al. (1999); (7) Kwak et al. (2002); (12) Proposed method

Table 4.8. *Statistical Parameters for Deep Beams ($a/d \leq 2.5$) without transverse reinforcement*

| Equation Number | Shear Equation | Mean | Range | Standard Deviation | Avg. Absolute Error (%) |
|---|---|---|---|---|---|
| (1) | ACI 318-14 (2014) | 1.39 | 0.44 - 3.55 | 0.38 | 39.81 |
| (2) | Sharma (1986) | 0.78 | 0.37 - 2.53 | 0.33 | 33.92 |
| (3) | Mansur et al. (1986) | 0.49 | 0.23 - 1.89 | 0.24 | 52.47 |
| (4) | Narayanan and Darwish (1987) | 0.92 | 0.49 - 1.83 | 0.33 | 28.38 |
| (5) | Ashour et al. (1992) | 0.94 | 0.18 - 1.81 | 0.32 | 27.67 |
| (6) | Khuntia et al. (1999) | 0.44 | 0.48 - 2.11 | 0.23 | 57.63 |
| (7) | Kwak et al. (2002) | 0.78 | 0.39 - 1.58 | 0.21 | 26.31 |
| (12) | Proposed Method | 0.72 | 0.32 - 1.40 | 0.23 | 31.80 |

Table 4.9. *Comparison of Predicted versus Experimental Strengths for Deep Beams ( $a/d \leq 2.5$ ) without transverse reinforcement*

| *Researcher* | *Specimen* | $a/d$ | $l_n/d$ | *Fiber* Type | $V_f$ (%) | $l_f/d_f$ | $V_{exp}$ $(MPa)$ | $V_{pre}/V_{exp}$ | | | | | | | |
|---|---|---|---|---|---|---|---|---|---|---|---|---|---|---|---|
| | | | | | | | | (1) | (2) | (3) | (4) | (5) | (6) | (7) | (12) |
| Mansur et al. (1986) | B1 | 2.0 | 10.2 | H | 0.5 | 60.0 | 75.0 | 1.3 | 0.9 | 0.5 | 0.8 | 0.4 | 0.8 | 0.6 | 1.0 |
| | C1 | 2.0 | 10.2 | H | 0.8 | 60.0 | 85.0 | 1.2 | 0.8 | 0.5 | 0.8 | 0.4 | 0.8 | 0.6 | 0.9 |
| | D1 | 2.0 | 10.2 | H | 1.0 | 60.0 | 93.0 | 1.1 | 0.8 | 0.5 | 0.9 | 0.4 | 0.8 | 0.6 | 0.8 |
| Lim et al. (1987) | 2/1,0/1,5 | 1.5 | 7.2 | H | 1.0 | 60.0 | 106.5 | 1.1 | 0.9 | 0.5 | 1.3 | 0.4 | 1.0 | 0.9 | 0.8 |
| | 2/1,0/2,5 | 2.5 | 9.5 | H | 1.0 | 60.0 | 60.2 | 2.0 | 1.4 | 0.8 | 0.9 | 0.8 | 1.1 | 0.9 | 1.0 |
| | 2/0.5/1.5 | 1.5 | 7.2 | H | 0.5 | 60.0 | 106.8 | 1.1 | 0.9 | 0.4 | 1.0 | 0.4 | 0.9 | 0.8 | 0.8 |
| | 2/0,5/2,5 | 2.5 | 9.5 | H | 0.5 | 60.0 | 58.0 | 2.1 | 1.4 | 0.7 | 0.8 | 0.7 | 0.9 | 0.8 | 1.0 |
| | 4/1/1.5 | 1.5 | 7.2 | H | 1.0 | 60.0 | 147.5 | 0.8 | 0.6 | 0.4 | 1.1 | 0.3 | 1.0 | 0.7 | 0.6 |
| | 4/1,0/2,5 | 2.5 | 9.5 | H | 1.0 | 60.0 | 82.6 | 1.5 | 1.0 | 0.6 | 0.9 | 0.6 | 1.0 | 0.8 | 1.1 |
| | 4/0.5/1.5 | 1.5 | 7.2 | H | 0.5 | 60.0 | 135.0 | 0.9 | 0.7 | 0.4 | 1.0 | 0.3 | 1.0 | 0.7 | 0.7 |
| | 4/0,5/2,5 | 2.5 | 9.5 | H | 0.5 | 60.0 | 63.7 | 1.9 | 1.3 | 0.7 | 0.9 | 0.6 | 1.0 | 0.9 | 1.4 |
| Cuchiara et al. (2004) | B10 | 2.0 | 10.5 | H | 1.0 | 60.0 | 115.0 | 1.1 | 0.8 | 0.5 | 0.9 | 0.4 | 0.8 | 0.7 | 0.8 |
| | B20 | 2.0 | 10.5 | H | 2.0 | 60.0 | 115.5 | 1.2 | 0.8 | 0.7 | 1.3 | 0.6 | 1.1 | 0.9 | 0.9 |
| Şen (2005) | BEAM-03 | 2.0 | 9.3 | H | 0.5 | 65.0 | 73.4 | 1.8 | 1.3 | 0.6 | 1.0 | 0.6 | 0.9 | 0.9 | 1.1 |
| | BEAM-05 | 2.0 | 9.3 | H | 0.8 | 65.0 | 79.0 | 1.7 | 1.2 | 0.7 | 1.0 | 0.6 | 0.9 | 0.9 | 1.1 |
| | BEAM-07 | 2.0 | 9.3 | H | 0.5 | 80.0 | 79.0 | 1.7 | 1.2 | 0.7 | 1.0 | 0.6 | 0.9 | 0.9 | 1.1 |
| | BEAM-09 | 2.0 | 9.3 | H | 0.8 | 80.0 | 90.8 | 1.5 | 1.0 | 0.7 | 1.0 | 0.7 | 0.9 | 0.9 | 0.9 |
| Kwak et al. (2002) | FHB2-2 | 2.0 | 5.9 | H | 0.5 | 62.5 | 135.0 | 1.0 | 0.7 | 0.4 | 0.5 | 0.4 | 0.5 | 0.5 | 0.6 |
| | FHB3-2 | 2.0 | 5.9 | H | 0.8 | 62.5 | 144.0 | 0.9 | 0.7 | 0.4 | 0.6 | 0.4 | 0.5 | 0.5 | 0.6 |
| | FNB2-2 | 2.0 | 5.9 | H | 0.5 | 62.5 | 107.1 | 0.9 | 0.6 | 0.3 | 0.6 | 0.3 | 0.5 | 0.4 | 0.6 |
| Rosenbusch andTeutsch (2003) | 2.2/2 | 1.5 | 8.8 | H | 0.3 | 65.0 | 280.0 | 0.7 | 0.6 | 0.3 | 0.6 | 0.3 | 0.6 | 0.5 | 0.5 |
| | 2.2/3 | 1.5 | 8.8 | H | 0.8 | 65.0 | 300.0 | 0.7 | 0.5 | 0.4 | 0.8 | 0.3 | 0.7 | 0.6 | 0.5 |
| | 2.3/2 | 2.5 | 8.8 | H | 0.3 | 65.0 | 82.5 | 2.5 | 1.7 | 0.9 | 0.9 | 0.8 | 0.8 | 0.8 | 1.2 |
| | 2.3/3 | 2.5 | 8.8 | H | 0.8 | 65.0 | 108.0 | 1.9 | 1.3 | 1.0 | 0.8 | 0.9 | 0.9 | 0.8 | 1.0 |
| | 2.4/2 | 2.5 | 8.8 | H | 0.3 | 65.0 | 108.0 | 1.9 | 1.3 | 0.7 | 0.8 | 0.6 | 0.8 | 0.7 | 1.3 |
| | 2.4/3 | 2.5 | 8.8 | H | 0.8 | 65.0 | 144.0 | 1.4 | 0.9 | 0.7 | 0.7 | 0.7 | 0.7 | 0.7 | 1.0 |

Table 4.9. *Comparison of Predicted versus Experimental Strengths for Deep Beams ( $a/d \leq 2.5$ ) without transverse reinforcement (continued)*

| $Researcher$ | $Specimen$ | $a/d$ | $l_n/d$ | $Fiber$ Type | $V_f$ (%) | $l_f/d_f$ | $V_{exp}$ $(MPa)$ | $V_{pre}/V_{exp}$ (1) | (2) | (3) | (4) | (5) | (6) | (7) | (12) |
|---|---|---|---|---|---|---|---|---|---|---|---|---|---|---|---|
| Dupontand Vandewalle (2003) | 14 | 1.5 | 8.8 | H | 0.3 | 65.0 | 280.0 | 0.7 | 0.6 | 0.3 | 0.6 | 0.3 | 0.6 | 0.5 | 0.5 |
| | 15 | 1.5 | 8.8 | H | 0.8 | 65.0 | 300.0 | 0.7 | 0.5 | 0.4 | 0.8 | 0.3 | 0.7 | 0.6 | 0.5 |
| | 17 | 2.5 | 8.8 | H | 0.3 | 65.0 | 82.5 | 2.5 | 1.7 | 0.9 | 0.9 | 0.8 | 0.9 | 0.8 | 1.2 |
| | 18 | 2.5 | 8.8 | H | 0.8 | 65.0 | 108.0 | 1.9 | 1.3 | 1.0 | 0.8 | 0.9 | 0.9 | 0.8 | 1.0 |
| | 20 | 2.5 | 8.8 | H | 0.3 | 65.0 | 108.0 | 1.9 | 1.3 | 0.7 | 0.7 | 0.6 | 0.8 | 0.7 | 1.3 |
| | 21 | 2.5 | 8.8 | H | 0.8 | 65.0 | 144.0 | 1.4 | 0.9 | 0.7 | 0.7 | 0.7 | 0.7 | 0.7 | 1.0 |
| | 26 | 2.5 | 8.8 | H | 0.3 | 45.0 | 100.0 | 1.7 | 1.1 | 0.5 | 0.6 | 0.5 | 0.6 | 0.5 | 1.0 |
| | 27 | 2.5 | 8.8 | H | 0.8 | 45.0 | 120.0 | 1.4 | 1.0 | 0.6 | 0.6 | 0.6 | 0.6 | 0.5 | 0.8 |
| | 29 | 2.5 | 8.8 | H | 0.3 | 45.0 | 100.0 | 1.7 | 1.1 | 0.6 | 0.7 | 0.5 | 0.7 | 0.6 | 1.2 |
| | 30 | 2.5 | 8.8 | H | 0.8 | 45.0 | 120.0 | 1.4 | 0.9 | 0.6 | 0.7 | 0.5 | 0.7 | 0.6 | 1.0 |
| | 31 | 2.5 | 8.8 | H | 0.5 | 65.0 | 130.0 | 1.7 | 1.2 | 0.8 | 0.6 | 0.7 | 0.7 | 0.7 | 0.8 |
| | 32 | 2.5 | 8.8 | H | 0.5 | 65.0 | 157.5 | 1.4 | 0.9 | 0.6 | 0.6 | 0.6 | 0.6 | 0.6 | 0.9 |
| | 33 | 2.5 | 8.8 | H | 0.5 | 80.0 | 147.5 | 1.5 | 1.0 | 0.8 | 0.6 | 0.8 | 0.6 | 0.6 | 0.7 |
| | 34 | 2.5 | 8.8 | H | 0.8 | 80.0 | 158.0 | 1.5 | 1.0 | 1.0 | 0.6 | 1.0 | 0.7 | 0.7 | 0.7 |
| | 41 | 2.5 | 10.7 | H | 0.6 | 80.0 | 162.0 | 1.4 | 0.9 | 0.7 | 0.6 | 0.7 | 0.6 | 0.6 | 0.6 |
| | 42 | 2.5 | 10.7 | H | 0.9 | 80.0 | 162.0 | 1.3 | 0.9 | 0.9 | 0.6 | 0.8 | 0.8 | 0.6 | 0.6 |
| | 43 | 2.5 | 10.7 | H | 0.4 | 80.0 | 162.0 | 1.3 | 0.9 | 0.6 | 0.5 | 0.6 | 0.5 | 0.5 | 0.6 |
| Imam et al. (1994) | B15 | 1.8 | 10.8 | H | 0.8 | 75.0 | 404.0 | 1.0 | 0.7 | 0.5 | 0.7 | 0.4 | 0.6 | 0.7 | 0.7 |
| | B5 | 2.5 | 10.8 | H | 0.8 | 75.0 | 269.0 | 1.5 | 1.0 | 0.7 | 0.6 | 0.7 | 0.7 | 0.7 | 0.9 |
| | B16 | 1.8 | 10.8 | H | 0.8 | 75.0 | 528.0 | 0.7 | 0.5 | 0.4 | 0.6 | 0.3 | 0.6 | 0.6 | 0.5 |
| | B6 | 2.5 | 10.8 | H | 0.8 | 75.0 | 284.0 | 1.4 | 0.9 | 0.7 | 0.6 | 0.6 | 0.7 | 0.8 | 1.0 |
| Tan et al. (1993) | 2 | 2.0 | 5.0 | H | 0.5 | 60.0 | 218.0 | 0.8 | 0.6 | 0.3 | 0.5 | 0.3 | 0.5 | 0.4 | 0.6 |
| | 3 | 2.0 | 5.0 | H | 0.8 | 60.0 | 180.9 | 0.9 | 0.7 | 0.4 | 0.7 | 0.3 | 0.6 | 0.5 | 0.7 |
| | 4 | 2.0 | 5.0 | H | 1.0 | 60.0 | 210.3 | 0.8 | 0.6 | 0.4 | 0.7 | 0.3 | 0.6 | 0.5 | 0.6 |
| | 5 | 2.5 | 5.0 | H | 1.0 | 60.0 | 154.2 | 1.2 | 0.8 | 0.5 | 0.6 | 0.4 | 0.7 | 0.6 | 0.8 |
| | 6 | 1.5 | 5.0 | H | 1.0 | 60.0 | 307.0 | 0.6 | 0.4 | 0.3 | 0.7 | 0.2 | 0.6 | 0.5 | 0.4 |

Table 4.9. *Comparison of Predicted versus Experimental Strengths for Deep Beams ( $a/d \leq 2.5$ ) without transverse reinforcement (continued)*

| *Researcher* | *Specimen* | $a/d$ | $l_n/d$ | *Fiber* Type | $V_f$ (%) | $l_f/d_f$ | $V_{exp}$ $(MPa)$ | $V_{pre}/V_{exp}$ | | | | | | | |
|---|---|---|---|---|---|---|---|---|---|---|---|---|---|---|---|
| | | | | | | | | (1) | (2) | (3) | (4) | (5) | (6) | (7) | (12) |
| Ashour et al. (1992) | B-2-l.O-L | 2.0 | 6.3 | H | 1.0 | 75.0 | 45.2 | 3.6 | 2.5 | 1.9 | 1.5 | 1.8 | 1.7 | 1.6 | 0.8 |
| | B-1-0.5-A | 1.0 | 4.3 | H | 0.5 | 75.0 | 244.3 | 0.7 | 0.6 | 0.3 | 1.1 | 0.3 | 1.1 | 1.1 | 0.5 |
| | B-2-0.5-A | 2.0 | 6.3 | H | 0.5 | 75.0 | 129.5 | 1.3 | 0.9 | 0.6 | 0.8 | 0.5 | 0.8 | 0.9 | 0.9 |
| | B-1-l.O-A | 1.0 | 4.3 | H | 1.0 | 75.0 | 342.4 | 0.5 | 0.4 | 0.3 | 0.9 | 0.2 | 0.9 | 0.8 | 0.3 |
| | B-2-l.O-A | 2.0 | 6.3 | H | 1.0 | 75.0 | 162.9 | 1.0 | 0.7 | 0.6 | 0.8 | 0.5 | 0.7 | 0.8 | 0.7 |
| | B-1-1.5-A | 1.0 | 4.3 | H | 1.5 | 75.0 | 374.9 | 0.4 | 0.4 | 0.3 | 1.0 | 0.3 | 0.8 | 0.8 | 0.3 |
| | B-2-1.5-A | 2.0 | 6.3 | H | 1.5 | 75.0 | 193.8 | 0.8 | 0.6 | 0.6 | 0.8 | 0.5 | 0.7 | 0.7 | 0.6 |
| | B-2-l.O-M | 2.0 | 6.3 | H | 1.0 | 75.0 | 180.9 | 0.9 | 0.6 | 0.5 | 0.8 | 0.5 | 0.8 | 0.8 | 0.7 |
| Choand Kim (2003) | F30-0.5-13 | 1.4 | 4.3 | H | 0.5 | 60.0 | 60.9 | 1.0 | 0.8 | 0.4 | 1.2 | 0.4 | 1.2 | 0.8 | 0.8 |
| | F30-1.0-13 | 1.4 | 4.3 | H | 1.0 | 60.0 | 79.4 | 0.8 | 0.6 | 0.4 | 1.2 | 0.3 | 1.1 | 0.7 | 0.6 |
| | F30-1.5-13 | 1.4 | 4.3 | H | 1.5 | 60.0 | 84.3 | 0.7 | 0.6 | 0.4 | 1.4 | 0.4 | 1.1 | 0.7 | 0.5 |
| | F30-2.0-13 | 1.4 | 4.3 | H | 2.0 | 60.0 | 91.4 | 0.7 | 0.6 | 0.5 | 1.6 | 0.4 | 1.1 | 0.8 | 0.5 |
| | F60-0.5-13 | 1.4 | 4.3 | H | 0.5 | 60.0 | 95.2 | 1.0 | 0.8 | 0.4 | 1.0 | 0.3 | 0.9 | 0.9 | 0.7 |
| | F60-1.0-13 | 1.4 | 4.3 | H | 1.0 | 60.0 | 103.0 | 1.0 | 0.7 | 0.4 | 1.1 | 0.4 | 1.0 | 0.9 | 0.7 |
| | F60-1.5-13 | 1.4 | 4.3 | H | 1.5 | 60.0 | 102.8 | 0.9 | 0.7 | 0.5 | 1.3 | 0.5 | 1.0 | 1.0 | 0.7 |
| | F60-2.0-13 | 1.4 | 4.3 | H | 2.0 | 60.0 | 114.9 | 0.9 | 0.7 | 0.5 | 1.4 | 0.5 | 1.0 | 0.9 | 0.6 |
| | F70-0.5-19 | 1.4 | 4.3 | H | 0.5 | 60.0 | 178.8 | 0.6 | 0.5 | 0.2 | 0.6 | 0.2 | 0.7 | 0.6 | 0.4 |
| | F70-1.0-19 | 1.4 | 4.3 | H | 1.0 | 60.0 | 169.5 | 0.6 | 0.5 | 0.3 | 0.8 | 0.3 | 0.8 | 0.7 | 0.4 |
| | F70-1.5-19 | 1.4 | 4.3 | H | 1.5 | 60.0 | 186.7 | 0.5 | 0.4 | 0.3 | 0.9 | 0.3 | 0.8 | 0.7 | 0.4 |
| | F70-2.0-19 | 1.4 | 4.3 | H | 2.0 | 60.0 | 198.5 | 0.5 | 0.4 | 0.3 | 0.9 | 0.3 | 0.8 | 0.7 | 0.4 |
| | F80-0.5-16 | 1.4 | 4.3 | H | 0.5 | 60.0 | 157.9 | 0.7 | 0.6 | 0.3 | 0.7 | 0.2 | 0.7 | 0.7 | 0.5 |
| | F80-1.0-16 | 1.4 | 4.3 | H | 1.0 | 60.0 | 162.8 | 0.7 | 0.5 | 0.3 | 0.8 | 0.3 | 0.7 | 0.7 | 0.5 |
| | F80-1.5-16 | 1.4 | 4.3 | H | 1.5 | 60.0 | 158.4 | 0.7 | 0.6 | 0.4 | 1.0 | 0.3 | 0.8 | 0.8 | 0.5 |
| | F80-2.0-16 | 1.4 | 4.3 | H | 2.0 | 60.0 | 179.5 | 0.6 | 0.5 | 0.4 | 1.0 | 0.4 | 0.8 | 0.7 | 0.5 |
| | F80-0.5-19 | 1.4 | 4.3 | H | 0.5 | 60.0 | 153.5 | 0.8 | 0.6 | 0.3 | 0.8 | 0.3 | 0.9 | 0.8 | 0.6 |
| | F80-1.0-19 | 1.4 | 4.3 | H | 1.0 | 60.0 | 170.6 | 0.7 | 0.5 | 0.3 | 0.9 | 0.3 | 0.8 | 0.8 | 0.5 |
| | F80-1.5-19 | 1.4 | 4.3 | H | 1.5 | 60.0 | 170.2 | 0.7 | 0.5 | 0.4 | 1.0 | 0.3 | 0.9 | 0.8 | 0.5 |
| | F80-2.0-19 | 1.4 | 4.3 | H | 2.0 | 60.0 | 176.0 | 0.7 | 0.5 | 0.4 | 1.1 | 0.4 | 0.9 | 0.9 | 0.5 |

Table 4.9. *Comparison of Predicted versus Experimental Strengths for Deep Beams ( $a/d \leq 2.5$ ) without transverse reinforcement (continued)*

| $Researcher$ | $Specimen$ | $a/d$ | $l_n/d$ | $Fiber$ Type | $V_f$ (%) | $l_f/d_f$ | $V_{exp}$ $(MPa)$ | $V_{pre}/V_{exp}$ | | | | | | | |
|---|---|---|---|---|---|---|---|---|---|---|---|---|---|---|---|
| | | | | | | | | (1) | (2) | (3) | (4) | (5) | (6) | (7) | (12) |
| Li et al. (1992) | M11 | 63.5 | 127.0 | C | 1.0 | 57.0 | 50.7 | 0.6 | 0.5 | 0.3 | 1.2 | 0.3 | 1.1 | 0.9 | 0.8 |
| | M12 | 63.5 | 127.0 | C | 1.0 | 57.0 | 33.4 | 0.9 | 0.7 | 0.5 | 1.0 | 0.4 | 0.9 | 0.8 | 0.7 |
| | M13 | 63.5 | 127.0 | C | 1.0 | 57.0 | 30.1 | 1.0 | 0.7 | 0.5 | 0.9 | 0.5 | 0.8 | 0.8 | 0.5 |
| | M14 | 63.5 | 127.0 | C | 1.0 | 57.0 | 25.8 | 1.1 | 0.8 | 0.6 | 0.9 | 0.5 | 0.8 | 0.8 | 0.6 |
| | M15 | 63.5 | 127.0 | C | 1.0 | 28.5 | 23.4 | 1.4 | 0.9 | 0.6 | 0.7 | 0.5 | 0.7 | 0.7 | 0.6 |
| | M16 | 63.5 | 127.0 | C | 1.0 | 28.5 | 20.5 | 1.6 | 1.0 | 0.6 | 0.7 | 0.6 | 0.7 | 0.7 | 0.5 |
| | C4 | 63.5 | 127.0 | H | 1.0 | 60.0 | 36.5 | 0.5 | 0.4 | 0.2 | 0.7 | 0.2 | 0.5 | 0.4 | 0.8 |
| Khalooand Kim (1997) | LC-0.5-16 | 125.0 | 220.0 | H | 0.5 | 29.0 | 102.9 | 0.8 | 0.7 | 0.3 | 1.7 | 0.2 | 2.1 | 1.3 | 0.6 |
| | LC-1.0-16 | 125.0 | 220.0 | H | 0.5 | 58.0 | 125.1 | 0.7 | 0.6 | 0.3 | 1.5 | 0.2 | 1.8 | 1.1 | 0.6 |
| | LC-1.5-16 | 125.0 | 220.0 | H | 1.0 | 29.0 | 146.3 | 0.6 | 0.5 | 0.3 | 1.3 | 0.2 | 1.5 | 0.9 | 0.6 |
| | LC-0.5-32 | 125.0 | 220.0 | H | 1.0 | 58.0 | 134.5 | 0.7 | 0.6 | 0.3 | 1.8 | 0.3 | 1.8 | 1.2 | 0.6 |
| | LC-1.0-32 | 125.0 | 220.0 | H | 1.5 | 29.0 | 145.5 | 0.6 | 0.5 | 0.3 | 1.5 | 0.2 | 1.6 | 1.0 | 0.5 |
| | LC-1.5-32 | 125.0 | 220.0 | H | 1.5 | 58.0 | 164.2 | 0.5 | 0.4 | 0.3 | 1.7 | 0.2 | 1.5 | 0.9 | 0.7 |
| | NC-0.5-16 | 125.0 | 220.0 | H | 0.5 | 29.0 | 123.5 | 0.8 | 0.7 | 0.3 | 1.5 | 0.2 | 1.8 | 1.4 | 0.7 |
| | NC-1.0-16 | 125.0 | 220.0 | H | 0.5 | 58.0 | 154.6 | 0.6 | 0.6 | 0.3 | 1.4 | 0.2 | 1.5 | 1.1 | 0.5 |
| | NC-1.5-16 | 125.0 | 220.0 | H | 1.0 | 29.0 | 170.0 | 0.6 | 0.5 | 0.3 | 1.3 | 0.2 | 1.4 | 1.1 | 0.6 |
| | NC-0.5-32 | 125.0 | 220.0 | H | 1.0 | 58.0 | 152.1 | 0.7 | 0.6 | 0.3 | 1.7 | 0.3 | 1.6 | 1.2 | 0.5 |
| | NC-1.0-32 | 125.0 | 220.0 | H | 1.5 | 29.0 | 176.8 | 0.6 | 0.5 | 0.3 | 1.3 | 0.2 | 1.4 | 1.0 | 0.5 |
| | NC-1.5-32 | 125.0 | 220.0 | H | 1.5 | 58.0 | 192.5 | 0.5 | 0.4 | 0.3 | 1.6 | 0.2 | 1.3 | 0.9 | 0.6 |
| | MC-0.5-16 | 125.0 | 220.0 | H | 0.5 | 29.0 | 153.2 | 0.7 | 0.6 | 0.3 | 1.3 | 0.2 | 1.5 | 1.3 | 0.5 |
| | MC-1.0-16 | 125.0 | 220.0 | H | 0.5 | 58.0 | 170.2 | 0.7 | 0.6 | 0.3 | 1.3 | 0.2 | 1.4 | 1.2 | 0.8 |
| | MC-1.5-16 | 125.0 | 220.0 | H | 1.0 | 29.0 | 199.1 | 0.6 | 0.5 | 0.2 | 1.1 | 0.2 | 1.2 | 1.0 | 0.7 |
| | MC-0.5-32 | 125.0 | 220.0 | H | 1.0 | 58.0 | 184.5 | 0.6 | 0.5 | 0.3 | 1.5 | 0.2 | 1.4 | 1.1 | 0.5 |
| | MC-1.0-32 | 125.0 | 220.0 | H | 1.5 | 29.0 | 222.8 | 0.5 | 0.5 | 0.2 | 1.1 | 0.2 | 1.1 | 0.9 | 0.6 |
| | MC-1.5-32 | 125.0 | 220.0 | H | 1.5 | 58.0 | 236.2 | 0.5 | 0.4 | 0.3 | 1.3 | 0.2 | 1.1 | 0.9 | 0.6 |
| Shin et al. (1994) | 1 | 100.0 | 200.0 | S | 0.5 | 100.0 | 119.7 | 0.8 | 0.6 | 0.3 | 0.6 | 0.3 | 0.6 | 0.6 | 0.5 |
| | 2 | 100.0 | 200.0 | S | 1.0 | 100.0 | 129.5 | 0.8 | 0.5 | 0.4 | 0.7 | 0.3 | 0.7 | 0.6 | 0.8 |

### 4.3.3. Comparison of Shear Prediction Equations for Deep Beams ($a/d$ > 2.5) with Transverse Reinforcement

The shear formulation of ACI 318-14 (2014) shown in Fig. 4.11 (1), has a high scatter of data, therefore, the mean (1.53), standard deviation (0.18) and AAE (56.67%) are relatively high, which raises a question on the validity of this equation for these members. The shear strength values obtained from Eqn. (2) by Sharma (1986) overpredict most of the experimental shear strength values (Table 4.10). Moreover, the mean (3.27), standard deviation (1.57) and AAE (231.18%) are higher than those of the other predictions. The error for this equation is especially high for the specimens of Batson et al. (1972), which are small scale specimens. This indicates that the equation does not provide accurate results for small scale members. The comparison of the proposed method with the experimental shear is given in Fig.4.11 (12). For the majority of the members, the experimental results are again underestimated (Table 4.9). Moreover, mean (0.78), standard deviation (0.12) and, AAE (25.13%) are much lower than that of other equations. Consequently, the proposed method leads to improved predictions, when compared with the others.

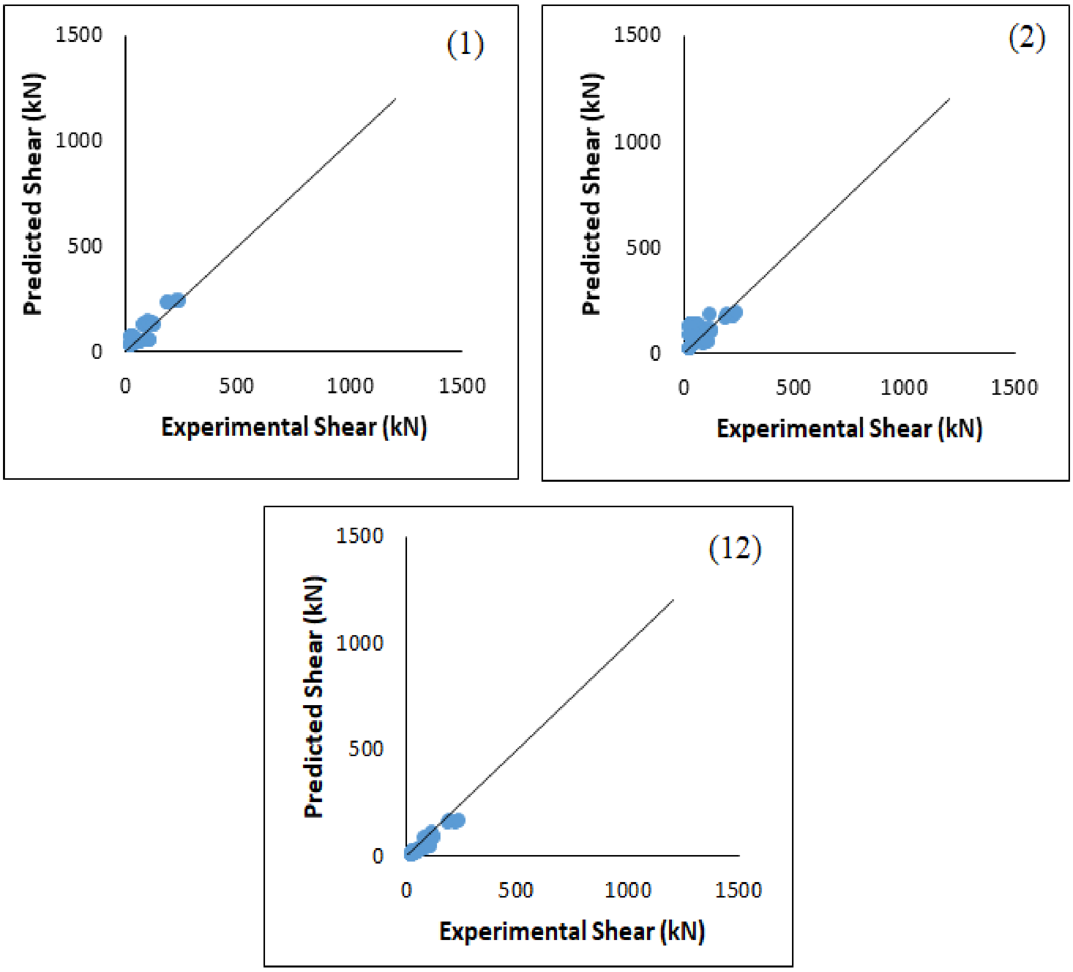


*Figure 4.11.* Shear strength predictions for Deep Beams ($a/d$ > 2.5) with transverse reinforcement: (1) ACI 318-14 (2014); (2) Sharma (1986); (12) Proposed method

Table 4.10. *Statistical Parameters for Deep Beams ($a/d$ > 2.5) with transverse reinforcement*

| Equation Number | Shear Equation | Mean | Range | Standard Deviation | Avg. Absolute Error (%) |
|---|---|---|---|---|---|
| (1) | ACI 318-14 (2014) | 1.53 | 0.55 - 3.86 | 0.18 | 56.67 |
| (2) | Sharma (1986) | 3.27 | 0.56 - 5.84 | 1.57 | 231.18 |
| (12) | Proposed Method | 0.78 | 0.52 - 1.19 | 0.12 | 25.13 |

Table 4.11. *Comparison of Predicted versus Experimental Strengths for Deep Beams ( $a/d$ > 2.5 ) with transverse reinforcement*

| $Researcher$ | $Specimen$ | $a/d$ | $l_n/d$ | $\rho_t$ (%) | $Fiber$ Type | $V_f$ (%) | $l_f/d_f$ | $V_{exp}$ $(MPa)$ | $V_{pre}/V_{exp}$ (1) | (2) | (12) |
|---|---|---|---|---|---|---|---|---|---|---|---|
| SwamyandBahia (1985) | B52 | 4.5 | 9.0 | 0.2 | C | 0.4 | 100.0 | 79.5 | 1.7 | 1.4 | 1.2 |
| | B53 | 4.5 | 9.0 | 0.2 | C | 0.8 | 100.0 | 114.0 | 1.2 | 1.0 | 0.8 |
| | B54 | 4.5 | 9.0 | 0.2 | C | 1.2 | 100.0 | 115.0 | 1.3 | 1.0 | 0.9 |
| | B55 | 4.5 | 9.0 | 0.2 | C | 0.8 | 100.0 | 118.2 | 1.2 | 0.9 | 0.8 |
| | B56 | 4.5 | 9.0 | 0.2 | C | 0.8 | 100.0 | 96.4 | 1.5 | 1.2 | 0.7 |
| | B63R | 4.5 | 9.0 | 0.2 | C | 0.8 | 100.0 | 75.5 | 1.8 | 1.4 | 0.8 |
| Batson et al. (1972) | A1 | 4.8 | 14.4 | 3.0 | S | 0.2 | 101.6 | 31.4 | 1.5 | 4.3 | 0.6 |
| | A2 | 4.8 | 14.4 | 3.0 | S | 0.2 | 101.6 | 26.7 | 1.7 | 5.1 | 0.8 |
| | A3 | 4.8 | 14.4 | 3.0 | S | 0.2 | 101.6 | 29.5 | 1.6 | 4.6 | 0.7 |
| | B1 | 4.4 | 14.4 | 3.0 | S | 0.2 | 101.6 | 32.7 | 1.4 | 4.2 | 0.7 |
| | B2 | 4.4 | 14.4 | 3.0 | S | 0.2 | 101.6 | 31.0 | 1.5 | 4.4 | 0.7 |
| | B3 | 4.4 | 14.4 | 3.0 | S | 0.2 | 101.6 | 31.6 | 1.5 | 4.3 | 0.7 |
| | C1 | 4.2 | 14.4 | 3.0 | S | 0.2 | 101.6 | 31.5 | 1.5 | 4.4 | 0.7 |
| | C2 | 4.2 | 14.4 | 3.0 | S | 0.2 | 101.6 | 27.9 | 1.7 | 4.9 | 0.8 |
| | C3 | 4.2 | 14.4 | 3.0 | S | 0.2 | 101.6 | 25.1 | 1.8 | 5.5 | 0.9 |
| | D1 | 4.3 | 14.4 | 3.0 | S | 0.2 | 101.6 | 32.5 | 1.4 | 4.2 | 0.7 |
| | D2 | 4.3 | 14.4 | 3.0 | S | 0.2 | 101.6 | 29.5 | 1.6 | 4.6 | 0.8 |
| | D3 | 4.3 | 14.4 | 3.0 | S | 0.2 | 101.6 | 27.9 | 1.7 | 4.9 | 0.8 |
| | E1 | 4.2 | 14.4 | 3.0 | S | 0.4 | 101.6 | 32.7 | 1.6 | 4.3 | 0.7 |
| | E2 | 4.2 | 14.4 | 3.0 | S | 0.4 | 101.6 | 32.9 | 1.5 | 4.3 | 0.7 |
| | E3 | 4.2 | 14.4 | 3.0 | S | 0.4 | 101.6 | 32.9 | 1.5 | 4.3 | 0.7 |
| | F1 | 4.0 | 14.4 | 3.0 | S | 0.4 | 101.6 | 33.1 | 1.5 | 4.2 | 0.8 |
| | F2 | 4.0 | 14.4 | 3.0 | S | 0.4 | 101.6 | 31.1 | 1.6 | 4.5 | 0.8 |
| | F3 | 4.0 | 14.4 | 3.0 | S | 0.4 | 101.6 | 33.1 | 1.5 | 4.2 | 0.8 |
| | G1 | 4.4 | 14.4 | 3.0 | S | 0.2 | 101.6 | 28.3 | 1.6 | 4.8 | 0.8 |
| | G2 | 4.4 | 14.4 | 3.0 | S | 0.2 | 101.6 | 28.8 | 1.6 | 4.8 | 0.8 |
| | G3 | 4.4 | 14.4 | 3.0 | S | 0.2 | 101.6 | 26.9 | 1.7 | 5.1 | 0.8 |

Table 4.11. *Comparison of Predicted versus Experimental Strengths for Deep Beams ( $a/d$ > 2.5 ) with transverse reinforcement (continued)*

| $Researcher$ | $Specimen$ | $a/d$ | $l_n/d$ | $\rho_t$ (%) | $Fiber$ Type | $V_f$ (%) | $l_f/d_f$ | $V_{exp}$ $(MPa)$ | $V_{pre}/V_{exp}$ | | |
|---|---|---|---|---|---|---|---|---|---|---|---|
| | | | | | | | | | (1) | (2) | (12) |
| Batson et al. (1972) | H1 | 3.8 | 14.4 | 3.0 | S | 0.9 | 101.6 | 38.0 | 1.3 | 3.7 | 0.7 |
| | H2 | 3.8 | 14.4 | 3.0 | S | 0.9 | 101.6 | 41.3 | 1.2 | 3.4 | 0.7 |
| | H3 | 3.8 | 14.4 | 3.0 | S | 0.9 | 101.6 | 37.9 | 1.3 | 3.7 | 0.7 |
| | I1 | 3.6 | 14.4 | 3.0 | S | 0.9 | 101.6 | 40.8 | 1.2 | 3.5 | 0.7 |
| | I2 | 3.6 | 14.4 | 3.0 | S | 0.9 | 101.6 | 38.2 | 1.3 | 3.7 | 0.8 |
| | I3 | 3.6 | 14.4 | 3.0 | S | 0.9 | 101.6 | 38.8 | 1.3 | 3.6 | 0.7 |
| | J1 | 2.8 | 14.4 | 3.0 | S | 1.8 | 101.6 | 51.8 | 1.0 | 2.8 | 0.8 |
| | J2 | 2.8 | 14.4 | 3.0 | S | 1.8 | 101.6 | 47.3 | 1.1 | 3.0 | 0.8 |
| | J3 | 2.8 | 14.4 | 3.0 | S | 1.8 | 101.6 | 46.9 | 1.1 | 3.1 | 0.8 |
| | K3 | 2.6 | 14.4 | 3.0 | S | 1.8 | 101.6 | 63.2 | 0.8 | 2.3 | 0.7 |
| | U1 | 4.0 | 14.4 | 3.0 | C | 0.2 | 101.6 | 30.1 | 1.5 | 4.6 | 0.8 |
| | U3 | 4.0 | 14.4 | 3.0 | C | 0.2 | 101.6 | 30.2 | 1.5 | 4.6 | 0.8 |
| | L1 | 4.0 | 14.4 | 3.0 | S | 0.2 | 101.6 | 33.1 | 1.4 | 4.2 | 0.7 |
| | L2 | 4.6 | 14.4 | 3.0 | S | 0.2 | 46.2 | 25.8 | 1.8 | 5.3 | 0.8 |
| | L3 | 4.4 | 14.4 | 3.0 | S | 0.2 | 46.2 | 27.1 | 1.7 | 5.1 | 0.8 |
| | M1 | 4.4 | 14.4 | 3.0 | C | 0.2 | 46.2 | 25.6 | 1.8 | 5.3 | 0.8 |
| | M2 | 5.0 | 14.4 | 3.0 | C | 0.2 | 46.2 | 24.3 | 1.9 | 5.6 | 0.8 |
| | M3 | 4.8 | 14.4 | 3.0 | C | 0.2 | 46.2 | 26.9 | 1.7 | 5.1 | 0.7 |
| | N1 | 5.0 | 14.4 | 3.0 | C | 0.2 | 46.2 | 26.0 | 1.8 | 5.2 | 0.7 |
| | N2 | 4.0 | 14.4 | 3.0 | C | 0.4 | 46.2 | 31.4 | 1.6 | 4.5 | 0.8 |
| | N3 | 4.4 | 14.4 | 3.0 | C | 0.4 | 46.2 | 31.1 | 1.6 | 4.5 | 0.7 |
| | O1 | 4.8 | 14.4 | 3.0 | C | 0.4 | 46.2 | 27.9 | 1.8 | 5.0 | 0.7 |
| | O2 | 4.2 | 14.4 | 3.0 | C | 0.4 | 46.2 | 33.7 | 1.5 | 4.2 | 0.7 |
| | O3 | 4.2 | 14.4 | 3.0 | C | 0.4 | 46.2 | 30.1 | 1.7 | 4.7 | 0.8 |
| | P1 | 4.2 | 14.4 | 3.0 | C | 0.4 | 46.2 | 32.5 | 1.6 | 4.3 | 0.7 |
| | P2 | 3.8 | 14.4 | 3.0 | C | 0.4 | 46.2 | 56.2 | 0.9 | 2.5 | 0.7 |
| | P3 | 3.8 | 14.4 | 3.0 | C | 0.4 | 46.2 | 60.6 | 0.8 | 2.4 | 0.7 |

Table 4.11. *Comparison of Predicted versus Experimental Strengths for Deep Beams ( $a/d$ > 2.5 ) with transverse reinforcement (continued)*

| $Researcher$ | $Specimen$ | $a/d$ | $l_n/d$ | $\rho_t$ (%) | $Fiber$ Type | $V_f$ (%) | $l_f/d_f$ | $V_{exp}$ $(MPa)$ | $V_{pre}/V_{exp}$ | | |
|---|---|---|---|---|---|---|---|---|---|---|---|
| | | | | | | | | | (1) | (2) | (12) |
| Batson et al. (1972) | Q1 | 4.4 | 14.4 | 3.0 | C | 0.4 | 46.2 | 29.7 | 1.7 | 4.7 | 0.8 |
| | Q2 | 4.4 | 14.4 | 3.0 | C | 0.4 | 46.2 | 30.1 | 1.7 | 4.6 | 0.8 |
| | Q3 | 4.4 | 14.4 | 3.0 | C | 0.4 | 46.2 | 30.4 | 1.7 | 4.6 | 0.7 |
| | R1 | 3.2 | 14.4 | 3.0 | C | 0.9 | 46.2 | 36.6 | 1.4 | 3.9 | 0.9 |
| | R2 | 3.4 | 14.4 | 3.0 | C | 0.9 | 46.2 | 34.2 | 1.5 | 4.1 | 0.9 |
| | R3 | 3.6 | 14.4 | 3.0 | C | 0.9 | 46.2 | 44.5 | 1.1 | 3.2 | 0.6 |
| | S1 | 3.4 | 14.4 | 3.0 | C | 0.9 | 46.2 | 33.1 | 1.5 | 4.3 | 0.9 |
| | S2 | 3.4 | 14.4 | 3.0 | C | 0.9 | 46.2 | 41.8 | 1.2 | 3.4 | 0.7 |
| | S3 | 3.4 | 14.4 | 3.0 | C | 0.9 | 46.2 | 39.4 | 1.3 | 3.6 | 0.7 |
| | T1 | 3.6 | 14.4 | 3.0 | C | 0.9 | 46.2 | 41.2 | 1.2 | 3.4 | 0.7 |
| | T2 | 3.6 | 14.4 | 3.0 | C | 0.9 | 46.2 | 40.6 | 1.2 | 3.5 | 0.7 |
| | T3 | 3.6 | 14.4 | 3.0 | C | 0.9 | 46.2 | 40.7 | 1.2 | 3.5 | 0.7 |
| | X1 | 4.8 | 14.4 | 3.0 | C | 0.2 | 46.2 | 24.2 | 1.9 | 5.6 | 0.8 |
| | X2 | 4.8 | 14.4 | 3.0 | C | 0.2 | 46.2 | 23.3 | 2.0 | 5.8 | 0.9 |
| | X3 | 4.8 | 14.4 | 3.0 | C | 0.2 | 46.2 | 26.0 | 1.8 | 5.2 | 0.8 |
| EI-Niema (1991) | 2 | 3.9 | 10.3 | 0.5 | C | 0.4 | 127.7 | 45.0 | 1.2 | 1.2 | 0.6 |
| | 3 | 3.9 | 10.3 | 0.5 | C | 0.7 | 127.7 | 46.5 | 1.3 | 1.2 | 0.6 |
| | 4 | 3.9 | 10.3 | 0.5 | C | 1.0 | 127.7 | 49.0 | 1.2 | 1.2 | 0.6 |
| | 5 | 3.9 | 10.3 | 0.5 | C | 0.4 | 95.8 | 40.5 | 1.3 | 1.4 | 0.7 |
| | 6 | 3.9 | 10.3 | 0.5 | C | 0.7 | 95.8 | 44.0 | 1.2 | 1.2 | 0.6 |
| | 7 | 3.9 | 10.3 | 0.5 | C | 1.0 | 95.8 | 45.5 | 1.2 | 1.2 | 0.6 |
| | 8 | 3.9 | 10.3 | 0.5 | C | 0.4 | 63.8 | 40.0 | 1.3 | 1.4 | 0.7 |
| | 9 | 3.9 | 10.3 | 0.5 | C | 0.7 | 63.8 | 41.5 | 1.3 | 1.3 | 0.6 |
| | 10 | 3.9 | 10.3 | 0.5 | C | 1.0 | 63.8 | 45.0 | 1.2 | 1.2 | 0.6 |
| SwamyandAlta'an(1981) | DR11 | 6.5 | 12.9 | 0.3 | C | 0.5 | 100.0 | 20.5 | 3.9 | 4.4 | 1.0 |
| | DR12 | 6.5 | 12.9 | 0.3 | C | 1.0 | 100.0 | 21.0 | 3.8 | 4.3 | 1.0 |
| | DR21 | 6.5 | 12.9 | 0.3 | C | 0.5 | 100.0 | 29.7 | 2.6 | 3.0 | 0.9 |

Table 4.11. *Comparison of Predicted versus Experimental Strengths for Deep Beams ( $a/d$ > 2.5 ) with transverse reinforcement (continued)*

| $Researcher$ | $Specimen$ | $a/d$ | $l_n/d$ | $\rho_t$ (%) | $Fiber$ Type | $V_f$ (%) | $l_f/d_f$ | $V_{exp}$ $(MPa)$ | $V_{pre}/V_{exp}$ | | |
|---|---|---|---|---|---|---|---|---|---|---|---|
| | | | | | | | | | $(1)$ | $(2)$ | $(12)$ |
| SwamyandAlta'an(1981) | DR22 | 6.5 | 12.9 | 0.3 | C | 0.5 | 100.0 | 31.0 | 2.6 | 2.9 | 0.9 |
| | DR31 | 6.5 | 12.9 | 0.3 | C | 1.0 | 100.0 | 25.3 | 3.1 | 3.6 | 0.8 |
| | DR32 | 3.8 | 10.6 | 0.2 | C | 1.0 | 33.4 | 27.2 | 3.0 | 3.4 | 0.8 |
| FurlanandHanai (1997) | P3A | 3.8 | 10.6 | 0.2 | C | 2.0 | 33.4 | 23.5 | 1.7 | 1.2 | 0.5 |
| | P4A | 3.8 | 10.6 | 0.2 | C | 1.0 | 50.1 | 20.0 | 1.9 | 1.4 | 0.7 |
| | P5A | 3.8 | 10.6 | 0.2 | C | 2.0 | 50.1 | 23.0 | 1.6 | 1.2 | 0.6 |
| | P6A | 3.8 | 10.6 | 0.2 | C | 0.5 | 50.1 | 22.0 | 1.8 | 1.3 | 0.6 |
| | P7A | 2.8 | 10.5 | 0.2 | C | 1.0 | 60.0 | 21.5 | 1.8 | 1.3 | 0.6 |
| Cuchiara et al. (2004) | A11 | 2.8 | 10.5 | 0.2 | H | 2.0 | 60.0 | 100.0 | 1.3 | 1.2 | 1.2 |
| | A21 | 2.8 | 10.5 | 0.6 | H | 1.0 | 60.0 | 123.0 | 1.1 | 1.0 | 1.0 |
| | A12 | 3.0 | 8.0 | 0.1 | H | 0.3 | 65.0 | 116.0 | 1.1 | 1.6 | 1.0 |
| Ding et al. (2011) | SFSCCB25-250 | 3.0 | 8.0 | 0.1 | H | 0.5 | 65.0 | 182.7 | 1.3 | 1.0 | 1.1 |
| | SFSCCB50-250 | 3.0 | 8.0 | 0.2 | H | 0.3 | 65.0 | 223.1 | 1.1 | 0.8 | 0.9 |
| | SFSCCB25-150 | 3.0 | 8.0 | 0.2 | H | 0.5 | 65.0 | 189.5 | 1.2 | 1.0 | 1.0 |
| | SFSCCB50-150 | 2.7 | 8.7 | 0.3 | H | 1.0 | 60.0 | 235.2 | 1.0 | 0.8 | 0.9 |
| Limand Oh (1999) | S0.50V1 | 2.7 | 8.7 | 0.4 | S | 1.0 | 60.0 | 86.0 | 0.7 | 0.6 | 0.6 |
| | S0.75V1 | 2.7 | 8.7 | 0.4 | S | 2.0 | 60.0 | 105.0 | 0.6 | 0.6 | 0.5 |
| | S0.50V2 | 6.5 | 12.9 | 0.3 | S | 0.5 | 100.0 | 102.0 | 0.6 | 0.6 | 0.6 |

### 4.3.4. Comparison of Shear Prediction Equations for Deep Beams ($a/d$ > 2.5) without Transverse Reinforcement

As can be observed from Table 4.12 and Figs. 4.12 (1), (2) and (11); ACI 318-14, Sharma (1986) and Dinh et al. (2011) overpredict most of the experimental shear strengths. Although the standard deviation of the Eqn. (1) is lower than others, it has the highest AAE (88.4%). Eqn. (6) has a low mean (0.62) and high AAE (43.93%). Results obtained from Eqns. (3), (4), (5), and (7) are comparable, however, they underestimate the shear strength for most of the specimens. When all the proposed equations in Table 4.12 are considered, the proposed method has the highest accuracy with lowest scatter of data.

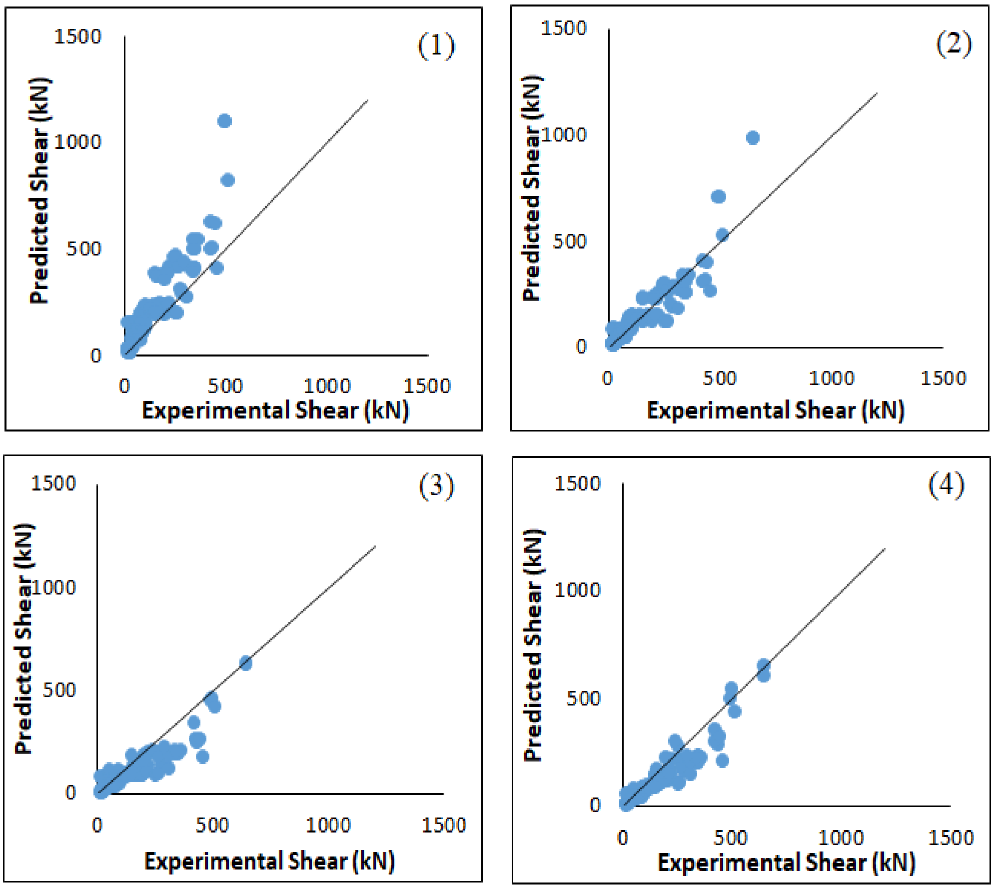


*Figure 4.12.* Shear strength predictions for Deep Beams ($a/d$ > 2.5) without transverse reinforcement: (1) ACI 318-14 (2014); (2) Sharma (1986); (3) Mansur et al. (1986); (4) Narayanan and Darwish (1987)

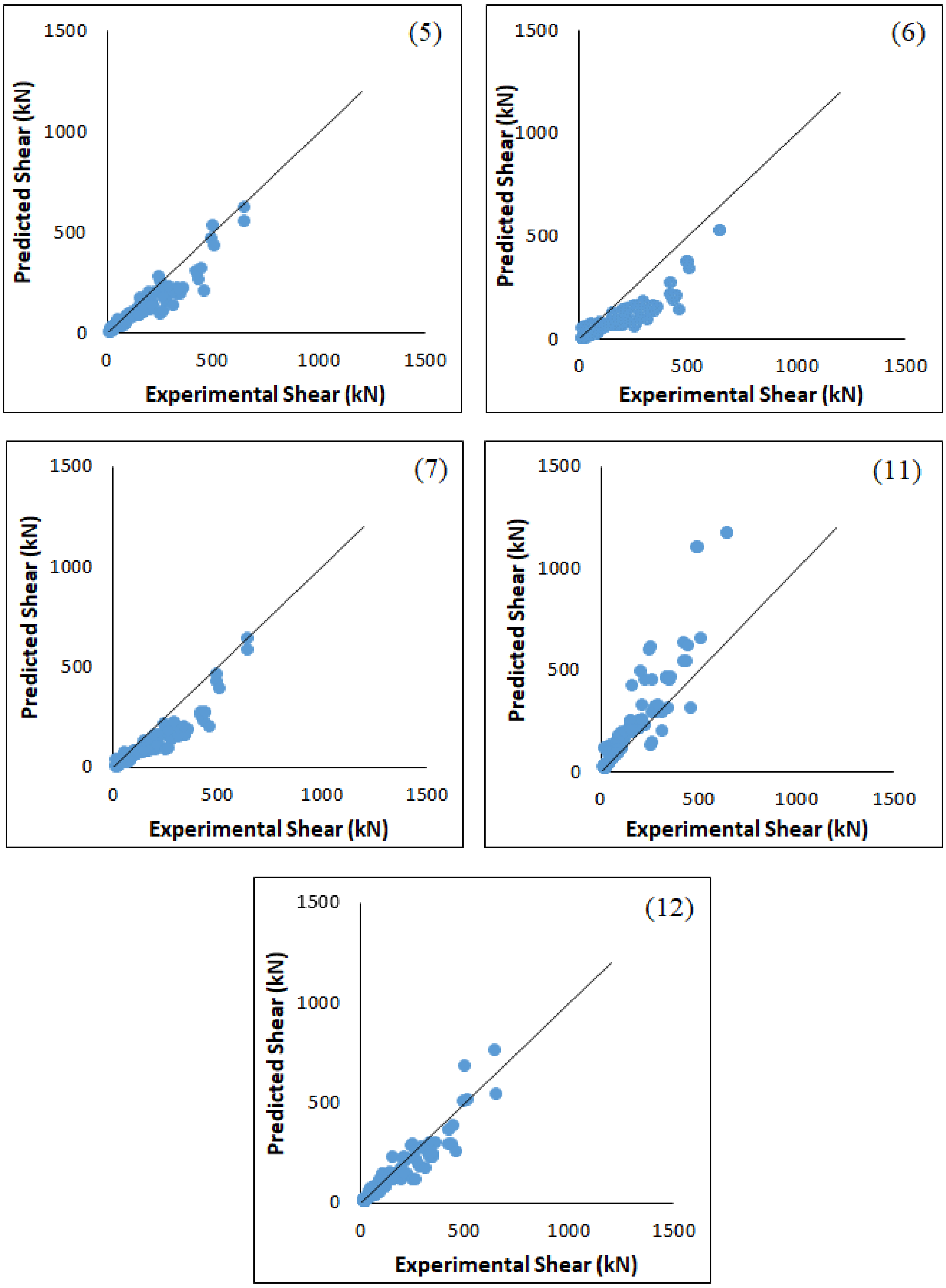


*Figure 4.12.* Shear strength predictions for Deep Beams ($a/d > 2.5$) without transverse reinforcement (continued):

(5) Ashour et al. (1992); (6) Khuntia et al. (1999); (7) Kwak et al. (2002); (11) Dinh et al. (2011); (12) Proposed method

Table 4.12. *Statistical Parameters for Deep Beams ($a/d$ > 2.5) without transverse reinforcement*

| Equation Number | Shear Equation | Mean | Range | Standard Deviation | Avg. Absolute Error (%) |
|---|---|---|---|---|---|
| (1) | ACI 318-14 (2014) | 1.31 | 0.77 - 10.76 | 0.16 | 88.4 |
| (2) | Sharma (1986) | 1.15 | 0.48 - 5.82 | 0.53 | 31.17 |
| (3) | Mansur et al. (1986) | 0.82 | 0.35 - 5.68 | 0.49 | 31.85 |
| (4) | Narayanan and Darwish (1987) | 0.85 | 0.40 - 2.07 | 0.34 | 24.66 |
| (5) | Ashour et al. (1992) | 0.80 | 0.26 - 3.80 | 0.19 | 23.43 |
| (6) | Khuntia et al. (1999) | 0.62 | 0.41 - 4.09 | 0.34 | 43.93 |
| (7) | Kwak et al. (2002) | 0.71 | 0.36 - 2.76 | 0.24 | 33.14 |
| (11) | Dinh et al. (2011) | 1.70 | 0.54 - 7.83 | 0.73 | 71.73 |
| (12) | Proposed Method | 0.98 | 0.56 - 1.64 | 0.22 | 18.11 |

Table 4.13. *Comparison of Predicted versus Experimental Strengths for Deep Beams ( $a/d$ > 2.5 ) without transverse reinforcement*

| $Researcher$ | $Specimen$ | $a/d$ | $l_n/d$ | $Fiber$ Type | $V_f$ (%) | $l_f/d_f$ | $V_{exp}$ $(MPa)$ | $V_{pre}/V_{exp}$ (1) | (2) | (3) | (4) | (5) | (6) | (7) | (11) | (12) |
|---|---|---|---|---|---|---|---|---|---|---|---|---|---|---|---|---|
| Dinh et al. (2010) | B18-1a | 3.4 | 8.2 | H | 0.8 | 55.0 | 167.9 | 1.4 | 0.9 | 0.6 | 0.6 | 0.4 | 0.6 | 0.5 | 1.3 | 0.9 |
| | B18-1b | 3.4 | 8.2 | H | 0.8 | 55.0 | 162.2 | 1.5 | 0.9 | 0.6 | 0.7 | 0.4 | 0.7 | 0.5 | 1.3 | 0.9 |
| | B18-2a | 3.5 | 5.9 | H | 1.0 | 55.0 | 173.7 | 1.3 | 0.8 | 0.5 | 0.6 | 0.4 | 0.7 | 0.5 | 1.3 | 0.8 |
| | B18-2b | 3.5 | 5.9 | H | 1.0 | 55.0 | 179.5 | 1.2 | 0.8 | 0.5 | 0.6 | 0.4 | 0.6 | 0.5 | 1.3 | 0.8 |
| | B18-2c | 3.5 | 5.9 | H | 1.0 | 55.0 | 202.7 | 1.1 | 0.7 | 0.5 | 0.6 | 0.3 | 0.6 | 0.5 | 1.1 | 0.8 |
| | B18-2d | 3.5 | 5.9 | H | 1.0 | 55.0 | 150.6 | 1.5 | 0.9 | 0.6 | 0.8 | 0.5 | 0.8 | 0.6 | 1.5 | 1.1 |
| | B18-3a | 3.4 | 8.2 | H | 1.5 | 55.0 | 150.6 | 1.3 | 0.8 | 0.7 | 0.9 | 0.5 | 0.9 | 0.7 | 1.7 | 1.0 |
| | B18-3b | 3.4 | 8.2 | H | 1.5 | 55.0 | 196.9 | 1.0 | 0.6 | 0.5 | 0.7 | 0.4 | 0.7 | 0.5 | 1.3 | 0.7 |
| | B18-3c | 3.4 | 8.2 | H | 1.5 | 55.0 | 191.1 | 1.3 | 0.8 | 0.6 | 0.7 | 0.5 | 0.8 | 0.6 | 1.3 | 0.9 |
| | B18-3d | 3.4 | 8.2 | H | 1.5 | 55.0 | 191.1 | 1.3 | 0.8 | 0.6 | 0.7 | 0.5 | 0.8 | 0.6 | 1.3 | 0.9 |
| | B18-5a | 3.4 | 8.2 | H | 1.0 | 80.0 | 173.7 | 1.5 | 0.9 | 0.8 | 0.8 | 0.6 | 0.9 | 0.7 | 1.3 | 1.1 |
| | B18-5b | 3.4 | 8.2 | H | 1.0 | 80.0 | 220.1 | 1.1 | 0.7 | 0.6 | 0.7 | 0.5 | 0.7 | 0.5 | 1.1 | 0.8 |
| | B18-7a | 3.4 | 8.2 | H | 0.8 | 80.0 | 191.1 | 1.2 | 0.8 | 0.5 | 0.6 | 0.4 | 0.6 | 0.5 | 1.1 | 0.8 |
| | B18-7b | 3.4 | 8.2 | H | 0.8 | 80.0 | 191.1 | 1.2 | 0.8 | 0.5 | 0.6 | 0.4 | 0.6 | 0.5 | 1.1 | 0.8 |
| | B27-1a | 3.4 | 5.8 | H | 0.8 | 55.0 | 359.1 | 1.5 | 1.0 | 0.6 | 0.6 | 0.4 | 0.6 | 0.5 | 1.3 | 0.8 |
| | B27-1b | 3.4 | 5.8 | H | 0.8 | 55.0 | 334.3 | 1.6 | 1.0 | 0.6 | 0.7 | 0.5 | 0.7 | 0.6 | 1.4 | 0.9 |
| | B27-2a | 3.4 | 5.8 | H | 0.8 | 80.0 | 346.7 | 1.2 | 0.7 | 0.6 | 0.6 | 0.4 | 0.7 | 0.5 | 1.3 | 0.8 |
| | B27-2b | 3.4 | 5.8 | H | 0.8 | 80.0 | 346.7 | 1.2 | 0.7 | 0.6 | 0.6 | 0.4 | 0.7 | 0.5 | 1.3 | 0.8 |
| | B27-3a | 3.5 | 5.8 | H | 0.8 | 55.0 | 334.3 | 1.5 | 0.9 | 0.6 | 0.6 | 0.4 | 0.6 | 0.5 | 1.4 | 0.7 |
| | B27-3b | 3.5 | 5.8 | H | 0.8 | 55.0 | 346.7 | 1.4 | 0.9 | 0.5 | 0.6 | 0.4 | 0.6 | 0.5 | 1.3 | 0.7 |
| | B27-4a | 3.5 | 5.8 | H | 0.8 | 80.0 | 260.0 | 1.6 | 1.0 | 0.8 | 0.8 | 0.6 | 0.9 | 0.6 | 1.7 | 0.9 |
| | B27-4b | 3.5 | 5.8 | H | 0.8 | 80.0 | 222.9 | 1.9 | 1.2 | 0.9 | 0.9 | 0.7 | 1.0 | 0.7 | 2.0 | 1.0 |
| | B27-5 | 3.5 | 5.8 | H | 1.5 | 55.0 | 433.4 | 1.2 | 0.7 | 0.6 | 0.6 | 0.4 | 0.7 | 0.5 | 1.3 | 0.7 |
| | B27-6 | 3.5 | 5.8 | H | 1.5 | 80.0 | 421.0 | 1.2 | 0.7 | 0.8 | 0.7 | 0.7 | 0.8 | 0.7 | 1.3 | 0.7 |
| Lim et al. (1987) | 2/1,0/3,5 | 3.5 | 9.5 | H | 1.0 | 60.0 | 46.5 | 2.6 | 1.6 | 1.1 | 1.1 | 0.8 | 1.2 | 0.9 | 2.9 | 0.9 |
| | 2/0,5/3,5 | 3.5 | 9.5 | H | 0.5 | 60.0 | 45.2 | 2.7 | 1.7 | 0.9 | 0.9 | 0.7 | 0.9 | 0.7 | 2.5 | 0.9 |
| | 4/1,0/3,5 | 3.5 | 9.5 | H | 1.0 | 60.0 | 67.4 | 1.8 | 1.1 | 0.8 | 0.9 | 0.6 | 1.0 | 0.7 | 2.0 | 1.1 |

Table 4.13. *Comparison of Predicted versus Experimental Strengths for Deep Beams ( $a/d$ > 2.5 ) without transverse reinforcement (continued)*

| $Researcher$ | $Specimen$ | $a/d$ | $l_n/d$ | $Fiber$ Type | $V_f$ (%) | $l_f/d_f$ | $V_{exp}$ $(MPa)$ | $V_{pre}/V_{exp}$ | | | | | | | | |
|---|---|---|---|---|---|---|---|---|---|---|---|---|---|---|---|---|
| | | | | | | | | (1) | (2) | (3) | (4) | (5) | (6) | (7) | (11) | (12) |
| Lim et al. (1987) | 4/0,5/3,5 | 254.0 | 221.0 | H | 0.5 | 60.0 | 49.4 | 2.5 | 1.5 | 0.9 | 1.1 | 0.6 | 1.1 | 0.8 | 2.3 | 1.4 |
| Cuchiara et al. (2004) | A10 | 240.0 | 219.0 | H | 1.0 | 60.0 | 96.4 | 1.4 | 0.9 | 0.6 | 0.7 | 0.5 | 0.7 | 0.6 | 1.4 | 1.0 |
| | A20 | 240.0 | 219.0 | H | 2.0 | 60.0 | 103.3 | 1.3 | 0.9 | 0.7 | 0.8 | 0.6 | 0.9 | 0.8 | 1.5 | 1.0 |
| Cohen (2012) | M15-0.5% | 250.0 | 212.5 | H | 0.5 | 55.0 | 43.3 | 2.9 | 1.8 | 1.0 | 0.9 | 0.7 | 0.9 | 0.8 | 2.2 | 1.0 |
| | M15-1.0% | 250.0 | 212.5 | H | 1.0 | 55.0 | 48.0 | 2.5 | 1.5 | 1.0 | 0.9 | 0.7 | 1.0 | 0.8 | 2.2 | 0.9 |
| | M15-1.5% | 250.0 | 212.5 | H | 1.5 | 55.0 | 46.1 | 2.7 | 1.6 | 1.3 | 1.1 | 1.0 | 1.3 | 1.1 | 2.6 | 1.0 |
| | M15-0.5%H | 250.0 | 212.5 | H | 0.5 | 80.0 | 45.2 | 2.6 | 1.6 | 0.9 | 0.9 | 0.6 | 0.9 | 0.8 | 2.0 | 0.9 |
| | M15-0.75%H | 250.0 | 212.5 | H | 0.8 | 80.0 | 46.6 | 2.4 | 1.5 | 0.9 | 0.9 | 0.6 | 1.0 | 0.8 | 2.1 | 0.9 |
| | M20-0.75% | 250.0 | 210.0 | H | 0.8 | 55.0 | 44.0 | 2.5 | 1.5 | 1.0 | 1.1 | 0.7 | 1.1 | 0.9 | 2.2 | 1.5 |
| | M20-1.0% | 250.0 | 210.0 | H | 1.0 | 55.0 | 57.5 | 1.9 | 1.2 | 0.8 | 0.9 | 0.6 | 0.9 | 0.7 | 1.8 | 1.1 |
| | M20-1.0%A | 250.0 | 210.0 | H | 1.0 | 55.0 | 59.0 | 2.0 | 1.2 | 0.9 | 0.9 | 0.6 | 0.9 | 0.8 | 1.8 | 1.1 |
| | M20-1.5%A | 250.0 | 210.0 | H | 1.5 | 55.0 | 61.9 | 1.9 | 1.2 | 0.9 | 1.0 | 0.7 | 1.0 | 0.8 | 1.9 | 1.1 |
| | M20-1.0%B | 250.0 | 210.0 | H | 1.0 | 55.0 | 51.5 | 2.3 | 1.4 | 0.9 | 1.0 | 0.7 | 1.0 | 0.9 | 2.1 | 1.3 |
| | M20-1.5%B | 250.0 | 210.0 | H | 1.5 | 55.0 | 59.7 | 2.0 | 1.2 | 1.0 | 1.0 | 0.7 | 1.1 | 0.9 | 1.9 | 1.1 |
| Şen (2005) | BEAM-04 | 250.0 | 215.0 | H | 0.5 | 65.0 | 41.9 | 3.1 | 1.9 | 1.1 | 1.0 | 0.8 | 1.0 | 0.9 | 2.3 | 1.0 |
| | BEAM-06 | 250.0 | 215.0 | H | 0.8 | 65.0 | 46.8 | 2.8 | 1.7 | 1.1 | 1.0 | 0.8 | 1.1 | 0.9 | 2.2 | 1.0 |
| | BEAM-08 | 250.0 | 215.0 | H | 0.5 | 80.0 | 37.4 | 3.5 | 2.1 | 1.4 | 1.2 | 1.0 | 1.2 | 1.1 | 2.5 | 1.2 |
| | BEAM-10 | 250.0 | 215.0 | H | 0.8 | 80.0 | 48.4 | 2.8 | 1.7 | 1.3 | 1.0 | 1.0 | 1.1 | 1.0 | 2.2 | 0.9 |
| Kwak et al. (2002) | FHB2-3 | 250.0 | 212.0 | H | 0.5 | 62.5 | 81.9 | 1.6 | 1.0 | 0.6 | 0.6 | 0.5 | 0.6 | 0.5 | 1.2 | 0.7 |
| | FHB3-3 | 250.0 | 212.0 | H | 0.8 | 62.5 | 90.1 | 1.5 | 1.0 | 0.7 | 0.6 | 0.6 | 0.6 | 0.6 | 1.2 | 0.7 |
| | FNB2-3 | 250.0 | 212.0 | H | 0.5 | 62.5 | 67.6 | 1.4 | 0.9 | 0.5 | 0.6 | 0.4 | 0.5 | 0.5 | 1.3 | 0.8 |
| | FHB2-4 | 250.0 | 212.0 | H | 0.5 | 62.5 | 63.9 | 2.1 | 1.2 | 0.8 | 0.7 | 0.6 | 0.7 | 0.6 | 1.5 | 0.7 |
| | FHB3-4 | 250.0 | 212.0 | H | 0.8 | 62.5 | 72.6 | 1.9 | 1.1 | 0.8 | 0.6 | 0.6 | 0.7 | 0.6 | 1.4 | 0.6 |
| | FNB2-4 | 250.0 | 212.0 | H | 0.5 | 62.5 | 53.0 | 1.7 | 1.0 | 0.7 | 0.6 | 0.5 | 0.6 | 0.5 | 1.7 | 0.7 |

Table 4.13. *Comparison of Predicted versus Experimental Strengths for Deep Beams ( $a/d$ > 2.5 ) without transverse reinforcement (continued)*

| $Researcher$ | $Specimen$ | $a/d$ | $l_n/d$ | $Fiber$ Type | $V_f$ (%) | $l_f/d_f$ | $V_{exp}$ $(MPa)$ | $V_{pre}/V_{exp}$ | | | | | | | | |
|---|---|---|---|---|---|---|---|---|---|---|---|---|---|---|---|---|
| | | | | | | | | (1) | (2) | (3) | (4) | (5) | (6) | (7) | (11) | (12) |
| Rosenbusc handTeutsc h (2003) | 1.2/2 | 300.0 | 260.0 | H | 0.3 | 65.0 | 110.0 | 2.0 | 1.3 | 0.7 | 0.9 | 0.5 | 0.8 | 0.7 | 1.4 | 1.5 |
| | 1.2/3 | 300.0 | 260.0 | H | 0.5 | 65.0 | 120.0 | 1.8 | 1.1 | 0.8 | 0.9 | 0.6 | 0.8 | 0.7 | 1.5 | 1.3 |
| | 1.2/4 | 300.0 | 260.0 | H | 0.8 | 65.0 | 155.0 | 1.5 | 0.9 | 0.7 | 0.7 | 0.5 | 0.7 | 0.6 | 1.3 | 1.1 |
| | 2.6/2 | 300.0 | 260.0 | H | 0.3 | 65.0 | 82.5 | 2.5 | 1.5 | 0.9 | 0.8 | 0.6 | 0.8 | 0.6 | 1.9 | 1.8 |
| | 2.6/3 | 300.0 | 260.0 | H | 0.8 | 65.0 | 117.0 | 1.8 | 1.0 | 0.8 | 0.7 | 0.6 | 0.8 | 0.6 | 1.7 | 1.3 |
| | 3.1/1 | 300.0 | 260.0 | H | 0.5 | 65.0 | 94.5 | 2.1 | 1.3 | 0.9 | 1.0 | 0.7 | 0.9 | 0.7 | 1.9 | 1.5 |
| | 3.1/1 F2 | 300.0 | 260.0 | H | 0.5 | 65.0 | 112.5 | 1.8 | 1.1 | 0.8 | 0.8 | 0.6 | 0.8 | 0.6 | 1.6 | 1.3 |
| Dupontand Vandewalle (2003) | 2 | 300.0 | 260.0 | H | 0.3 | 65.0 | 110.0 | 2.0 | 1.2 | 0.7 | 0.9 | 0.5 | 0.8 | 0.7 | 1.4 | 1.5 |
| | 3 | 300.0 | 260.0 | H | 0.5 | 65.0 | 120.0 | 1.8 | 1.1 | 0.8 | 0.9 | 0.6 | 0.8 | 0.7 | 1.5 | 1.3 |
| | 4 | 300.0 | 260.0 | H | 0.8 | 65.0 | 155.0 | 1.4 | 0.9 | 0.7 | 0.7 | 0.5 | 0.7 | 0.6 | 1.3 | 1.1 |
| | 23 | 300.0 | 260.0 | H | 0.3 | 65.0 | 82.5 | 2.5 | 1.5 | 0.9 | 0.8 | 0.6 | 0.8 | 0.6 | 1.9 | 1.8 |
| | 24 | 300.0 | 260.0 | H | 0.8 | 65.0 | 117.0 | 1.8 | 1.1 | 0.9 | 0.7 | 0.6 | 0.8 | 0.6 | 1.7 | 1.3 |
| Imam et al. (1994) | B4 | 350.0 | 300.0 | H | 0.8 | 75.0 | 197.5 | 2.0 | 1.2 | 0.9 | 0.7 | 0.7 | 0.8 | 0.7 | 1.3 | 1.4 |
| | B11 | 350.0 | 300.0 | H | 0.8 | 75.0 | 151.0 | 2.6 | 1.5 | 1.2 | 0.8 | 0.9 | 1.0 | 0.9 | 1.7 | 1.9 |
| | B7 | 350.0 | 300.0 | H | 0.8 | 75.0 | 209.0 | 1.9 | 1.2 | 0.9 | 0.8 | 0.7 | 0.8 | 0.8 | 1.2 | 1.4 |
| | B12 | 350.0 | 300.0 | H | 0.8 | 75.0 | 212.0 | 1.9 | 1.1 | 0.9 | 0.7 | 0.6 | 0.8 | 0.7 | 1.2 | 1.4 |
| Aoude et al. (2012) | A0.5 | 250.0 | 202.0 | H | 0.5 | 55.0 | 48.0 | 1.8 | 1.2 | 0.6 | 0.7 | 0.5 | 0.7 | 0.6 | 2.1 | 1.3 |
| | A1 | 250.0 | 202.0 | H | 1.0 | 55.0 | 57.0 | 1.5 | 0.9 | 0.6 | 0.7 | 0.5 | 0.8 | 0.6 | 2.0 | 1.1 |
| | B0.5 | 500.0 | 437.0 | H | 0.5 | 55.0 | 154.0 | 2.4 | 1.6 | 0.9 | 1.2 | 0.7 | 1.1 | 0.8 | 2.8 | 1.8 |
| | B1 | 500.0 | 437.0 | H | 1.0 | 55.0 | 198.0 | 1.8 | 1.2 | 0.8 | 1.1 | 0.6 | 1.1 | 0.8 | 2.5 | 1.3 |
| Ashour et al. (1992) | B-4-1 .0-L | 250.0 | 215.0 | H | 1.0 | 75.0 | 24.0 | 6.7 | 4.0 | 3.5 | 1.5 | 2.7 | 2.6 | 1.9 | 4.9 | 4.9 |
| | B-6-l.O-L | 250.0 | 215.0 | H | 1.0 | 75.0 | 15.1 | 10.8 | 5.8 | 5.7 | 2.1 | 3.8 | 4.1 | 2.8 | 7.8 | 7.9 |
| | B-4-0.5-A | 250.0 | 215.0 | H | 0.5 | 75.0 | 61.0 | 2.7 | 1.6 | 1.1 | 1.0 | 0.8 | 1.0 | 0.9 | 1.7 | 2.0 |
| | B-6-0.5-A | 250.0 | 215.0 | H | 0.5 | 75.0 | 52.4 | 3.1 | 1.7 | 1.3 | 1.0 | 0.7 | 1.1 | 1.0 | 2.0 | 2.3 |
| | B-4-l.O-A | 250.0 | 215.0 | H | 1.0 | 75.0 | 85.2 | 1.9 | 1.2 | 1.1 | 0.8 | 0.8 | 0.9 | 0.8 | 1.4 | 1.4 |
| | B-6-l.O-A | 250.0 | 215.0 | H | 1.0 | 75.0 | 52.7 | 3.2 | 1.7 | 1.7 | 1.2 | 1.1 | 1.4 | 1.2 | 2.3 | 2.3 |
| | B-4-1.5-A | 250.0 | 215.0 | H | 1.5 | 75.0 | 94.3 | 1.7 | 1.0 | 1.2 | 0.9 | 0.9 | 1.0 | 0.8 | 1.4 | 1.3 |

Table 4.13. *Comparison of Predicted versus Experimental Strengths for Deep Beams ( $a/d$ > 2.5 ) without transverse reinforcement (continued)*

| $Researcher$ | $Specimen$ | $a/d$ | $l_n/d$ | $Fiber$ Type | $V_f$ (%) | $l_f/d_f$ | $V_{exp}$ $(MPa)$ | $V_{pre}/V_{exp}$ | | | | | | | | |
|---|---|---|---|---|---|---|---|---|---|---|---|---|---|---|---|---|
| | | | | | | | | (1) | (2) | (3) | (4) | (5) | (6) | (7) | (11) | (12) |
| Ashour et al. (1992) | B-6-1.5-A | 6.0 | 14.3 | H | 1.5 | 75.0 | 53.2 | 3.2 | 1.7 | 2.1 | 1.3 | 1.5 | 1.6 | 1.6 | 2.4 | 2.3 |
| | B-4-l.O-M | 4.0 | 10.3 | H | 1.0 | 75.0 | 104.3 | 1.6 | 0.9 | 0.9 | 0.8 | 0.6 | 0.8 | 0.8 | 1.1 | 1.1 |
| | B-6-l.O-M | 6.0 | 14.3 | H | 1.0 | 75.0 | 78.7 | 2.1 | 1.1 | 1.1 | 0.9 | 0.7 | 1.0 | 1.0 | 1.5 | 1.5 |
| Ding et al. (2012) | SF20- | 4.0 | 9.3 | H | 0.3 | 80.0 | 24.0 | 1.9 | 1.1 | 0.7 | 0.9 | 0.4 | 0.9 | 0.9 | 1.5 | 1.4 |
| | SF40- | 4.0 | 9.3 | H | 0.5 | 80.0 | 36.1 | 1.2 | 0.7 | 0.5 | 0.7 | 0.3 | 0.7 | 0.7 | 1.1 | 0.9 |
| | SF60- | 4.0 | 9.3 | H | 0.8 | 80.0 | 37.3 | 1.3 | 0.8 | 0.7 | 0.7 | 0.5 | 0.8 | 0.8 | 1.2 | 1.0 |
| FurlanandHanai (1997) | P3B | 3.8 | 10.6 | C | 1.0 | 33.0 | 18.5 | 2.1 | 1.3 | 0.8 | 0.7 | 0.6 | 0.7 | 0.7 | 1.9 | 1.5 |
| | P4B | 3.8 | 10.6 | C | 2.0 | 33.0 | 23.5 | 1.6 | 1.0 | 0.8 | 0.7 | 0.6 | 0.7 | 0.7 | 1.7 | 1.2 |
| | P5B | 3.8 | 10.6 | C | 1.0 | 50.0 | 20.0 | 1.9 | 1.1 | 0.8 | 0.7 | 0.6 | 0.8 | 0.8 | 1.7 | 1.4 |
| | P6B | 3.8 | 10.6 | C | 2.0 | 50.0 | 22.5 | 1.7 | 1.0 | 1.1 | 0.8 | 0.8 | 1.0 | 1.0 | 1.8 | 1.3 |
| | P7B | 3.8 | 10.6 | C | 0.5 | 50.0 | 17.5 | 2.2 | 1.3 | 0.8 | 0.7 | 0.6 | 0.7 | 0.7 | 1.7 | 1.6 |
| Shin et al. (1994) | 3 | 3.0 | 6.0 | S | 0.5 | 100.0 | 55.8 | 1.7 | 1.1 | 0.7 | 0.8 | 0.5 | 0.8 | 0.8 | 1.2 | 1.3 |
| | 4 | 3.0 | 6.0 | S | 1.0 | 100.0 | 71.8 | 1.4 | 0.9 | 0.6 | 0.8 | 0.5 | 0.8 | 0.8 | 1.0 | 1.0 |
| | 5 | 4.5 | 9.0 | S | 0.5 | 100.0 | 48.7 | 2.0 | 1.2 | 0.7 | 0.8 | 0.5 | 0.9 | 0.9 | 1.3 | 1.5 |
| | 6 | 4.5 | 9.0 | S | 1.0 | 100.0 | 60.2 | 1.6 | 0.9 | 0.7 | 0.8 | 0.5 | 0.9 | 0.9 | 1.2 | 1.2 |
| Mansur et al. (1986) | B2 | 2.8 | 10.2 | H | 0.5 | 60.0 | 52.5 | 1.9 | 1.2 | 0.7 | 0.8 | 0.6 | 0.8 | 0.8 | 1.9 | 1.4 |
| | B3 | 3.6 | 10.2 | H | 0.5 | 60.0 | 45.0 | 2.2 | 1.4 | 0.8 | 0.8 | 0.5 | 0.8 | 0.8 | 2.2 | 1.6 |
| | B4 | 4.4 | 10.2 | H | 0.5 | 60.0 | 38.0 | 2.6 | 1.5 | 0.9 | 0.9 | 0.6 | 0.9 | 0.9 | 2.6 | 1.9 |
| | C2 | 2.8 | 10.2 | H | 0.8 | 60.0 | 60.0 | 1.7 | 1.1 | 0.6 | 0.7 | 0.6 | 0.8 | 0.8 | 1.8 | 1.2 |
| | C3 | 3.6 | 10.2 | H | 0.8 | 60.0 | 47.5 | 2.1 | 1.3 | 0.8 | 0.9 | 0.6 | 0.9 | 0.9 | 2.3 | 1.5 |
| | C4 | 4.4 | 10.2 | H | 0.8 | 60.0 | 41.0 | 2.5 | 1.4 | 0.9 | 0.9 | 0.6 | 1.0 | 1.0 | 2.6 | 1.8 |
| | C5 | 2.8 | 12.5 | H | 0.8 | 60.0 | 37.5 | 2.7 | 1.8 | 1.0 | 1.0 | 0.9 | 1.1 | 1.1 | 2.9 | 2.0 |
| | C6 | 2.8 | 10.2 | H | 0.8 | 60.0 | 65.0 | 1.5 | 1.0 | 0.6 | 0.8 | 0.5 | 0.8 | 0.8 | 1.7 | 1.1 |
| | D2 | 2.8 | 10.2 | H | 1.0 | 60.0 | 65.0 | 1.6 | 1.0 | 0.6 | 0.7 | 0.6 | 0.8 | 0.8 | 1.8 | 1.1 |
| | D3 | 3.6 | 10.2 | H | 1.0 | 60.0 | 50.5 | 2.0 | 1.2 | 0.8 | 0.9 | 0.6 | 1.0 | 1.0 | 2.3 | 1.5 |
| | D4 | 4.4 | 10.2 | H | 1.0 | 60.0 | 44.0 | 2.3 | 1.3 | 0.9 | 1.0 | 0.6 | 1.1 | 1.1 | 2.6 | 1.7 |
| | E1 | 2.8 | 12.5 | H | 0.8 | 60.0 | 35.0 | 2.4 | 1.6 | 0.9 | 1.0 | 0.8 | 1.1 | 1.1 | 3.1 | 1.8 |

Table 4.13. *Comparison of Predicted versus Experimental Strengths for Deep Beams ( $a/d$ > 2.5 ) without transverse reinforcement (continued)*

| $Researcher$ | $Specimen$ | $a/d$ | $l_n/d$ | $Fiber$ Type | $V_f$ (%) | $l_f/d_f$ | $V_{exp}$ $(MPa)$ | $V_{pre}/V_{exp}$ | | | | | | | | |
|---|---|---|---|---|---|---|---|---|---|---|---|---|---|---|---|---|
| | | | | | | | | (1) | (2) | (3) | (4) | (5) | (6) | (7) | (11) | (12) |
| Mansur et al. (1986) | E2 | 2.8 | 10.2 | H | 0.8 | 60.0 | 45.0 | 1.9 | 1.2 | 0.7 | 0.9 | 0.6 | 1.0 | 0.7 | 2.4 | 1.4 |
| | E3 | 2.8 | 10.2 | H | 0.8 | 60.0 | 60.0 | 1.4 | 0.9 | 0.6 | 0.8 | 0.5 | 0.8 | 0.6 | 1.8 | 1.0 |
| | F1 | 2.8 | 12.5 | H | 0.8 | 60.0 | 46.8 | 2.3 | 1.5 | 0.9 | 0.8 | 0.8 | 0.9 | 0.8 | 2.4 | 1.7 |
| | F2 | 2.8 | 10.2 | H | 0.8 | 60.0 | 75.0 | 1.4 | 0.9 | 0.5 | 0.6 | 0.5 | 0.6 | 0.6 | 1.5 | 1.0 |
| | F3 | 2.8 | 10.2 | H | 0.8 | 60.0 | 86.0 | 1.2 | 0.8 | 0.5 | 0.6 | 0.4 | 0.6 | 0.5 | 1.3 | 0.9 |
| Shoaib et al. (2014) | N31 | 3.0 | 6.0 | H | 1.0 | 55.0 | 211.0 | 1.1 | 0.7 | 0.5 | 0.7 | 0.4 | 0.7 | 0.5 | 1.6 | 0.8 |
| | N32 | 3.0 | 6.0 | H | 1.0 | 55.0 | 281.0 | 1.1 | 0.7 | 0.5 | 0.6 | 0.4 | 0.7 | 0.5 | 1.1 | 0.8 |
| | H31 | 3.0 | 6.0 | H | 1.0 | 55.0 | 278.0 | 1.1 | 0.7 | 0.5 | 0.6 | 0.4 | 0.6 | 0.5 | 1.1 | 0.8 |
| | H32 | 3.0 | 6.0 | H | 1.0 | 55.0 | 458.0 | 0.9 | 0.6 | 0.4 | 0.5 | 0.3 | 0.5 | 0.4 | 0.7 | 0.7 |
| | N61 | 3.0 | 6.0 | H | 1.0 | 55.0 | 252.0 | 1.9 | 1.2 | 0.8 | 1.0 | 0.7 | 1.1 | 0.8 | 2.4 | 1.4 |
| | N62 | 3.0 | 6.0 | H | 1.0 | 55.0 | 242.0 | 1.9 | 1.2 | 0.9 | 1.2 | 0.7 | 1.2 | 0.9 | 2.5 | 1.4 |
| | E2 | 3.0 | 6.0 | H | 1.0 | 55.0 | 423.0 | 1.5 | 1.0 | 0.6 | 0.7 | 0.5 | 0.7 | 0.6 | 1.5 | 1.1 |
| | E3 | 3.0 | 6.0 | H | 1.0 | 55.0 | 444.0 | 1.4 | 0.9 | 0.6 | 0.7 | 0.5 | 0.7 | 0.6 | 1.4 | 1.0 |
| | F1 | 3.0 | 6.0 | H | 1.0 | 55.0 | 492.0 | 2.2 | 1.4 | 0.9 | 1.0 | 0.8 | 1.0 | 0.9 | 2.3 | 1.6 |
| | F2 | 3.0 | 6.0 | H | 1.0 | 55.0 | 497.0 | 2.2 | 1.4 | 0.9 | 1.1 | 0.8 | 1.1 | 0.9 | 2.2 | 1.6 |
| | F3 | 3.0 | 6.0 | H | 1.0 | 55.0 | 646.0 | 2.4 | 1.5 | 1.0 | 0.9 | 0.8 | 0.9 | 0.9 | 1.8 | 1.7 |
| | N31 | 3.0 | 6.0 | H | 1.0 | 55.0 | 644.0 | 2.4 | 1.5 | 1.0 | 1.0 | 0.8 | 1.0 | 1.0 | 1.8 | 1.7 |
| Noghabai (2000) | 3typeB | 2.8 | 5.5 | H | 1.0 | 50.0 | 310.0 | 0.9 | 0.6 | 0.4 | 0.5 | 0.3 | 0.5 | 0.5 | 0.7 | 0.7 |
| | 5 type A | 3.3 | 6.7 | H | 0.5 | 86.0 | 252.0 | 0.8 | 0.5 | 0.3 | 0.4 | 0.3 | 0.4 | 0.4 | 0.5 | 0.6 |
| | 6 type A | 3.3 | 6.7 | H | 0.8 | 86.0 | 262.0 | 0.8 | 0.5 | 0.4 | 0.4 | 0.3 | 0.4 | 0.4 | 0.6 | 0.6 |
| | 7 type C | 2.9 | 7.3 | H | 0.5 | 86.0 | 264.0 | 1.6 | 1.0 | 0.7 | 0.7 | 0.6 | 0.7 | 0.7 | 1.1 | 1.2 |
| | 8 type C | 2.9 | 7.3 | H | 0.5 | 86.0 | 312.0 | 1.4 | 0.9 | 0.6 | 0.7 | 0.5 | 0.7 | 0.6 | 1.0 | 1.0 |
| | 9 type C | 2.9 | 7.3 | H | 0.8 | 86.0 | 339.0 | 1.2 | 0.8 | 0.6 | 0.7 | 0.5 | 0.7 | 0.6 | 0.9 | 0.9 |
| | 10 type C | 2.9 | 7.3 | H | 0.8 | 86.0 | 292.0 | 1.5 | 1.0 | 0.8 | 0.8 | 0.6 | 0.8 | 0.8 | 1.1 | 1.1 |
| | 4 type D | 3.0 | 8.8 | H | 0.8 | 86.0 | 509.0 | 1.6 | 1.0 | 0.8 | 0.9 | 0.7 | 0.9 | 0.8 | 1.3 | 1.2 |
| Majdzadeh et al. (2006) | B12 | 3.0 | 6.7 | H | 0.5 | 80.0 | 51.0 | 1.5 | 1.0 | 0.7 | 0.8 | 0.5 | 0.8 | 0.7 | 1.2 | 1.1 |
| | B13 | 3.0 | 6.7 | H | 1.0 | 80.0 | 62.5 | 1.2 | 0.8 | 0.7 | 0.8 | 0.6 | 0.8 | 0.6 | 1.2 | 0.9 |

Table 4.13. *Comparison of Predicted versus Experimental Strengths for Deep Beams ( $a/d$ > 2.5 ) without transverse reinforcement (continued)*

| $Researcher$ | $Specimen$ | $a/d$ | $l_n/d$ | $f'_c$ $(MPa)$ | $Fiber$ Type | $V_f$ (%) | $l_f/d_f$ | $V_{exp}$ $(MPa)$ | $V_{pre}/V_{exp}$ | | | | | | | | |
|---|---|---|---|---|---|---|---|---|---|---|---|---|---|---|---|---|---|
| | | | | | | | | | (1) | (2) | (3) | (4) | (5) | (6) | (7) | (11) | (12) |
| Majdzadeh et al. (2006) | B14 | 150.0 | 150.0 | 150.0 | H | 1.5 | 80.0 | 59.5 | 1.2 | 0.8 | 0.9 | 0.9 | 0.7 | 1.0 | 0.8 | 1.3 | 0.9 |
| Ding et al. (2011) | SFSCCB25-∞ | 200.0 | 300.0 | 300.0 | H | 0.3 | 65.0 | 105.0 | 2.2 | 1.4 | 0.8 | 0.9 | 0.6 | 0.9 | 0.8 | 1.6 | 1.6 |
| | SFSCCB50-∞ | 200.0 | 300.0 | 300.0 | H | 0.6 | 65.0 | 142.0 | 1.7 | 1.1 | 0.7 | 0.8 | 0.5 | 0.8 | 0.7 | 1.5 | 1.3 |
| Li et al. (1992) | M1 | 63.5 | 127.0 | 127.0 | C | 1.0 | 28.5 | 16.5 | 1.8 | 1.1 | 0.7 | 0.7 | 0.6 | 0.7 | 0.7 | 1.6 | 1.3 |
| | M2 | 127.0 | 228.0 | 228.0 | C | 1.0 | 28.5 | 50.5 | 2.3 | 1.5 | 0.9 | 0.9 | 0.8 | 0.9 | 0.8 | 2.1 | 1.7 |
| | M3 | 63.5 | 127.0 | 127.0 | C | 2.0 | 28.5 | 20.8 | 1.4 | 0.9 | 0.7 | 0.7 | 0.6 | 0.7 | 0.6 | 1.5 | 1.0 |
| | M4 | 127.0 | 228.0 | 228.0 | C | 2.0 | 28.5 | 66.3 | 1.7 | 1.1 | 0.9 | 0.8 | 0.7 | 0.8 | 0.7 | 1.8 | 1.3 |
| | M5 | 63.5 | 127.0 | 127.0 | C | 1.0 | 28.5 | 17.7 | 1.8 | 1.2 | 0.7 | 0.7 | 0.6 | 0.7 | 0.7 | 1.5 | 1.3 |
| | M6 | 127.0 | 228.0 | 228.0 | C | 1.0 | 28.5 | 61.4 | 2.1 | 1.3 | 0.8 | 0.8 | 0.7 | 0.8 | 0.8 | 1.7 | 1.5 |
| | M7 | 63.5 | 127.0 | 127.0 | C | 2.0 | 28.5 | 24.5 | 1.2 | 0.8 | 0.6 | 0.6 | 0.5 | 0.6 | 0.5 | 1.3 | 0.9 |
| | M8 | 63.5 | 127.0 | 127.0 | C | 1.0 | 57.0 | 23.0 | 1.4 | 0.9 | 0.7 | 0.6 | 0.6 | 0.7 | 0.6 | 1.2 | 1.0 |
| | M9 | 127.0 | 228.0 | 228.0 | C | 1.0 | 57.0 | 89.4 | 1.4 | 0.9 | 0.7 | 0.6 | 0.6 | 0.7 | 0.6 | 1.2 | 1.0 |
| | M10 | 127.0 | 228.0 | 228.0 | C | 2.0 | 57.0 | 94.0 | 1.3 | 0.8 | 0.9 | 0.8 | 0.8 | 0.8 | 0.7 | 1.3 | 0.9 |
| | M17 | 63.5 | 127.0 | 127.0 | C | 1.0 | 28.5 | 17.8 | 1.8 | 1.2 | 0.7 | 0.7 | 0.6 | 0.7 | 0.7 | 1.5 | 1.3 |
| | M18 | 63.5 | 127.0 | 127.0 | C | 1.0 | 28.5 | 12.8 | 2.5 | 1.6 | 1.0 | 0.8 | 0.8 | 0.8 | 0.8 | 2.1 | 1.8 |
| | M19 | 63.5 | 127.0 | 127.0 | C | 1.0 | 28.5 | 17.8 | 1.8 | 1.2 | 0.7 | 0.8 | 0.6 | 0.8 | 0.8 | 1.5 | 1.3 |
| | M20 | 63.5 | 127.0 | 127.0 | C | 1.0 | 57.0 | 25.3 | 1.2 | 0.8 | 0.6 | 0.6 | 0.5 | 0.7 | 0.6 | 1.0 | 0.9 |
| | C1 | 127.0 | 228.0 | 228.0 | H | 1.0 | 60.0 | 79.0 | 1.0 | 0.6 | 0.4 | 0.6 | 0.3 | 0.6 | 0.5 | 1.3 | 0.7 |
| | C2 | 63.5 | 127.0 | 127.0 | H | 1.0 | 60.0 | 20.5 | 0.9 | 0.6 | 0.4 | 0.6 | 0.3 | 0.6 | 0.4 | 1.2 | 0.7 |
| | C3 | 63.5 | 127.0 | 127.0 | H | 1.0 | 60.0 | 15.7 | 1.2 | 0.8 | 0.5 | 0.6 | 0.4 | 0.7 | 0.5 | 1.6 | 0.9 |
| | C5 | 127.0 | 228.0 | 228.0 | H | 1.0 | 100.0 | 79.0 | 1.0 | 0.7 | 0.5 | 0.7 | 0.4 | 0.8 | 0.6 | 1.3 | 0.8 |
| | C6 | 63.5 | 127.0 | 127.0 | H | 1.0 | 100.0 | 23.0 | 0.9 | 0.6 | 0.5 | 0.7 | 0.4 | 0.7 | 0.5 | 1.1 | 0.7 |

Table 4.13. *Comparison of Predicted versus Experimental Strengths for Deep Beams ( $a/d$ > 2.5 ) without transverse reinforcement (continued)*

| $Researcher$ | $Specimen$ | $a/d$ | $l_n/d$ | $f_c'$ $(MPa)$ | $Fiber$ Type | $V_f$ (%) | $l_f/d_f$ | $V_{exp}$ $(MPa)$ | $V_{pre}/V_{exp}$ | | | | | | | | |
|---|---|---|---|---|---|---|---|---|---|---|---|---|---|---|---|---|---|
| | | | | | | | | | (1) | (2) | (3) | (4) | (5) | (6) | (7) | (11) | (12) |
| Greenough andNehdi (2008) | S-HE-50-0.5 | 200.0 | 300.0 | 300.0 | H | 0.5 | 50.0 | 91.0 | 2.5 | 1.6 | 1.0 | 0.9 | 0.8 | 0.9 | 0.8 | 2.0 | 1.8 |
| | S-HE-50-0.75 | 200.0 | 300.0 | 300.0 | H | 0.8 | 50.0 | 105.0 | 1.9 | 1.2 | 0.9 | 0.8 | 0.7 | 0.8 | 0.7 | 1.9 | 1.4 |
| | S-HE-50-1.0 | 200.0 | 300.0 | 300.0 | H | 1.0 | 50.0 | 149.0 | 1.4 | 0.9 | 0.7 | 0.6 | 0.6 | 0.7 | 0.6 | 1.4 | 1.1 |
| | S-FE-50-0.5 | 200.0 | 300.0 | 300.0 | F | 0.5 | 50.0 | 115.0 | 1.9 | 1.2 | 0.8 | 0.7 | 0.6 | 0.7 | 0.6 | 1.6 | 1.4 |
| | S-FE-50-0.75 | 200.0 | 300.0 | 300.0 | F | 0.8 | 50.0 | 144.0 | 1.5 | 1.0 | 0.7 | 0.6 | 0.6 | 0.6 | 0.6 | 1.4 | 1.1 |
| | S-FE-50-1.0 | 200.0 | 300.0 | 300.0 | F | 1.0 | 50.0 | 147.0 | 1.4 | 0.9 | 0.7 | 0.6 | 0.6 | 0.7 | 0.6 | 1.4 | 1.0 |
| | S-FE-30-0.5 | 200.0 | 300.0 | 300.0 | F | 0.5 | 43.0 | 106.0 | 2.3 | 1.5 | 0.8 | 0.8 | 0.6 | 0.8 | 0.8 | 1.7 | 1.7 |
| | S-FE-30-0.75 | 200.0 | 300.0 | 300.0 | F | 0.8 | 43.0 | 123.0 | 1.8 | 1.2 | 0.7 | 0.7 | 0.6 | 0.7 | 0.6 | 1.6 | 1.3 |
| | S-FE-30-1.0 | 200.0 | 300.0 | 300.0 | F | 1.0 | 43.0 | 151.0 | 1.4 | 0.9 | 0.6 | 0.6 | 0.5 | 0.6 | 0.5 | 1.4 | 1.0 |

### 4.3.5. Comparison of Shear Prediction Equations for FRC Coupling Beams with Transverse Reinforcement

In Fig. 4.13 (1), almost all the shear strength values are overpredicted with a mean value of 1.37. In Fig. 4.13 (8), most of the capacities are underestimated with a mean of 0.7, which leads to an increase in standard deviation (0.26) and AAE (35.33%). In Figs. 4.13 (9) and (10), the overestimation of data points is predominant. As a result, mean values are 1.13 and 1.56, respectively. Especially for Eqn. (10) by Cai et al. (2016) almost all the shear strengths are overestimated significantly. This results in a high error margin of 56.81%. The proposed methodology, the results of which are shown in Fig. 4.13 (12), is the most accurate one with lowest scatter of data. As a result, mean, standard deviation and AAE turn out to be 0.99, 0.17 and 13.59%, respectively.

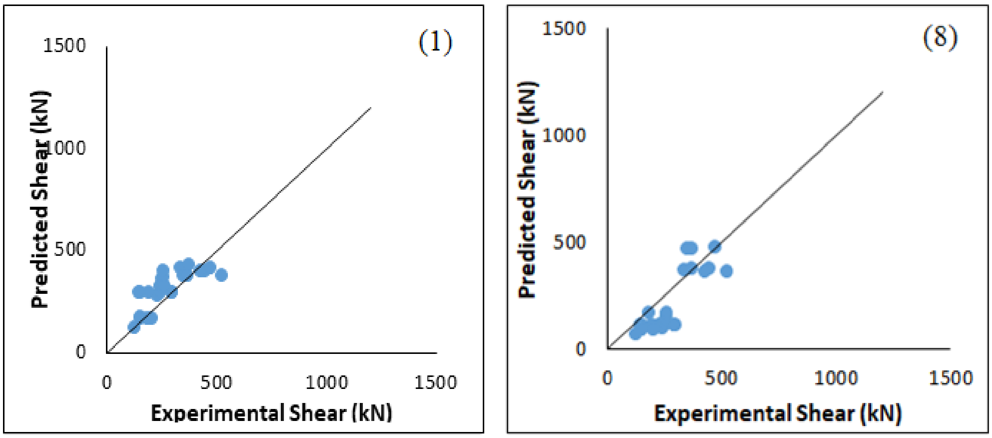


*Figure 4.13.* Shear strength predictions for FRC Coupling Beams with transverse reinforcement: (1) ACI 318-14 (2014); (8) Canbolat (2004)

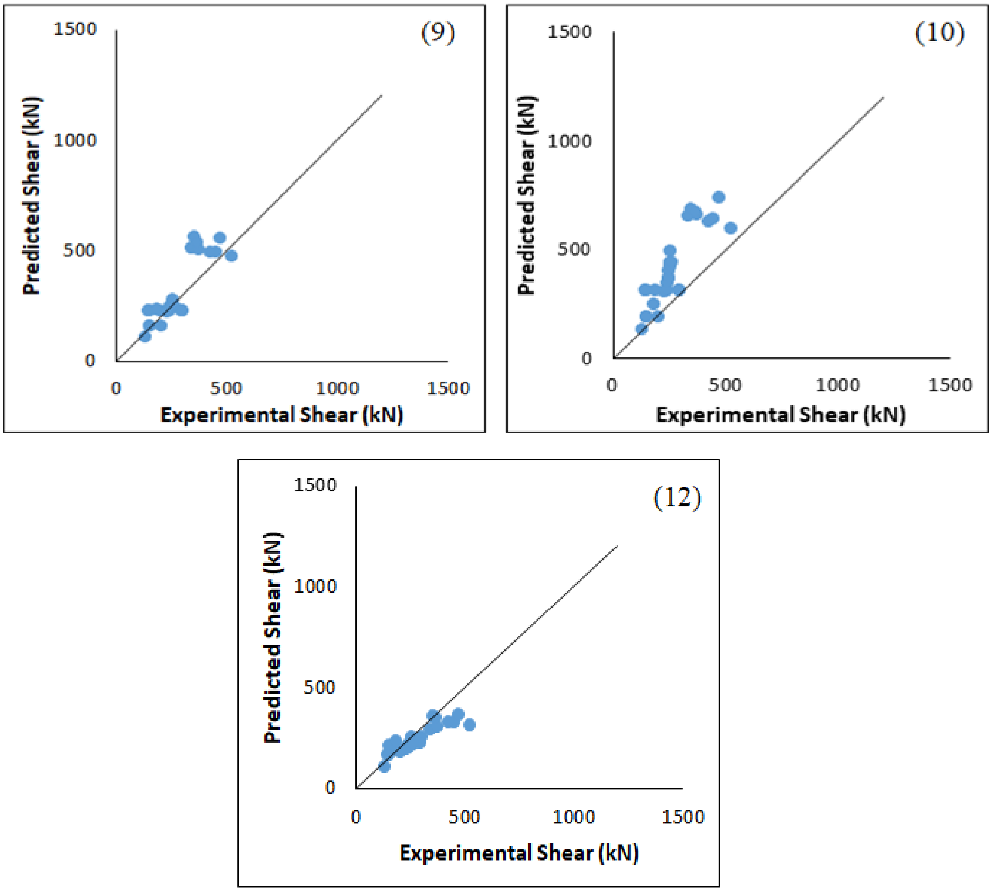


*Figure 4.13.* Shear strength predictions for FRC Coupling Beams with transverse reinforcement (continued):

(9) Lequesne (2011); (10) Cai et al. (2016); (12) Proposed method

Table 4.14. *Statistical Parameters for FRC Coupling Beams with transverse reinforcement*

| Equation Number | Shear Equation | Mean | Range | Standard Deviation | Avg. Absolute Error (%) |
|---|---|---|---|---|---|
| (1) | ACI 318-14 (2014) | 1.37 | 0.7 - 2.1 | 0.30 | 28.37 |
| (8) | Canbolat (2004) | 0.70 | 0.4 - 1.4 | 0.26 | 35.33 |
| (9) | Lequesne (2011) | 1.13 | 0.8 - 1.6 | 0.24 | 19.24 |
| (10) | Cai et al. (2016) | 1.56 | 1.0 - 2.3 | 0.33 | 56.81 |
| (12) | Proposed Method | 0.99 | 0.7 - 1.4 | 0.17 | 13.59 |

Table 4.15. *Comparison of Predicted versus Experimental Strengths for FRC Coupling Beams with transverse reinforcement*

| *Researcher* | *Specimen* | $l_n/d$ | $\rho_t$ (%) | $f'_c$ $(MPa)$ | *Fiber* Type | $V_f$ (%) | $l_f/d_f$ | $V_{exp}$ $(MPa)$ | $V_{pre}/V_{exp}$ | | | | |
|---|---|---|---|---|---|---|---|---|---|---|---|---|---|
| | | | | | | | | | (1) | (8) | (9) | (10) | (12) |
| Cai et al. (2016) | CCB3-30-2-1F-S | 2.2 | 0.6 | 40.5 | S | 1.0 | 42.0 | 227.0 | 1.3 | 0.5 | 1.0 | 1.4 | 1.0 |
| | CCB3-40-2-1F-S | 2.2 | 0.6 | 43.1 | S | 1.0 | 42.0 | 238.0 | 1.2 | 0.5 | 1.0 | 1.3 | 0.9 |
| | CCB3-50-2-1F-S | 2.2 | 0.6 | 52.9 | S | 1.0 | 42.0 | 243.0 | 1.3 | 0.5 | 1.0 | 1.5 | 1.0 |
| | CCB3-60-2-1F-S | 2.2 | 0.6 | 66.7 | S | 1.0 | 42.0 | 250.0 | 1.5 | 0.5 | 1.1 | 1.7 | 1.1 |
| | CCB3-70-2-1F-S | 2.2 | 0.6 | 70.1 | S | 1.0 | 42.0 | 253.0 | 1.5 | 0.5 | 1.1 | 1.8 | 1.1 |
| | CCB3-80-2-1F-S | 2.2 | 0.6 | 80.7 | S | 1.0 | 42.0 | 255.0 | 1.6 | 0.5 | 1.1 | 1.9 | 1.1 |
| | CCB3-40-1-1F-S | 1.1 | 0.6 | 43.1 | S | 1.0 | 42.0 | 295.0 | 1.0 | 0.4 | 0.8 | 1.1 | 1.0 |
| | CCB3-40-1.5-1F-S | 1.7 | 0.6 | 43.1 | S | 1.0 | 42.0 | 292.0 | 1.0 | 0.4 | 0.8 | 1.1 | 0.9 |
| | CCB3-40-2.5-1F-F/S | 2.8 | 0.6 | 43.1 | S | 1.0 | 42.0 | 190.0 | 1.5 | 0.6 | 1.2 | 1.7 | 1.1 |
| | CCB3-40-3.0-1F-F/S | 3.3 | 0.6 | 43.1 | S | 1.0 | 42.0 | 147.0 | 2.0 | 0.8 | 1.6 | 2.2 | 1.4 |
| | CCB3-40-3.5-1F-F | 3.9 | 0.6 | 43.1 | S | 1.0 | 42.0 | 140.0 | 2.1 | 0.8 | 1.6 | 2.3 | 1.4 |
| | CCB3-50-2-0.5F-S | 2.2 | 0.6 | 54.5 | S | 0.5 | 42.0 | 238.0 | 1.4 | 0.4 | 1.0 | 1.5 | 1.0 |
| | CCB3-55-2-1F-S | 2.2 | 0.6 | 54.8 | S | 1.0 | 42.0 | 244.0 | 1.4 | 0.5 | 1.0 | 1.5 | 1.0 |
| | CCB3-50-2-1.5F-S | 2.2 | 0.6 | 55.9 | S | 1.5 | 42.0 | 249.5 | 1.3 | 0.6 | 1.0 | 1.6 | 1.0 |
| | CCB3-50-2-2F-S | 2.2 | 0.6 | 55.3 | S | 2.0 | 42.0 | 255.5 | 1.3 | 0.6 | 1.0 | 1.7 | 1.0 |
| | CCB3-50-2.5F-F/S | 2.2 | 0.6 | 54.1 | S | 2.5 | 42.0 | 257.0 | 1.3 | 0.7 | 1.0 | 1.7 | 1.0 |
| Baczkowski (2007) | C-10/M | 1.1 | 0.6 | 33.7 | H | 1.0 | 47.6 | 150.0 | 1.2 | 0.6 | 1.1 | 1.3 | 1.3 |
| | C-15/M | 1.7 | 0.6 | 32.8 | H | 1.0 | 47.6 | 200.0 | 0.9 | 0.5 | 0.8 | 1.0 | 0.8 |
| | C-15/S | 1.7 | 1.1 | 31.9 | H | 1.0 | 47.6 | 180.0 | 0.9 | 1.0 | 1.3 | 1.4 | 1.1 |
| | C-20/M | 2.2 | 0.6 | 32.2 | H | 1.0 | 47.6 | 150.0 | 1.1 | 0.6 | 1.1 | 1.3 | 1.0 |
| | C-30/M | 3.1 | 0.6 | 31.4 | H | 1.0 | 47.6 | 125.0 | 1.0 | 0.6 | 0.9 | 1.1 | 0.7 |
| Pérez-Irizarry and Parra-Montesinos (2016) | CB1 | 3.4 | 1.0 | 53.7 | H | 1.3 | 64.0 | 520.0 | 0.7 | 0.7 | 0.9 | 1.2 | 0.7 |
| | CB2 | 3.4 | 1.0 | 59.9 | H | 1.3 | 64.0 | 445.0 | 0.9 | 0.9 | 1.1 | 1.4 | 0.8 |
| | CB3 | 3.4 | 1.0 | 58.5 | H | 1.3 | 55.0 | 423.0 | 0.9 | 0.9 | 1.2 | 1.5 | 0.8 |
| | CB4 | 3.4 | 1.0 | 63.3 | H | 1.0 | 55.0 | 334.0 | 1.2 | 1.1 | 1.5 | 2.0 | 0.9 |
| | CB5 | 3.4 | 1.0 | 67.5 | H | 1.0 | 79.0 | 369.0 | 1.2 | 1.0 | 1.4 | 1.8 | 0.8 |
| | CB6 | 2.4 | 1.2 | 57.4 | H | 1.5 | 64.0 | 347.0 | 1.1 | 1.4 | 1.6 | 2.0 | 1.2 |
| | CB7 | 2.4 | 1.2 | 70.4 | H | 1.5 | 79.0 | 467.0 | 0.9 | 1.0 | 1.2 | 1.6 | 0.9 |
| | CB8 | 2.4 | 1.2 | 58.7 | H | 1.5 | 79.0 | 365.0 | 1.0 | 1.3 | 1.5 | 1.9 | 1.1 |

### 4.3.4. Comparison of Shear Prediction Equations for FRC Coupling Beams without transverse reinforcement

The ACI 318-14 equation overpredicts most of the shear strength values within the range of 1.52 to 2.53 with a mean value of 1.99. While Equation (8) by Canbolat et al. (2005) (Fig. 4.14 (8)) underestimates all experimental shear strengths significantly, Eqn. (10) by Cai et al. (2016) (Fig. 4.14 (10)) overestimates all. The rest of the equations give similar predictions and have comparable statistical parameters. It should be noted that only one set of experiments is available for this group, namely the specimens tested by Adebar et al. (1997). More experiments should be performed to verify the validity of all shear prediction equations.

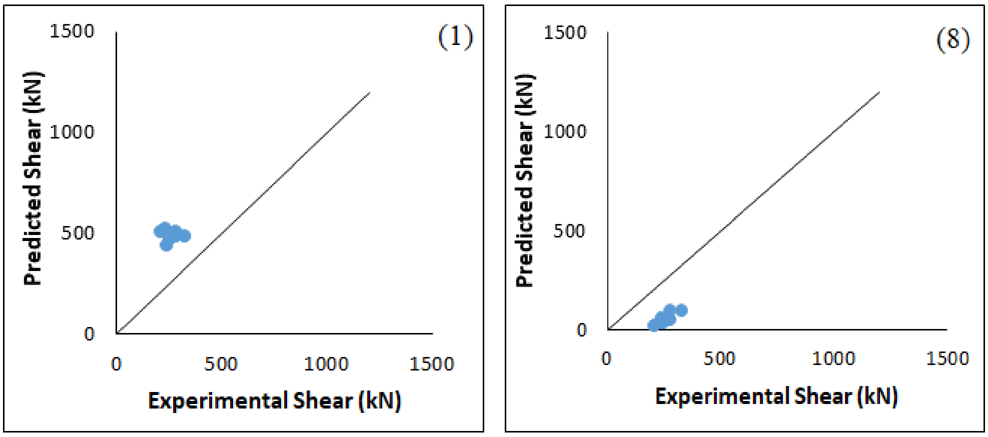


*Figure 4.14.* Shear strength predictions for FRC Coupling Beams without transverse reinforcement: (1) ACI 318-14 (2014); (8) Canbolat (2004)

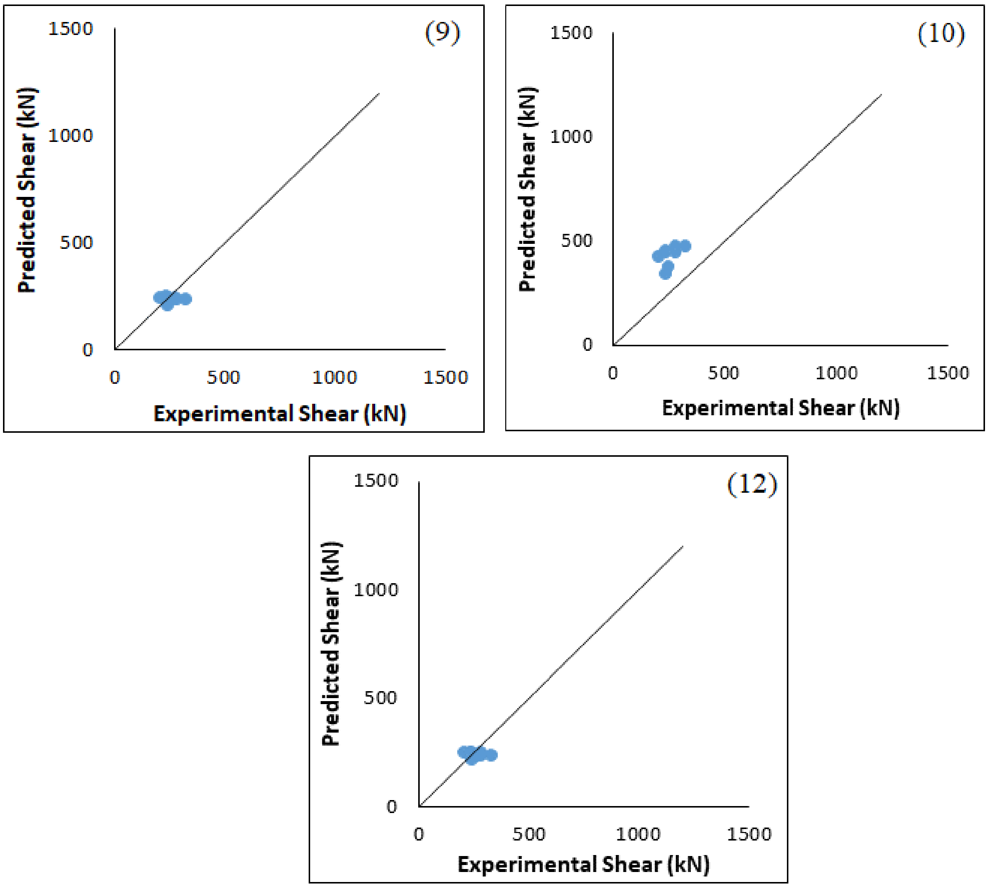


*Figure 4.14.* Shear strength predictions for FRC Coupling Beams without transverse reinforcement (continued):

(9) Lequesne (2011); (10) Cai et al. (2016); (12) Proposed method

Table 4.16. *Statistical Parameters for FRC Coupling Beams without transverse reinforcement*

| Equation Number | Shear Equation | Mean | Range | Standard Deviation | Avg. Absolute Error (%) |
|---|---|---|---|---|---|
| (1) | ACI 318-14 (2014) | 1.99 | 1.52 - 2.53 | 0.29 | 98.75 |
| (8) | Canbolat (2004) | 0.23 | 0.14 - 0.37 | 0.07 | 76.96 |
| (9) | Lequesne (2011) | 0.96 | 0.73 - 1.22 | 0.14 | 12.91 |
| (10) | Cai et al. (2016) | 1.72 | 1.47 - 2.10 | 0.23 | 72.03 |
| (12) | Proposed Method | 1.13 | 0.86 - 1.44 | 0.17 | 16.40 |

Table 4.17. *Comparison of Predicted versus Experimental Strengths for FRC Coupling Beams without transverse reinforcement*

| *Researcher* | *Specimen* | $l_n/d$ | $f_c'$ $(MPa)$ | *Fiber* Type | $V_f$ (%) | $l_f/d_f$ | $V_{exp}$ $(MPa)$ | $V_{pre}/V_{exp}$ | | | | |
|---|---|---|---|---|---|---|---|---|---|---|---|---|
| | | | | | | | | (1) | (8) | (9) | (10) | (12) |
| Adebar et al. (1997) | FC2 | 2.7 | 54.1 | H | 0.8 | 60.0 | 276.0 | 1.9 | 0.2 | 0.9 | 1.6 | 1.1 |
| | FC3 | 2.7 | 49.9 | H | 1.5 | 60.0 | 324.0 | 1.5 | 0.3 | 0.7 | 1.5 | 0.9 |
| | FC5 | 2.7 | 54.1 | H | 0.8 | 60.0 | 237.0 | 2.2 | 0.2 | 1.0 | 1.9 | 1.2 |
| | FC6 | 2.7 | 49.9 | H | 1.5 | 60.0 | 278.0 | 1.8 | 0.4 | 0.9 | 1.7 | 1.0 |
| | FC8 | 2.7 | 54.8 | H | 0.4 | 60.0 | 204.0 | 2.5 | 0.1 | 1.2 | 2.1 | 1.4 |
| | FC9 | 2.7 | 56.5 | H | 0.6 | 60.0 | 232.0 | 2.3 | 0.2 | 1.1 | 2.0 | 1.3 |
| | FC10 | 2.7 | 46.9 | H | 0.4 | 100.0 | 247.0 | 1.9 | 0.2 | 0.9 | 1.5 | 1.1 |
| | FC11 | 2.7 | 40.8 | H | 0.6 | 100.0 | 237.0 | 1.9 | 0.3 | 0.9 | 1.5 | 1.1 |

#### 4.3.7. Comparison of Shear Prediction Equations for HPFRC Coupling Beams with Transverse Reinforcement

Eqn. (1) underpredicts nearly all data with a mean value of 0.55, which is significantly low. Although the mean of Eqns. (8) and (9) are 1.04 and 1.08, respectively, as it can be observed from Figs. 4.15 (8) and (9), there is a significant scatter in the data and nearly half of the shear strengths are overestimated while others are underestimated significantly. Moreover, these equations have a large range of predictions; between 0.44 and 1.71 for Eqn. (8) and 0.52 and 1.54 for Eqn. (9). The results obtained by using the proposed method are given in Fig. 4.15 (12) Majority of the experimental results are underestimated (Table 4.18) and the highest overestimation is 4%. Furthermore, mean is 0.93, while AAE is quite low, at a level of 9.86%. Standard deviation of the proposed method (0.13) and therefore the scatter of data are smaller than those of other equations. Consequently, the proposed equation has the most accurate and conservative results when compared to the others.

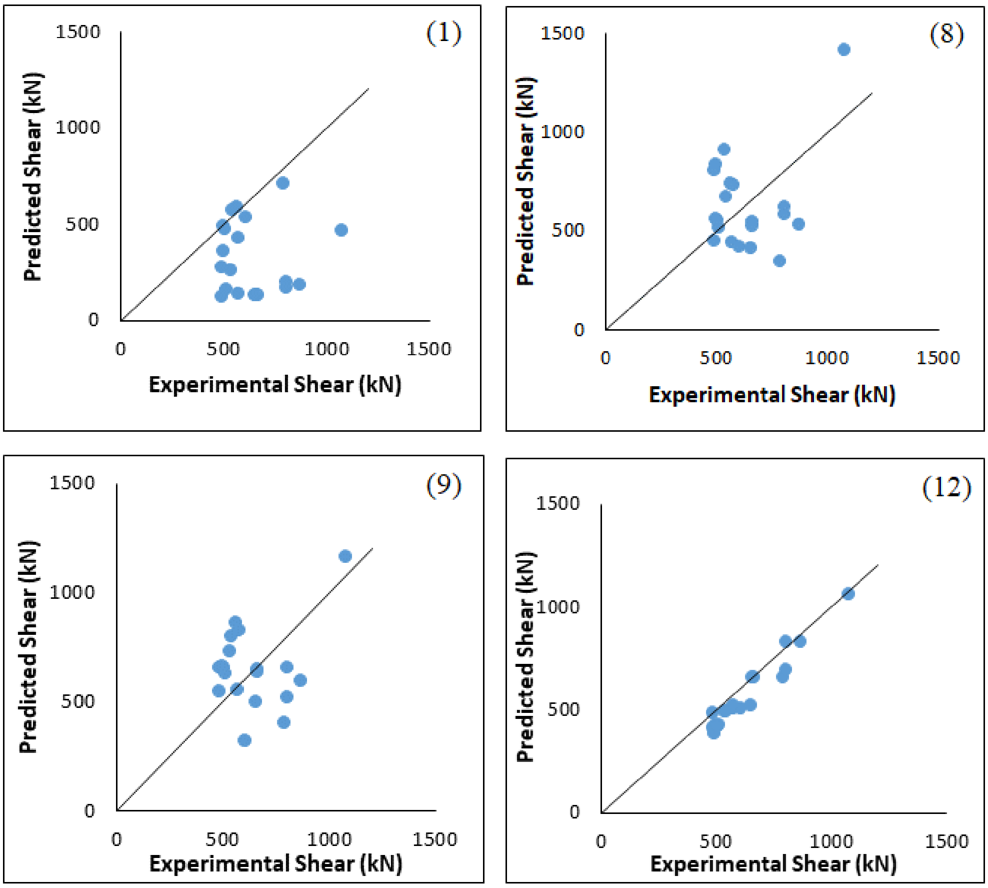


*Figure 4.15.* Shear strength predictions for HPFRC Coupling Beams with transverse reinforcement: (1) ACI 318-14 (2014); (8) Canbolat (2004); (9) Lequesne (2011); (12) Proposed method

Table 4.18. *Statistical Parameters for HFRC Coupling Beams with transverse reinforcement*

| Equation Number | Shear Equation | Mean | Range | Standard Deviation | Avg. Absolute Error (%) |
|---|---|---|---|---|---|
| (1) | ACI 318-14 (2014) | 0.55 | 0.21 - 1.07 | 0.32 | 46.11 |
| (8) | Canbolat (2004) | 1.04 | 0.44 - 1.71 | 0.37 | 31.34 |
| (9) | Lequesne (2011) | 0.94 | 0.52 - 1.54 | 0.10 | 9.22 |
| (12) | Proposed Method | 0.94 | 0.82 - 1.02 | 0.11 | 9.80 |

Table 4.19. *Comparison of Predicted versus Experimental Strengths for HPFRC Coupling Beams with transverse reinforcement*

| $Researcher$ | $Specimen$ | $l_n/d$ | $\rho_t$ (%) | $\rho_d$ (%) | $f_c'$ $(MPa)$ | $Fiber$ Type | $V_f$ (%) | $l_f/d_f$ | $V_{exp}$ $(MPa)$ | $V_{pre}/V_{exp}$ | | | |
|---|---|---|---|---|---|---|---|---|---|---|---|---|---|
| | | | | | | | | | | (1) | (8) | (9) | (12) |
| Shin et al. (2014) | 1CF2Y | 4.2 | 1.4 | 0.0 | 49.2 | PVA | 2.0 | 307.7 | 491.0 | 0.74 | 1.71 | 1.35 | 0.82 |
| | 1DF2Y | 4.2 | 0.9 | 1.5 | 49.2 | PVA | 2.0 | 307.7 | 533.0 | 0.49 | 1.71 | 1.38 | 0.93 |
| Yun et al. (2008) | CB2 | 1.1 | 0.2 | 2.0 | 57.0 | PE+T | 0.75+0.75 | 342.1+100 | 865.69 | 0.22 | 0.62 | 0.69 | 1.02 |
| | CB3 | 1.1 | 0.2 | 0.0 | 57.0 | PE+T | 0.75+0.75 | 342.1+100 | 785.14 | 0.91 | 0.44 | 0.52 | 0.86 |
| Setkit (2012) | CB-1 | 2.9 | 0.5 | 3.7 | 49.6 | H | 1.5 | 80.0 | 568.0 | 0.26 | 0.79 | 0.98 | 0.90 |
| | CB-2 | 2.9 | 0.6 | 3.7 | 59.0 | H | 1.5 | 80.0 | 508.0 | 0.32 | 1.02 | 1.25 | 0.85 |
| | CB-3 | 3.6 | 0.6 | 3.1 | 61.0 | H | 1.5 | 80.0 | 484.0 | 0.27 | 0.94 | 1.14 | 0.87 |
| | CB-5 | 3.6 | 1.1 | 0.0 | 68.0 | H | 1.5 | 80.0 | 496.0 | 0.99 | 1.15 | 1.35 | 0.86 |
| | CB-6 | 2.9 | 1.1 | 0.0 | 67.6 | H | 1.5 | 80.0 | 562.0 | 1.06 | 1.32 | 1.54 | 0.90 |
| Canbolat (2004) | Specimen 2 | 1.1 | 0.3 | 0.0 | 57.0 | PE | 2.0 | 342.1 | 600.0 | 0.89 | 0.71 | 0.53 | 0.88 |
| | Specimen 3 | 1.1 | 0.3 | 3.7 | 57.0 | PE | 2.0 | 342.1 | 800.0 | 0.25 | 0.79 | 0.65 | 0.94 |
| | Specimen 4 | 1.1 | 0.5 | 1.5 | 63.4 | T | 1.5 | 100.0 | 800.0 | 0.22 | 0.73 | 0.83 | 1.00 |
| Lequesne (2011) | CB-1 | 1.8 | 0.6 | 2.9 | 45.0 | H | 1.5 | 78.9 | 660.0 | 0.21 | 0.83 | 0.99 | 0.90 |
| | CB-2 | 1.8 | 0.6 | 2.9 | 52.0 | H | 1.5 | 78.9 | 655.0 | 0.21 | 0.81 | 0.98 | 0.92 |
| | CB-3 | 1.8 | 0.5 | 2.9 | 34.0 | H | 1.5 | 78.9 | 650.0 | 0.21 | 0.64 | 0.77 | 0.89 |
| C18 Han et al. (2015) | FC-05-2,0 | 2.1 | 0.6 | 4.5 | 41.0 | PVA | 2.0 | 307.7 | 1073.0 | 0.44 | 1.32 | 1.09 | 0.93 |
| | FC-0,5-3,5 | 3.9 | 0.6 | 4.6 | 41.0 | PVA | 2.0 | 307.7 | 484.0 | 0.57 | 1.67 | 1.36 | 1.01 |
| Parra-Montesinos et al. (2017) | 1 | 2.4 | 1.8 | 0.0 | 63.0 | H | 1.5 | 78.9 | 570.0 | 0.76 | 1.30 | 1.45 | 0.99 |
| | 2 | 2.9 | 1.2 | 0.0 | 68.3 | H | 1.5 | 78.9 | 540.0 | 1.07 | 1.26 | 1.48 | 0.92 |
| | 3 | 3.6 | 1.2 | 0.0 | 68.3 | H | 1.5 | 78.9 | 500.0 | 0.95 | 1.12 | 1.32 | 0.85 |

### 4.3.8. Comparison of Shear Prediction Equations for HPFRC Coupling Beams without Transverse Reinforcement

In Fig. 4.16 (1), the experimental shear strengths are underestimated, whereas in Fig. 4.16 (8), they are overestimated. Eqn. (9) by Lequesne (2011) has the same prediction for both beams, therefore, the standard deviation is 0.0. The proposed method has adequate accuracy in predicting the shear strength. Since, there are only two experiments performed for this type of members, more tests are required to verify the reliability of the proposed equations.

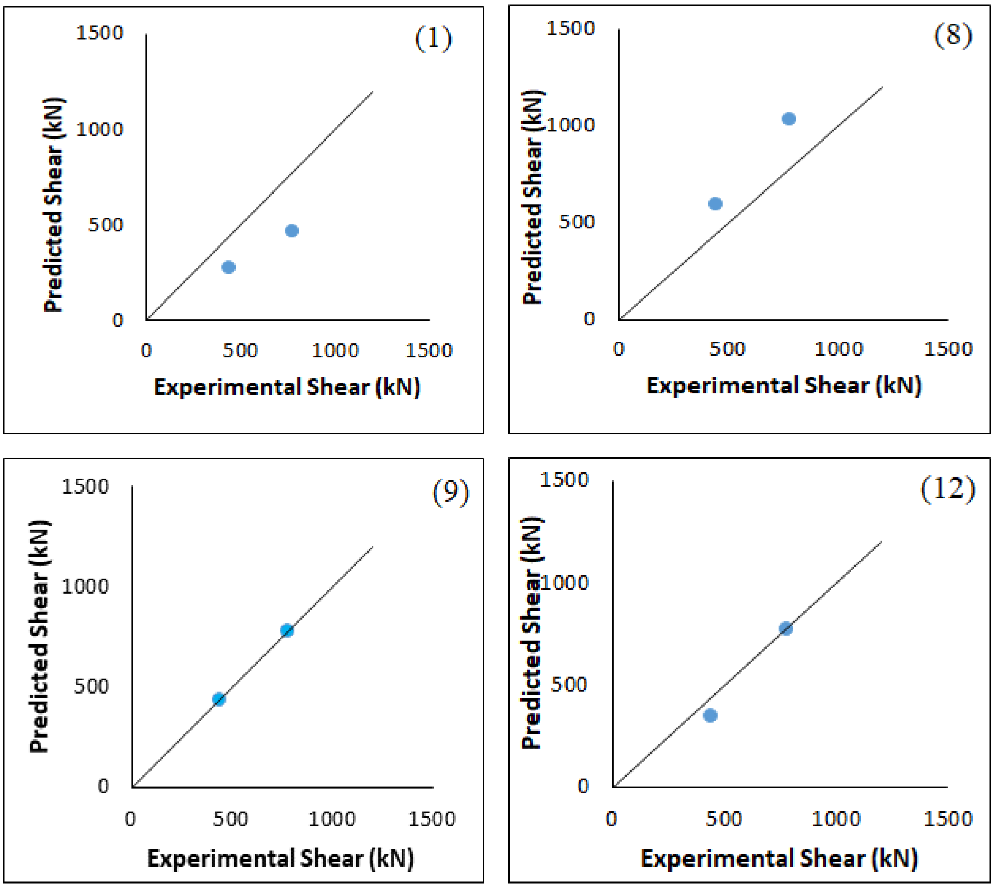


*Figure 4.16.* Shear strength predictions for HPFRC Coupling Beams without transverse reinforcement: (1) ACI 318-14 (2014); (8) Canbolat (2004); (9) Lequesne (2011); (12) Proposed method

Table 4.20. *Statistical Parameters for HPFRC Coupling Beams without transverse reinforcement*

| Equation Number | Shear Equation | Mean | Range | Standard Deviation | Avg. Absolute Error (%) |
|---|---|---|---|---|---|
| (1) | ACI 318-14 (2014) | 0.62 | 0.61 - 0.63 | 0.01 | 37.76 |
| (8) | Canbolat (2004) | 1.36 | 1.34 - 1.37 | 0.02 | 35.58 |
| (9) | Lequesne (2011) | 1.01 | 1.01 - 1.01 | 0.00 | 1.43 |
| (12) | Proposed Method | 0.95 | 0.88 - 1.02 | 0.07 | 7.21 |

Table 4.21. *Comparison of Predicted versus Experimental Strengths for HPFRC Coupling Beams without transverse reinforcement*

| $Researcher$ | $Specimen$ | $l_n/d$ | $\rho_d$ (%) | $f_c'$ $(MPa)$ | $Fiber$ Type | $V_f$ (%) | $l_f/d_f$ | $V_{exp}$ $(MPa)$ | $V_{pre}/V_{exp}$ | | | |
|---|---|---|---|---|---|---|---|---|---|---|---|---|
| | | | | | | | | | (1) | (8) | (9) | (12) |
| Kwon et al. (2013) | FC-0.0 | 2.2 | 4.5 | 41.0 | PVA | 2.0 | 307.7 | 775.0 | 0.61 | 1.34 | 1.01 | 1.02 |
| Han et al. (2015) | FC-0-3.5 | 4.1 | 4.6 | 41.0 | PVA | 2.0 | 307.7 | 437.0 | 0.63 | 1.37 | 1.01 | 1.08 |

### 4.3.9. Comparison of Shear Prediction Equations for all the Beams in the Database

In Figs. 4.17 and 4.18, comparison of prediction equations is shown for deep beams and coupling beams, respectively. Furthermore, statistical parameters are given in Tables 4.22 and 4.23. In these figures and tables, only the equations applicable to the given beam types are considered. It can be observed that, although a single proposed equation is used for beams with different material properties and loading conditions, the obtained results are mostly conservative, have adequate accuracy and provide improved predictions when compared with other available prediction equations. The proposed prediction equation works best for HPFRC coupling beams with transverse reinforcement. The highest error and scatter of data are observed for deep beams ($a/d \leq 2.5$) without transverse reinforcement.

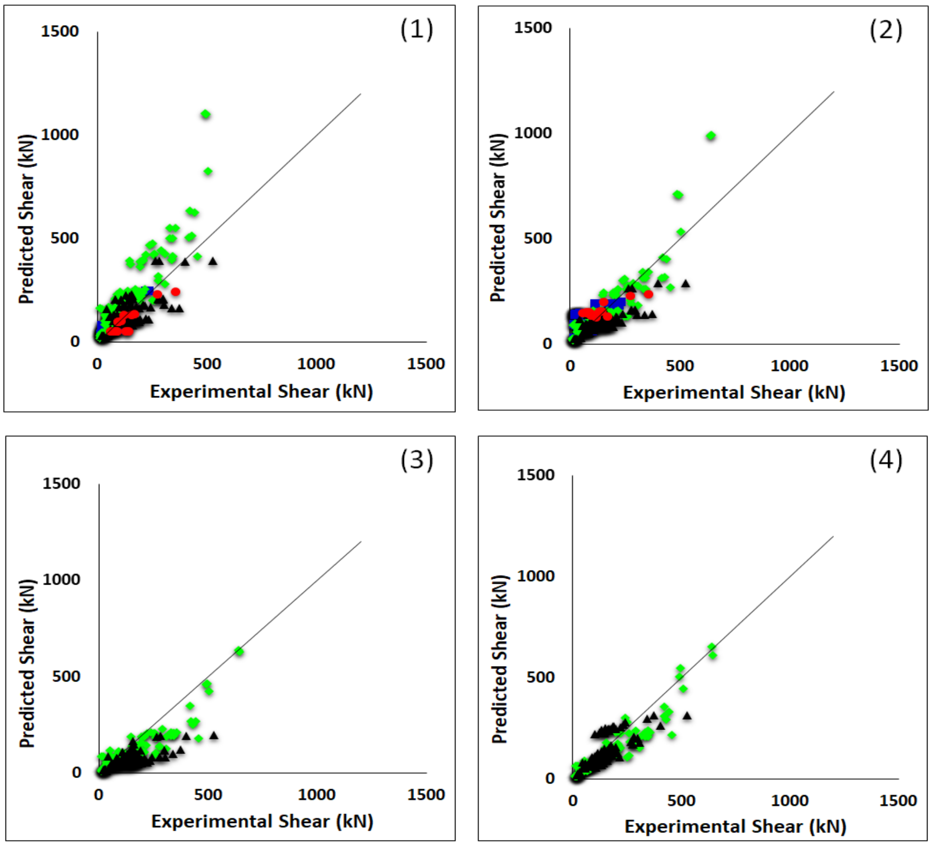


*Figure 4.17.* Shear strength predictions for Deep Beams:
(1) ACI 318-14 (2014); (2) Sharma (1986); (3) Mansur et al. (1986); (4) Narayanan and Darwish (1987)

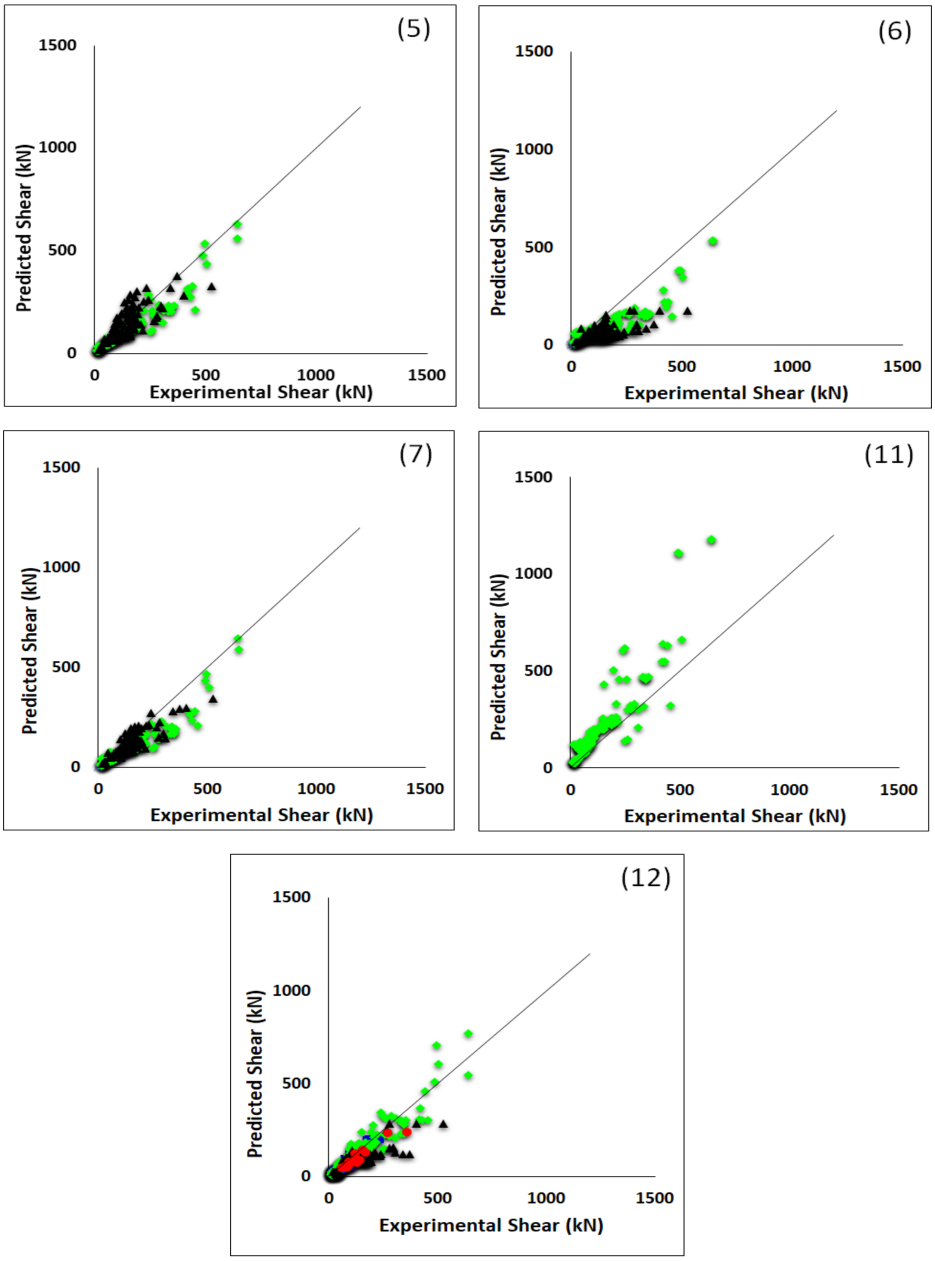


Deep beams ($a/d \le 2.5$) with transverse reinforcement

Deep beams ($a/d \le 2.5$) without transverse reinforcement

Deep beams ($a/d > 2.5$) with transverse reinforcement

Deep beams ($a/d > 2.5$) without transverse reinforcement

*Figure 4.17.* Shear strength predictions for Deep Beams (continued):

(5) Ashour et al. (1992); (6) Khuntia et al. (1999); (7) Kwak et al. (2002); (11) Dinh et al. (2011);

(12) Proposed method

Table 4.22. *Statistical Parameters for Deep Beams*

| Equation Number | Shear Equation | Mean | Range | Standard Deviation | Avg. Absolute Error (%) |
|---|---|---|---|---|---|
| (1) | ACI 318-14 (2014) | 1.36 | 0.35 - 10.76 | 0.23 | 63.82 |
| (2) | Sharma (1986) | 1.60 | 0.37 - 5.84 | 0.73 | 83.7 |
| (3) | Mansur et al. (1986) | 0.90 | 0.23 - 5.68 | 0.51 | 52.45 |
| (4) | Narayanan and Darwish (1987) | 1.14 | 0.4 - 2.07 | 0.43 | 34.24 |
| (5) | Ashour et al. (1992) | 1.10 | 0.18 - 3.80 | 0.32 | 32.89 |
| (6) | Khuntia et al. (1999) | 0.71 | 0.41 - 4.09 | 0.37 | 64.68 |
| (7) | Kwak et al. (2002) | 0.96 | 0.36 - 2.76 | 0.30 | 39.88 |
| (11) | Dinh et al. (2011) | 1.70 | 0.54 - 7.83 | 0.73 | 71.73 |
| (12) | Proposed Method | 0.84 | 0.32 - 1.64 | 0.19 | 24.13 |

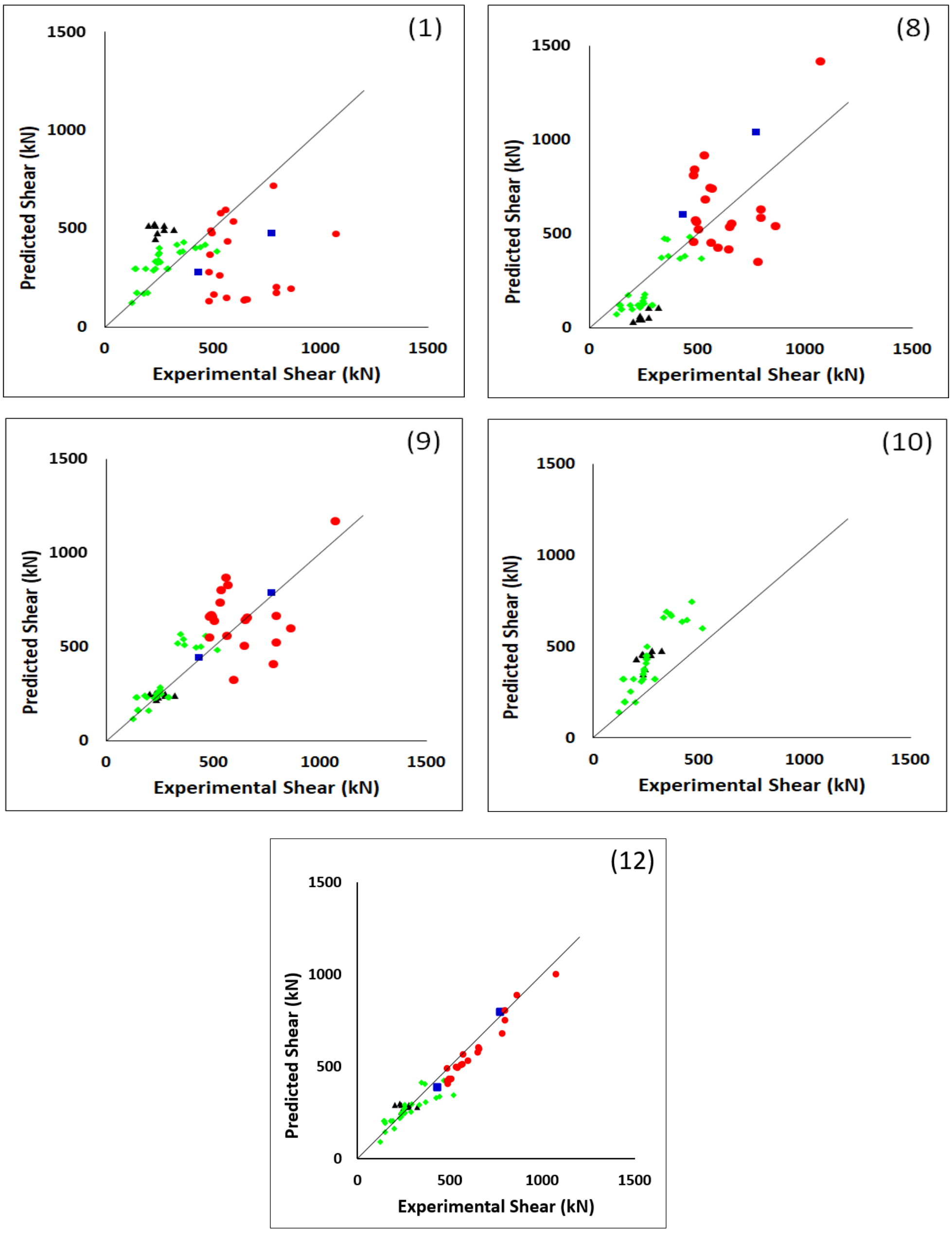


● HPFRC coupling beams with transverse reinforcement
■ HPFRC coupling beams without transverse reinforcement
◆ FRC coupling beams with transverse reinforcement
▲ FRC coupling beams without transverse reinforcement

*Figure 4.18.* Shear strength predictions for Coupling Beams:

(1) ACI 318-14 (2014); (8)Canbolat (2004); (9) Lequesne (2011); (10) Cai et al. (2016); (12) Proposed method

Table 4.23. *Statistical Parameters for Coupling Beams*

| Equation Number | Shear Equation | Mean | Range | Standard Deviation | Avg. Absolute Error (%) |
|---|---|---|---|---|---|
| (1) | ACI 318-14 (2014) | 1.15 | 0.21 - 2.53 | 0.29 | 44.24 |
| (8) | Canbolat (2004) | 0.77 | 0.14 - 1.71 | 0.26 | 39.63 |
| (9) | Lequesne (2011) | 1.04 | 0.52 - 1.60 | 0.17 | 14.38 |
| (10) | Cai et al. (2016) | 1.59 | 1.00 - 2.30 | 0.31 | 60.10 |
| (12) | Proposed Method | 0.99 | 0.70 - 1.44 | 0.15 | 12.47 |

# CHAPTER 5

# VERIFICATION OF THE PROPOSED MODEL BY NONLINEAR ANALYSIS

In order to verify the applicability of the proposed method to predict the shear strength of shear critical deep beams, selected specimens are analyzed using ETABS 17 (2017). First, moment-curvature relationships for conventionally and diagonally reinforced fiber reinforced composite coupling beams are obtained. Nonlinear analytical models of coupling beam subassemblies previously tested under cyclic loading are generated and the analytical results are then compared with the experimental ones

## 5.1. Subassembly Modeling

Coupling beam subassemblies are composed of a shear critical deep beam connecting two reinforced concrete wall segments on each end. The commonly used test setup is to attach one of the wall segments to the strong floor and apply the load to the upper wall segment. The specimens considered in the database are loaded under two different configurations. In the first case, the predetermined displacement history based on the drift levels, are applied to the top reinforced concrete wall through a rigid steel plate, the line of action of which is passing through the midspan of the beam in order to obtain zero moment at the midspan of the coupling beam. In the second case, the predetermined displacement history is directly applied to the center of the top wall segment. For these specimens, two steel arms are placed at the ends of the top wall segment to prevent wall rotation. The aforementioned test setups and generated ETABS 2017 models of the test specimens are shown in Fig. 5.1 (a) and (b) and Fig.5.2 (a) and (b), respectively.

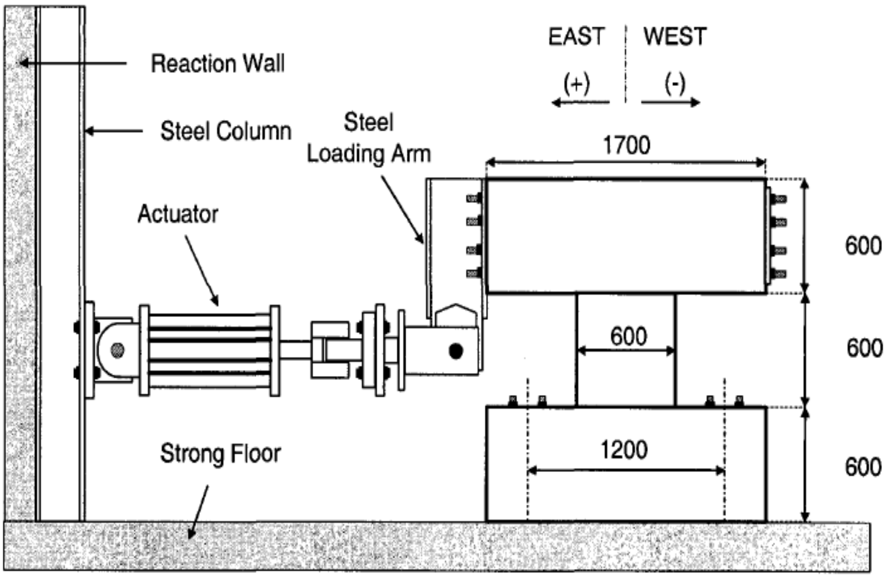


a) Specimen model when there are no arms holding the ends of the top wall segment (Canbolat, 2004)

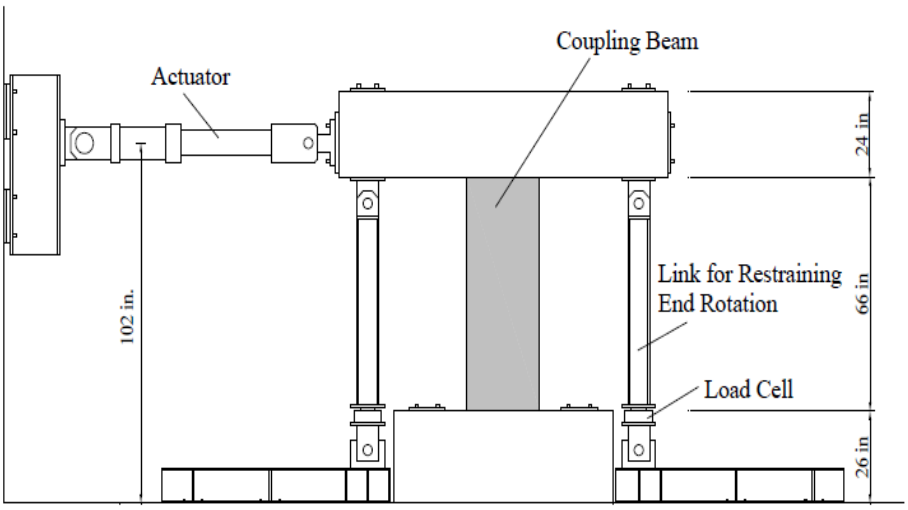


b) Test setup when there are arms holding the ends of the top wall segment

*Figure 5.1.* Test setup

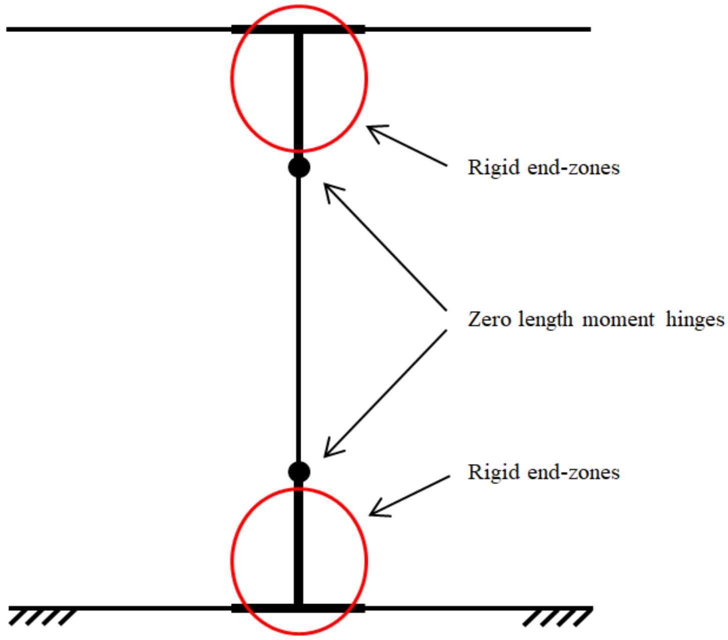


a) Specimen model when there are no arms holding the ends of the top wall segment

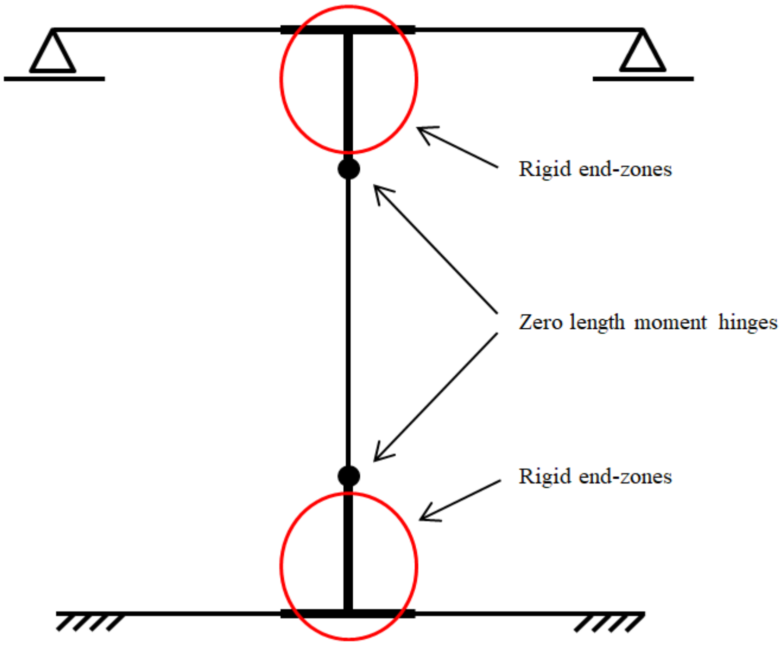


b) Specimen model when there are arms holding the ends of the top wall segment

*Figure 5.2*. Specimen models

The beam element is modeled as a cracked elastic segment in between the axis of the walls with cracked stiffness. At the two ends of the beam, there are two semi-rigid end zones within the walls and zero length moment hinges on the face of the walls (Fig.5.2). The wall segments are modeled as cracked elastic segments with rigid end zone elements along the depth of the beam (Fig. 5.2). Rigid end-zone factor is used to determine the relative rigidity of the beam-to-wall connections and it ranges from 0 to 1. The value 0 refers to the case, where the connection is infinitely flexible and the beam is free to rotate at the face of the wall; 1 is used to define full rigidity, so the portion of the beam embedded in the wall can not rotate. In this analytical study, rigid end zone factor is taken as 0.5, because fiber reinforced precast beams experience some slip under applied loading.

The main parameters which are required to define the elastic member behavior are cross-sectional dimensions, moment of inertia, elastic modulus, and Poisson's ratio. Since multiple cracking is expected in fiber reinforced composite beams, cracked moment of inertia is considered. Different approaches for obtaining the cracked moment of inertia and the values used in this study for the nonlinear analysis are discussed in Section 5.2.3 in detail. Thomas and Ramaswamy (2007) observed that the value of Poisson's ratio varied from 0.18 to 0.22 for different grades of concrete. This variation depends on the aggregate amount and the rate of loading. Moreover, fiber type and volumetric ratio affect Poisson's ratio. In this study, Poisson's ratio is considered to be constant and taken as 0.2 for both fiber reinforced and high performance fiber reinforced composites.

### 5.2. Nonlinear Analysis

For the verification of the proposed shear strength prediction method, nonlinear static analysis similar to pushover analysis is performed on previously tested subassemblies and the analytical results are compared with the experimental ones. In the analysis, the top wall segment in Fig. 5.2 (a) and (b) is displaced following the given displacement history for each specimen.

### 5.2.1. Beam Model

In the Seismic Rehabilitation and Retrofit of Existing Buildings Document (ASCE 41-13, 2013), the generalized force-deformation relationship for reinforced concrete elements or components is given in Fig.5.3. The modeling parameters recommended to be used in nonlinear analysis of reinforced concrete coupling beams controlled by flexure are presented in Table 5.1.

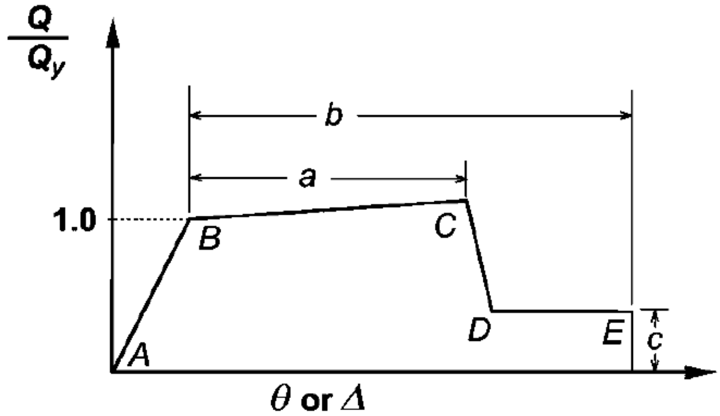


*Figure 5.3.* Generalized force versus deformation curve (ASCE 41, 2013)

Table 5.1. *Modeling Parameters for Coupling Beams (ASCE 41, 2013)*

| Conditions | | | Plastic Hinge Rotation (radians) | | Residual Strength Ratio | Acceptable Plastic Hinge Rotation[a] (radians) | | |
|---|---|---|---|---|---|---|---|---|
| | | | | | | Performance Level | | |
| | | | $a$ | $b$ | $c$ | IO | LS | CP |
| i. Shear walls and wall segments | | | | | | | | |
| $\frac{(A_s - A_s')f_y + P}{t_w l_w f_c'}$ | $\frac{V}{t_w l_w \sqrt{f_c'}}$ | Confined Boundary[b] | 0.015 | | | | | |
| ≤0.1 | ≤4 | Yes | 0.010 | 0.020 | 0.75 | 0.005 | 0.015 | 0.020 |
| ≤0.1 | ≥6 | Yes | 0.009 | 0.015 | 0.40 | 0.004 | 0.010 | 0.015 |
| ≥0.25 | ≤4 | Yes | 0.005 | 0.012 | 0.60 | 0.003 | 0.009 | 0.012 |
| ≥0.25 | ≥6 | Yes | 0.008 | 0.010 | 0.30 | 0.0015 | 0.005 | 0.010 |
| ≤0.1 | ≤4 | No | 0.006 | 0.015 | 0.60 | 0.002 | 0.008 | 0.015 |
| ≤0.1 | ≥6 | No | 0.003 | 0.010 | 0.30 | 0.002 | 0.006 | 0.010 |
| ≥0.25 | ≤4 | No | 0.002 | 0.005 | 0.25 | 0.001 | 0.003 | 0.005 |
| ≥0.25 | ≥6 | No | 0.002 | 0.004 | 0.20 | 0.001 | 0.002 | 0.004 |
| ii. Shear wall coupling beams[c] | | | | | | | | |
| Longitudinal reinforcement and transverse reinforcement[d] | | $\frac{V}{t_w l_w \sqrt{f_c'}}$ | | 0.050 | | | | |
| Conventional longitudinal reinforcement with conforming transverse reinforcement | | ≤3 | 0.025 | 0.040 | 0.75 | 0.010 | 0.025 | 0.050 |
| | | ≥6 | 0.020 | 0.035 | 0.50 | 0.005 | 0.020 | 0.040 |
| Conventional longitudinal reinforcement with nonconforming transverse reinforcement | | ≤3 | 0.020 | 0.025 | 0.50 | 0.006 | 0.020 | 0.035 |
| | | ≥6 | 0.010 | 0.050 | 0.25 | 0.005 | 0.010 | 0.025 |
| Diagonal reinforcement | | NA | 0.030 | 0.050 | 0.80 | 0.006 | 0.030 | 0.050 |

[a]Linear interpolation between values listed in the table shall be permitted.
[b]A boundary element shall be considered confined where transverse reinforcement exceeds 75% of the requirements given in ACI 318 and spacing of transverse reinforcement does not exceed $8d_b$. It shall be permitted to take modeling parameters and acceptance criteria as 80% of confined values where boundary elements have at least 50% of the requirements given in ACI 318 and spacing of transverse reinforcement does not exceed $8d_b$. Otherwise, boundary elements shall be considered not confined.
[c]For coupling beams spanning <8 ft 0 in., with bottom reinforcement continuous into the supporting walls, acceptance criteria values shall be permitted to be doubled for LS and CP performance.
[d]Conventional longitudinal reinforcement consists of top and bottom steel parallel to the longitudinal axis of the coupling beam. Conforming transverse reinforcement consists of (a) closed stirrups over the entire length of the coupling beam at a spacing ≤ $d/3$, and (b) strength of closed stirrups $V_s \geq 3/4$ of required shear strength of the coupling beam.

Based on the recommendations of ASCE 41 (2013), the backbone curve given in Fig. 5.4 is generated for the beam-moment rotation response.

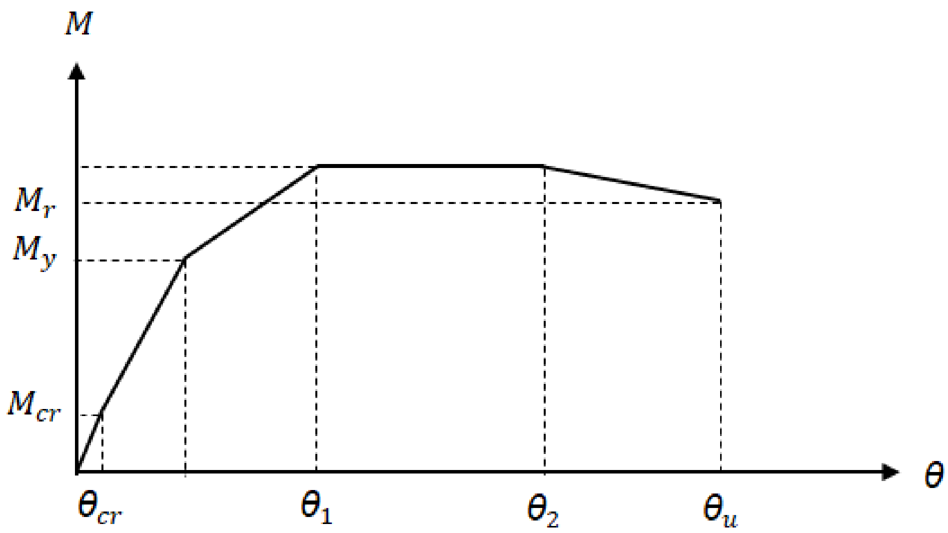


*Figure 5.4.* Moment-rotation backbone curve for beams

Five different regions are used to define the behavior of coupling beams. First region of the member response represents the uncracked behavior. The point where beam cracking results in the loss of stiffness is identified as the cracking point and denoted as $M_{cr}$, which is assumed to be 10% of the computed moment capacity. This additional point is considered to increase the accuracy of the predicted rigidity of a specimen.

After the primary cracks are formed in the member, although the stiffness does not reduce considerably, the beam starts to deviate from elastic behavior and continues to carry the load with increasing strength. This region ends at the point where the inelastic activity increases and crack maturation occurs and the stiffness loss of the beam becomes significant. Second performance point, which is defined as the point of inelasticity and denoted as $M_y$, is set equal to 70% of the computed moment capacity.

The third region represents the inelastic activity region where the stiffness of the beam is considerably reduced, although the strength of the beam is still increasing. The end point of this third region is denoted as $M_u$.

From the test results, it is observed that after reaching the maximum flexural capacity, $M_u$, remained almost constant through a transition region, where the tensile strength of reinforcing bars increase due to strain hardening and the tensile strength of high performance fiber reinforced composite decrease after the material reaches its peak tensile strength.

The last performance point is specified as the termination point of the descending region and the remaining moment is denoted by $M_r$. Although higher reduction in capacity is defined in ASCE 41-13 (2013), since fiber reinforced composites do not exhibit a sudden loss of strength, after some trial analytical runs, a 10% reduction in the beam moment capacity is used.

The rotation at cracking, $\theta_{cr}$, and yield rotation, $\theta_y$, are calculated from the following equations:

$$\theta_{cr} = \left(\frac{0.1\ M_u}{E_c I_g}\right) l_p \qquad (5-1)$$

$$\theta_y = \left(\frac{0.7\ M_u}{E_c\ I_{cr}}\right) l_p \qquad (5-2)$$

where, $I_g$ : gross moment of inertia of the section,

$M_u$ : ultimate moment capacity considered to be the moment capacity obtained by considering the predicted shear strength,

$E_c$ : elastic modulus,

$I_{cr}$ : cracked moment of inertia of the section,

$l_p$ : plastic hinge length.

$$l_p = \begin{cases} \frac{d}{2} & for\,\frac{a}{d} > 2.5 \\ 0.05\; l_n + \frac{0.1\, f_y\, d_b}{\sqrt{f_c'}} & for\,\frac{a}{d} \leq 2.5 \text{ (Berry et al., 2008)} \end{cases} \qquad (5-3)$$

where, $l_n$ : clear length of member,

$f_y$: yield strength of longitudinal bars,

$d_b$: bar diameter,

$f_c'$ : concrete compressive strength (MPa).

The resulting moment versus rotation relationships for conventionally reinforced fiber reinforced coupling beams (CCBs) and diagonally reinforced fiber reinforced coupling beams (DCBs) are given in Fig. 5.5.

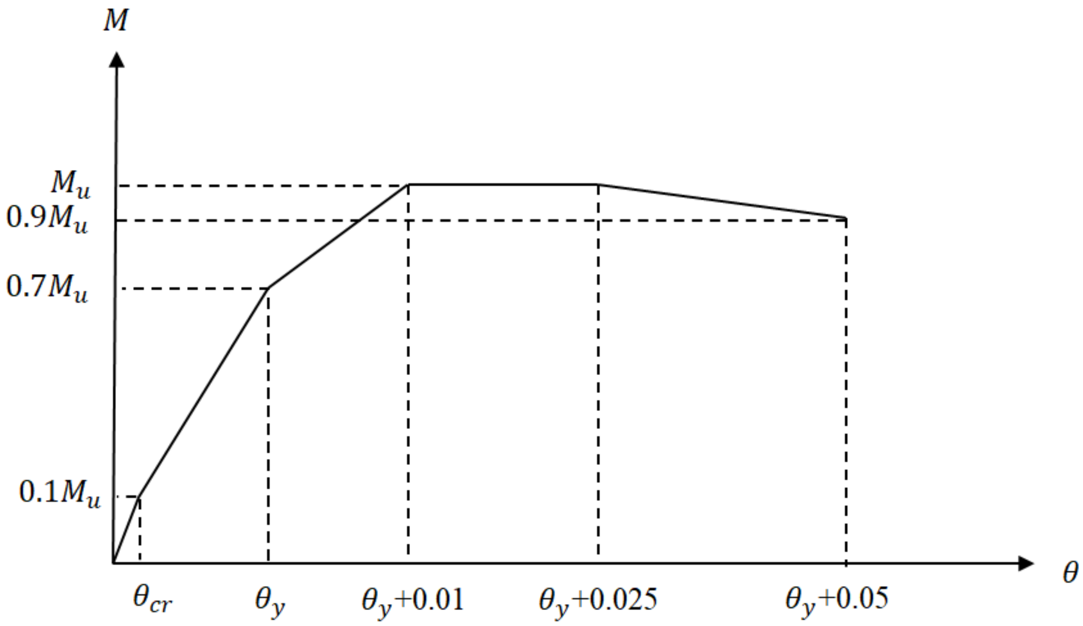


a) Moment-rotation relationship for CCBs.

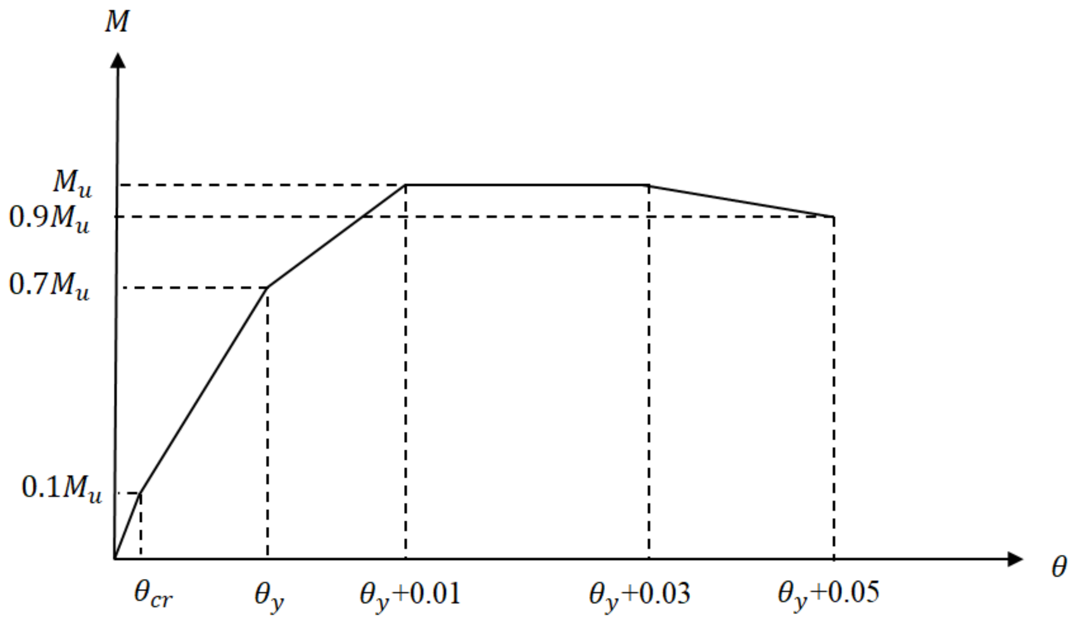


b) Moment-rotation relationship for DCBs

*Figure 5.5.* Moment versus rotation relationships for coupling beams

### 5.2.2. Modulus of Elasticity

The accuracy of modeling members, the behavior of which are controlled by flexure depends on defining a realistic flexural rigidity, $E_c\, I$, where $E_c$ is elastic modulus of concrete and $I$ is the moment of inertia.

ACI 318-14 provides two different formulations for the concrete modulus of elasticity. The first equation is:

$$E_c = w_c^{1,5}\ 33\sqrt{f_c'} \qquad (psi) \qquad (5-4)$$

where, $w$ is the unit weight of concrete in $lb/ft^3$. This equation was derived from short-time tests on concrete and systematically overestimates $E_c$ in regions where low modulus aggregates are prevalent.

The second equation used for normal-weight concrete is:

$$E_c = 57000\sqrt{f_c'} \qquad (psi) \tag{5-5}$$

Wafa (1990) stated that, modulus of elasticity of fiber reinforced composites increases with increasing fiber content. It was reported that for each 1% increase in fiber content by volume there is an increase of 3% in the modulus of elasticity. Moreover, Naaman (1987) proposed the following equation to predict the upper bound elastic modulus of FRC.

$$E_c = E_m V_m + E_f V_f \tag{5-6}$$

where, $E$ is the elastic modulus, $V$ is volume fraction, and the subscripts $c, m$, and $f$ represent the composite, matrix, and fiber, respectively.

In the current study, second formulation of ACI 318-14 is adopted in SI units as follows:

$$E_c = 4750\sqrt{f_c'} \qquad (MPa) \tag{5-7}$$

### 5.2.3. Moment of Inertia

As mentioned earlier, the accuracy of a nonlinear model depends on defining a realistic flexural rigidity, so moment of inertia plays an important role in modeling. Under seismic loading, cracks are formed in the coupling beams and the rigidity of member reduces. As the applied load increases crack lengths and widths will also increase and the member stiffness continues to reduce. For this reason, it is important to estimate a realistic cracked stiffness ($I_{cr}$) value for the member.

ACI 318-14 recommends taking the cracked flexural rigidity of beams as $0.35\ E_c I_g$ in seismic design, and recommended Eqn. 5-8 for the effective stiffness. ASCE 41-13 (2013) uses a lower value for the cracked flexural rigidity equal to 0.3 $E_c I_g$.

$$I_e = (0.1 + 25\rho_s)\left(1.2 - 0.2\frac{b}{d}\right) I_g \leq 0.5\ I_g \qquad (5-8)$$

where, $\rho_s$: longitudinal reinforcement ratio,

$b$ : web width,

$d$ : effective depth,

$I_g$ : gross moment of inertia.

The New Zealand standard (NZS 3101, 1995) provides different equations for conventionally reinforced coupling beams (CCBs) and diagonally reinforced coupling beams (DCBs). The effective stiffness of CCBs is considered to be only a function of the member aspect ratio (Eqn. 5-9), whereas, for DCBs the expected ductility demand is also taken into account (Eqn. 5-10).

$$I_e = \frac{0.4\ I_g}{1+8\left(\frac{d}{l}\right)^2} \qquad (5-9)$$

$$I_e = \frac{A\, I_g}{B + C\left(\frac{d}{l}\right)^2} \tag{5-10}$$

In the above equation, the coefficients A, B, and C vary with damping, μ. For $\mu = 1.5$; $A = 1.0$, $B = 1.7$, and $C = 1.3$. For $\mu = 6.0$; the parameters are considered as $A = 0.4$, $B = 1.7$, and $C = 2.7$. Linear interpolation should be used in between these values.

Paulay and Priestley (1992) proposed Eqn. 5-11 to compute $I_e$ of CCBs with effective depth, $d$, and clear span, $l$, and Eqn. 5-12 for DCBs.

$$I_e = \frac{0.2\, I_g}{1 + 3\left(\frac{d}{l}\right)^2} \tag{5-11}$$

$$I_e = \frac{0.4\, I_g}{1 + 3\left(\frac{d}{l}\right)^2} \tag{5-12}$$

Taranath (1997) considered the effect of Poisson's ratio, $\nu$, in the calculation of the effective stiffness, $I_e$, for reinforced concrete coupling beams:

$$I_e = \frac{I_g}{1 + 2.4\left(\frac{d}{l}\right)^3 (1+\nu)} \tag{5-13}$$

Vu et al. (2014) proposed the following equations to estimate $I_e$ for CCBs (Eqn. 5-14) and DCBs (Eqn. 5-15).

$$\kappa_{CCB} = \frac{I_e}{I_g} = 0.67\left(1.8\frac{l}{d} + 0.4\frac{l^2}{d^2}\right)(0.9 + 0.7\rho_v + 1.1\rho_s)\left(0.5 + \frac{11}{f_c'}\right) \qquad (5-14)$$

$$\kappa_{DCB} = \frac{I_e}{I_g} = 0.65\left(1.6 + 0.9\frac{l}{d}\right)(0.4 + 1.7\rho_{sd})\left(0.7 + \frac{14}{f_c'}\right) \qquad (5-15)$$

where, $\kappa_{CCB}$ : dimensionless stiffness factor for CCBs,

$\kappa_{DCB}$ : dimensionless stiffness factor for DCBs,

$I_e$ : effective moment of inertia,

$I_g$ : gross moment of inertia,

$l$ : length of the coupling beam,

$d$ : effective depth of the coupling beam,

$\rho_v$ : transverse reinforcement ratio,

$\rho_s$ : longitudinal reinforcement ratio,

$\rho_{sd}$ : diagonal reinforcement ratio,

$f_c'$ : concrete compressive strength.

Based on the test results, Naish (2010) found out that $0.2\,EI$ should be used as the cracked rigidity of coupling beams. Lequesne (2011) tested three HPFRC coupling beams that have $l_n/h$ ratios of 1.75 and also recommended to use a cracked rigidity of 0.2 $EI$. Furthermore, Setkit (2012) reported that the cracked rigidity varied between $0.13 - 0.2\,EI$ for HPFRC precast coupling beams with $l_n/h$ ranging between 2.75 and 3.3. However, it should be noted that these proposed flexural rigidity values also include the effect of slip/extension between the coupling beam and the reinforced concrete wall.

The contribution of slip/extension to the yield rotation, $\theta_y$, can also be estimated by following the methodology developed by Alsiwat and Saatcioglu (1992), where the crack width that develops at the beam-wall interface depends on bar slip and bar extension in terms of strains.

$$u_e = u_{ACI} = \frac{f_y\, d_b}{4\, l_d} \tag{5-16}$$

$$l_d = \frac{400\, A_b}{K\sqrt{f_c'}} \frac{f_y}{400} 300 \qquad (mm) \tag{5-17}$$

$$L_e = \frac{f_s d_b}{4\, u_e} \tag{5-18}$$

$$u_u = \left(20 - \frac{d_b}{4}\right)\sqrt{\frac{f_c'}{30}} \tag{5-19}$$

$$\delta_{s1} = \sqrt{\frac{30}{f_c'}} \tag{5-20}$$

$$\delta_s = \delta_{s1}\left(\frac{u_e}{u_u}\right)^{2.5} \tag{5-21}$$

$$\delta_{exty} = 1.25\, \varepsilon_y\, \frac{L_e}{2} \tag{5-22}$$

$$\delta_{total} = \delta_s + \delta_{exty} \tag{5-23}$$

$$\theta = \frac{\delta_{total}}{d-c} \tag{5-24}$$

where, $u_e$ : elastic bond stress,

$d_b$ : reinforcing bar diameter,

$A_b$ : tension reinforcement area,

$K$ : factor to take into account confinement and bar spacing (recommended to be taken as $3d_b$),

$L_e$ : length of the elastic region,

$u_u$ : peak bond stress,

$\delta_{s1}$ : local slip at peak bond stress,

$\delta_s$: slip of the reinforcement,

$\delta_{exty}$: extension of the reinforcement at yield,

$\delta_{total}$: total displacement of the reinforcement at yield,

$\theta$: angle of the crack that opens at the beam-wall interface due to the slip/extension of the bar at yield,

$d$ : effective depth,

$c$ : depth of the compressive stress block.

The cracked moment of inertia which included the slip calculated using the slip-extension formulae of Alsiwat and Saatcioglu (1992) are significantly similar with the values computed by using the formulae of Paulay and Priestley (1992) for $l_n/d > 2.5$. The resulting cracked rigidities computed by Alsiwat and Saatcioglu (1992) equations range between 0.2-0.22 for $l_n/d > 2.5$. However, these formulae give unrealistically low rigidity values between 0.08 and 0.14 for $l_n/d \leq 2.5$.

In order to decide which cracked rigidity assumption works best with the developed model, Specimen CB-1 ($l_n/h$ = 1.75) tested by Lequesne (2011) and Specimen CB-6 ($l_n/h = 2.75$) tested by Setkit (2012) are analyzed considering cracked rigidity equal to 0.2 $E_cI_g$, 0.25 $E_cI_g$, and 0.3 $E_cI_g$. For these specimens, the cracked rigidity computed by considering slip–anchorage action is significantly low; 0.09 and 0.16 for Specimens CB-1 and CB-6, respectively. Even when the cracked rigidity is considered to be 0.2 $E_cI_g$, the member becomes too flexible, therefore, these lower values are not used in the analyses. In Fig. 5.6, the obtained shear stress vs. drift responses for Lequesne, Specimen CB-1are presented for different flexural rigidities. As it can be observed from the figures, member stiffness is underestimated by the model, when the cracked rigidity is considered to be $0.2\,E_cI_g$ or $0.25\,E_cI_g$. Fig. 5.7 shows the shear stress vs. drift relationships for Setkit, Specimen CB-6. Since this specimen has a higher shear clear span-to-depth ratio, the use of different cracked rigidities does not affect the behavior as much as the specimen with lower $l_n/h$.

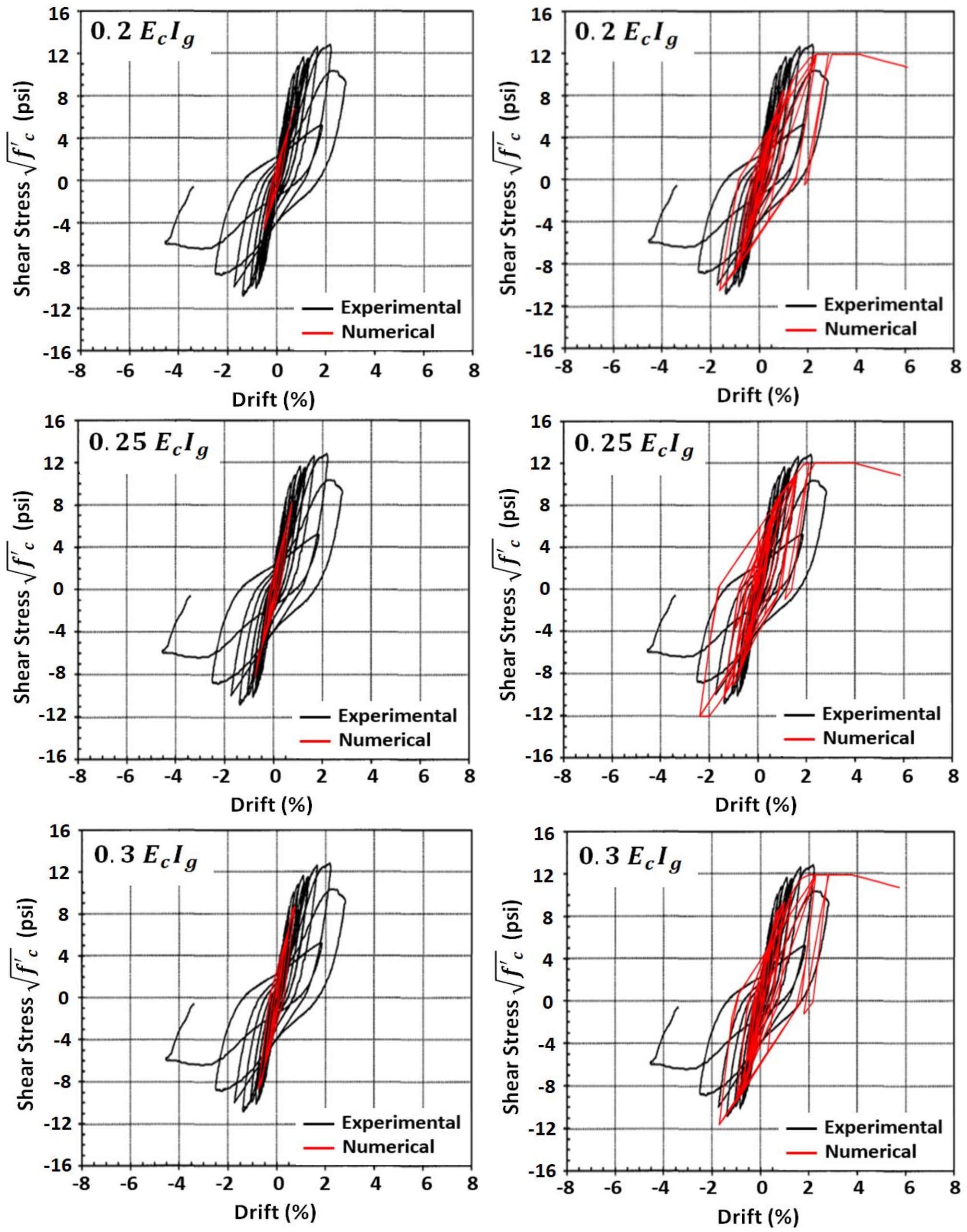


*Figure 5.6.* Shear stress vs. drift response for Specimen CB-1 (Lequesne, 2011)

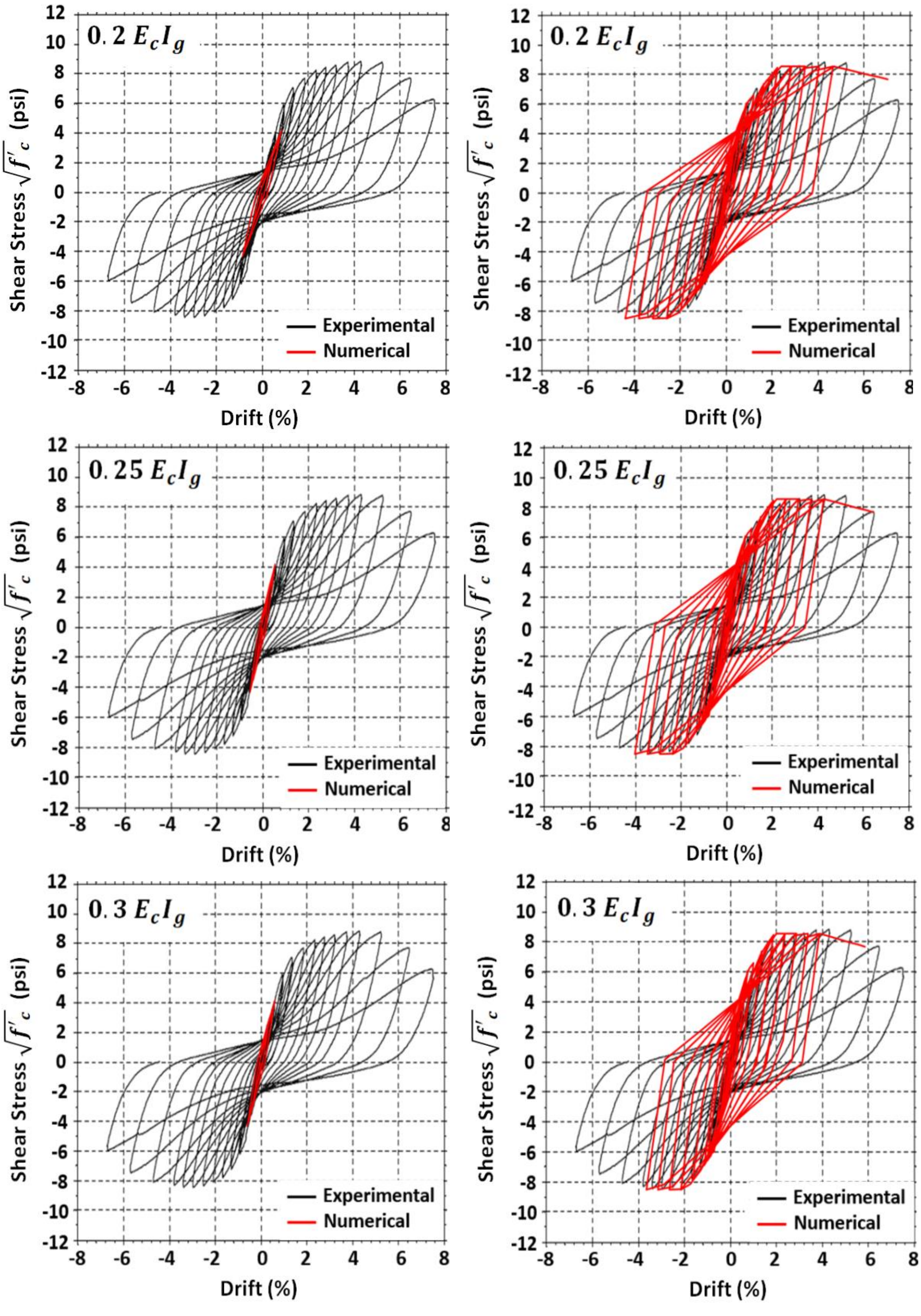


*Figure 5.7.* Shear stress vs. drift response for Specimen CB-6 (Setkit, 2012)

### 5.3. Analytical Verification of the Proposed Model

In order to verify the accuracy of the proposed model, the results obtained from pushover analysis of subassemblies using ETABS 17 (2017) are compared with the experimental results. In all the comparison graphs, analytical results are shown with red straight lines. The graphs on the left are provided to investigate whether the selected cracked rigidity of the beams matches with the experimental rigidity. The graphs on the right present the comparison of the overall behavior. The envelope curves are also provided at the bottom to clarify the comparison.

#### 5.3.1. Specimens of Setkit (2012)

Setkit (2012) evaluated the use of high-performance fiber reinforced composites to reduce or totally eliminate the need for diagonal and transverse reinforcement. For this purpose, five precast coupling beams were tested under large displacement reversals. The considered parameters were the coupling beam shear span-to-depth ratio (2.75 and 3.3) and the contribution of diagonal reinforcement to shear strength. All specimens had 1.5% volume fraction of hooked steel fibers with aspect ratio of 80. Beam width kept constant for all specimens.

*Specimen CB-1*

The first specimen has a clear span-to-depth ratio of 2.75 and a composite compressive strength of 49.6 MPa. The beam depth is 609 mm. There are two layers of main flexural bars at the bottom and top, two groups of diagonal reinforcement with two layers of bars in each group, transverse reinforcement, dowel bars, and longitudinal bars at nearly mid-depth of the beam. The main difference of this specimen with the others in this series is that this one has more reinforcement at the bottom and top of the beam and low aspect ratio (Fig. 5.8). Shear stress vs. drift response of the specimen is shown in Fig. 5.9. The predicted initial rigidity is close to that of the specimen. The ultimate moment capacity, strength and stiffness degradation, and the overall behavior are also predicted with adequate accuracy, being on the conservative side.

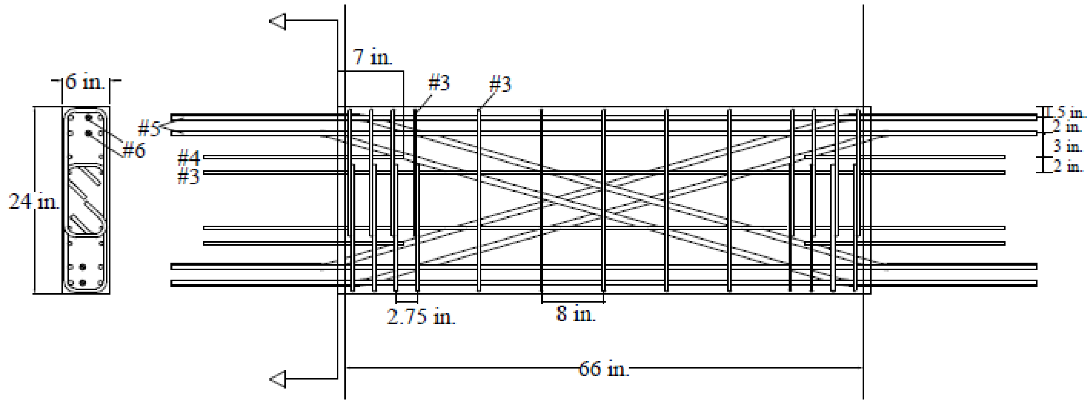


*Figure 5.8.* Reinforcement detailing of Specimen CB-1

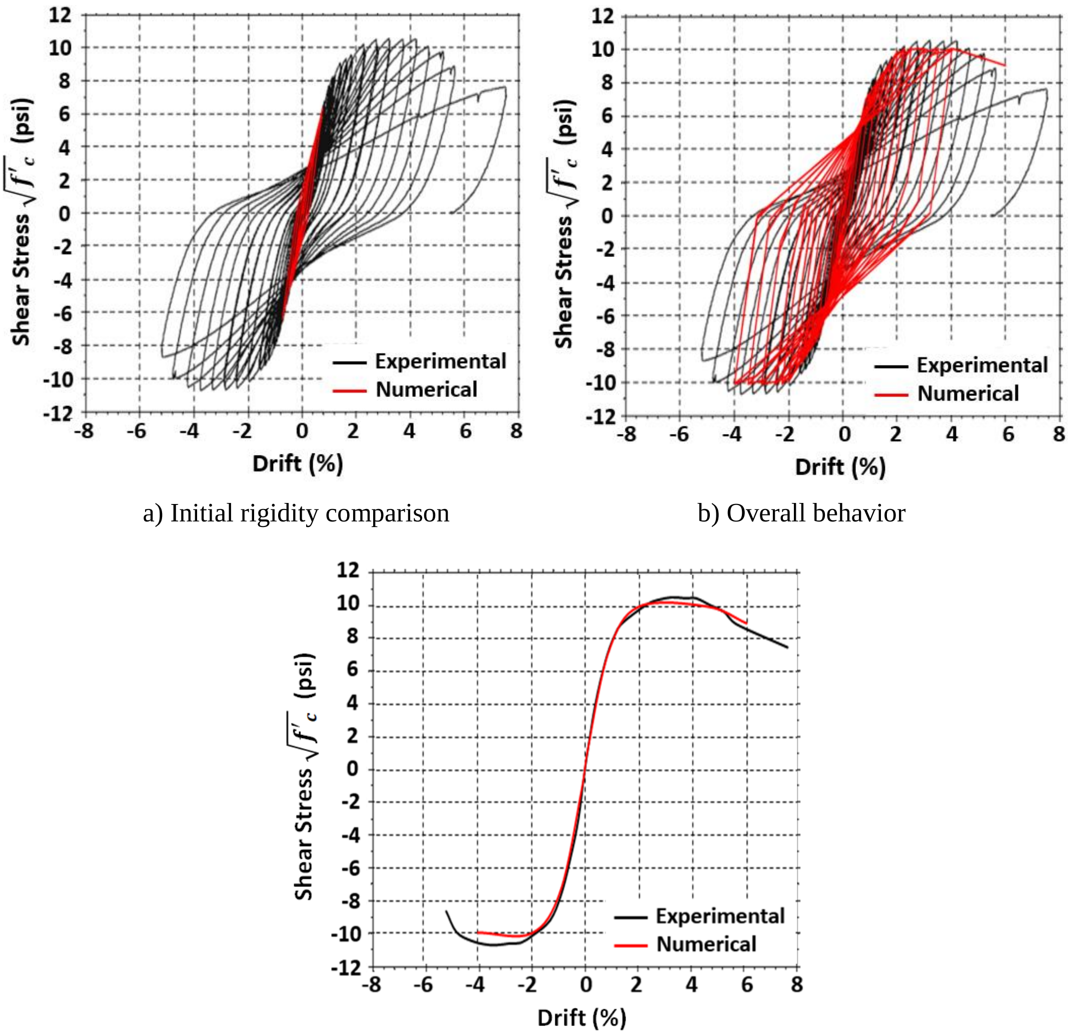


a) Initial rigidity comparison

b) Overall behavior

c) Envelope curve

*Figure 5.9*. Shear stress vs. drift response of Specimen CB-1

*Specimen CB-2*

This specimen with a clear span-to-depth ratio of 2.75 has a composite compressive strength of 59 MPa. and a beam depth of 609 mm. The reinforcement detailing is provided as one layer of main flexural bars at the bottom and top, two groups of diagonal reinforcement with two layers of bars in each group, transverse reinforcement, U-shaped dowel bars, and longitudinal bars at nearly mid-depth of the beam (Fig. 5.10). Shear stress vs. drift response of the specimen is shown in Fig. 5.11. The analytical model seems to work conservatively for this specimen as well. However, the strength degradation at failure is underestimated.

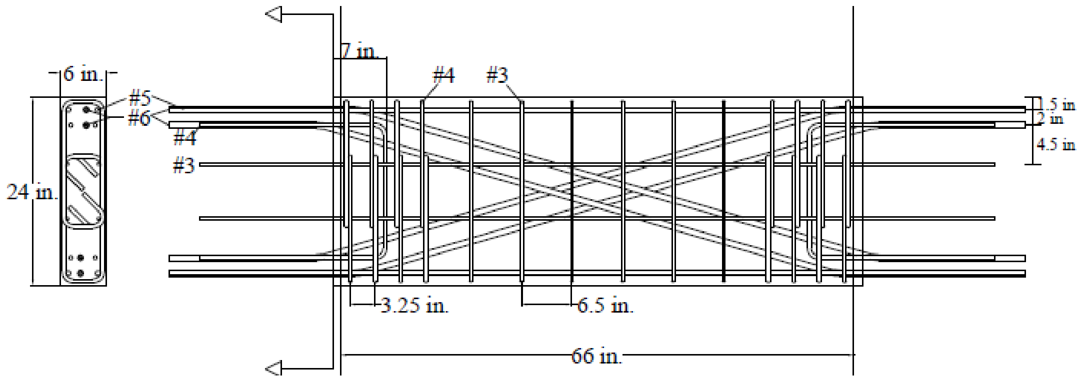


*Figure 5.10.* Reinforcement detailing of Specimen CB-2

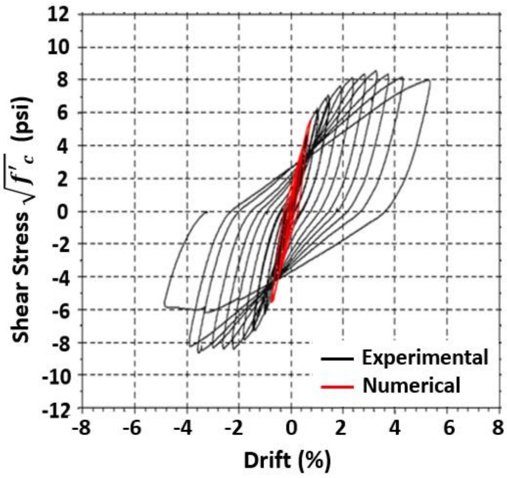


a) Initial rigidity comparison

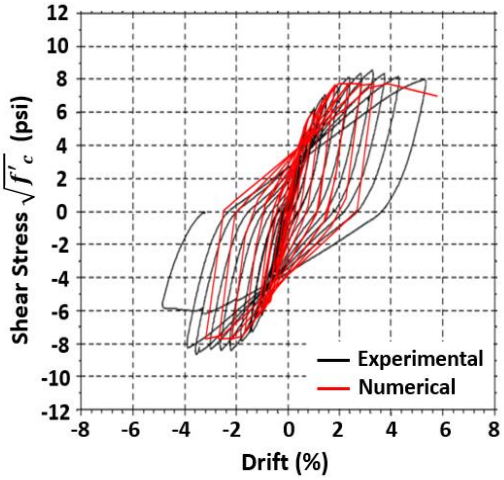


b) Overall behavior

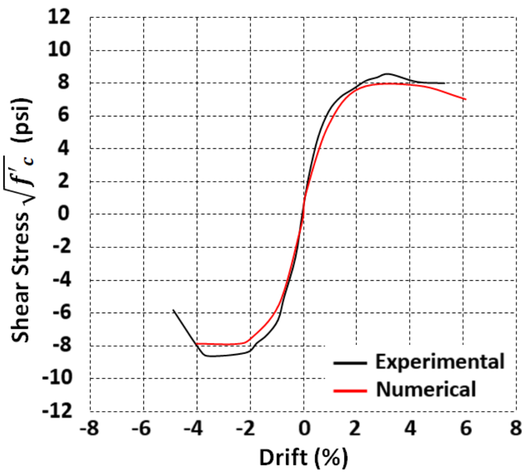


c) Envelope curve

*Figure 5.11.* Shear stress vs. drift response of Specimen CB-2

*Specimen CB-3*

This specimen has a clear span-to-depth ratio of 3.3, composite compressive strength of 61 MPa., and a beam depth of 508 mm. The reinforcement detailing is provided as one layer of main flexural bars at the bottom and top, two groups of diagonal reinforcement with two layers of bars in each group, transverse reinforcement, U-shaped dowel bars, and longitudinal bars at nearly mid-depth of the beam (Fig. 5.12). This specimen has a shallower depth and a higher aspect ratio. Fig. 5.13 indicates that the predicted capacity is lower than the experimental results for this specimen, but the maximum expected drift matches the results.

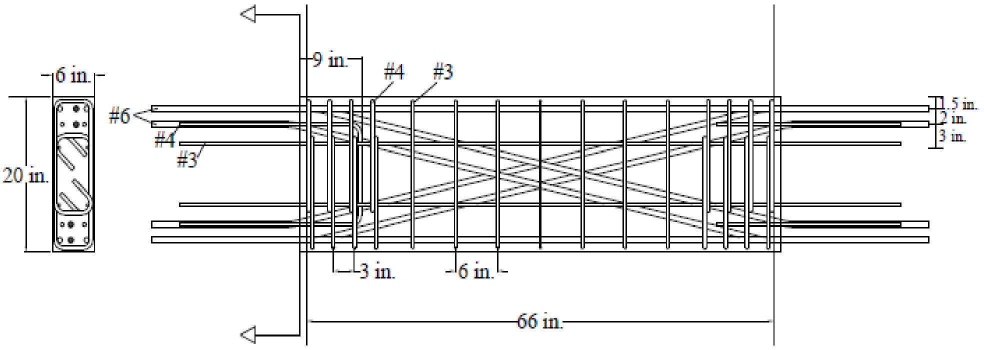


*Figure 5.12.* Reinforcement detailing of Specimen CB-3

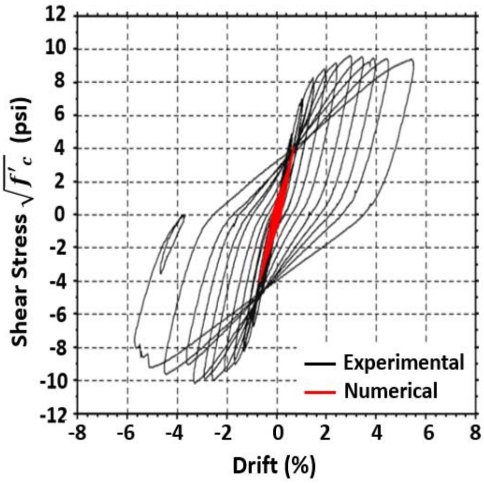


a) Initial rigidity comparison

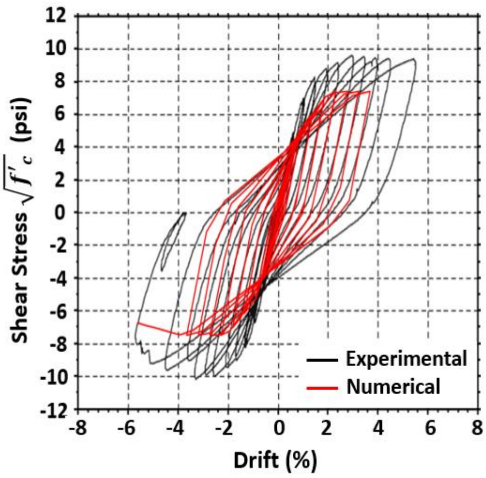


b) Overall behavior

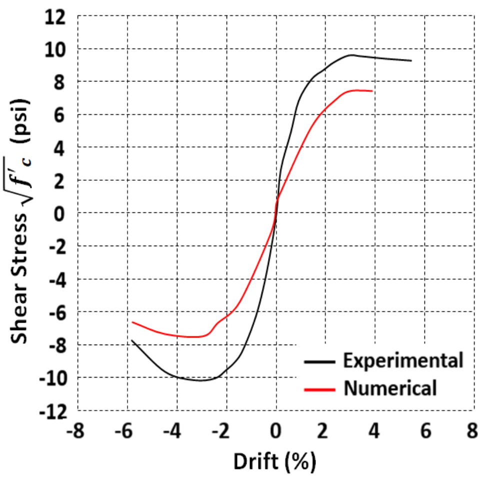


c) Envelope curve

Figure 5.13. Shear stress vs. drift response of Specimen CB-3

*Specimen CB-5*

Specimen CB-4 is not analyzed, since it was a reinforced concrete control beam. Specimen CB-5 ($l_n/h = 3.3$) has a composite compressive strength of 68 MPa. and a beam depth of 508 mm. The reinforcement detailing is provided as one layer of main flexural bars at the bottom and top, transverse reinforcement, U-shaped dowel bars, and longitudinal bars at nearly mid-depth of the beam (Fig. 5.14). Although, the strength of this specimen is not significantly different from CB-3; since there are no diagonal bars, the initial rigidity is lower and higher drift ratios are observed for this specimen. The analytical response of Specimen CB-5 shown in Fig. 5.15, has higher strength and stiffness degradation when compared to the experimental results due to the absence of diagonal reinforcement.

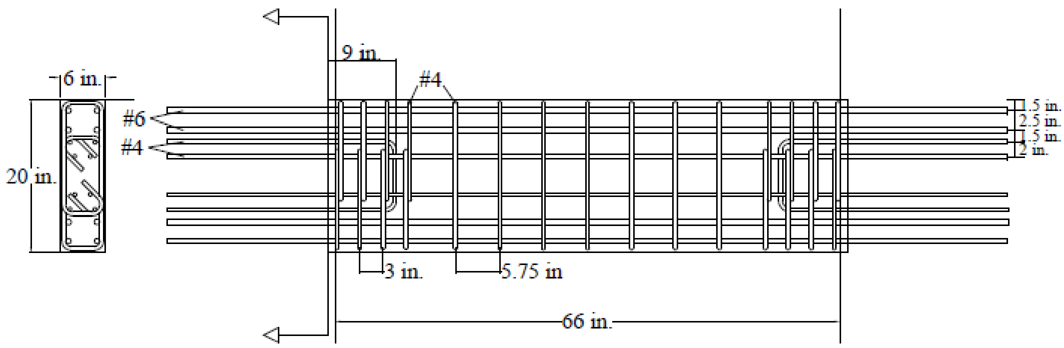


*Figure 5.14.* Reinforcement detailing of Specimen CB-5

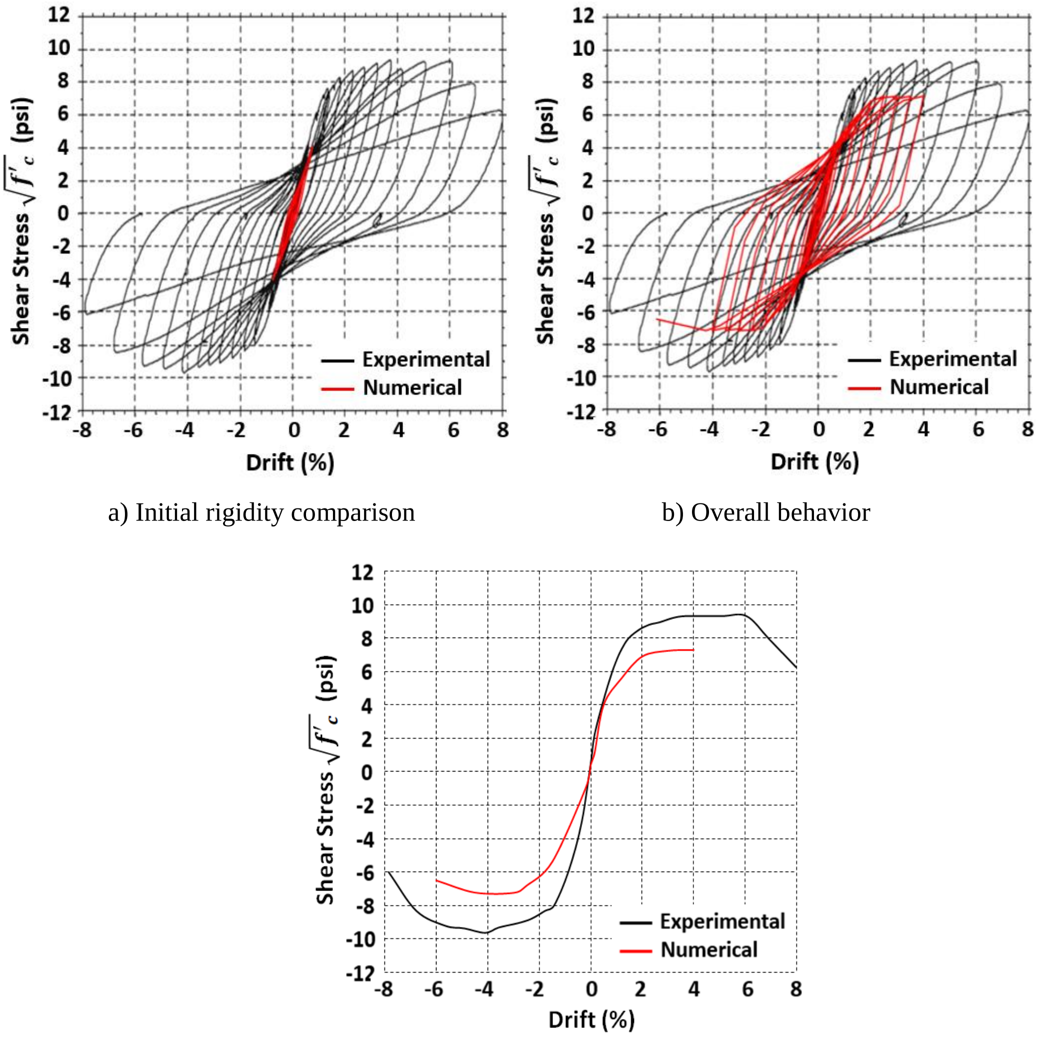


a) Initial rigidity comparison

b) Overall behavior

c) Envelope curve

*Figure 5.15.* Shear stress vs. drift response of Specimen CB-5

*Specimen CB-6*

The final specimen has an aspect ratio of 2.75, composite compressive strength of 67.6 MPa, and a beam depth of 609 mm. The reinforcement detailing of this specimen is the similar to that of Specimen CB-5 (Fig. 5.16). The analytical results given in Fig. 5.17 are in reasonable conformity with the test results, although this specimen has no diagonal reinforcement either. This indicates that the prediction equation worked better for deeper beams.

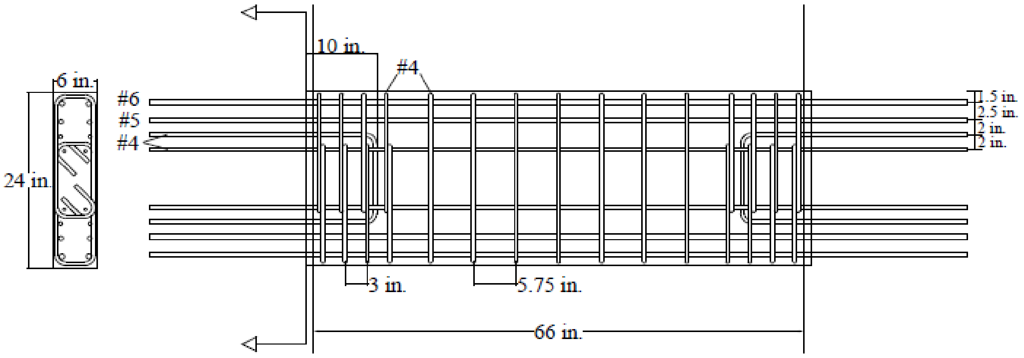


*Figure 5.16.* Reinforcement detailing of Specimen CB-6

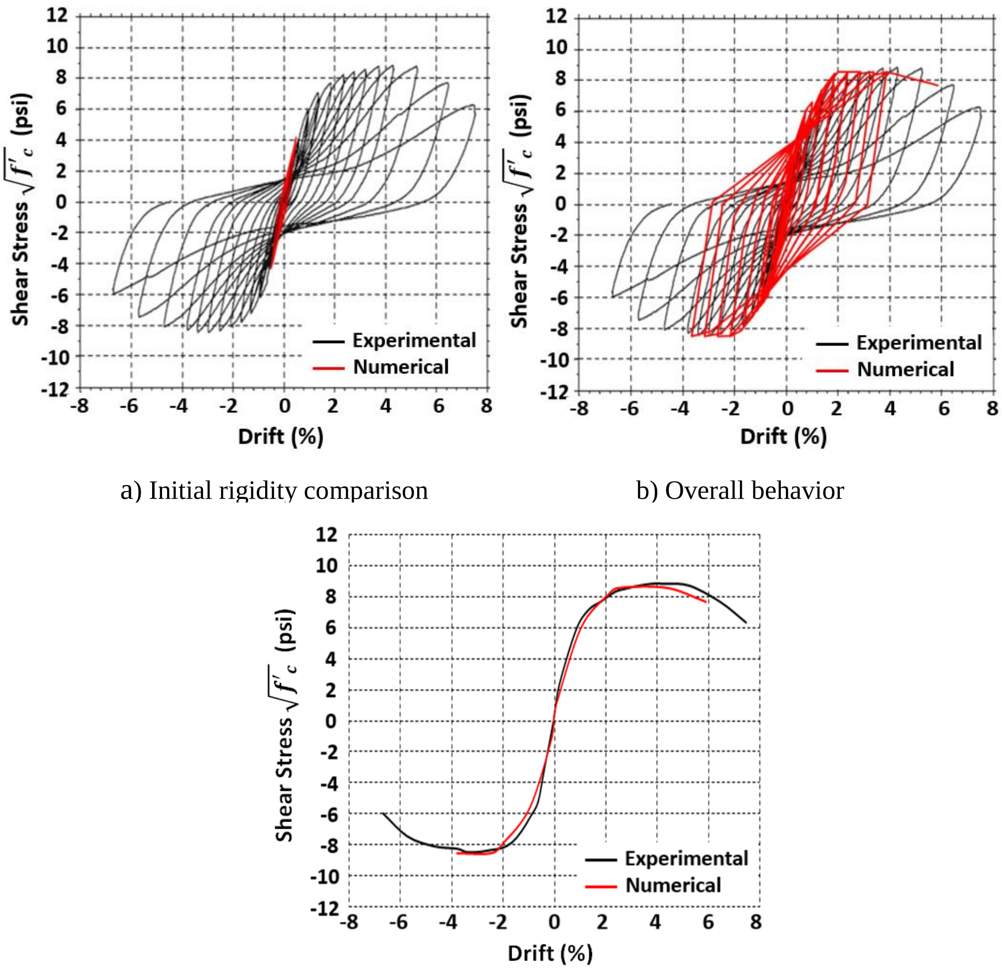


a) Initial rigidity comparison

b) Overall behavior

c) Envelope curve

*Figure 5.17.* Shear stress vs. drift response of Specimen CB-6

### 5.3.2. Specimens of Lequesne et al. (2011)

Three large scale precast coupling beam subassemblies with clear span-to-depth ratios of 1.75 were subjected to reversed cyclic loading. Main difference in between the specimens is the connection of the beams to the reinforced concrete walls by using different dowel detailing. Hooked steel fibers are used in the composite with a 1.5% volume fraction and have an aspect ratio of 80. Beam sizes and reinforcement layouts for both longitudinal and diagonal reinforcements kept the same for all specimens.

Shear stress vs. drift responses of specimens are shown in Figs. 5.19, 5.21 and 5.23. For all specimens, ultimate moment capacity and initial rigidity are reasonable when compared with test results. In Specimen CB-3 (Fig. 5.22), in addition to lowering the transverse reinforcement ratio by 25%, straight dowel bars were placed across the beam-to-wall interface to enable plastic hinging to occur within the beam, replacing the U-shaped dowel bars used in Specimens CB-1 and CB-2 (Figs. 5.18, 5.20). It was reported that, in the third specimen, the beam experienced slip and the response of Specimen CB-3 was dominated by flexural rotations at the ends of the coupling beam. The proposed model would have given more accurate results, if the rigid end-zone factor was taken below 0.5. However, the detailing of the connection regions is not a parameter investigated in this study and semi-rigid connections are considered for all the subassemblies without any modifications. Therefore, the strength and stiffness degradation and high drift ratios observed in Specimen CB-3 cannot be predicted precisely, although the observed ultimate drift level is close to the experimental value.

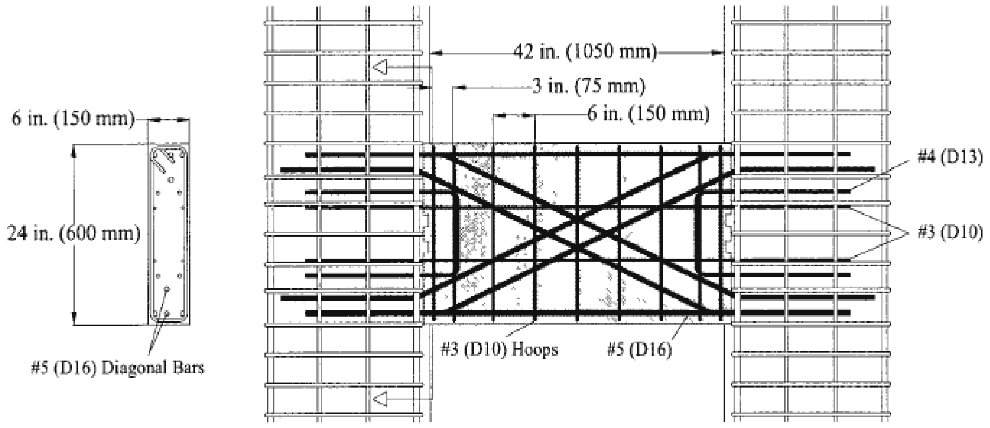


*Figure 5.18.* Reinforcement detailing of Specimen CB-1

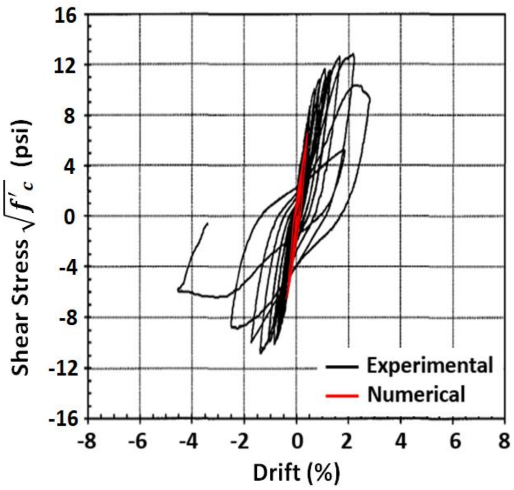


a) Initial rigidity comparison

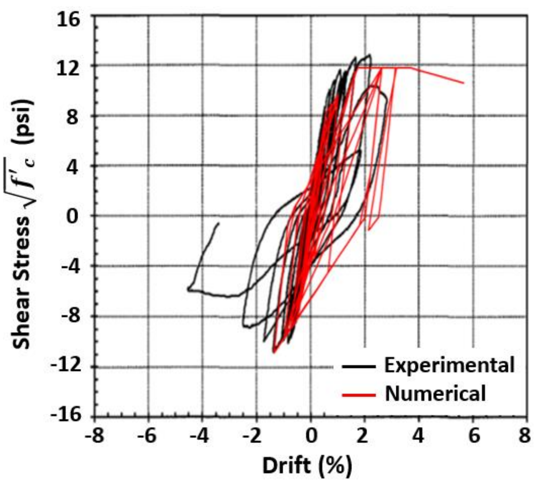


b) Overall behavior

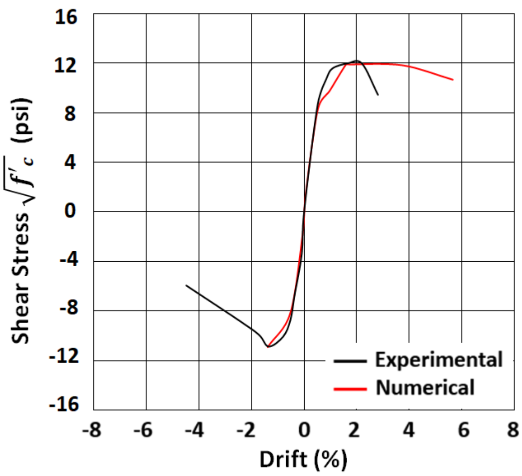


c) Envelope curve

*Figure 5.19.* Shear stress vs. drift response of Specimen CB-1

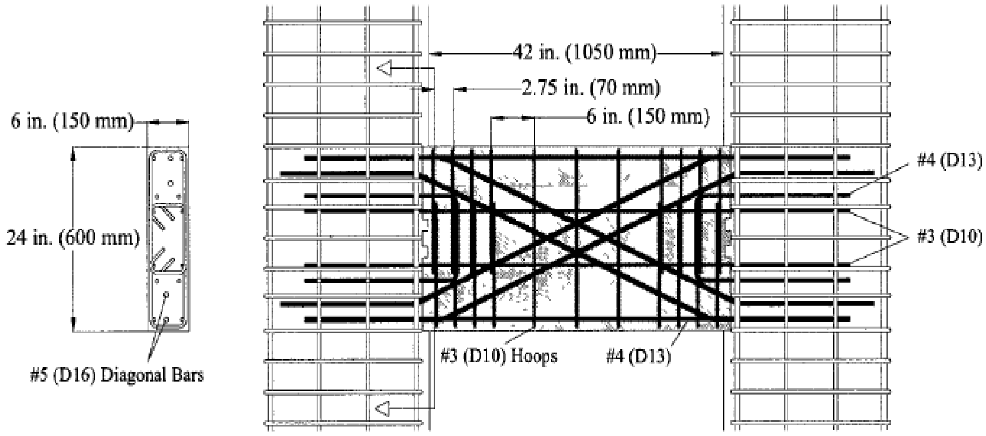


*Figure 5.20*. Reinforcement detailing of Specimen CB-2

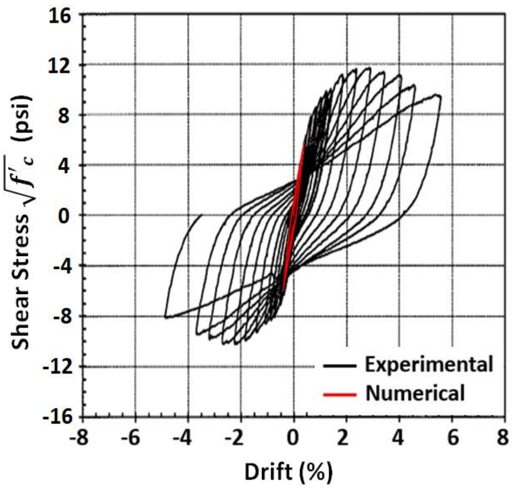


a) Initial rigidity comparison

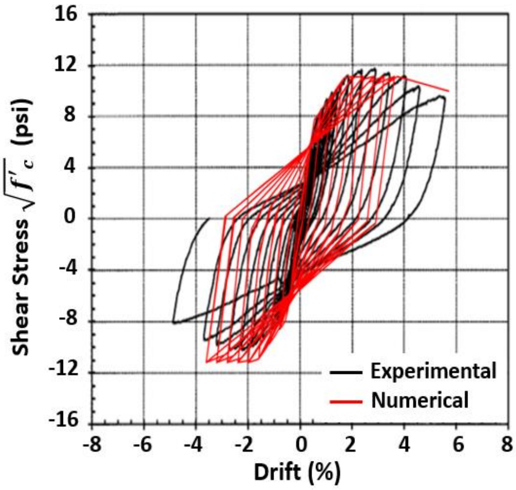


b) Overall behavior

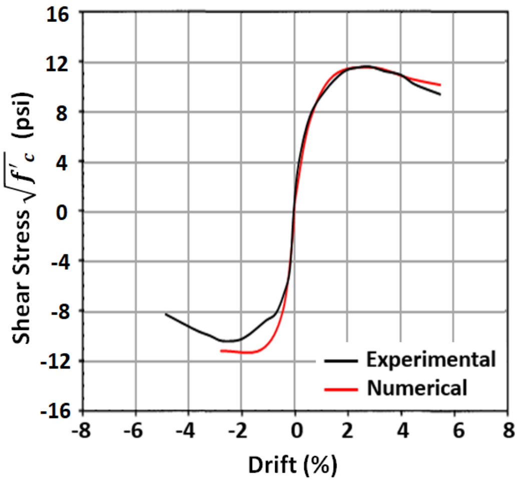


c) Envelope curve

*Figure 5.21*. Shear stress vs. drift response of Specimen CB-2

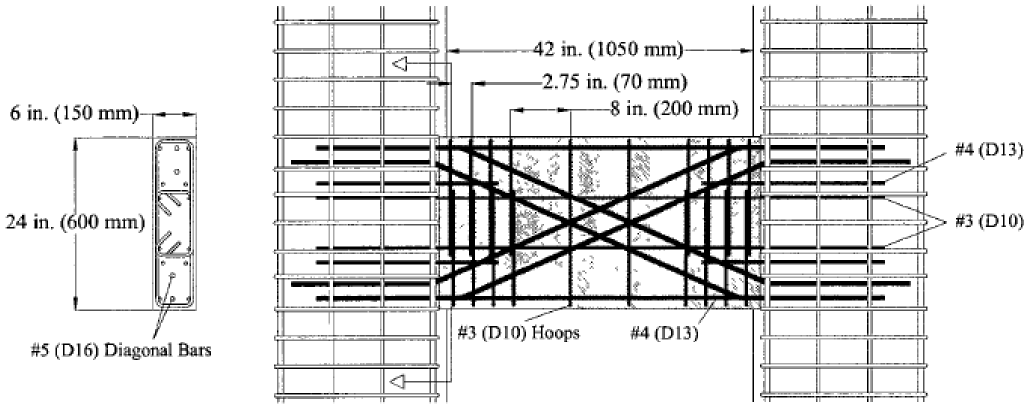


*Figure 5.22*. Reinforcement detailing of Specimen CB-3

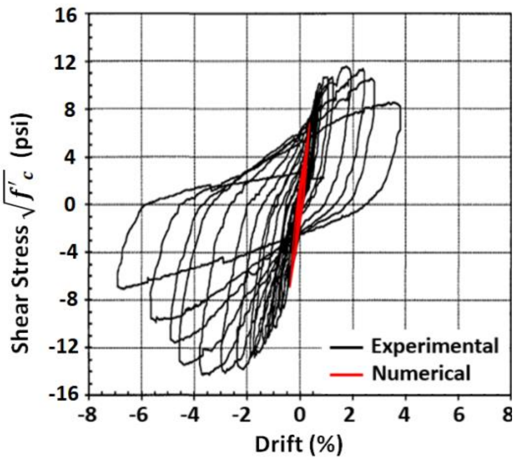


a) Initial rigidity comparison

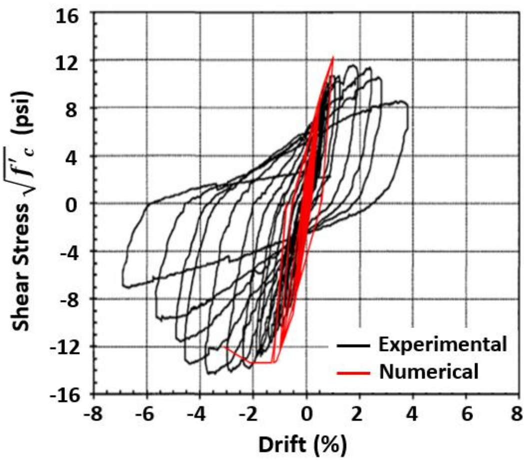


b) Overall behavior

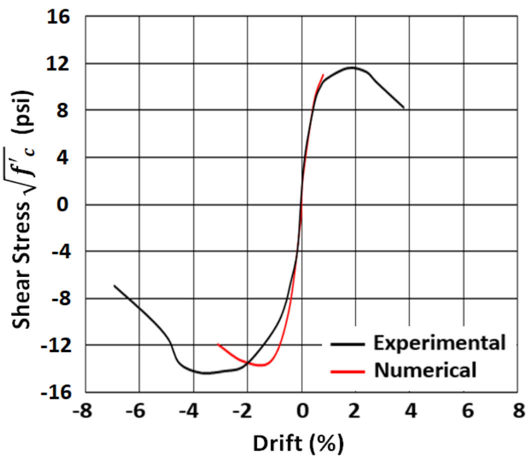


c) Envelope curve

*Figure 5.23*. Shear stress vs. drift response of Specimen CB-3

### 5.3.3. Specimens of Canbolat et al. (2005)

High performance fiber reinforced composite subassemblies of Canbolat et al. (2005) are $3/4$ scale with 1.0 clear span-to-depth ratio. The main experimental variables are the fiber type and reinforcement detailing. In Specimen 2 and Specimen 3, 2.0% volume fraction of spectra fiber was used. In Specimen 4, torex steel fiber with a volumetric ratio of 1.5% was used. Specimen 2 is conventionally reinforced coupling beam (Fig. 5.24) and others are diagonally reinforced coupling beams (Figs. 5.26, 5.28). The comparisons of experimental and analytical results are given in Figs. 5.25, 5.27, 5.29. For Specimen 2, it was reported that all the reinforcing bars remained elastic up to 1.5% and strength loss occurred when major diagonal cracks are formed at approximately 2.0% drift. Although the capacity is estimated well for this specimen, the initial rigidity is higher than the experimental one and strength degradation cannot be captured. For Specimens 3 and 4 similar problems are observed in the analytical response. This indicates that the diagonal reinforcement detailing is as important as its amount in predicting the strength and stiffness degradation.

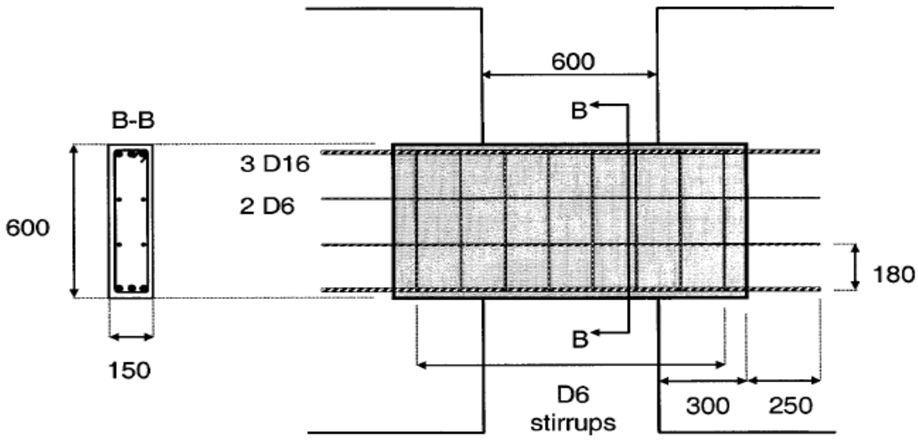


*Figure 5.24.* Reinforcement detailing of Specimen 2

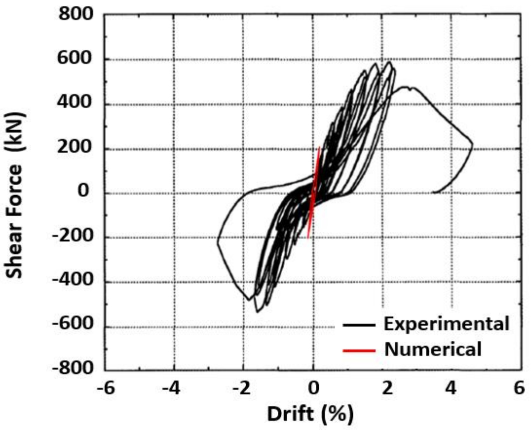


a) Initial rigidity comparison

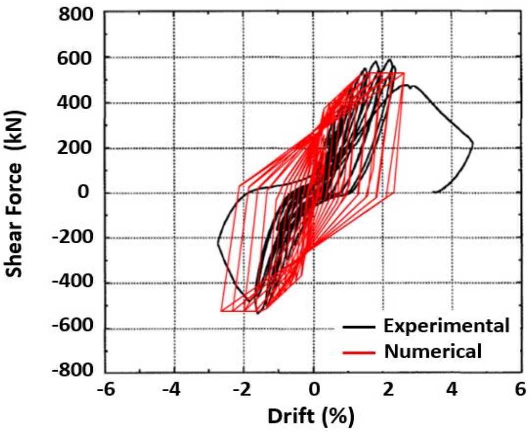


b) Overall behavior

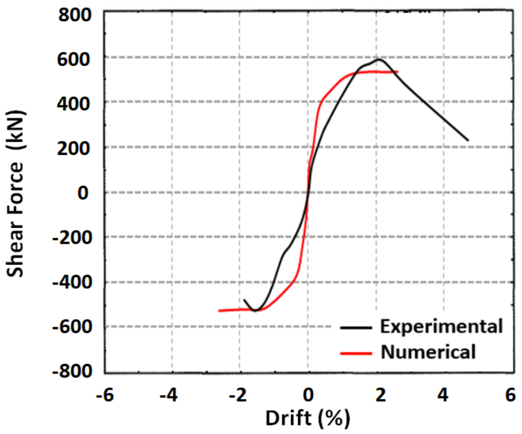


c) Envelope curve

*Figure 5.25.* Shear stress vs. drift response of Specimen 2

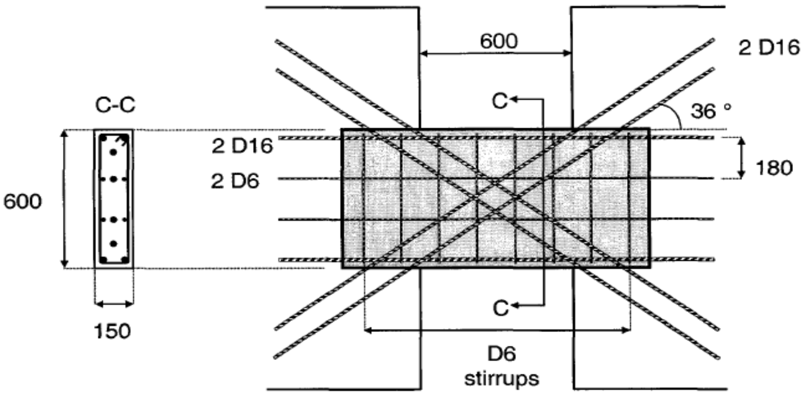


Figure 5.26. Reinforcement detailing of Specimen 3

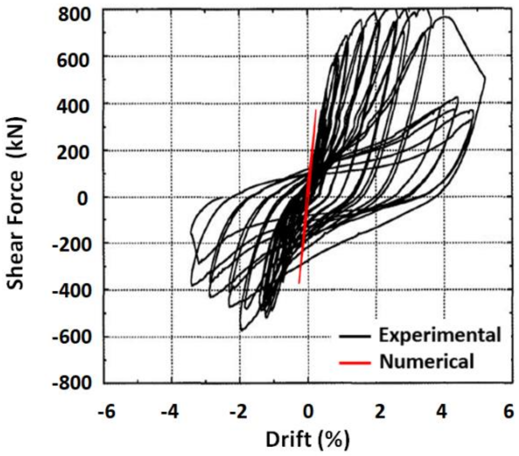


a) Initial rigidity comparison

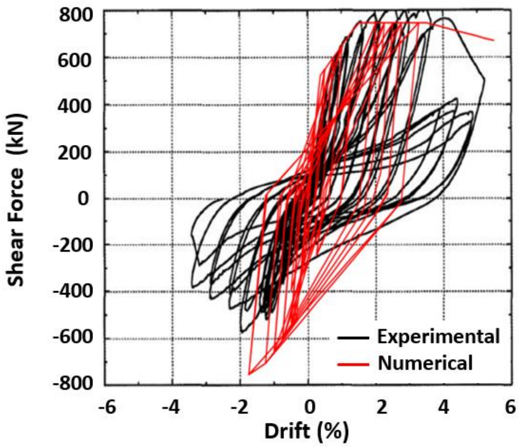


b) Overall behavior

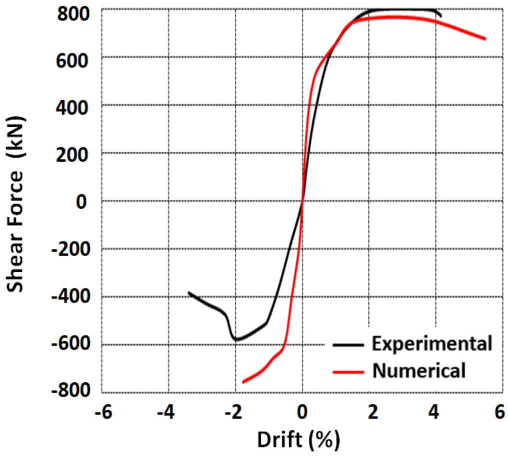


c) Envelope curve

*Figure 5.27.* Shear stress vs. drift response of Specimen 3

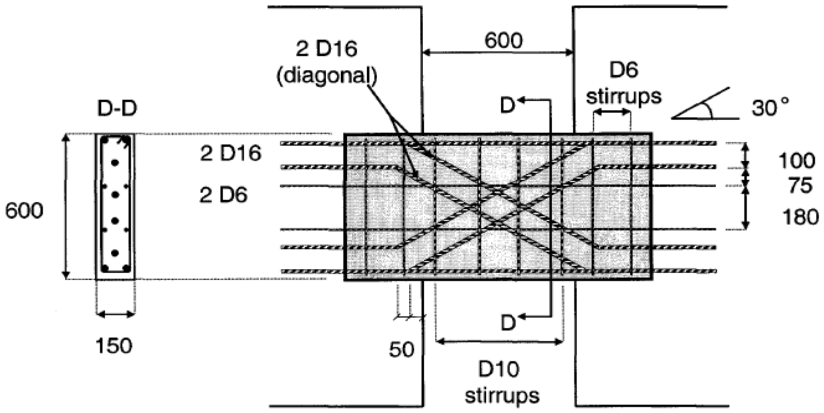


*Figure 5.28.* Reinforcement detailing of Specimen 4

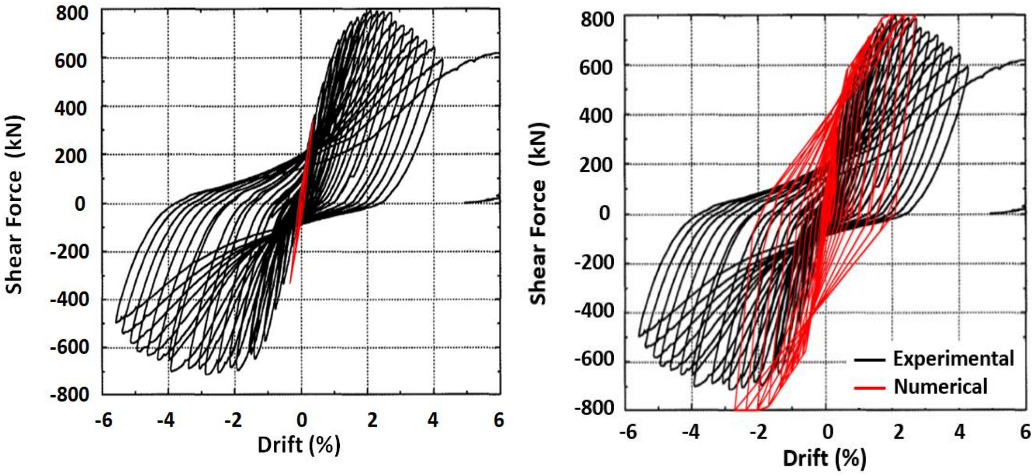


a) Initial rigidity comparison

b) Overall behavior

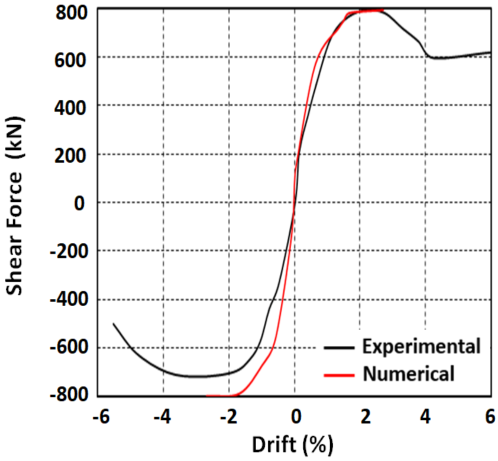


c) Envelope curve

*Figure 5.29.* Shear stress vs. drift response of Specimen 4

### 5.3.4. Specimens of Han et al. (2015)

Three high performance fiber reinforced composite coupling beams with 2% PVA fibers were tested. The main variables of the experimental study by Han et al. are the reinforcement detailing and shear span-to-depth ratio. Specimens FC-0.5-2.0 and FC-0.5-3.5 have transverse and diagonal reinforcement (Figs. 5.30 and 5.32), but FC-0.0-3.5 has only diagonal reinforcement (Fig. 5.34). Furthermore, shear span-to-depth ratio of FC-0.5-2.0 is 2.0 and for FC-0.5-3.5 and FC-0.0-3.5, this ratio is 3.5. For all the subassemblies, the analytical results match with the experimental results accurately up to the ultimate strength capacity (Figs. 5.31, 5.33, 5.35). In this series, analytical results are again better for deeper members. It can be concluded that, the expected ultimate drift values of the model need an enhancement for relatively slender members.

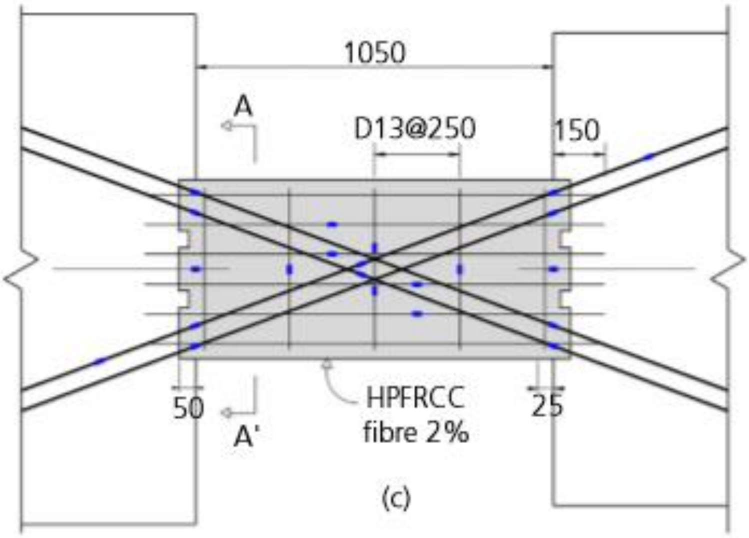


*Figure 5.30.* Reinforcement detailing of Specimen FC-0.5-2.0

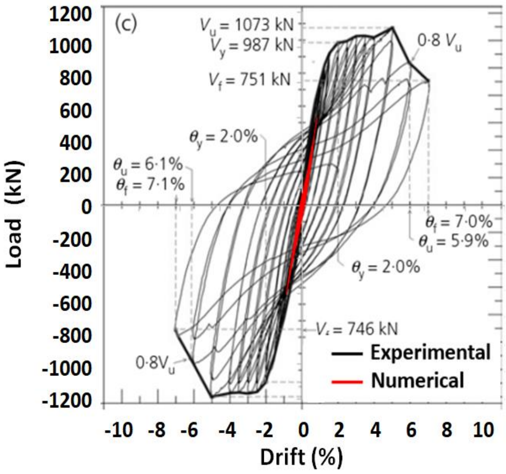


a) Initial rigidity comparison

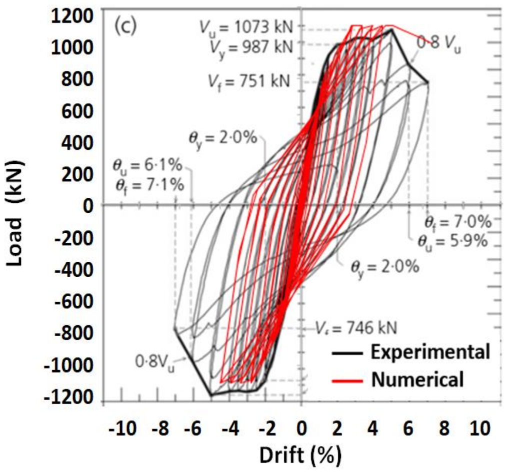


b) Overall behavior

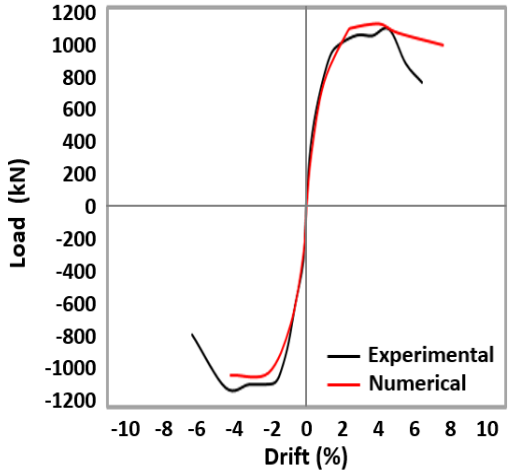


c) Envelope curve

*Figure 5.31.* Shear stress vs. drift response of Specimen FC-0.5-2.0

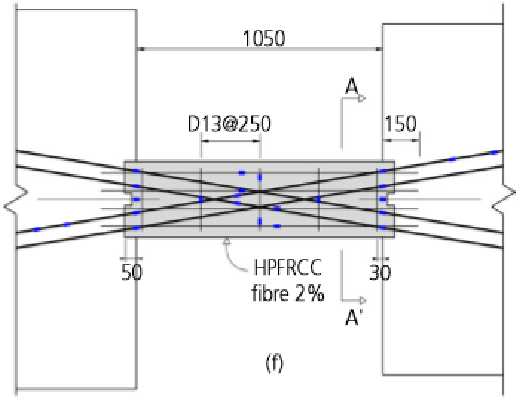


*Figure 5.32.* Reinforcement detailing of Specimen FC-0.5-3.5

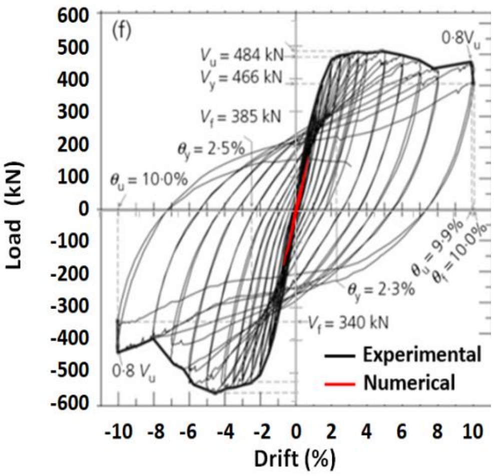


a) Initial rigidity comparison

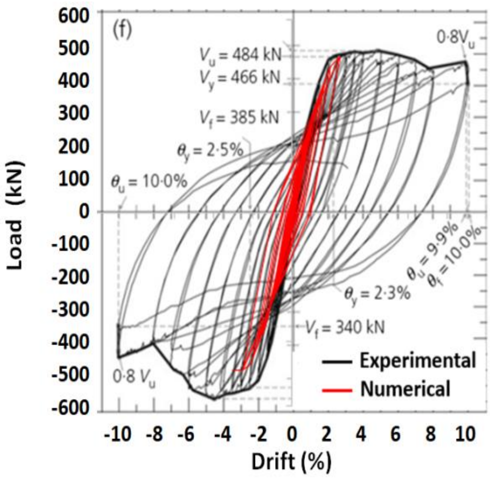


b) Overall behavior

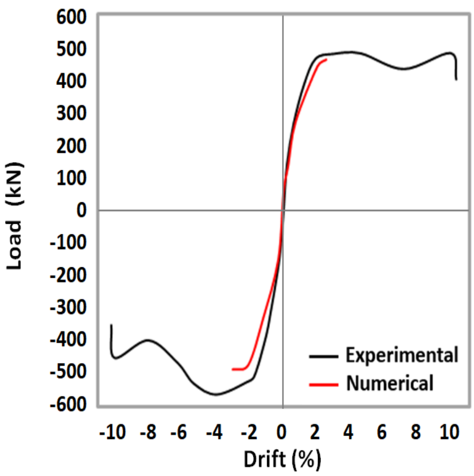


c) Envelope curve

*Figure 5.33*. Shear stress vs. drift response of Specimen FC-0.5-3.5

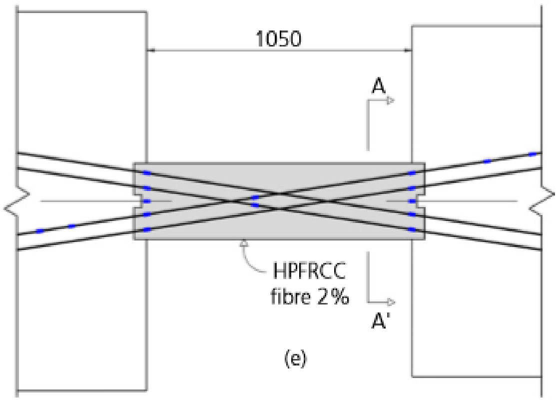


*Figure 5.34.* Reinforcement detailing of Specimen FC-0.0-3.5

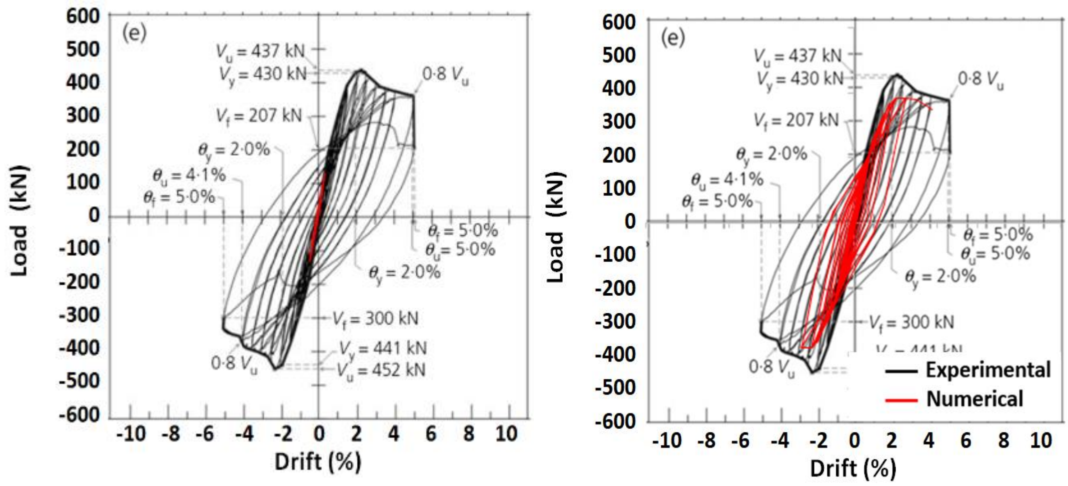


a) Initial rigidity comparison

b) Overall behavior

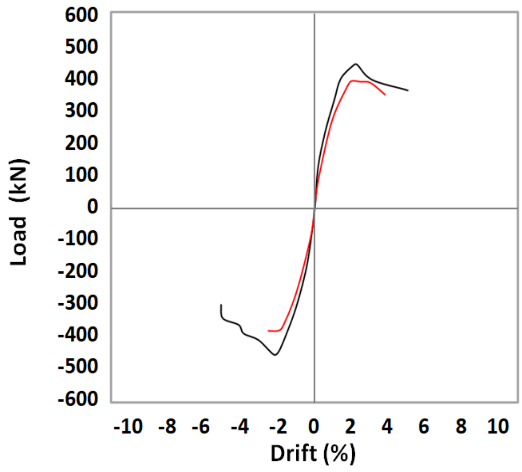


c) Envelope curve

*Figure 5.35.* Shear stress vs. drift response of Specimen FC-0.0-3.5

### 5.3.5. Specimens of Shin et al. (2014)

In this test group, there are two 1/2 scale high-performance fiber reinforced composite coupling beams with 3.5 clear span-to-depth ratio and 2% PVA fibers. Specimen 1CF2Y is a conventionally reinforced coupling beam (Fig. 5.36 (a)) and 1DF2Y is a diagonally reinforced coupling beam (Fig. 5.36 (b)). The rigidity and the expected drift ratios of these specimens with synthetic fibers are underestimated, but the shear strength prediction is not far off (Figs. 5.37 and 5.38).

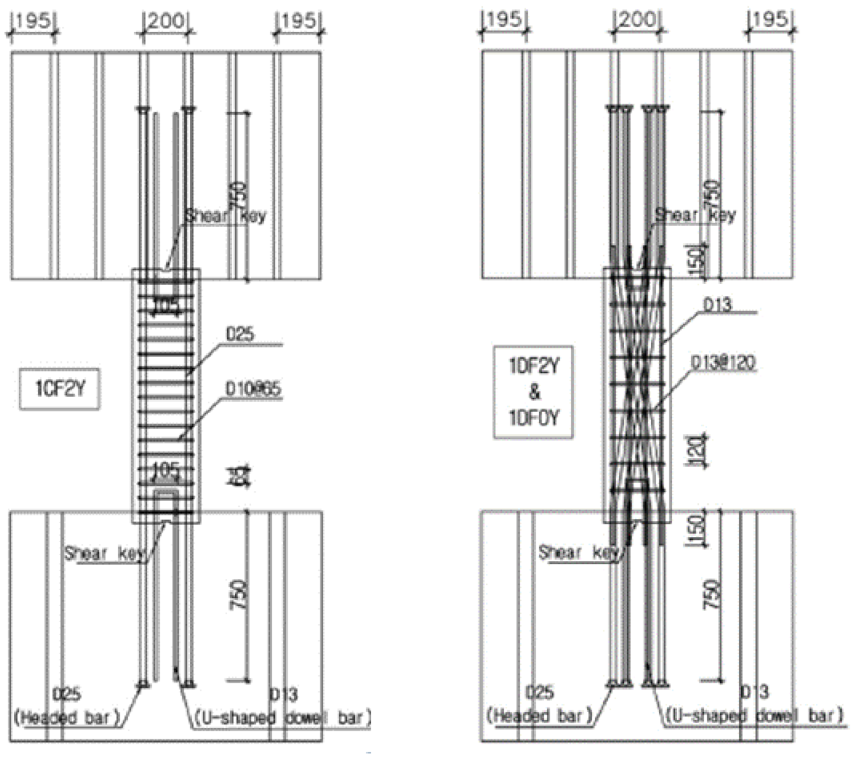


a) Specimen 1CF2Y b) Specimen 1DF2Y

*Figure 5.36.* Reinforcement detailing of Specimens

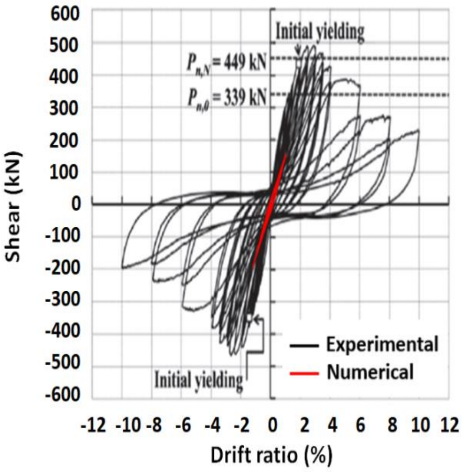


a) Initial rigidity comparison

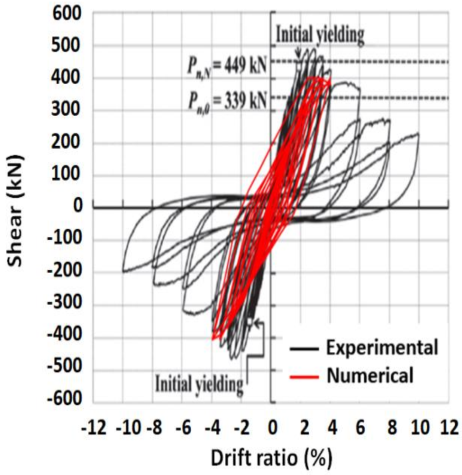


b) Overall behavior

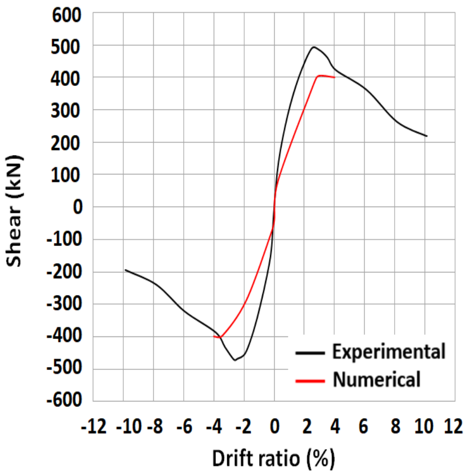


c) Envelope

*Figure 5.37*. Shear stress vs. drift response of Specimen 1CF2Y

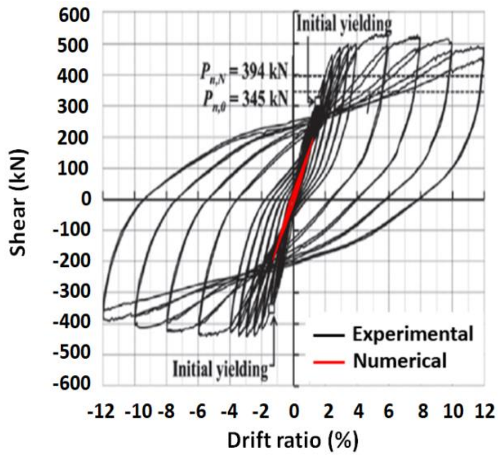


a) Initial rigidity comparison

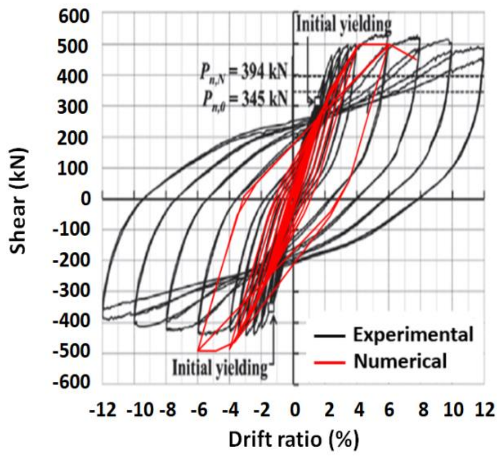


b) Overall behavior

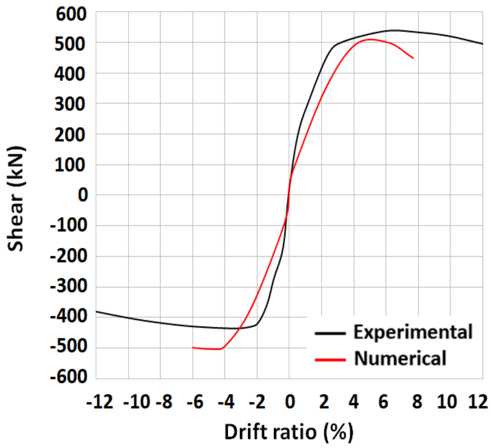


c) Envelope curve

*Figure 5.38*. Shear stress vs. drift response of Specimen 1DF2Y

### 5.3.6. Specimens of Yun et al. (2008)

In this study, two high performance fiber reinforced composite deep coupling beams with different reinforcement arrangements were tested. Vertical and longitudinal reinforcement layouts are the same for both specimens (Fig. 5.39), but CB3 also has diagonal reinforcement. Both subassemblies have a shear span-to-depth ratio of 1.0 and reinforced with a 0.75% volume fraction of PE fibers and 0.75% fraction of torex fibers. Comparison of the results is provided in Figs. 5.40 and 5.41. For both specimens, the ultimate displacement levels are predicted accurately. The initial stiffness of specimen CB3 is predicted correctly, but for CB2 the prediction is too stiff. This is the test series for which the proposed model gives the worst shear strength predictions. More data is required to investigate the influence of the use of more than one type of fiber in a coupling beam.

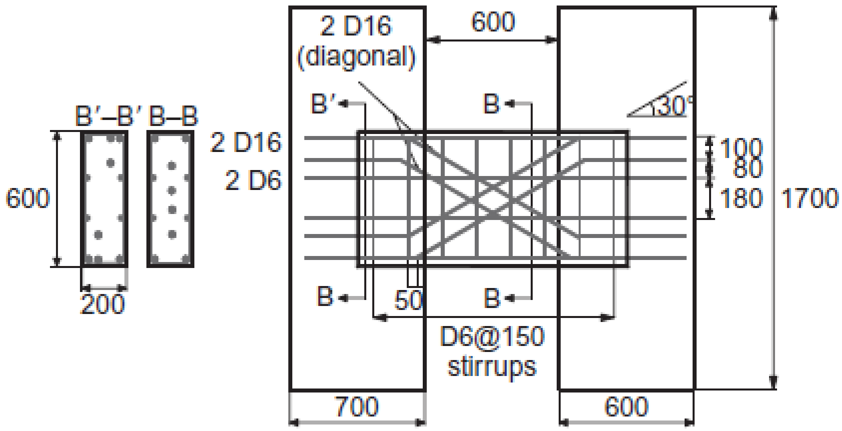


(a)

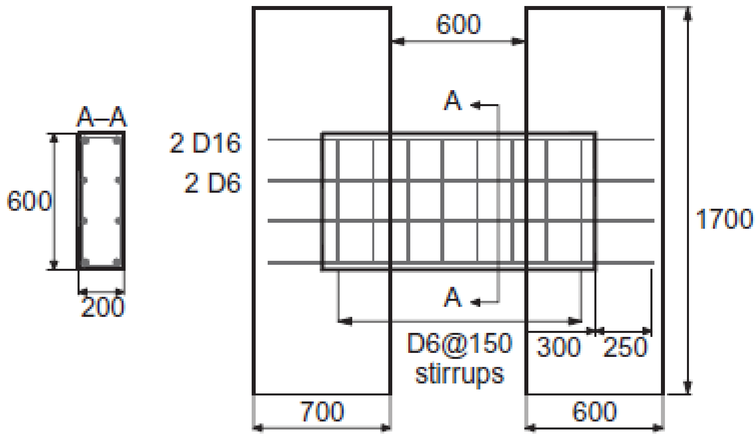


(b)

*Figure 5.39.* Reinforcement detailing of (a) Specimen CB2 and (b) Specimen CB3

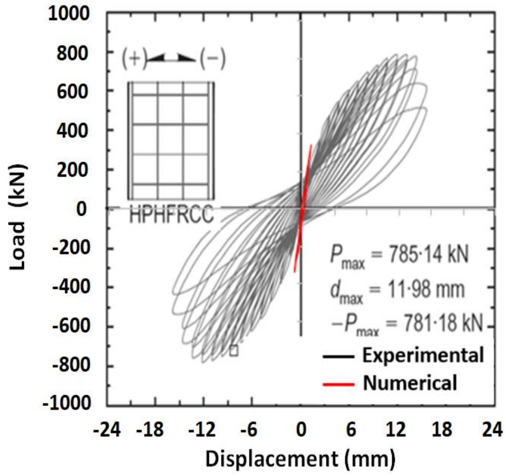


a) Initial rigidity comparison

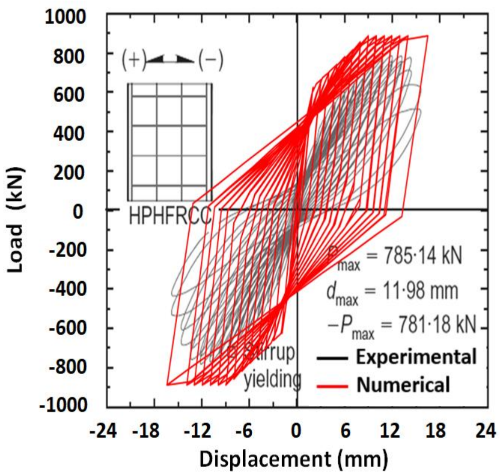


b) Overall behavior

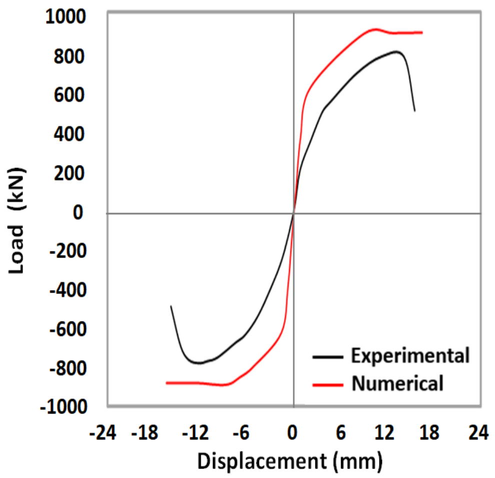


c) Envelope curve

*Figure 5.40.* Shear stress vs. drift response of Specimen CB2

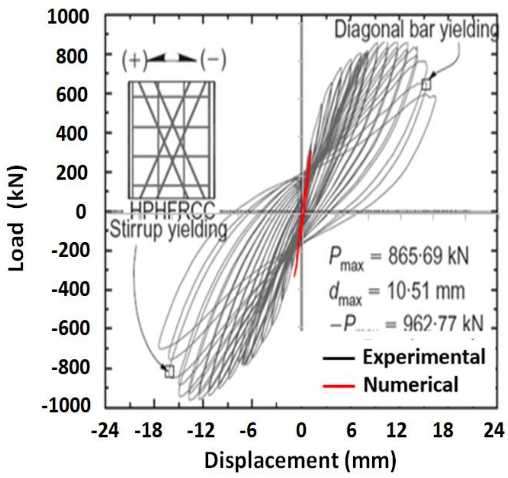


a) Initial rigidity comparison

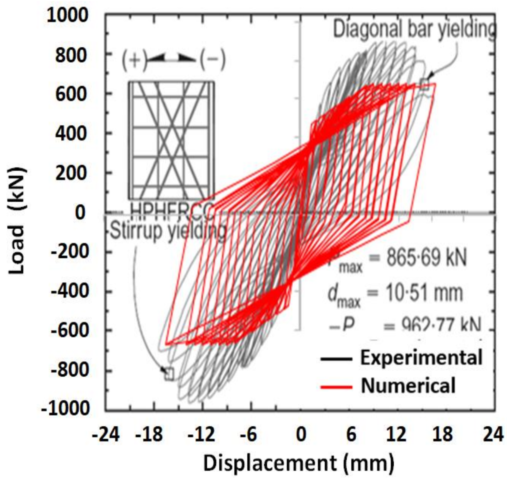


b) Overall behavior

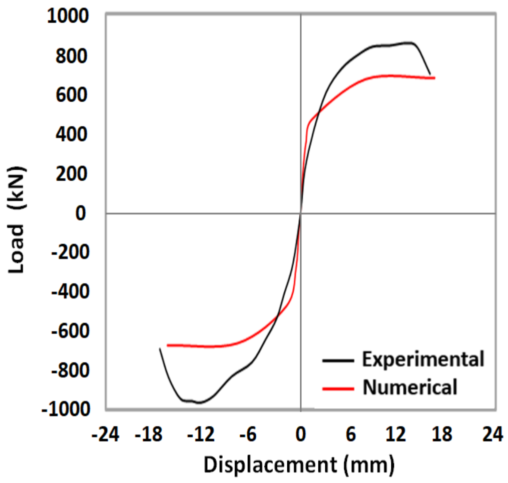


c) Envelope curve

*Figure 5.41.* Shear stress vs. drift response of Specimen CB3

### 5.3.7. Specimens of Kwon et al. (2013)

A high-performance fiber reinforced composite coupling beam, which has a shear span-to-depth ratio of 2.0, a beam depth of 525 mm., and 2.0% PVA fibers without any transverse reinforcement, FC-0.0, (Fig. 5.42) was tested by Kwon et al. (2013). As seen in Fig.5.43, the yield strength of the member is 95% of the ultimate strength, which indicates that the fibers provide shear transfer up to the yield point. This way, the cracks remained narrow and the reinforcement strain did not reach yielding. The shear strength of the member is reasonably predicted; however the strength degradation is underestimated. This indicates the need to define higher strength degradation for the specimens with no transverse reinforcement.

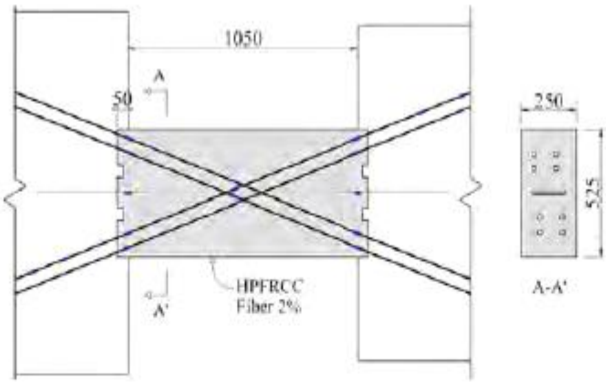


*Figure 5.42*. Reinforcement detailing of Specimen FC-0.0

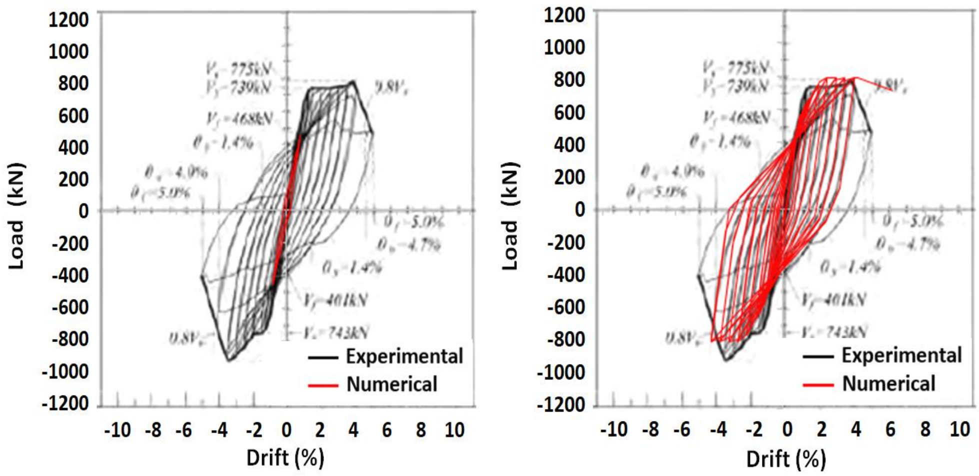


a) Initial rigidity comparison

b) Overall behavior

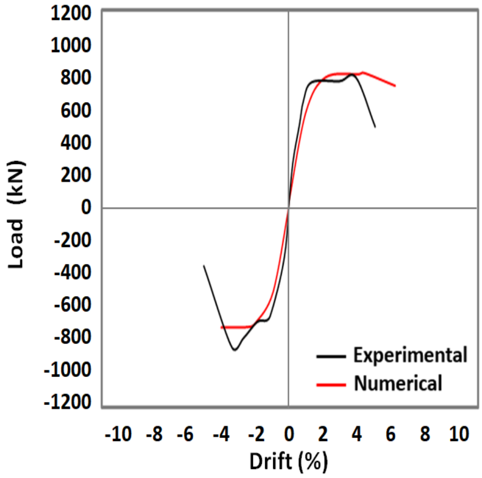


c) Envelope curve

*Figure 5.43.* Shear stress vs. drift response of Specimen FC-0.0

### 5.3.8. Specimens of Parra-Montesinos et al. (2017)

Parra-Montesinos et al. (2017) tested three high performance fiber reinforced composite coupling beams with 1.5% hooked steel fiber to investigate the effect of fibers on the capacity of members with different aspect ratios. Specimen 1 (Fig. 5.44 (a)) has an aspect ratio of 2.2, the experimental results of which are shown with black line in the graph (Fig. 5.45). Specimen 2 ($l_n/h = 2.75$) (Fig. 5.44 (b)) and Specimen 3 ($l_n/h = 3.3$) (Fig. 5.44 (c)) are shown with blue (Fig. 5.46) and red (Fig. 5.47) dashed lines, respectively. The analytical results match with the experimental results with reasonable accuracy up to ultimate strength and strength degradation is captured as well. However, the ultimate drifts are underestimated.

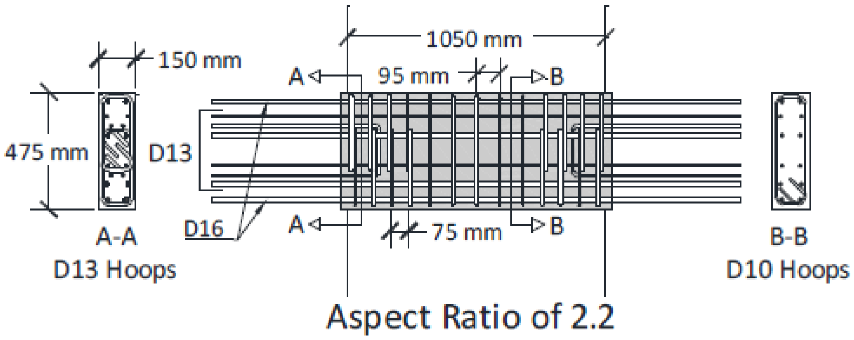


a) Specimen 1

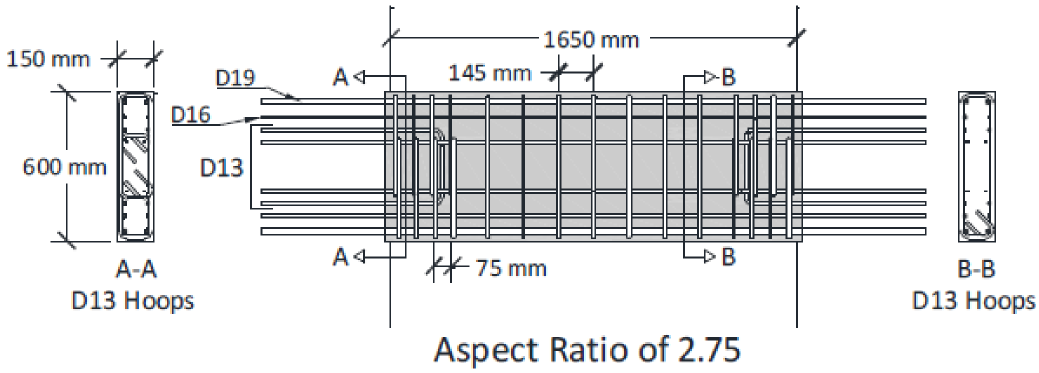


b) Specimen 2

*Figure 5.44*. Reinforcement detailing of Specimens

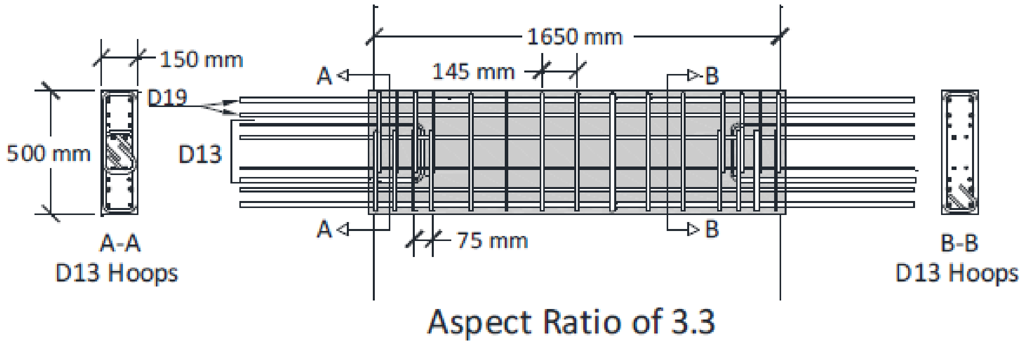


c) Specimen 3

*Figure 5.45.* Reinforcement detailing of Specimens (continued)

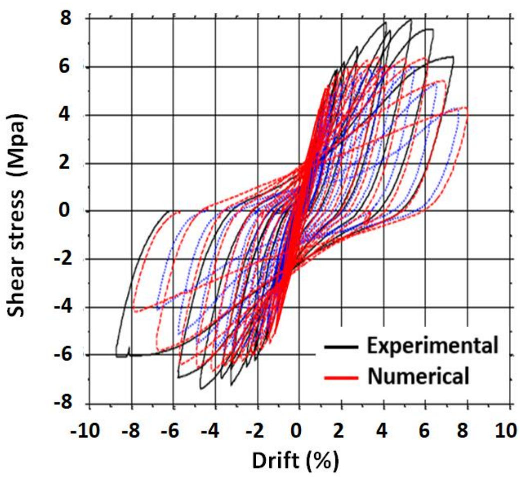


a) Initial rigidity comparison

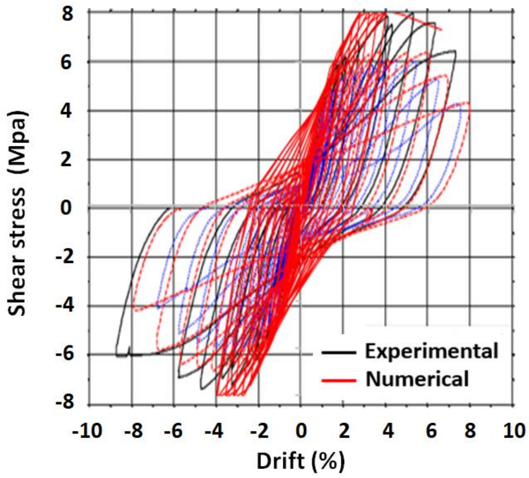


b) Overall behavior

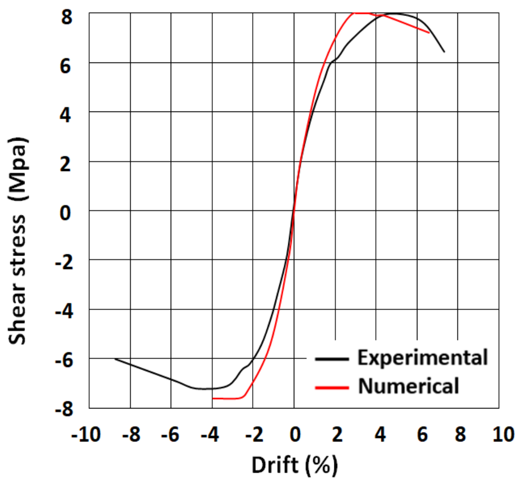


c) Envelope curve

*Figure 5.46.* Shear stress vs. drift response of Specimen 1 (Aspect ratio = 2.2)

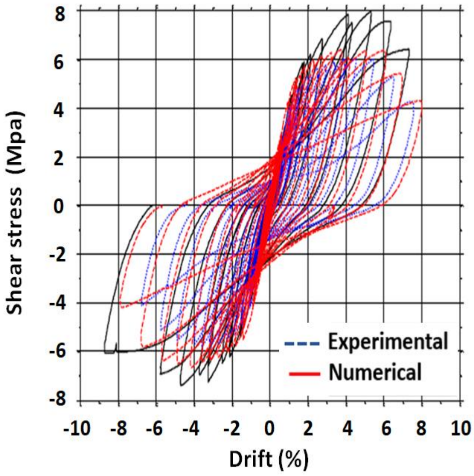


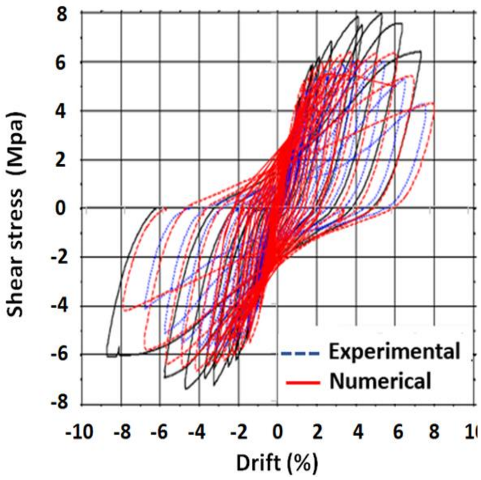


a) Initial rigidity comparison b) Overall behavior

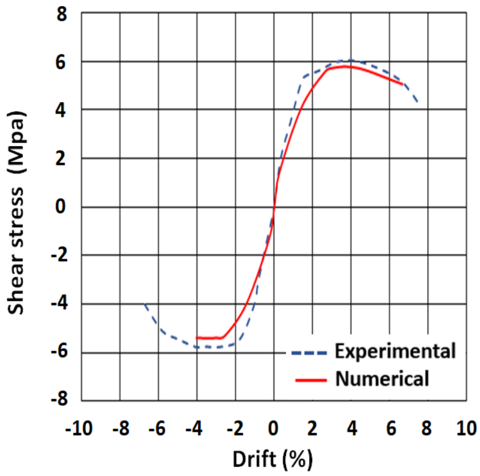


c) Envelope curve

*Figure 5.47*. Shear stress vs. drift response of Specimen 2 (Aspect ratio = 2.75)

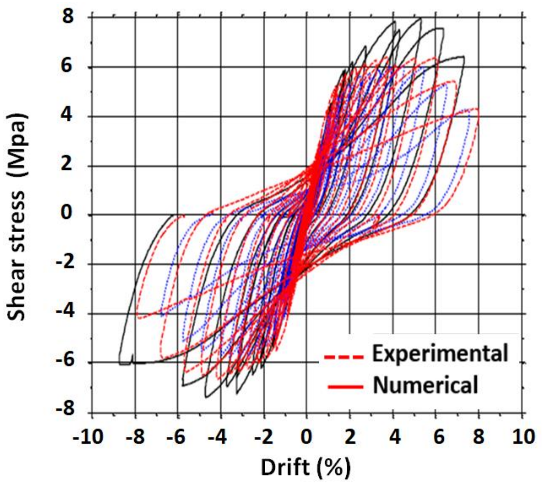

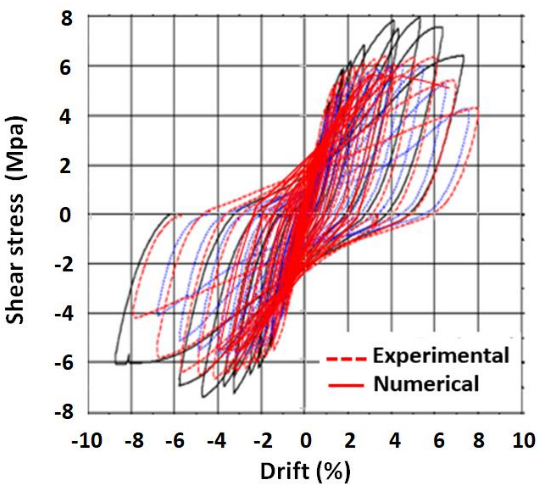


a) Initial rigidity comparison

b) Overall behavior

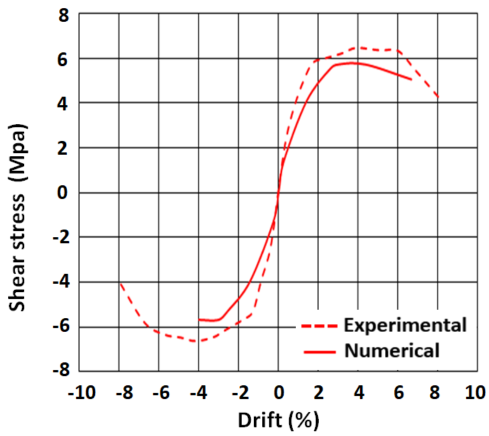


c) Envelope curve

*Figure 5.48.* Shear stress vs. drift response of Specimen 3 (Aspect ratio = 3.3)

### 5.3.9. Pérez-Irizarry and Parra-Montesinos (2016)

CB4 (Fig. 5.48), and CB8 (Fig. 5.50) are the two conventionally reinforced fiber reinforced composite coupling beams tested in this experimental study. The two specimens differ from one another in terms of clear span-to-depth ratio, which is 3 for CB4 and 2 for CB8; fiber aspect ratio 60 and 80 and fiber volumetric ratio 1% and 1.5%, respectively. The behavior of Specimen CB4 is accurately predicted in terms of initial stiffness, ultimate shear capacity and drift (Fig. 5.49). However, ultimate capacity of CB8 is quite far from the predicted value, although the initial stiffness matches well (Fig. 5.51). It was reported that horizontal through-depth crack at the bottom plastic hinge and the opening of a gap between the coupling beam and the reinforced concrete wall were observed while testing CB8. This explains the lower strength and higher drift values and emphasizes the need to investigate the influence of coupling beam-to-wall connection detailing on the strength and deformation capacity of these shear critical beams.

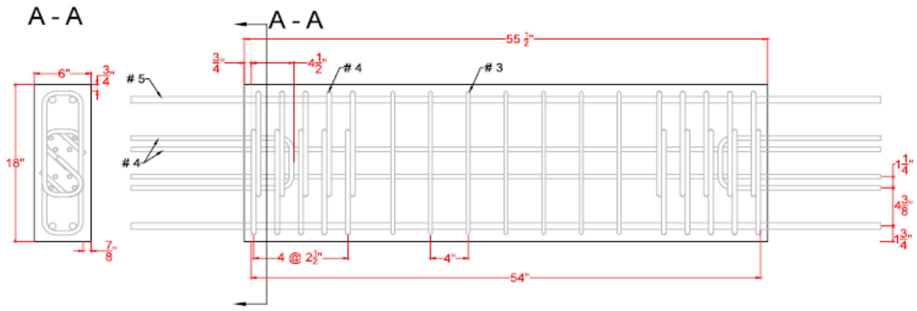


*Figure 5.49.* Rinforcement detailing of Specimen CB4

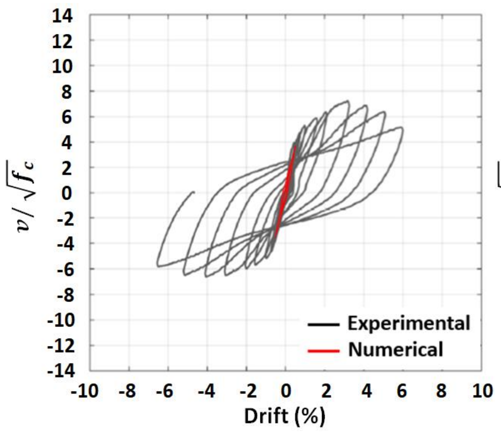


a) Initial rigidity comparison

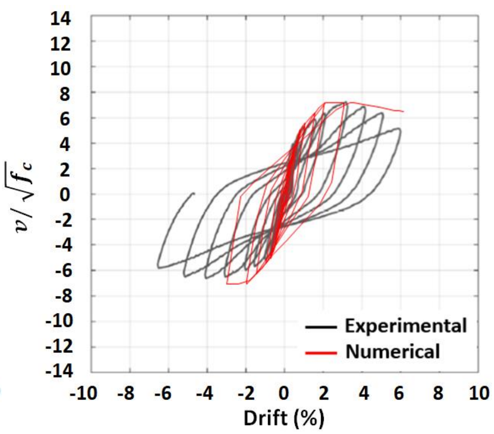


b) Overall behavior

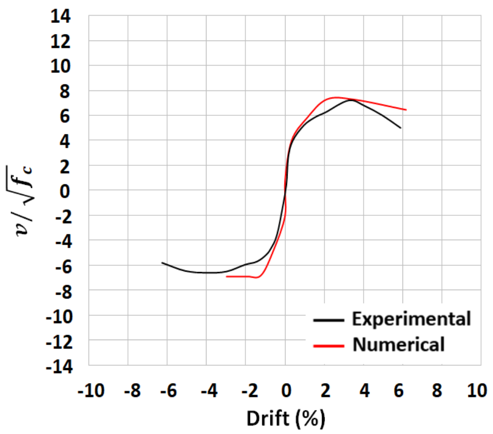


c) Envelope curve

*Figure 5.50.* Shear stress vs. drift response of Specimen CB4

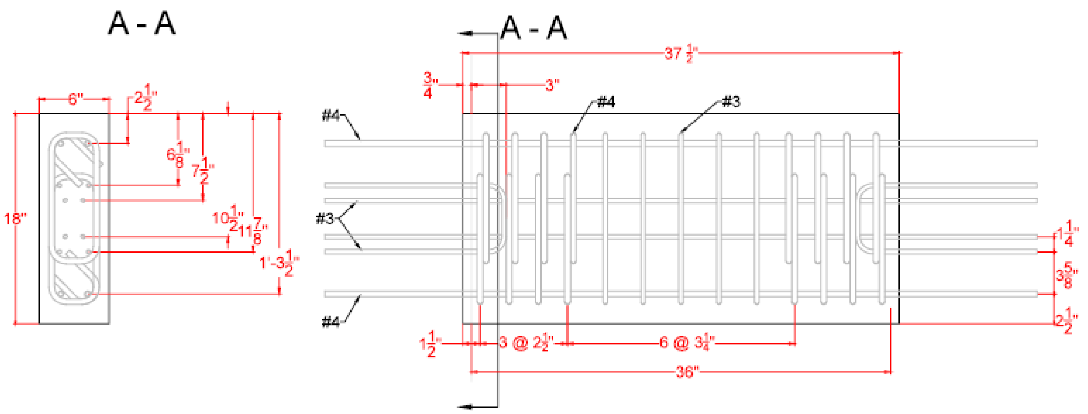


Figure 5.51. Reinforcement detailing of Specimen CB8

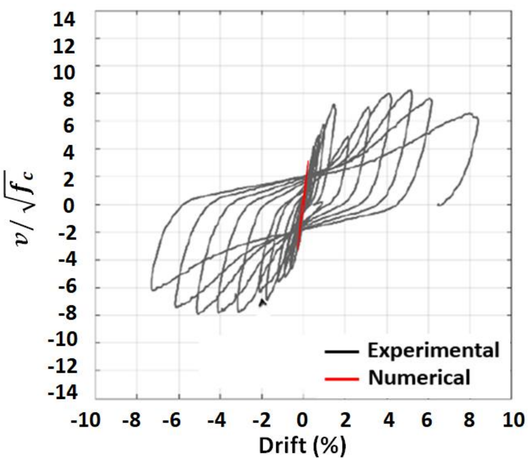


a) Initial rigidity comparison

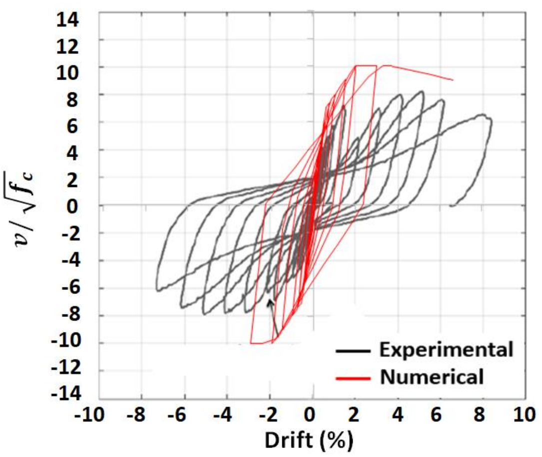


b) Overall behavior

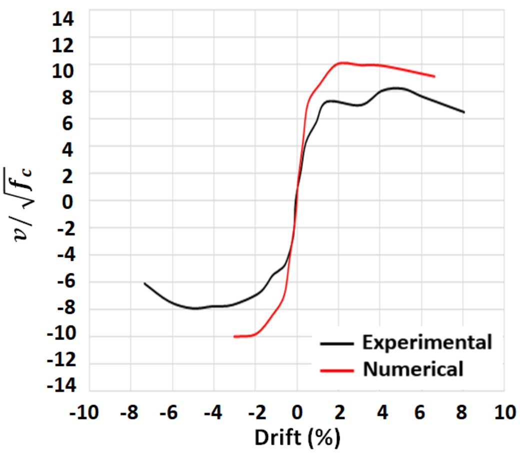


c) Envelope curve

*Figure 5.52.* Shear stress vs. drift response of Specimen CB8

### 5.4. Coupled Wall Systems (Lequesne et al. (2012))

In order to verify the applicability of the proposed analytical model to the coupled wall systems, two approximately 1/3 scale four-story coupled wall specimens (CW-1 and CW-2) tested by Lequesne et al. (2012), under the combined action of axial and lateral loads are analyzed using ETABS 17 (2017).

Each coupled wall specimen has two T-shaped structural wall segments and four coupling beams, as shown in Fig. 5.52. The lateral displacement history given in Fig. 5.53 is applied to the fourth floor, while 60% of these displacements are applied to the second floor. The axial load is considered to be 0.3 $A_g$, where, $A_g$ is the cross sectional area of the wall. Each of the two specimens has a reinforced concrete coupling beam (Beam 2) and three high performance fiber reinforced composite (HPFRC) coupling beams (Beams 1, 3 and 4). The reinforcement detailing of coupling beams is given in Fig. 5.54. Moreover, the first two stories of CW-2 were cast using high performance fiber reinforced composites.

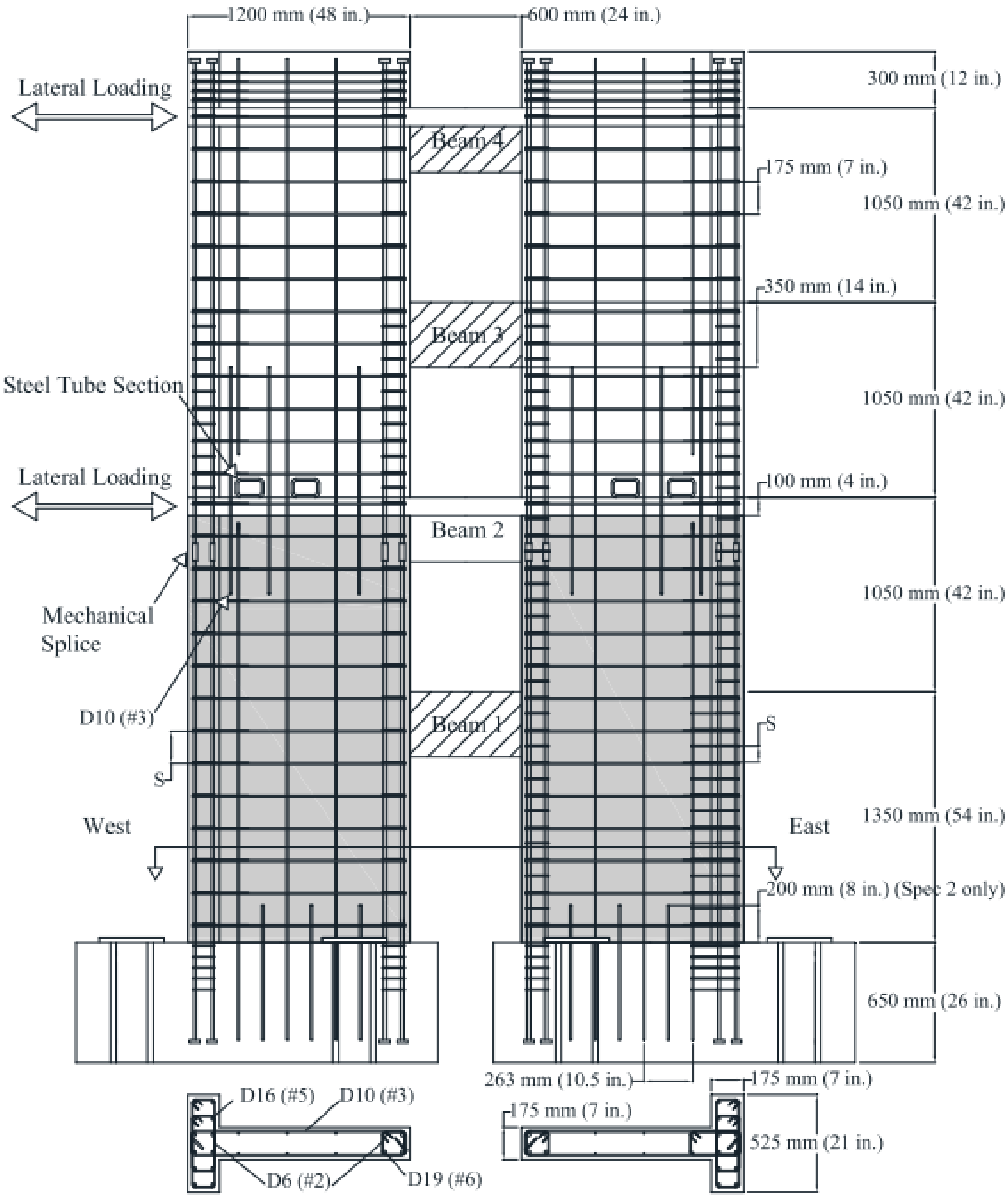


*Figure 5.53.* Coupled wall system

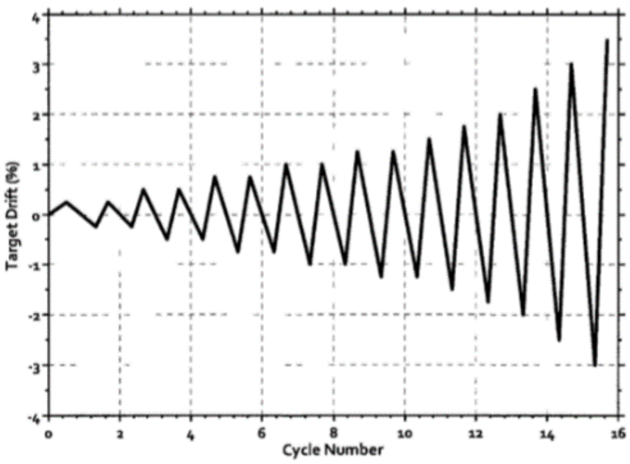


*Figure 5.54.* Lateral displacement history for coupled wall systems

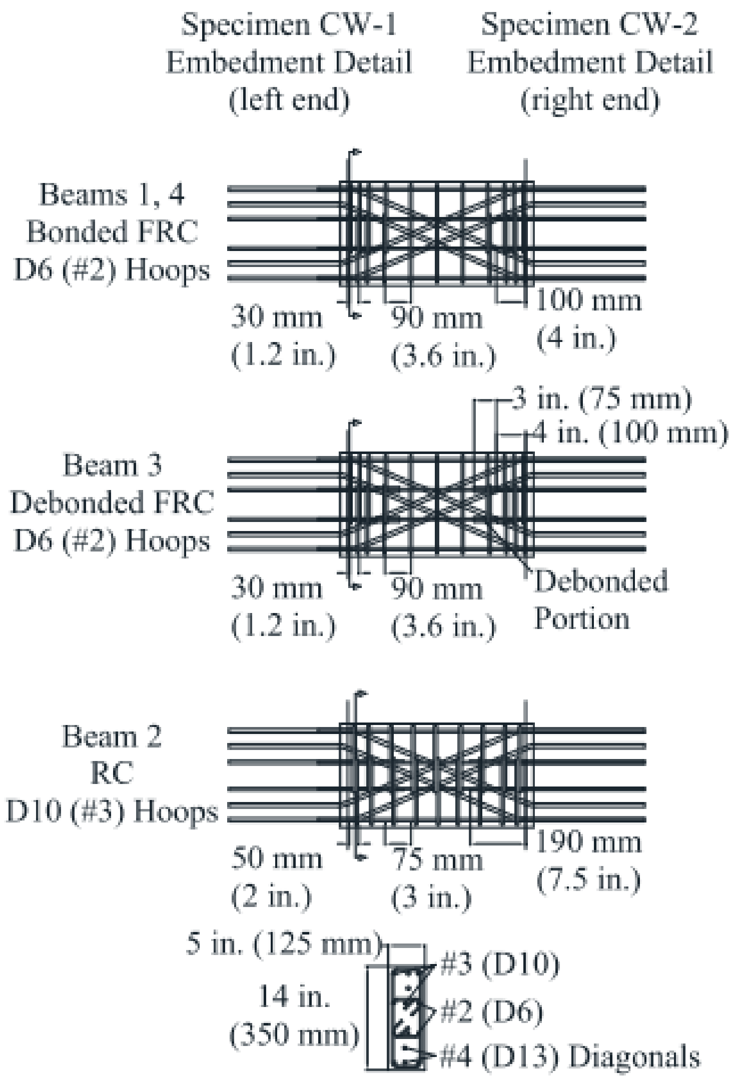


*Figure 5.55.* Coupling beam reinforcement detailing for CW-1 and CW-2

The ETABS 2017 model of the test specimens is shown in Fig. 5.55. In the model, fixed end supports are considered at the base of each wall. The coupling beams and walls are modeled as elastic members that have cracked flexural rigidity. The cracked flexural rigidity is taken as 0.3 $EI_g$ for coupling beams and 0.5 $EI_g$ for wall segments as recommended by ASCE 41-13 (2013). At the two ends of the coupling beams, semi-rigid end zones are defined within the walls and zero length moment hinges at the face of the walls (Fig.5.55). The wall segments are modeled as members with rigid end zones within the depth of the beam (Fig. 5.55) and P-M-M hinges at their bases, which take into account the effect of combined axial load and bending. In this analytical study, rigid end zone factor is taken as 0.5 for beams, to take into account the slip of precast beams from the walls, and 1.0 for walls. Elastic modulus is calculated by using Eqn. 5-5 and Poisson's ratio is taken as 0.2 for both reinforced concrete and high performance fiber reinforced composite members.

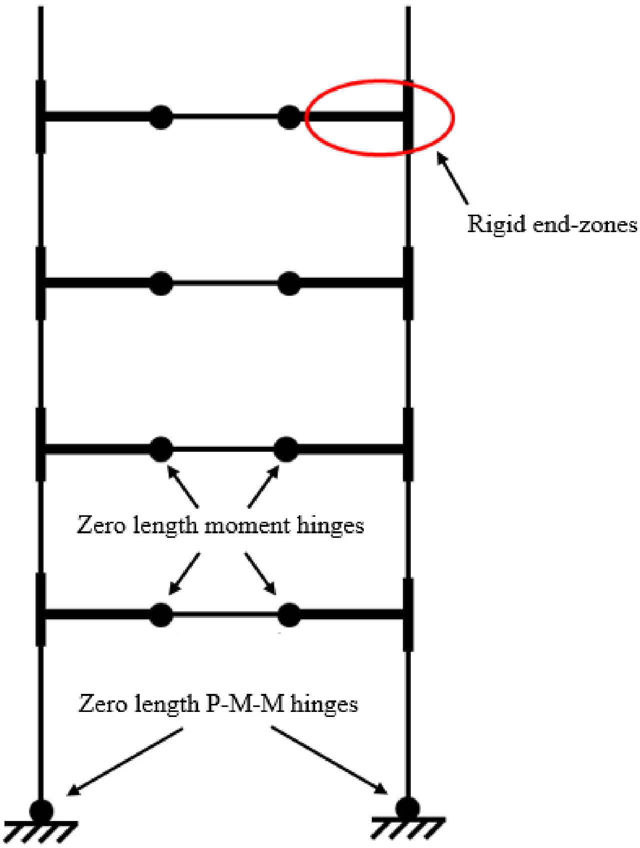


*Figure 5.56.* Specimen model

The modeling parameters used in the nonlinear analysis of reinforced concrete shear walls controlled by flexure are presented in Table 5.1. Based on the recommendations of ASCE 41-13 (2013), the backbone curves given in Fig. 5.56 are generated for the wall moment-rotation and axial load-moment responses. Yield moment, $M_y$, is set equal to 70% of the computed moment capacity of the wall, and yield rotation, $\theta_y$, is computed from Eqn. 5-2. The results of the nonlinear analysis are given in Figs. 5.57 and 5.58 for specimens CW-1 and CW-2, respectively. As it can be observed from these figures, the proposed method accurately and conservatively predicts the overall behavior.

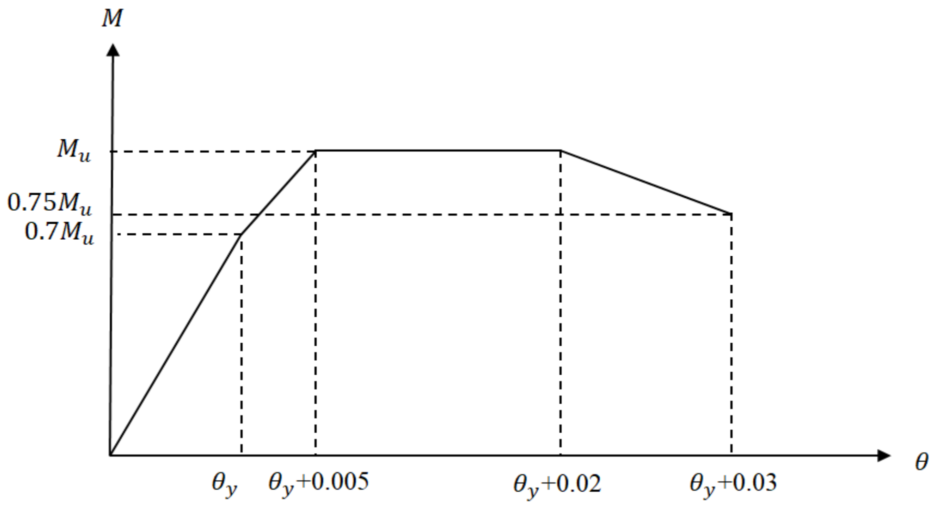


(a) Moment-rotation relationship

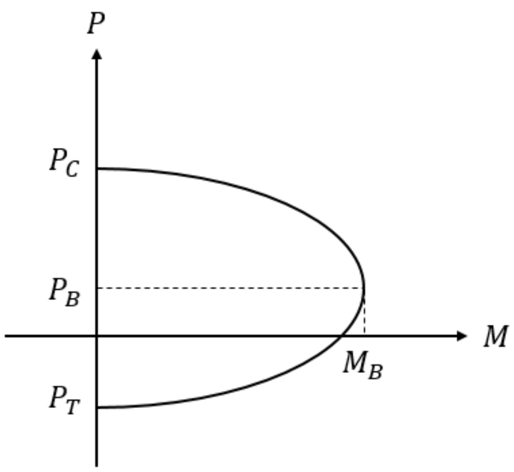


(b) Axial load-moment relationship

*Figure 5.57.* Backbone curves for walls

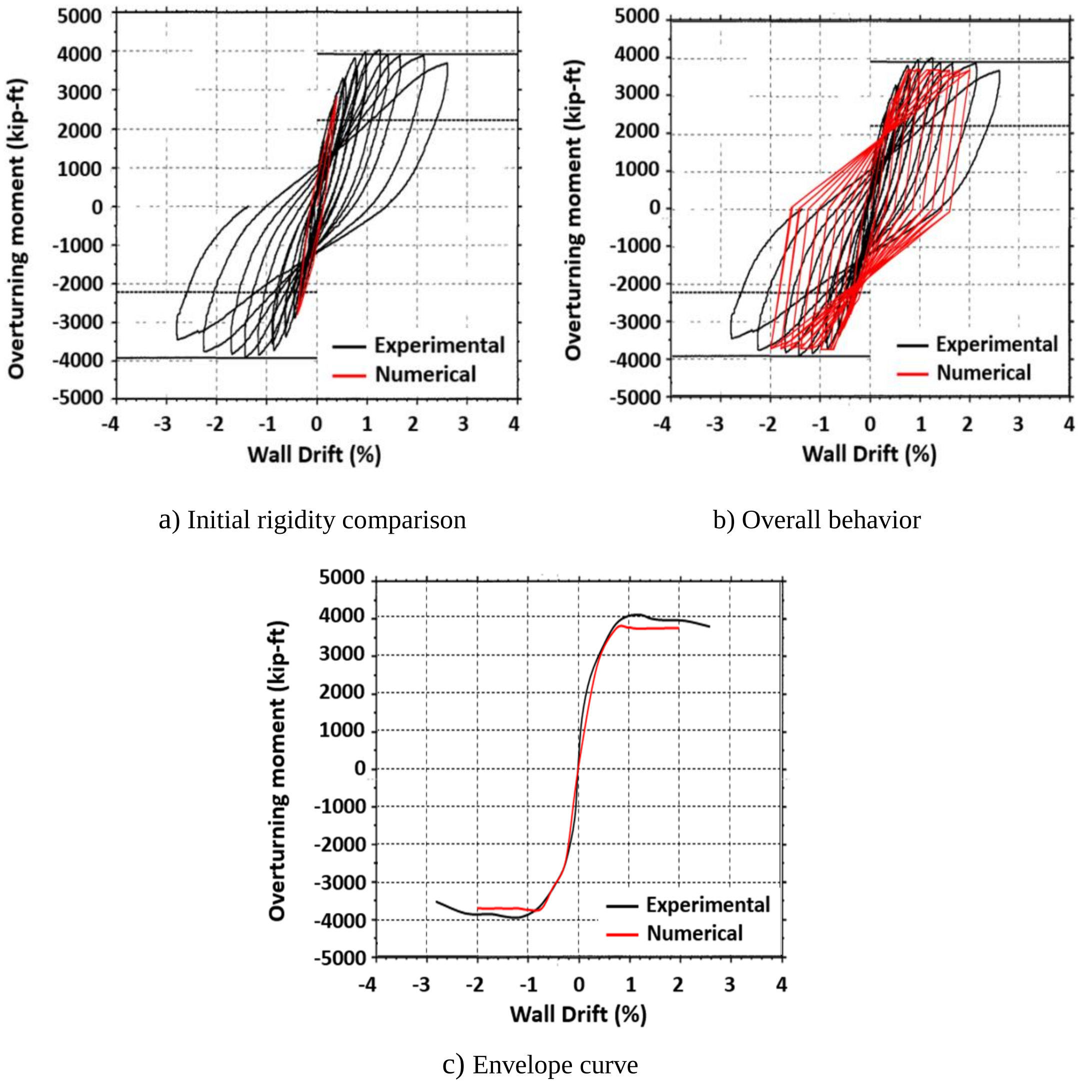


*Figure 5.58.* Shear stress vs. drift response of Specimen CW-1

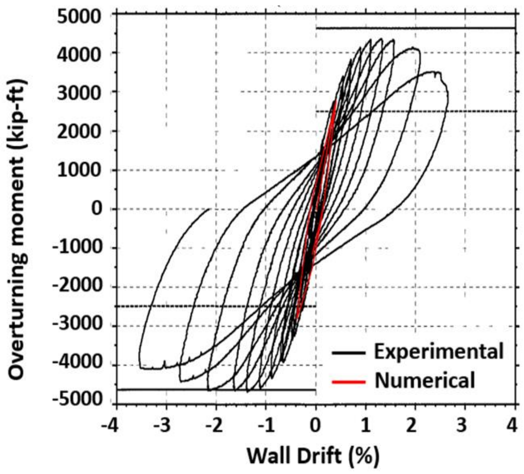


a) Initial rigidity comparison

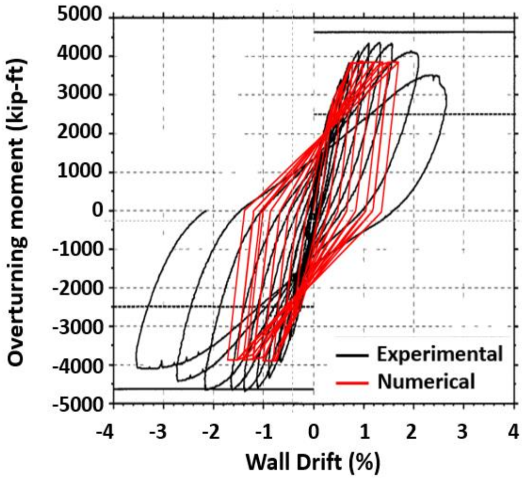


b) Overall behavior

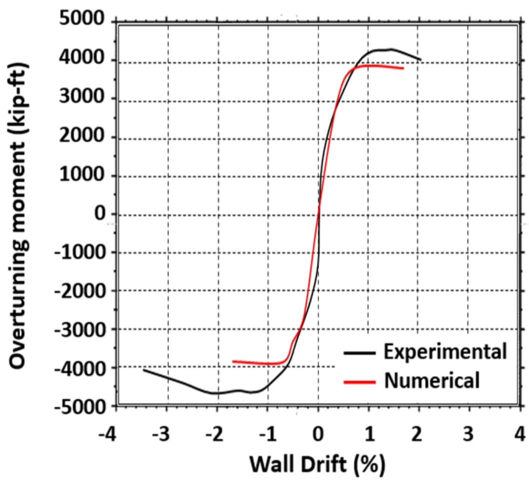


c) Envelope curve

*Figure 5.59.* Shear stress vs. drift response of Specimen CW-2

# CHAPTER 6

# SUMMARY AND CONCLUSIONS

## 6.1. Summary and Conclusions

Under seismic loading, reinforced concrete beams have flexural or shear failure based on material and cross sectional properties of the members. In order to prevent brittle shear failure, randomly distributed short fibers can be aded to the concrete mix, which increases the tensile and shear strengths and provides load transfer in between cracked surfaces.

Various researchers proposed analytical equations to predict the shear strength of fiber reinforced concrete composites within some limitations. Although, each model agrees well with the test results from which they are derived, when the analytical results from these models are compared with other test results, their accuracy diminish significantly. Moreover, most of the prior research studies do not compare flexural and shear strengths to take into account different failure modes. The key limitations of the prior methods are the fiber type used in the mix and member shear span-to-depth ratio. The main objective of this analytical study is to develop a simple equation to accurately predict the shear strength of fiber reinforced composite shear critical beams, which is applicable to any type and volumetric ratio of fibers, reinforcement layouts and member properties. For this purpose, a large variety of shear critical beam subassemblies having different geometric and material properties under different loading conditions are considered in the constructed database.

After thorough investigation of the behavior of specimens included in the database, a shear strength equation and a method to obtain the flexural strength are proposed. By comparing the two, the failure mode of the members can also be determined. Then, moment-rotation relationships are generated for conventionally and diagonally reinforced fiber reinforced coupling beams. Finally, coupling beam subassemblies and coupled wall systems are modeled under the experimental displacement histories using ETABS 17. The analytical results are compared with the experimental ones in order to verify the accuracy of the developed model.

It was observed that the shear strength of fiber reinforced composite deep and coupling beams can be reasonably estimated by using the same formulation for different types of fibers, geometric properties and reinforcement layouts. The key parameters that influence the behavior of beams are found to be effective depth to clear length ratio, $d/l_n$, and transverse reinforcement ratio, $\rho_t$.

From the comparison of experimental results with the analytical ones using the proposed method, as well as other existing predictions, the following conclusions can be drawn:

- For deep beams that have $a/d \leq 2.5$ and transverse reinforcement, the proposed shear strength equation leads to more accurate predictions (mean, standard deviation and average absolute error of 0.73, 0.12, and 27.54, respectively) when compared to the existing shear strength models.
- For deep beams that have $a/d \leq 2.5$ and no transverse reinforcement, the analytical results can be improved by considering the effect of beam-to-wall connection rigidity. This can be accomplished by taking into account the dowel action, either by modifying the rigid end zone factor or defining a slip component based on the detailing of the dowel bars in the connection region.
- For deep beams that have $a/d > 2.5$ and transverse reinforcement, proposed equation gives more conservative results than the others (mean, standard deviation and average absolute error of 0.78, 0.12, and 25.13, respectively).
- For deep beams that have $a/d > 2.5$ and no transverse reinforcement, when compared to other models, the proposed method predicts the ultimate shear strength with significant accuracy (mean, standard deviation and average absolute error of 0.98, 0.22, and 18.11, respectively).

- While the proposed method is adequate for FRC coupling beams with transverse reinforcement (mean, standard deviation and average absolute error of 0.99, 0.17, and 13.59, respectively), it overestimates the shear strength of FRC coupling beams without transverse reinforcement (mean, standard deviation and average absolute error of 1.13, 0.17, and 16.40, respectively). However, it should be mentioned that the number of specimens in the constructed database is not enough to determine the accuracy of the proposed method for FRC coupling beams without transverse reinforcement.
- For HPFRC coupling beams with or without transverse reinforcement, the proposed method has the highest accuracy among all other predictions.
- Coupled wall system test results are also obtained with adequate accuracy, which indicates that the proposed model can be used conservatively in structural analysis and design.
- In this study, the cracked rigidity of fiber reinforced composite coupling beams is considered to be 30% of the gross sectional rigidity as recommended by ASCE 41-13. It is observed that some of the equations to predict cracked rigidity give unrealistically low values.
- Considering a constant bond strength for different fiber types without taking into account the fiber volumetric and aspect ratios results in inaccurate prediction of the shear strength. Therefore, an equation is proposed in this study to account for the influence of these parameters on the bond strength. The use of this equation rather than constant values is believed to be one of the reasons for the improvement in the accuracy of the shear prediction.

## 6.2. Recommendations for Future Research

Although the proposed method gives reasonable results for most of the subassemblies in the database further improvement may be accomplished by considering more parameters in the prediction equations and adding new experimental results to the database. More experimental research should be conducted especially on coupling beams that evaluates the effect of using different fiber types and two or more fibers in the same composite. A different moment-rotation backbone curve could be obtained for FRC coupling beams without transverse reinforcement. The dowel action can be integrated into the proposed model, either by modifying the rigid end zone factor or defining a slip component based on the detailing of the dowel bars in the beam-to-wall connection region.

# REFERENCES


ACI Committee 318, (2014), Building code requirements for structural concrete (ACI 318-14) and commentary. Farmington Hills, MI: American Concrete Institute, Detroit, 519 p.

ACI Committee 318, (2011), Building code requirements for structural concrete (ACI 318-11) and commentary. Farmington Hills, MI: American Concrete Institute, Detroit, 503p.

ACI Committee 318-83, (1983), Building Code Requirements for Reinforced Concrete, American Concrete Institute, Detroit, 111 p.

ACI Committee 363, (1997), Report on High-Strength Concrete (ACI 363R-92, Reapproved 1997), ACI Manual of Concrete Practice, American Concrete Institute, Farmington Hills, MI, 55 p.

ACI 544.1R-96 (Reappoved 2009): Report on Fiber Reinforced Concrete, 66p.

ACI 544.3R-93 (1998): Guide for Specifying, Proportioning, Mixing, Placing and Finishing Steel Fiber Reinforced Concrete, 186 p.

ACI 544.4R88, (1999), Design Considerations for Steel Fiber Reinforced Concrete, American Concrete Institute, Detroit, 186 p.

Adebar, P., Mindess, S., St.-Pierre, D., Olund, B., (1997), Shear Tests of Fiber Concrete Beams without Stirrups, ACI Structural Journal, 94(1), 68-76.

Alsiwat, J. M., Saatçioğlu, M., (1992), Modeling Anchorage Slip for Dynamic Analysis, Earthquake Engineering Tenth World Conference, Balkema, Rotterdam, 2627-2632.

Aoude, H., Belghiti, M., Cook, W. D., and Mitchell D., (2012), Response of Steel Fiber-Reinforced Concrete Beams with and without Stirrups, ACI structural journal, 109(3), 359-367.

Araújo, D. L., Nunes, F. G. T., Filho, R. D. S., Andrade, M. A. S., (2014), Shear Strength of Steel Fiber-Reinforced Concrete Beams, Acta Scientiarum Technology, 36(3), 389-397.

Aristizabal-Ochoa, J. D., (1982), Dynamic response of coupled wall systems, ASCE Journal of the Structural Division, 108(8), 1846-1857.

ASCE Standard: ASCE/SEI 41-06, (2007), Seismic Rehabilitation of Existing Buildings, American Society of Civil Engineers, 194 p.

ASCE Standard: ASCE 41-13, (2013), Seismic Evaluation and Retrofit of Existing Buildings, American Society of Civil Engineers, 194 p.

Ashour, S. A., Hasanain, G. S., and Wafa, F. F., (1992), Shear Behavior of High-Strength Fiber Reinforced Concrete Beams, ACI Structural Journal, 89(2), 176-184.

Baczkowski, B. J., (2007), Steel Fibre Reinforced Concrete Coupling Beams, Ph.D. Thesis, The Hong Kong University of Science and Technology, 306 p.

Barney, G. B. et al., (1978), Earthquake Resistant Structural Walls - Test of Coupling Beams, Report to NSF, submitted by Portland Cement Association, Research and Development, Skokie, IL.

Batson, G., Jenkins, E., Spatney, R., (1972), Steel Fibers as Shear Reinforcement in Beams, ACI Structural Journal, 69(61), 640-644.

Berry, M. P., Lehman, D. E., andLowes, L. N., (2008), Lumped-Plasticity Models for Performance Simulation of Bridge Columns, ACI Structural Journal, 105(3), 270-279.

Birrcher, D. B., Tuchscherer, R. G., Huizinga, M., and Bayrak, O., (2014), Depth Effect in Deep Beams, ACI Structural Journal, 111(4), 731-740.

Bresler, B., and Scordelis, A. C., (1963), Shear Strength of Reinforced Concrete Beams, ACI Structural Journal, 60(1), 51-74.

Cai, G., Zhao, J., Degee, H., Vandoren, B., (2016), Shear Capacity of Steel Fibre Reinforced Concrete Coupling Beams Using Conventional Reinforcements, Engineering Structures, 128, 428-440.

Canbolat, B. A., (2004), Seismic Behavior of High-Performance Fiber Reinforced Cementitious Composite Coupling Beams, Ph.D. Thesis, The University of Michigan, 209 p.

Canbolat, B. A., Parra-Montesinos, G. J., Wight, J. K., (2005), Experimental Study on Seismic Behavior of High Performance Fiber Reinforced Cement Composite Coupling Beams, ACI Structural Journal, 102(1), 159-166.

Casanova, P., Rossi, P., (1997), Can Steel Fibers Replace Transverse Reinforcements in Reinforced Concrete Beams, ACI Material Journal, 94(5), 341-354.

Champione, G., (2012), Flexural Behavior of Steel Fibrous Reinforced Concrete Deep Beams, ASCE, 138(2), 235-246.

Cho, S. H., and Kim, Y. I., (2003), Effects of Steel Fibers on Short Beams Loaded in Shear, ACI Structural Journal, 100(6), 765-774.

Choi, K-K., Park H-G., Wight, J. K., (2007), Shear Strength of Steel Fiber-Reinforced Concrete Beams without Web Reinforcement, ACI Structural Journal, 104(1),12-21.

Cohen, M., (2012), Structural Behavior of Self Consolidating Steel Fiber Reinforced Concrete Beams, Ottawa-Carleton Institute for Civil Engineering MS thesis, 208 p.

Cucchiara, C., Mendola, L. L., Papia, M., (2004), Effectiveness of stirrups and steel fibres as shear reinforcement, Cement and concrete composites, 26, 777–786.

Ding, Y.,Youb, Z., Jalali, S., (2011), The composite effect of steel fibres and stirrups on the shear behaviour of beams using self-consolidating concrete, Engineering Structures, 33, 107-117.

Ding, Y., Zhang, F., Fernando, T., and Zhang, Y., (2012), Shear Behavior of Steel Fibre Reinforced Self-Consolidating Concrete Beams Based on the Modified Compression Field Theory, Composite Structures, 1-20.

Dinh, H. H., Parra-Monteinos, G. J., and Wight, J. K. (2010), Shear Behavior of Steel Fiber-Reinforced Concrete Beams without Stirrup Reinforcement, ACI Structural Journal, 107(5), 597-606.

Dupont, D., and Vandewalle, L., (2003), Shear Capacity of Concrete Beams Containing Longitudinal Reinforcement and Steel Fibers, ACI Structural Journal, 216(6), 79-94.

Dong, J.K., El-Tawil, S., Naaman, A. E., (2008), Loading Rate Effect on Pullout Behavior of Deformed Steel Fibers, ACI Structural Journal, 105(6), 576-584.

El-Niema, E. I., (1991), Reinforced Concrete Beams with Steel Fibers under Shear, ACI Structural Journal, 88(2), 178-183.

Ersoy U., Özcebe G., Tankut T., (2008), Reinforced Concrete, Metu Press, 388 p.

ETABS 17, (2017), Computer and Structures Inc., USA.

FEMA 356, (2000), Prestandard and Commentary for the Seismic Rehabilitation of Buildings/ Prepared for Federal Emergency Management Agency, American Society of Civil Engineers.

Furlan, S., and Hanai, J. B., (1997), Shear Behavior of Fiber Reinforced Concrete Beams, Cement and Concrete Composites, 19, 359-366.

Galano, L., Vignoli, A., (2000), Seismic Behavior of Short Coupling Beams with Different Reinforcement Layouts, ACI Structural Journal, 97(6), 876-885.

Gopalaratnam, V.S., Jin-Cheng, (1987), In Material Research Society Symposium Proceedings 114; Materials Research Society Pittsburgh, 225-232.

Greenough, T., Nehdi, M., (2008), Shear behavior of fiber-reinforced self-Consolidating Concrete Slender Beams, ACI structural journal, 105(5), 468-477.

Guerrero, P., (1999), Bond Stress-Slip Mechanisms in High Performance Fiber Reinforced Cement Composites, Ph.D. Thesis, The University of Michigan, 249 p.

Han, S. W., Lee, C. S., Kwon, H-W., Lee, K. H., Shin, M. S., (2015), Behaviour of Fibre-Reinforced Beams with Diagonal Reinforcement, Magazine of Concrete Research, 67(24), 1287-1300.

Henager C. H. and Doherty T. J., (1976), Analysis of Reinforced Fibrous Concrete Beams. Proceeding, ASCE, 102(1), 177-188.

Hanson, J. A., (1961), Tensile Strength and Diagonal Tension Resistance of Structural Lightweight Concrete, ACI Journal Proceedings, 58(1), 1-40.

Hull, D. and Clyne, T.W. (1996) An Introduction to Composite Materials. 2nd Edition, Cambridge University Press, Cambridge, 344 p.

Imam, M., L. Vandewalle, L., and Mortelmans, F., (1994), Shear Capacity of Steel Fiber High-Strength Concrete Beams, ACI Structural Journal, 149(13), 227-241.

Imam, M., Vandewalle, L., and Mortelmans, F., (1995), Shear-Moment Analysis of Reinforced High Strength Concrete Beams Containing Steel Fibres, Canadian Journal of Civil Engineering, 22, 462-470.

Ivey, D. L., Buth, E., (1967), Shear Capacity of Light-weight Concrete Beams, ACI Journal Proceedings, 64(10), 634-643.

Jenq, Y. S., and Shah, S. P., (1987), Fracture Mechanics and Constitutive Modeling of Concrete, Proceedings, Constitutive Laws for Engineering Materials, Tucson, AZ, Elsevier, 21, 1055.

Khaloo, A. R., and Kim, N., (1997), Influence of Concrete and Fiber Characteristics on Behavior of Steel Fiber-Reinforced Concrete under Direct Shear, ACI Structural Journal, 94(6), 592-600.

Khuntia, M., Stajodinovic, B., and Goel, S. C., (1999), Shear Strength of Normal and High-Strength Fiber Reinforced Concrete Beams without Stirrups, ACI Structural Journal, 96(2), 282-289.

Khuntia, M., and Stojadinovic, B., (2001), Shear Strength of Reinforced Concrete Beams without Transverse Reinforcement, ACI Structural Journal, 98(5).

Kurtz, S., Balaguru, P., (2000), Postcrack Creep of Polymeric Fiber Reinforced Concrete in Flexure, Cement and Concrete Research, 30(2), 183-190.

Kwak, Y. K., Eberhard, M. O., Kim, W. S., and Kim, J., (2002), Shear Strength of Steel Fiber-Reinforced Concrete Beams without Stirrups, ACI structural journal, 99(4), 530-538.

Kwon, H-W., Jeon, Y-R., Lee, K-H., Shin, M-S., Han, S-W., (2013), Cyclic Behavior of High-Performance Fiber-Reinforced Cement Composite Coupling Beam Having Diagonal Reinforcement, JKCI, 25(6), 649-656.

Lequesne, R., (2011), Behavior and Design of High-Performance Fiber-Reinforced Concrete Coupling Beams and Coupled-Wall Systems, Ph.D. Thesis, The University of Michigan, 299 p.

Lequesne, R., Parra-Montesinos, G. J., Wight, J. K., (2012), Seismic Behavior of Detailing of High-Performance Fiber-Reinforced Concrete Coupling Beams and Coupled Wall Systems, Journal of Structural Engineering, 139(8), 1362-1370.

Li, V. C., Ward, R., and Hamza, A. M., (1992), Steel and synthetic fibers as shear reinforcement, ACI Struct. J., 89(5), 499-508.

Lim, T. Y., Paramasivam, P., Leet, S. L., (1987), Shear and Moment Capacity of Reinforced Steel-Fibre-Concrete Beams, Magazine of Concrete Research, 39(140), 148-160.

Lim, D. H., Oh B. H., (1999), Experimental and theoretical investigation on the shear of steel, Engineering Structures, 21, 937–944.

Lim, D. H., Oh B. H., (1999), Experimental and theoretical investigation on the shear of steel, Engineering Structures, 21, 937–944.

Luo, X., Sun, W., Chan, Y. N., (2000), Characteristics of High Performance Steel Fiber Reinforced Concrete Subject to High Velocity Impact, Cement and Concrete Research, 30(6), 907-914.

Majdzadeh, F., Soleimani, S. M., and Banthia, N., (1985), Shear Strength of Reinforced Concrete Beams with a Fiber Concrete Matrix, Journal of Canadian Civil Engineering, 33, 726-734.

Mansur, M. A., Ong, K. C. G., and Paramasivam, P., (1986), Shear Strength of Fibrous Concrete Beams without Stirrups, ASCE, 112(9), 2066-2079.

Mansur, M. A., and Ong, K. C. G., (1991), Behavior of reinforced fiber concrete deep beams in shear, ACI Struct. J., 88(1), 98-105.

Mattock, A. H., Kriz, L. B., Hognestad, E., (1961), Rectangular Concrete Stress Distribution in Ultimate Strength Design, ACI Structural Journal, 57(8), 875-926.

Mohamed, K., Farghaly, A.S., Benmokrane, B., (2016), Strut Efficiency-Based Design for Concrete Deep Beams Reinforced with Fiber-Reinforced Polymer Bars, ACI Structural Journal, 113(4), 791-800.

Moody, K.G., Viest, I.M., Elstner, R.C. and Hognestad, E., (1954), Shear strength of reinforced concrete beams, Part 1- Tests of simple beams, ACI Journal Proceedings, 51(12), 317–332.

Muttoni A., Ruiz F. M. (2010), Shear in Slabs and Beams: Should They Be Treated in the Same Way?", Fédération Internationale du Béton, 57, 105-128.

Naaman, A.E., (1987), High Performance Fiber Reinforced Cement Composites, Proceeding IABSE Symposium on Concrete Structures for the Future, Paris, France, September, 371-376.

Naaman, A. E., Nammur, G., Najm, H., and Alwan, J. M., (1989), Bond mechanisms in fiber reinforced cement-based composites." Report UMCE, Dept. of Civ. Eng., Univ. of Michigan, 254 p.

Naaman, A. E., Namur, G. G., Alwan, J. M., and Najm, H. S., (1991), Fiber Pullout and Bond Slip. I: Analytical Study, ASCE, 117(9), 2769-2790.

Naaman, A. E., and Reinhardt, H. W., (1995), Characterization of High Performance Fiber Reinforced Cement Composites, Proceedings of the Second Int. Workshop: HPFRCC, Ann Arbor, USA, 1-24.

Naaman, A. E., and Reinhardt, H. W., (1996), Characterization of High Performance Fiber Reinforced Cement Composites-HPFRCC 2, RILEM, 31, 1-24.

Naaman, A.E., (1998), New fiber technology: Cement, ceramic and polymetric composites, Concrete International, 20(7), 57-62.

Naaman, A. E., (2003), Strain Hardening and Deflection Hardening Fiber Reinforced Cement Composites, HPFRCC4: International Workshop High Performance Fiber Reinforced Cement Composites, 95-113.

Naaman, A.E., (2003), Engineered Steel Fibers with Optimal Properties for Reinforcement of Cement Composites, Journal of Advanced Concrete Technology, 1(3), 241-252.

Naaman, A. E., and Reinhardt, H. W., (2006), Proposed Classification of HPFRC Composires Based on Their Tensile Stress, Materials and Structures, 39, 547-555.

Naaman, A. E., (2007), High Performance Fiber Reinforced Cement Composites: Classification and Applications, CBM-CI International Workshop, Karachi, Pakistan.

Narayanan, R., Kareem-Palanjian, A. S., (1984), Torsion in Plain and Prestressed Concrete Beams Containing Polypropylene Fibres, Magazine of Concrete Research, 36, 22-30.

Narayanan, R., and Darwish, I. Y. S., (1987), Use of Steel Fibers as Shear Reinforcement, ACI Structural Journal, 84(3), 216-227.

Narayanan, R., Darwish, I. Y. S., (1989), Fiber Concrete Deep Beams in Shear, ACI Structural Journal, 85(17), 141-149.

Naish,, D. A. B., (2010), Testing and Modeling of Reinforced Concrete Coupling Beams, Ph.D. Thesis, University of California, 251 p.

Noghabai, K., (2000), Beams of Fibrous Concrete in Shear and Bending: Experimental and Model, ASCE, 126(2), 243-251.

NZS 3101: Standards New Zealand, (1995), Concrete Structures Standard, 309 p.

Oh, H. C., Lee, K., Han, S. W., Shin, M., Jo, Y. W., (2015), Hysteretic Behavior Evaluation of a RC Coupling Beam using a Steel Fiber and Diagonal Reinforcement, Journal of the Korea Concrete Institute, 27(3), 291-298.

Parra-Montesinos, G. J., (2000), Seismic Behavior, Strength and Retrofit of Exterior RC Column-to-Steel Beam Connections, Ph.D. Thesis, The University of Michigan.

Parra-Montesinos, G.J., Wight, J. K., Kopczynski, C., Lequesne, R. D., Setkit, M., Conforti, A., Ferzli, J., (2017), Earthquake-Resistant Fibre-Reinforced Concrete Coupling Beams without Diagonal Bars, SP-310, ACI.

Paulay, T., (1971), Coupling Beams of Reinforced Concrete Shear Walls, ASCE, 97(3), 843-862.

Paulay, T., Binney, J.R., (1974), Diagonally Reinforced Coupling Beams of Shear Walls, Shear in Reinforced Concrete, SP-42- ACI, 2, 579-598.

Pauley, T., Priestley, M. J. N., (1992), Seismic Design of Reinforced Concrete Masonry Buildings, Wiley-Interscience, 1st Edition, 768 p.

Paulay, T., and Taylor, R. G., (1981), Slab coupling of earthquake-resisting shear walls, ACI Journal, 78(2), 130-140.

Pérez-Irizarry, A. L., Parra-Montesinos, G. J., (2016), Evaluation of Seismic Behavior of Coupling Beams with Various Types of Steel Fiber Reinforced Concrete, Research Project, The University of Wisconsin, Medison, 120 p.

Puertas, F., Amat, T., Fernandez-Jimenez, A., Varguez, T., (2003), Mechanical and Durable Behaviour of Alkali Cement Mortars Reinforced with Polypropylene Fibers, Cement and Concrete Research, 33(12), 2031-2036.

Ritter, W., (1899), Die Bauweise Hennebique, Schweizerische Bauzeitung, Bd, XXXIII, 7

Rosenbusch J., and Teutsch M., (2003), Shear Design with Shear-Strain Method, RILEM TC 162-TDF Workshop, Bochum, Germany, 105-117.

Sanad, A. & Saka, M.P. (2001), Prediction of ultimate shear strength of reinforced-concrete deep beams using neural networks. J Struct Eng, ASCE, 127(7), 818–28.

SAP 2000, (1998), Graphic User Interface Manual, Computer and Structures, USA, Version 7, 159 p.

Seo, S.Y., Yun, H.D., Chun, Y.S., (2017), Hysteretic Behavior of Conventionally Reinforced Concrete Coupling Beams in Reinforced Concrete Coupled Shear Wall, International Journal of Concrete Structures and Materials, 11(4), 599-616.

Setkit, M., (2012), Seismic Behavior of Slender Coupling Beams Constructed with High-Performance Fiber-Reinforced Concrete, Ph.D. Thesis, The University of Michigan, 261 p.

Sharma, A. K., (1986), Shear Strength of Steel Fiber Reinforced Concrete Beams, ACI Journal, 83(56), 624-628.

Shah, S. P., Peled, A., Aldea, C. M., and Akkaya, Y, (1999), Scope of High Performance Fiber Reinforced Cement Composites-HPFRCC3, RILEM, 10, 113-129.

Shahnewaz, M., Alam, M. S., (2014), Improved Shear Equations for Steel-Fiber Reinforced Concrete Deep and Slender Beams, ACI Structural Journal, 111(4), 851-860.

Shin, S. W., Oh, J. G., and Ghosh, S. K., (1994), Shear Behavior of Laboratory-Sized High-Strength Concrete Beams Reinforced with Bars and Steel Fibers, ACI Structural Journal, 142, 181-200.

Shin, M., Gwon S-W., Lee, K., Han, S. W., Jo, Y. W., (2014), Effectiveness of High Performance Fiber-Reinforced Cement Composites in Slender Coupling Beams, Construction and Building Materials, 68, 476-490.

Shiu, N. K., Barney, G. B., Fiorato, A. E. and Corley, W. G., (1981), Earthquake Resistant Walls - Coupled Wall Test, Report to NSF submitted by Portland Cement Association, Research and Development, Skokie, Illinois.

Shoaib, A., Lubell, A. S., Bindiganavile, V. S., (2014), Size Effect in Shear for Steel Fiber-Reinforced Concerte Members without Stirrups, ACI Structural Journal, 111(5), 1081-1090.

Shui N. K., Barney G. B., Fiorata A. E., Corley W. G., (1981), Earthquake Resistant Walls Coupled Wall Test, Report to NSF submitted by Portland Cement Association, Research and Development, Illinois.

Subedi, N. K., (1991), RC-Coupled Shear Wall Structures. I: Analysis of Coupling Beams, Journal of Structural Engineering, ASCE, 117(3), 667-680.

Swamy, R.N., Mangat, P.S., and Rao, C.V.S.K., (1974), The Mechanics of Fiber Reinforcement of Cement Matrices, ACI Special Publication, 44, 1-28.

Swamy, R. N., Al-Ta'an, S. A., (1981), Deformation and Ultimate Strength in Flexure of Reinforced Concrete Beams Made with Steel Fiber Concrete, ACI Structural Journal, 78(5), 395-405.

Swamy, R. N., Bahia, H. M., (1985), The Effectiveness Steel Fibers as Shear Reinforcement, Concrete International: Design and Construction, 7(3), 35-40.

Şen, M., (2005), Shear Behavior of FRC Beams without Web Reinforcement Using Steel Fibres with Different Aspect Ratios, Msc Thesis, Boğaziçi University, 79 p.

Tan, K. H., Murugappan, K., Paramasivam, P., (1993), Shear Behavior of Steel Fiber Reinforced Concrete Beams, ACI Structural Journal, 89(6), 3-11.

Tassios, T., Moretti, M., and Bezas, A., (1996), On the Behavior and Ductility of Reinforced Concrete Coupling Beams of Shear Walls, ACI Structural Journal, 93(6), 711-720.

Taranath, B. S., (1997), Steel, Concrete, and Composite Design of Tall Buildings, McGraw-Hill Education, 2nd Edition, 1024 p.

Takeda, T., Sozen, M.A. and Nielsen, N.M., (1970), Reinforced Concrete Response to Simulated Earthquakes, ASCE , 96 (ST12), 2557-2573.

Yun, H-D., Kim, S-W., Jeon, E., Park, W-S., Lee, Y-T., (2008), Effects of Fibre-Reinforced Cement Composites' Ductility on the Seismic Performance of Short Coupling Beams, Magazine of Concrete Research, 60(3), 223-233.

Wafa, F. F., (1990), Properties and Applications of Fiber Reinforced Concrete, JKAU: Engineering Science, 2, 49-63.

Wang, Y., Li, V. C, and Backer, S., (1987), Analysis of synthetic fiber pullout from a cement matrix."Symp. Proc, Materials Research Society, 114, 159-165.

Whitney, C., (1937), Design of Reinforced Concrete Members Under Flexure or Combined Flexure and Direct Compression, ACI Journal Proceedings, 8(4), 483-498.

Wight, J. K., MacGregor, J. G., (2011), Reinforced Concrete Mechanics and Design, 6th edition, Pearson.

Zsutty, T., (1968), Beam Shear Strength Prediction by Analysis of Existing Data,ACI Journal Proceedings, 65(11), 943-951.

## CURRICULUM VITAE

### Education

| Year | Degree (*) | University | Department |
|---|---|---|---|
| 2012 | Master | Erciyes University | Civil Engineering |
| 2009 | Bachelor degree | Erciyes University | Civil Engineering |

**Master Thesis:**

**“Çelik Lif Katkılı Betondan İmal Edilmiş Kolonların Performans Düzeylerinin İncelenmesi”.**

Advisor : Prof. Dr. Fatih Altun